A pilot study investigating specific immune regulatory cells and microRNA in patients with advanced Pancreatic Adenocarcinoma treated with intravenous omega-3 fish oil infusion and Gemcitabine.

Thesis submitted for degree of
Doctor of Medicine
At the University of Leicester

By
John David Isherwood

Department of Cancer Studies

University of Leicester

June 2017

Abstract

Introduction

Pancreatic adenocarcinoma (PAC) is a devastating disease and the majority of patients have advanced pancreatic cancer (APC) and incurable disease at the time of presentation, and die within a few months. The overall survival of pancreatic cancer has not changed significantly in the past forty years with multiple trials demonstrating disappointing results. PAC features a profound inflammatory response and immune dysregulation, both systemically and locally that contributes to tumour progression. Immune modulatory cells particularly myeloid derived suppressor cells (MDSCs), T regulator cells (Tregs), endothelial progenitor cells (EPCs) in addition to micro RNAs are important mediators in PAC. Omega 3 fatty acids (ω-3FAs) have been shown to have anti-inflammatory and anti-cancer properties. There is good evidence demonstrating the benefit of ω-3FAs in PAC including growth inhibition, induction of apoptosis, inhibition of proliferation and invasion, augmentation of the effect of gemcitabine, reduced pro inflammatory mediators and growth factors and an improved quality of life.

Methods

This was a single centre cohort study investigating intravenous ω-3FAs and gemcitabine chemotherapy versus gemcitabine therapy only in patients with APC. The primary outcome measures were the levels of specific immune modulatory cells and micro RNAs in trial versus control patients. The secondary outcome measure was the correlation of demonstrated changes with progression free and overall survival.

Results

Eighteen trial and nine control patients were recruited. There was significant benefit in progression free survival in trial compared to control patients (P=0.0003). Median survival in trial patients was 5.65 months compared to 1.8 months in control patients. There was no significant benefit in overall survival in trial compared to control patients (P=0.13). Medial survival in trial patients was 7 months compared to 2.9 months in control patients. There was a significant benefit in progression free survival in trial compared to control patients (P=0.0003). MDSCs were significantly decreased in trial patients (P=0.0001) but not control patients. Tregs were significantly increased in control patients (P=0.005) but not in trial patients. Three EPC phenotypes ($CD45^-$, $CD31^+$, $CD133^+$ (P=0.04), $CD45^-$, $CD31^+$, $CD34^+$ (P=0.001), and $CD45^-$, $CD34^+$, $CD31^+$ and $CD133^+$(P=0.006) were significantly increased in the trial patients but not control patients. In addition EPCs ($CD45^-$, $CD31^+$, $CD34^+$ (P=0.0001) and $CD45^-$, $CD34^+$, $CD31^+$ and $CD133^+$ (P=0.0001)) were significantly increased compared to controls on comparison regression analysis over treatment. There was no significant change seen in any micro RNA measured in either cohort.

Conclusion

Administration of ω-3FAs with gemcitabine chemotherapy in APC results in a significant decrease of MDSCs and stability of Tregs. This may be secondary to the

reduction of pro inflammatory mediators. A phase three randomised trial is indicated to further validate these results.

Acknowledgements

This thesis is dedicated to my family, my father, mother and brothers, without your love and support I would not be here and this would not be possible. An enormous thank you to my wife and son. Your love and understanding have been incredible. This is for you both.

Thank you to my supervisor Professor Ashley Dennison. Thank you for your belief, patience, time, knowledge and understanding. You have set the bar for me to aspire to.

I would also like to thank Mr Matthew Metcalfe for his on-going support and guidance. Many thanks to Dr Wen Chung for all your help with laboratory protocols and the Taiwan collaboration, I hope to work with you on numerous future projects. I must also thank Mr Ali Arshad; you have been an incredible inspirational senior colleague. Thanks to Mr François Runau and Mr Amar El-Tweri for assistance in trial logistics. A considerable mention must be made to Ms Jill Cooke whose research support and advice was appreciated throughout. Thanks to Professor William Stewart and his team, particularly Ms Sarah Porter, whose help in recruiting and managing the trial patients was greatly appreciated. Thank you to Dr Lynne Howells and Dr Jenny Fishwick for their advice, support and expertise with my specimen analysis. Thanks to Professor John Thompson for his unwavering support and patience with the data analysis.

Finally I would like to thank all of the patients who have participated in this study who are no longer with us. Without your support for research this would not be possible.

Prizes, publications and presentations

Prizes

September 2016: European society for clinical nutrition and metabolism (ESPEN), International Conference. Copenhagen, Denmark. Presented - Prize winning oral presentation.
Isherwood J, Arshad A, Chung W, Runau F, Eltweri A, Mann C, Cooke J, Pollard C, Howells L, Fishwick J, Thompson JR, Metcalfe MS, Steward W, Dennison AR.
Investigation of immune regulatory cells (Myeloid derived supressor cells & T-regulator cells) in pancreatic cancer patients recieving gemcitabine and intravenous omega-3 fatty acids.
Published: Clinical Nutrition, Vol.35, S8. Published in issue: September 2016.

Publications

Under review: To be published:

Isherwood J, Arshad A, Chung W, Runau F, Eltweri A, Mann C, Cooke J, Pollard C, Howells L, Fishwick J, Thompson JR, Metcalfe MS, Steward W, Dennison AR. Omega 3 fatty acids significantly reduce Myeloid Derived Supressor Cells in advanced pancreatic cancer patients recieving gemcitabine and intravenous omega-3 fatty acids.

Isherwood, J, Arshad A, Chung W, Runau F, Cooke J, Pollard C, Thompson J, Metcalfe MS, Dennison AR. Parenteral Omega 3 significantly increases Endothelial Progenitor Cells in palliative pancreatic patients receiving Gemcitabine and intravenous Omega 3 compared to patient receiving Gemcitabine only.

Presentations

1.
September 2017: European society for clinical nutrition and metabolism (ESPEN), International Conference. The Hague, Netherlands.
Isherwood, J, Arshad A, Chung W, Runau F, Cooke J, Pollard C, Thompson J, Steward W, Metcalf MS, Dennison AR.
Parenteral Omega 3 significantly reduces Myeloid-Derived Suppressor Cells in palliative pancreatic patients receiving Gemcitabine and intravenous Omega 3 compared to patients receiving Gemcitabine only treatment.
Published: Clinical Nutrition, Vol. 36, S93-94. Published in issue: September 2017.

2.
September 2017: European society for clinical nutrition and metabolism (ESPEN), International Conference. The Hague, Netherlands. Accepted.
Isherwood, J, Arshad A, Chung W, Runau F, Cooke J, Pollard C, Thompson J, Steward W, Metcalf MS, Dennison AR.

T regulator cells are significantly increased in palliative pancreatic patients treated with gemcitabine alone compared to patients receiving Gemcitabine and intravenous Omega 3.
Published: Clinical Nutrition, Vol. 36, S94. Published in issue: September 2017.

3.
September 2017: European society for clinical nutrition and metabolism (ESPEN), International Conference. The Hague, Netherlands.
Isherwood, J, Arshad A, Chung W, Runau F, Cooke J, Pollard C, Thompson J, Metcalfe MS, Dennison AR.
Parenteral Omega 3 significantly increases Endothelial Progenitor Cells in palliative pancreatic patients receiving Gemcitabine and intravenous Omega 3 compared to patient receiving Gemcitabine only.
Published: Clinical Nutrition, Vol. 36, S93. Published in issue: September 2017.

4.
September 2016: European society for clinical nutrition and metabolism (ESPEN), International Conference. Copenhagen, Denmark.
Isherwood J, Arshad A, Chung W, Runau F, Eltweri A, Mann C, Cooke J, Pollard C, Howells L, Fishwick J, Thompson JR, Metcalfe MS, Steward W, Dennison AR.
Parenteral Omega 3 significantly increases Endothelial Progenitor Cells in palliative pancreatic patients receiving Gemcitabine and intravenous Omega 3.
Published: Clinical Nutrition, Vol. 35, S75-76. Published in issue: September 2016.

5.
September 2016: European society for clinical nutrition and metabolism (ESPEN), International Conference. Copenhagen, Denmark.
Isherwood J, Arshad A, Chung W, Runau F, Eltweri A, Mann C, Cooke J, Pollard C, Howells L, Fishwick J, Thompson JR, Metcalfe MS, Steward W, Dennison AR.
Parenteral Omega 3 significantly reduces Myeloid Derived Suppressor cells in palliative pancreatic patients receiving Gemcitabine and intravenous Omega 3.
Published: Clinical Nutrition, Vol.35, S8. Published in issue: September 2016.

6.
September 2015: European society for clinical nutrition and metabolism (ESPEN), International Conference. Lisbon. Portugal.
Isherwood J, Arshad A, Chung W, Runau F, Eltweri A, Cooke J, Chi-Sheng W, Steward W, Metcalfe MS, Chang Y-S, Dennison AR.
Micro RNA analysis in palliative care pancreatic cancer patients recieving Gencitabine and intravenous Omega 3 therapy.
Published: Clinical Nutrition, Vol 34, S158. Published in issue: September 2015.

Abbreviations used

AA - Arachadonic acid
Akt - Protein kinase B
ALP – Alkaline phosphatase
ALT – Alanine transaminase
APC – Advanced pancreatic cancer
CCR5 - Chemokine receptor type 5
CECs - Circulating endothelial cells / Circulating endothelial progenitors
Cetuximab - Anti-EGFR monoclonal antibody
COX2 - Cyclooxygenase-2
CSF1 - Colony stimulating factor 1
CXCL5 - C-X-C motif chemokine ligand 5 / Epithelial neutrophil-activating peptide-78
CXCL17 - Chemokine (C-X-C motif) ligand 17
CTLs - Cytotoxic T lymphocytes
CDK4 - Cyclin-dependent kinase 4
DHA - Docosahexaenoic acid
DNA - Deoxyribonucleic acid
DMSO - Dimethyl sulfoxide
EDTA - Ethylenediaminetetraacetic acid
EGF – Epidermal growth factor
EGFR -Epidermal growth factor type 1
ERK - Extracellular signal-regulated kinase
ENO1 - α-Enolase
EPA - Eicosapentaenoic acid
EPC – Endothelial progenitor cells
ERCP - Endoscopic retrograde cholangiopancreatography
FAS-L - FAS-ligand
FACS – Fluorescence-activated cell sorting
FGF – Fibroblast growth factor
FOLFRINOX - Oxaliplatin, irinotecan, leucovorin and fluorouracil
5-FU - Fluorouracil
G-CSF - Granulocyte colony stimulating factor
HMGB1 - High mobility group box 1
HLA1 - Human leukocyte antigen 1
IDO - Indoleamine 2,3 dioxygenase
IF-γ - Interferon gamma
IGF1R - Insulin growth factor receptor 1
IGF – Insulin-like growth factor
ICAM2 - Intercellular adhesion molecule
iNOS - Inducible nitric oxide synthase
IL – Interleukin
IL-1β – Interleukin 1 beta
IL-1ra - IL-1 receptor agonist
LOX - Lipoxygenase
LT - Leukotrienes

MDSC – Myeloid derived suppressor cells
MHC-1 - Major histocompatibility complex 1
MHRA - Medicines and Healthcare Products Regulatory Agency
MiRNA – Micro RNA
MMPs - Matrix metalloproteinases
NS - Natural suppressor cells
NFκB - Nuclear factor-kappaB
NICE - National institute for health and care excellence
NO - Nitric oxide
ω-3FA – Omega 3 fatty acid
ω-3FAs – Omega 3 fatty acids
ω-6FA – Omega 6 fatty acid
ω-6FAs – Omega 6 fatty acids
ω-9FAs – Omega 9 fatty acids
OS – Overall survival
PAC – Pancreatic adenocarcinoma
PSCs - Pancreatic stromal cells
PBS – Phosphate buffered solution
PCD1 - Programmed cell death protein-1
PDGF – Platelet derived growth factor
PECAM-1 - Platelet and endothelial cell adhesion molecule 1
PPAR - Peroxisome proliferator-activated receptor
PFS – Progression free survival
PG - Prostaglandins
PGE2 - Prostaglandin-E2
PMBC – Peripheral blood mononuclear cell
PUFA - Polyunsaturated fatty acids
PDL-1 - Programmed cell death ligand-1
PSC - Pancreatic stromal cells
PTEN - Phosphatase and tensin homolog
RCT – Randomised control trial
ROS - Reactive oxygen species
RECIST - Response evaluation criteria in solid tumours
RNA – Ribonucleic acid
S-1 - An oral fluropyrimidine derivative
SMADs – Small mothers against decapentaplegic receptors
STAT - Signal transducer and activator of transcription
STAT 3 - Signalling transducer and activator of transcription 3
TCRζ - T cell receptor signalling molecule zeta
TGF-β - Transforming growth factor-beta
TH2 - T-helper 2
TNFα - Tumor necrosis factor- α
Tregs – T regulator cells
TRL - Troll-like receptors
TX - Thromboxanes
UTRs - Untranslated regions
VEGF – Vascular endothelial growth factor

VEGFR2 - Vascular endothelial growth factor receptor 2
ZEB2 - Zinc finger E-box-binding homeobox 2 protein

Table of Contents

1 Chapter One: Introduction

1.1 Epidemiology of pancreatic cancer

Pancreatic adenocarcinoma (PAC) is a devastating disease and the majority of patients have advanced pancreatic cancer (APC) and incurable disease at the time of presentation and die within a few months. The incidence of the disease approximates to the mortality, with around 7,500 to 8,000 new cases and deaths each year in the UK, making it the 5th most common cause of cancer death[1]. In the USA there are approximately 53,000 new cases of pancreatic cancer[2,3], with a 7% 5 year survival rate[2]. Pancreatic cancer is expected to become the second cause of cancer related death by 2030[4]. The overall survival of pancreatic cancer has not changed significantly in the past forty years contrasting with other cancers such as bowel and breast cancer, which have demonstrated a significant increase in overall survival (Figure 1.1). The anatomical position of the pancreas means that small tumours often develop undetected and this results in patients presenting at a late stage with advanced disease. The presenting symptoms depend on the anatomical site of cancer in the pancreas with approximately 75% of adenocarcinomas developing in the head of the gland explaining why patients often present with obstructive jaundice[5].

The common presenting signs and symptoms of pain, anorexia, weight loss, nausea, vomiting, malaise and jaundice are protean and patients are often misdiagnosed until the disease is at an advanced stage. Diabetes is present in approximately 50% of newly diagnosed patients[6]. Evaluation of a patient with suspected pancreatic cancer should involve diagnosis and staging of the disease, assessment of resectability and treatment of any symptoms[7]. Computed tomography with intravenous contrast is presently the gold standard investigative modality although other useful investigations include positron-emission tomography (PET), endoscopic ultrasonography (EUS) and endoscopic retrograde cholangiopancreatography (ERCP). Endoscopic ultrasonography has the added benefit of facilitating tissue collection for a definitive pathological diagnosis. ERCP can be used to provide brushings and to place an endoscopic stent in patients with an obstructed biliary system. Discussion of all patients at a

multidisciplinary team meeting allows peer review of a patient's case with the high-quality input of various allied specialities. Approximately 5-10 % of patients have a family history of pancreatic cancer[8] and the risk of developing pancreatic cancer is increased by eighteen fold in first degree relatives[9]. In addition to the genetic risk other causative factors include age, smoking, alcohol intake, chronic pancreatitis and obesity.

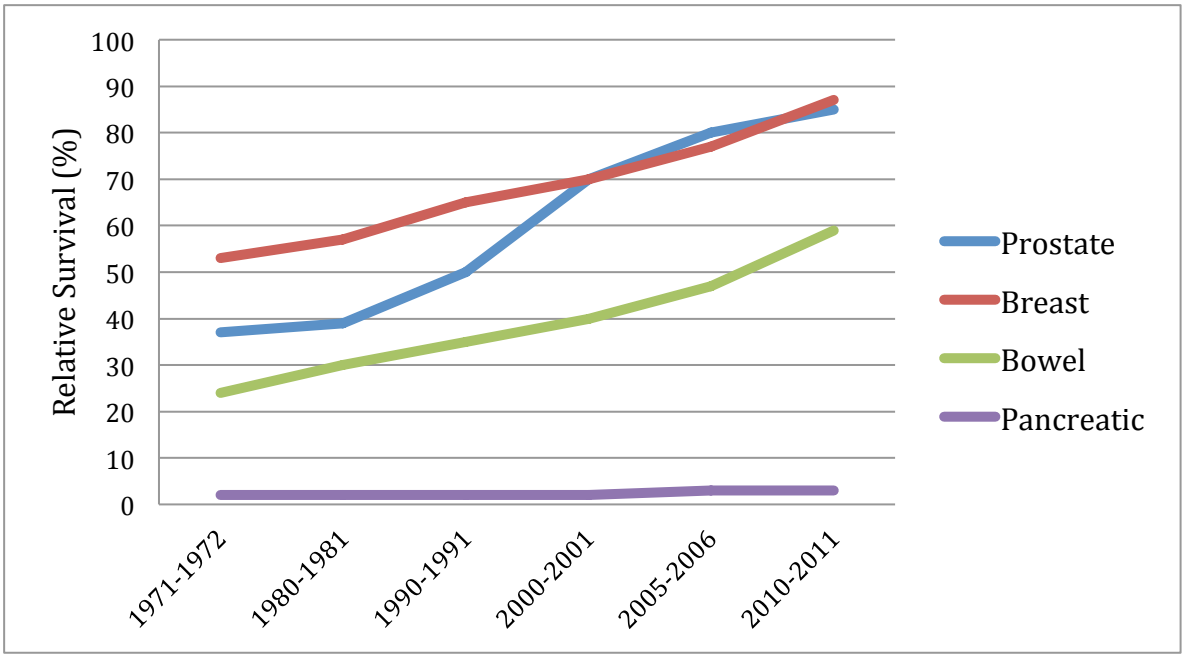

Figure 1.1. Trends in cancer survival of pancreatic cancer from 1971-2011 compared to other common cancers. The relative survival of pancreatic cancer has remained static for over forty years (data from pancreatic cancer UK).

1.2 Current treatment of pancreatic cancer

Pancreatic adenocarcinoma regularly metastasises, predominantly to the liver, lung and abdomen and invades important surrounding anatomical structures at an early stage[10]. When a patient with a pancreatic adenocarcinomas presents, approximately 20% will be considered potentially operable with curative intent, resulting in the majority of patients being considered for palliative treatment[11] (Figure 1.2). Surgery involves a major operation and if the cancer is in the head of the pancreas, patients will undergo a pancreaticodudenectomy (Whipple's procedure), or a distal pancreatectomy if the cancer is in the distal body or tail of the gland. Patients who are

found to be inoperable intra-operatively frequently undergo a biliary bypass involving generally a Roux loop to the bile duct and generally also a gastrojejunostomy. This helps prevent symptoms of obstructive cholestasis and gastric outlet obstruction. Patients with apparently resectable disease with curative intent who undergo surgery nevertheless still only have a five year survival of approximately 20%[11]. For those diagnosed with unresectable cancer the median life expectancy is approximately 8 months[12,13].

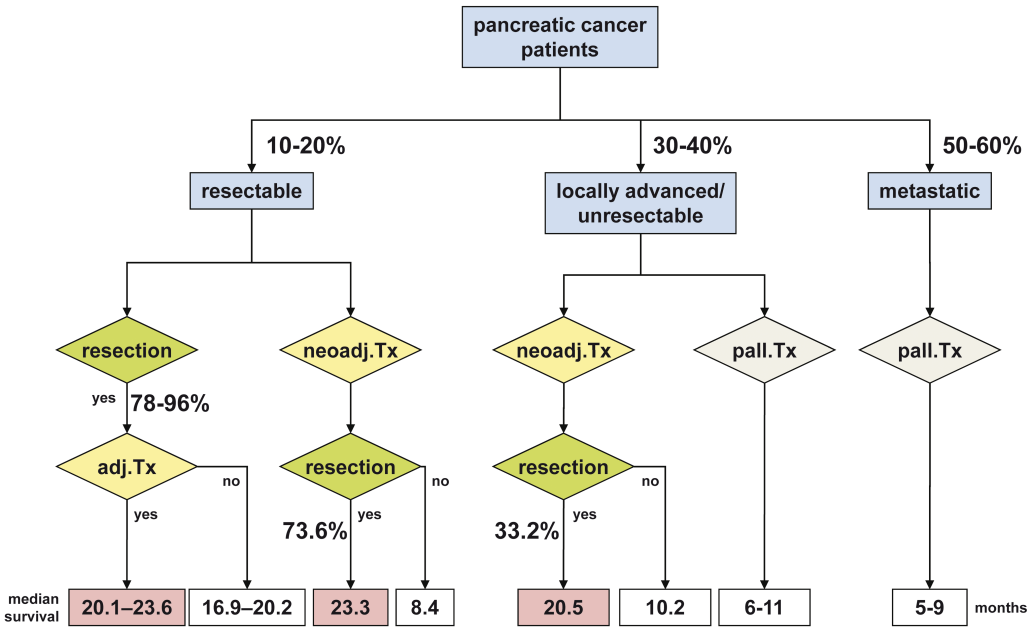

Figure 1.2. Summary overview of survival of different groups of patients with pancreatic cancer. Figure from Gillen S, et al, Preoperative/Neoadjuvant Therapy in Pancreatic Cancer: A Systematic Review and Meta-analysis of Response and Resection Percentages, [13]. Reproduced with permission.

1.3 Palliative pancreatic cancer treatment

Patients with locally advanced or unresectable disease not amenable to neo-adjuvant treatment and metastatic disease are considered for palliative treatment (Figure 1.2). APC has proved very difficult to treat and there have not been any significant treatment developments in the past twenty years. Treatment options include symptomatic relief and palliative chemotherapy. Prior to 1997 the main

chemotherapeutic agent used was Fluorouracil (5-FU) which had minimal effect on either disease related symptoms or survival.

1.4 Gemcitabine mono therapy

Gemcitabine is a pyrimidine analog that is phosphorylated to disphosphate and triphosphate forms to inhibit both ribonucleotide and DNA polymerase[14]. The triphosphate form replaces cytidine during DNA replication and arrests tumour growth. In 1997 Burris et al published a seminal paper that established the superiority of gemcitabine chemotherapy over 5-FU[15]. One hundred and twenty-six patients were randomised to receive gemcitabine or 5-FU and there was a clinical benefit response of 23.8% in the gemcitabine-treated patients compared with 4.8% of 5-FU-treated patients (P=0.002). This became the gold standard treatment for twenty years and patients treated with gemcitabine demonstrated an improved median survival of 5.56 months compared to 4.41 months in the 5-FU treated cohort (P=0.002). The survival rate at twelve months was 18% for gemcitabine patients and 2% for 5-FU patients. The most frequent toxic side effect of gemcitabine was neutropenia, but it was otherwise generally well tolerated[14]. Over the past forty years there have been copious trials that have demonstrated minimal or no survival benefit compared with gemcitabine alone. Multiple phase two and three trials have explored gemcitabine mono-therapy versus numerous combinations of gemcitabine with other chemotherapeutic agents and targeted medications[4]. The vast majority of these trials have demonstrated disappointing results with no trial having demonstrated a median survival of greater than 12 months although a number have shown promise. The key trials are discussed further below (Table 1.1, 1.2 & 1.3).

Trial	Number of patients	Treatment	Median Overall Survival (Months)	P value
Burris et al. (1997). [15]	126	Fluorouracil (5-FU) Gemcitabine	4.4 5.6	0.002
Moore et al. (2007). [16]	569	Gemcitabine Gemcitabine & erlotinib	5.91 6.24	0.038
Cunningham et al. (2009). [17]	533	Gemcitabine Gemcitabine & Capecitabine	6.2 7.1	0.08
Ueno et al. (2013). [18]	834	Gemcitabine S-1 Gemcitabine & S-1	8.8 9.7 10.1	<0.001 (Non-inferiority) 0.15 (Superiority of combination treatment)
Conroy et al. (2011). [19]	342	Gemcitabine FOLFIRINOX	6.8 11.1	<0.001
Von Hoff et al. (2013). [20]	861	Gemcitabine Gemcitabine & nab-paclitaxel	6.7 8.5	<0.001
Neoptolemos et al (2017). [21]	732	Gemcitabine & Capecitabine Gemcitabine	28.0 25.5	0.032

Table 1.1. Key trials in palliative pancreatic cancer treatment. FOLFIRINOX denotes oxaliplatin, irinotecan, leucovorin and fluorouracil.

1.5 Gemcitabine and erlotinib

In 2007 Moore et al published a phase three trial comparing standard gemcitabine treatment versus gemcitabine and erlotinib treatment[16] in metastatic or unresectable pancreatic cancer. Pancreatic cancers frequently over express human epidermal growth factor (EGFR), which was associated with a worse prognosis. Erolinib is a tyrosine kinase inhibitor that acts on EGFR. They demonstrated a hazard ration of 0.82 for survival (P=0.038), which translated into a median survival advantage of 0.33 months compared to gemcitabine only treatment. One-year survival was also significantly improved with erlotinib plus gemcitabine (23% versus 17%; P=0.02). The main disadvantage with erlotinib was that its toxic side effects did not justify the modest survival benefit which meant that the treatment was not widely adopted. A systematic review into gemcitabine and erlotinib combination treatment examined sixteen studies containing 1,308 patients and reported that up to 62.9% of patients experienced severe adverse events, the most prominent being a dermatological rash (57.9%), leucopenia (71.2%), neutropenia (32.9%), thrombocytopenia (32.4%) and anaemia (30.6%)[22]. Pooled data demonstrated an overall survival of 27.9% at one year[22], a disappointing outcome.

1.6 Gemcitabine and capecitabine

Capecitabine is an oral chemotherapy agent that is metabolised to 5-FU. Cunningham et al[17] demonstrated a non-significant trend towards improved overall survival in patients treated with both gemcitabine and capecitabine compared to gemcitabine alone (7.1 months versus 6.2 months, P=0.08). On combination with two further studies in a meta-analysis of nine hundred and thirty five patients they demonstrated an improvement in overall survival in favour of the combination treatment (P=0.02)[17,23,24]. No study individually demonstrated an improved survival over gemcitabine only treatment and this chemotherapy regime only provided oncologists with a well-tolerated oral alternative to gemcitabine mono-therapy.

1.7 Gemcitabine and S-1

S-1 is an oral fluropyrimidine derivative designed to improve antitumor activity and reduce the toxicity of 5-FU[25]. It consists of a pro-drug of 5-FU combined with two 5-FU

biochemical modulators aimed at decreasing the phosphorylation of 5-FU in the gastrointestinal tract, thereby decreasing the effects of nausea, vomiting, stomatitis and diarrhoea[25]. Ueno and colleagues demonstrated a significant non-inferiority to gemcitabine (P=<0.001) but a non-significant superiority of gemcitabine plus S-1 (P=0.15)[18]. Patients experienced increased toxic side effects with combination treatment. This study had a selection bias as it only included patients with an Eastern Cooperative Oncology Group performance status (ECOG) of 0 or 1 (Appendix 1). No improvement compare to standard gemcitabine treatment meant this treatment had limited therapeutic implementation but remained a convenient oral alternative.

1.8 Gemcitabine and FOLFIRINOX

The first trial demonstrating the superiority of a combination treatment utilised a combination of four chemotherapy agents; oxaliplatin, irinotecan, leucovorin and fluorouracil (FOLFIRINOX)[19]. This multicentre randomised trial demonstrated that patients treated with FOLFIRINOX had a significantly improved progression free and overall survival compared to gemcitabine alone (6.4 months versus 3.3 months (P<0.001), and 11.1 months versus 6.8 months, P<0.001) respectively[19]. Patients also reported significant improvements in global health status and quality of life (P<0.001)[19]. However patients treated with FOLFIRINOX had a significant increase in toxic side events including neutropenia, febrile neutropenia, thrombocytopenia, diarrhoea and sensory neuropathy and 42% of patients received supplementary treatment with filgrastim, a granulocyte colony-stimulating factor medication. Patients selected for this study also had a better baseline performance status (ECOG 0 or 1), than previous trials. This was a limitation as the majority of patients diagnosed with pancreatic cancer are frail and elderly, who would consequently be ineligible for this therapeutic regime. Because of the toxic side effects and selection bias, this chemotherapy regime has generally been reserved for patients with an good baseline performance status.

1.9 Gemcitabine and nab-paclitaxel

The most recent pioneering breakthrough in metastatic pancreatic cancer treatment came in 2013 with the publication of a phase 1-2 trial by Von Hoff et al[20]. Paclitaxel is a mitotic inhibitor, preventing the breakdown of microtubules during cell division[26]. Preclinical data demonstrated that nab-paclitaxel led to stromal depletion and increasing microvasculature in PAC, resulting in higher gemcitabine penetration into and subsequent concentration within the tumour[14]. The concentration of gemcitabine in tumour cells was increased by 2.8 fold in mice receiving combination treatment[27], potentially increasing the gemcitabine efficacy. Although this phase three trial did not replicate the impressive median overall survival of 12.2 months from the phase two trial[27], the results were impressive. Eight hundred and sixty-one patients were randomised to receive nab-paclitaxel and gemcitabine or gemcitabine only treatment. There was a significant improvement in progression free and overall survival in the combination treatment (5.5 months versus 3.7 months ($P<0.001$), and 8.5 months versus 6.7 months, $P<0.001$) respectively. However there were again increased side effects in the combination treatment group including neutropenia, fatigue and neuropathy. Although this treatment regimen was adopted as standard worldwide in 2015, the National Institute for Health and Care Excellence (NICE) withdrew routine funding for nab-paclitaxel in England, explaining that it did not find the treatment cost effective. This is despite one cycle treatment only costing £1481 per cycle, and each patient's treatment costing an average of £5035. This is a clear demonstration of the low funding priority allocated to PAC within the National Health Service.

1.10 Gemcitabine and Capecitabine versus gemcitabine monotherapy. ESPAC-4

A recent publication by the European Study Group for Pancreat Cancer (ESPAC-4, Neoptolemos et al[21]) in 2017 demonstrated that the adjuvant combination of gemcitabine and capecitabine was superior to gemcitabine monotherapy following surgical resection for PAC. The group conducted a phase 3, two-group, open-label, multicentre, randomised clinical trial at 92 hospitals in England, Scotland, Wales,

Germany, France and Sweden. Patients were enrolled following surgical resection for PAC. Patients were either assigned to receive six cycles of gemcitabine alone administered once a week for three of every four weeks or with oral capecitabine administered for 21 days followed by 7 days rest. Seven hundred and thirty two patients were enrolled. Patients receiving combination treatment had a medial overall survival of 28.0 months versus 25.5 months for those treated with gemcitabine monotherapy (hazard ratio 0.82, p=0.032). However the study reported increased grade 3-4 adverse events in the combination treatment group (608 versus 481).

Gemcitabine monotherapy is well tolerated and recommended to patients with a poor performance status. The combination treatments of erlotinib, FOLFIRINOX or nab-paclitaxel and gemcitabine are recommended for patients with a good or excellent performance status[14]. ESPAC-4 recently demonstrated that gemcitabine in combination with capecitabine was superior to gemcitabine monotherapy however this is only following surgical resection. This is on the background of numerous Phase III trials that have produced very disappointing results (table 1.2). Recently there have been several phase III trials that have explored the potential of immune therapies in APC and the results of these are summarised in table 1.3.

Trial	Year	Treatment	Patient No.	PFS - months	P value	OS - months	P value
Burris et al.[15]	1997	Gemcitabine 5-FU	63 63	2.3 0.9	0.0002	5.7 4.4	0.002
Berlin et al.[28]	2002	Gemcitabine Gemcitabine/ 5FU	162 160	2.2 3.4	0.22	6.7 5.4	0.09
Colucci et al.[29]	2002	Gemcitabine Gemcitabine/Cisplatin	54 53	1.8 4.6	0.048	4.6 6.9	0.48
Decreux et al.[30]	2002	5-FU 5-FU/Cisplatin	103 104	1.9 2.4	ns	3.4 3.7	0.1
Bramhall et al.[31]	2002	Gem/Marimastat Gemcitabine/Placebo	120 119	3.0 3.2	ns	5.4 5.4	ns
Van Cutsem et al.[32]	2004	Gem/Tipifarnib Gem/Placebo	341 347	3.7 3.6	ns	6.3 6.0	0.75
Oettle et al.[33]	2005	Gemcitabine Gem/Pemetrexed	282 283	3.3 3.9	0.11	6.3 6.2	0.84
Louvet et al.[34]	2005	Gemcitabine Gem / Oxaliplatin	156 157	3.7 5.8	0.04	7.1 9.0	0.13
Heinemann et al.[35]	2006	Gemcitabine Gem/Cisplatin	97 98	3.1 5.3	0.53	6.0 7.5	0.15
Abou-Alfa et al.[36]	2006	Gemcitabine Gem/Exatecan	174 175	3.7 3.6	ns	6.2 6.7	0.52
Stathopoulos et al.[37]	2006	Gemcitabine Gem/Irinotecan	74 71	2.9 2.8	ns	6.5 6.4	0.6
Hermann et al.[23]	2007	Gemcitabine Gem/Capecitabine	159 160	3.9 4.3	0.22	7.2 8.4	0.23
Moore et al.[16]	2007	Gemcitabine/Placebo Gemcitabine/Erlotinib	280 282	3.6 3.8	0.004	5.9 6.2	0.038
Eckhardt et al.[38]	2009	Gem/Placebo Gem/Tipifarnib	120 124	3.0 2.3	0.4	7.4 6.7	0.66
Van Cutsem et al.[39]	2009	Gemcitabine/Erlotinib Gem/Erlotinib/ Bevacisumab	301 306	3.6 4.6	0.0002	6.0 7.1	0.2
Poplin et al.[40]	2009	Gemcitabine Gemcitabine (FDR) Gem/Oxaliplatin	275 277 272	2.6 3.5 2.7	0.09	4.9 6.2 5.7	0.15

Cunningham et al. [17]	2009	Gemcitabine Gem/Capecitabine	266 276	3.8 5.3	0.04	6.2 7.1	0.08
Ciuleanu et al.[41]	2009	Best supportive care Glufosamide	155 148	/	/	2.8 3.5	0.19
Dahan et al.[42]	2010	Gem, 5-FU/LV/Cis 5-FU/LV/Cis, Gem	100 102	3.5 3.4	0.67	8.0 6.7	0.85
Kindler et al.[43]	2010	Gemcitabine/Placebo Gemcitabine/Bevacizum	300 302	2.9 3.8	0.07	5.9 5.8	0.95
Philip et al. [44]	2010	Gemcitabine Gemcitabine/Cetuximab	371 372	3.0 3.4	0.18	5.9 6.3	0.19
Conroy et al.[19]	2011	Gemcitabine FOLFRINOX	171 171	3.3 6.4	<0.00 1	6.8 11.1	<0.001
Goncalves et al.[45]	2012	Gem/Placebo Gem/Sorafenib	52 52	5.7 3.8	0.902	9.2 8.0	0.231
Von Hoff et al.[20]	2013	Gemcitabine Gem/Nab-paclitaxel	430 431	3.7 5.5	<0.00 1	6.6 8.7	<0.001
Heinemann et al. [46]	2013	Gem/Erl, Cap Cap/Erl, Gem	143 131	3.2 2.2	0.003	6.2 6.9	0.90
Ueno et al.[18] (GEST)	2013	Gemcitabine S-1 Gem/S-1	277 280 275	4.1 3.8 5.7	ns	8.8 9.7 10.1	<0.001 (non inferiority) 0.15 (superiority)
Rougier et al.[47]	2013	Gemcitabine/Placebo Gem/Aflibercept	275 271	3.7 3.7	ns	7.8 6.5	0.2 -
Middleton et al.[48] (TeloVac)	2014	Gem/Cap Gem/Cap, GV1001 Gem/Cap/GV1001	358 350 354	6.4 4.5 6.6	 ns	7.9 6.9 8.4	 0.11 0.05
Fuchs et al.[49]	2015	Gemcitabine Gem/Ganitumab (12mg) Gem/Ganitumab (20mg)	322 318 160	3.7 3.7 3.6	 0.403 0.520	7.2 7.1 7.0	- 0.494 0.397
Deplanque et al. [50]	2015	Gemcitabine/Placebo Gem/Masitinib	178 175	/	/	7.0 7.7	Ns -
Yamaue et al.[51] (PEGASUS-PC)	2015	Gemcitabine Gemcitabine/Elpamotide	53 100	/	/	8.5 8.3	0.897 -
O'neil et al.[52]	2015	Gemcitabine Gemcitabine/Rigosertib	47 106	3.4 3.4	Ns	6.4 6.1	Ns -

Wang-Gillam et al.[53] (NAPOLI-1) *Second line	2016	5-FU/folinic acid Irinotecan Irinotecan/5-FU/Folonic acid	119 151 117	1.5 2.7 3.1	0.0001	4.2 4.9 6.1	- - 0.012
Lee et al. [54]	2017	Gemcitabine Gem/Capecitabine	106 108	5.3 6.2	0.08	7.5 10.3	0.06
Okusaka et al.[55] (GEST update)	2017	Gemcitabine S-1 Gemcitabine/S-1	277 280 275	/	/	8.8 9.7 9.9	- - <0.001(non inferiority)
Neoptolemos et al (2017). [21]	732	Gemcitabine & Capecitabine Gemcitabine	364 366	/	/	28.0 25.5	0.032

Table 1.2. Table summarising phase III trials in APC over the past twenty years.
Patient No; Number of patients in trial. PFS; Progression free survival. OS; Overall survival. Gem; Gemcitabine. Gem (FDR); Gemcitabine – Fixed dose rate. 5-FU; Fluorouracil. Marimastat; orally administered matrix metalloproteinase inhibitor. Tipifarnib; farnesyltransferase inhibitor. Pemetrexed; folate antimetabolite. Exatecan mesylate; hexacyclic, water-soluble, topoisomerase-1 inhibitor. Irinotecan; DNA replication and transcription inhibitor. 5-FU/LV/Cis; 5-fluorouracil (5FU), folinic acid and cisplatin. Sorafenib; Chemotherapy agent targeting Ras-dependent signaling and angiogenic pathways. Gem/Erl, Cap; Gemcitabine plus erlotinib followed by capecitabine. Aflibercept; Vascular endothelial growth factor (VEGF) inhibtor. MM-398; Irinotecan liposome injection. LV; leucovorin. GV1001; telomerase vaccination. Ganitumab; monoclonal antibody against insulin growth factor receptor 1. Elpamotide; vascular endothelial growth factor 2 peptide. Rigosertib; A Ras mimetic. Cetuximab; Anti-EGFR monoclonal antibody.

1.11 Immunotherapies in pancreatic cancer

Pancreatic adenocarcinoma (PAC) overexpresses multiple growth factors including epidermal growth factor (EGF), fibroblast growth factor (FGF), insulin-like growth factor (IGF), platelet derived growth factor (PDGF) and vascular endothelial growth factor (VEGF) and receptors which favour angiogenesis and proliferation[56,57]. Recent studies have investigated chemo-immunotherapy treatments that target these growth factor receptors and their downstream signaling pathways. Preclinical data have

demonstrated that the epidermal growth factor receptor (EGFR) pathway was a potential therapeutic target. Cetuximab is a monoclonal antibody against the ligand binding domain of the EGFR receptor[44]. Philip et al[44] randomised 745 patients and demonstrated no significant benefit in patients treated with gemcitabine and cetuximab versus gemcitabine monotherapy.

A telomere is a region at the end of a chromosome that protects the end of a chromosome from fusion or deterioration. Telomere instability and mutations or the shortening and up-regulation of telomerase (a reverse transcriptase enzyme that can elongate telomeres) lead to genetic instability. With telomerase up-regulated in up to 85% of human cancers this would theoretically provide a promising treatment target[58]. GV1001 is a telomerase vaccination, specifically a peptide that is recognized by the immune system that reacts by killing telomerase active cells[58]. TeloVac was a three-group, open-label, randomised phase three trial. One thousand and sixty two patients were randomly assigned chemotherapy (gemcitabine and capecitabine) alone, chemotherapy with sequential GV1001, or chemotherapy with concurrent GV1001 but disappointingly there was no benefit in overall survival in either arm treated with GV1001[48].

Ganitumab is a human monoclonal antibody against insulin growth factor receptor 1 (IGF1R). In vivo studies have demonstrated an anticancer effect of ganitumab in pancreatic cancer and that it displayed an additive effect on anti tumour activity with gemcitabine[59]. IGF1R has been shown to be overexpressed in pancreatic cancer and it is therefore another potential therapeutic target [60]. The GAMMA trial was a double blind, phase three study that randomly allocated patients to receive gemcitabine plus placebo, ganitumab 12mg/kg, or ganitumab 20mg/kg. There was no significant benefit in overall survival in either arm treated with ganitumab[49].

Masitinib is a selective oral tyrosine-kinase inhibitor and pre-clinical trials have reported that masitinib can sensitise gemcitabine–refractory pancreatic cell lines[61]. A phase two trial demonstrated promising but non-significant survival and median time to progression outcomes[62]. A randomised phase three trial of 353 patients receiving

masitinib plus gemcitabine or placebo and gemcitabine demonstrated no significant overall survival benefit[50]. Interestingly subgroup analysis demonstrated a significant median overall survival in patients who over expressed acyl-CoA oxidase-1 in their blood (OS=11.7 months, P=0.001) and in patients who had an increased baseline pain intensity threshold (OS=8 months, P=0.012).

Vascular endothelial growth factor receptor 2 (VEGFR2) is a target for tumour angiogenesis. Pancreatic cancer has been shown to express high levels of VEGF and it is dependent on angiogenesis for development[63]. Elpamotide is a VEGF2 peptide that targets VEGF expressing cells[51]. A phase one trial of 18 patients demonstrated a median overall survival of 8.7 months[64]. Yamaue et al[51] conducted a phase three trial of one hundred and fifty three patients with APC, administering gemcitabine and placebo or gemcitabine and elpamotide. There was no benefit in overall survival in patients receiving elpamotide compared to placebo (8.36 months versus 8.54 months). Rigosertib is a first-in-class Ras mimetic and small-molecule inhibitor of multiple signaling pathways[52], specifically the polio like kinase-1 and phosphatidylinositol-4,5-bisphosphate 3 kinase pathways[65]. O'Neil et al randomized one hundred and sixty patients to receive gemcitabine and rigosertib or gemcitabine only treatment[52]. The median progression free survival in both groups was 3.4 months and there was no significant difference in overall survival in both groups.

There have been some interesting results from second line treatments after patients have completed gemcitabine treatment. NAPOLI-1 is a recent multicentre phase three randomised, open label trial. It included 417 patients with metastatic pancreatic cancer who had previously been treated with gemcitabine. Irinotecan is a chemotherapy agent previously used to treat colon, rectal and lung cancer. This study examined an encapsulated form of irinotecan as a nano-liposome. They demonstrated that patients treated with nano-liposomal irinotecan in combination with 5-FU and folinic acid had an overall survival of 6.1 months compared to patients treated with 5-FU and folinic acid (4.2 months, P=0.012)[53]. However, patients treated with triple therapy experienced increased side effects of neutropenia (27%), diarrhoea (13%),

vomiting (11%) and fatigue (14%)[53] demonstrating the perennial problem with PAC treatment research.

Trial	Number of patients	Treatment	Median Overall Survival (Months)	P value
Philip et al. (2010). [44]	745	Gemcitabine Gemcitabine & Cetuximab	5.9 6.3	0.19
Middleton et al. (2007). [66]	1062	Combination Chemotherapy (Gemcitabine & Capecitabine) With sequential GV1001 With concurrent GV1001	7.9 6.9 8.4	 0.05 0.64
Fuchs et al. (2015). [49] The GAMMA trial	800	Gemcitabine & placebo Gemcitabine & ganitumab (12mg/kg) Gemcitabine & ganitumab (20mg/kg)	7.2 7.0 7.1	 0.494 0.397
Deplanque et al. (2015). [50]	353	Gemcitabine & placebo Gemcitabine & masitinib	7.1 7.7	0.695
Yamaue et al. (2015). [67]	153	Gemcitabine & placebo Gemcitabine & elpamotide	8.54 8.36	0.897
O'Neil et al. (2015). [52]	160	Gemcitabine Gemcitabine & rigosertib	6.4 6.1	ns
Wang-Gillam et al (2016).[53]	417	Nanoliposomal irinotecan & fluorouracil & folinic acid Nanoliposomal irinotecan Fluorouracil & folinic acid	6.1 4.9 4.2	0.012 0.94

Table 1.3. Key trials utilising biologic agents in pancreatic cancer treatment

1.12 APC research trials: future directions

Despite all the excitement following the development of treatments targeting potentially promising new areas these myriad trials have very disappointing outcomes. In a recent systematic review and meta-analysis of targeted therapy in APC that included twenty-seven randomised trials and 8205 patients[68], there was a significant benefit for anti-EGFR agents on overall survival (OS, P=0.011), but on pooled survival there was no OS or PFS benefit for target based therapies compared to standard treatments[68]. A recent meta-analysis of randomised phase three trials into gemcitabine mono-therapy versus gemcitabine plus additional targeted treatments (including erlotinib, cetuximab, rigosertib, elpamotide, bevacizumab, aflibercept, axitinib, masitinib and ganitumab) that included nine studies and 4564 patients[57], had very disappointing results and there was no significant heterogeneity or improvement in overall survival among the nine trials. There has clearly been a lack of meaningful breakthroughs in new treatments for APC for several decades. The high molecular and genetic heterogeneity of pancreatic cancer, its persistent chemo-resistance and the poor vascularisation of the surrounding stroma are significant factors that are responsible for the disappointing results of clinical trial. Others believe that the poor selection of patients for phase III trials, that do not demonstrated clinical meaningful benefits in survival, have been diverting patients away from earlier-stage trials[69]. There has been a 37% increase in the number of PAC trials open in the United Stated in 2014-2015 compared to 2011-2012[70]. Demand for patients far exceeds recruitment and Thota et al[71] found that of thirty randomised control trials from 1997, only 13% first line phase III trials in APC were successful, and that interestingly only 30% were predecated based on preclinical in vitro cell line data. There is a suggestion that a move to faster, smaller trials, with emphasis on targeted therapies, immunotherapies and stromal targets could provide more promising results than the last few decades of disappointing research[70].

2 Chapter Two: The Immune Network in Pancreatic Cancer

The link between inflammation and cancer was first postulated by Virchow in 1863[72] and there is clear link between increased inflammation and pancreatic cancer. Chronic inflammation is considered a major risk factor in its development and it is well documented that chronic pancreatitis can lead to the development of pancreatic cancer[73,74]. Chronic pancreatitis increases the risk of developing cancer by 10 to 20 fold[75], and there are similar inflammatory components and downstream effectors in chronic pancreatitis and pancreatic cancer suggesting some commonality of developmental pathways. Pancreatic cancer is an inflammatory process and there is a clear inflammatory component incorporated within and surrounding PAC. The tumour microenvironment in PAC has an increase in immune/inflammatory cell infiltrates[76]. Within the tumour microenvironment there is widespread dysfunction, leading to an immunosuppressive environment that causes impaired activation of the inflammatory infiltrates and ensuing processes[77,78]. The tumour microenvironment also comprises a desmoplastic reaction that drives fibrosis. Pancreatic stellate cells are the prominent cell type that drives this desmoplastic response to the inflammatory process and immune dysfunction[79]. An inflammatory stromal cuff classically surrounds pancreatic cancer and immune dysregulation drives the desmoplastic response contributing to this surrounding inflammation.

Pancreatic cancer develops with the combined interaction of disordered genetic and environmental factors. Subclinical injuries accumulate and become chronic, leading to genetic instability and mutagenesis[78]. These mutations lead to premalignant and malignant cell changes. The cancer immune-editing hypothesis was originally proposed by Burnet and Thomas[80] in 1957 (the classic cancer immune surveillance hypothesis), although it was Ehrlich in 1909 who first linked the possibility of the immune system repressing carcinomas[81]. This hypothesis proposes that these malignancies are recognised by the immune system and either eliminated, achieve dynamic equilibrium or escape[81]. Accumulation of mutations allows the immune response to become overwhelmed, and tumours subsequently acquire immune resistance. This occurs in tandem with the dysregulation of immune and inflammatory mediators, growth

factors and immune modulatory cells favouring immune suppression that results in further tumorigenesis, growth and invasion[82]. This means that any clinically detectable tumour has reduced immunogenicity and a dysregulated immune network[83]. Research supporting this comes from immunodeficient mouse models where key molecules or pathways are deficient, including perforin[84] or interferon-γ (IFγ)[85] which demonstrated that spontaneous tumours in these knockout mice were more common than in their wild type counterparts. Indeed it is well evidenced that immunocompromised patients, such as those with HIV and AIDS are significantly more susceptible to developing cancer (e.g. Lymphomas and Kaposi sarcoma).

The immune system can be broadly divided into two components, the innate and adaptive systems. Innate immunity refers to non-specific, inborn immunity while adaptive immunity refers to acquired immunity with highly specialised, specific and complex cells, pathways and processes that protect the body from pathogens. Tumorigenesis involves the failure of both the innate and adaptive immune systems, however this is a complex and dynamic process involving a multitude of intricate exchanges between the cancer and its microenvironment[86]. Cancer cells use at least three mechanisms to modulate and evade the immune system and its cells. Contact dependent factors (expression of immune system checkpoint ligands such as programmed cell death ligand-1 (PDL-1)), secretion of immunosuppressive factors (such as interleukin-10 (IL-10) and transforming growth factor-beta (TGF-β) and interference with major histocompatibility complex I (MHC1) peptide presentation[87]. There are numerous mediators involved in pancreatic cancer immune dysregulation and the important contributors are discussed below.

2.1 Cytokines and chemokines

Cytokines and chemokines are important facilitators of both the innate and adaptive immune systems. They are secreted proteins that are widely implicated in a broad range of immune processes including, immune responses, immune cell trafficking, antigen presentation and cellular activation[88]. The cytokine produced depends on the insult and in addition they can act alone or in synergy with each other and cytokines

may have different roles depending on the cellular source, target and phase of immune response they are acting in[89]. Cytokines can broadly be divided into pro-inflammatory and anti-inflammatory and a number have the potential to be both. Interleukin-6 (IL-6), interleukin-1 (IL1), and IL-10 have been shown to be dysregulated in PAC.

IL-6 has been shown to correlate with tumour stage, cachexia and survival[88] and has also been demonstrated to have use as a prognostic marker in pancreatic cancer progression[90]. IL-6 promotes PAC development by enhancing the pro-tumorigenic signalling transducer and activator of transcription 3 (STAT-3) signalling pathway, which in turn regulates transcription, anti-apoptotic and pro-proliferative genes[88]. The interleukin 1 (IL-1) family comprises IL-1α, IL-1β and IL-1 receptor agonist (IL-1ra) that have been shown to be increased in pancreatic cancer and levels correlate with survival[91]. IL-1 has been shown to promote pancreatic tumorigenesis by acting primarily through nuclear factor-κB (NKκB), a protein complex that controls DNA transcription, cytokine production and cell survival[88]. IL-10 has been demonstrated to be up regulated in PAC and demonstrated a strong correlation with tumour stage[92]. IL-10 induces an anti-inflammatory microenvironment, leading to a shift in T-helper 2 (TH2) cytokines and an altered cell function of numerous cells[88,93].

Chemokine's are a group of small chemotactic cytokines that induce direct chemotaxis in nearby cells and they are also important in inflammation and cellular migration[88]. Various chemokine's are aberrantly expressed in PAC. IL-8, a pro-inflammatory chemokine, is over expressed in PAC, and it is known that tumors with higher serum IL-8 levels grow more rapidly than those with lower levels[94]. Chemokine MCP-1/CCL-2, a monocyte chemo-attractant is aberrantly expressed and increased levels have been associated with tumour macrophage infiltration that correlates negatively with tumour cell proliferation, suggesting that the chemokine could be a relevant negative regulator of PAC progression[95]. Epithelial neutrophil-activating peptide-78 (CXCL5), a chemokine has been shown to be up regulated in PAC, and is correlated with worse tumour differentiation, advanced clinical stage and shorted patient survival[96]. In addition CXCL5 mediates tumour derived angiogenesis through the activation of several

signaling pathways including protein kinase B (Akt), extracellular signal-regulated kinase (ERK) and signal transducer and activator of transcription (STAT) in endothelial cells[96]. Chemokine ligand 17 (CXCL17) is produced early on by PAC and induces the accumulation of a potent immune cell collectively known as myeloid derived suppressor cells (MDSCs)[97]. CXCL17, produced by pancreatic stellate cells (PSCs), has also been shown to coat cancer cells and prevent T cell infiltration[98]. SMADs are a group of intracellular proteins that transduce extracellular signals from transforming growth factor beta (TGF-β) ligands to the nucleus to activate downstream gene transcription. SMAD4 is a key participant in apoptosis and its mutations have been found in up to 50% of PAC[99]. TGF-β is a key cytokine in PAC and its loss of co-ordination, in conjunction with SMAD4 mutations influence pancreatic tumorigenesis. A KRAS (V-Ki-ras2 Kirsten rat sarcoma viral oncogene homolog, an enzyme coded by the KRAS gene[100]) activated mouse model with TGF-β receptor II knockout developed aggressive PAC, with a strong expression of connective tissue growth factor (CTGF), a profibrotic and tumour–promoting factor which suggests an active tumour-stromal interaction[101]. This mouse model demonstrated increased CXCR2 chemokine's, which interestingly resulted in reduced tumour progression when treated with a CXCR2 inhibitor[101]. Cytokines and chemokine's are therefore key players in the PAC microenvironment.

2.2 Pancreatic cancer immune suppression

Pancreatic cancer involves dysregulation of both the innate and adaptive immune systems by immunosuppression and local and systemic dysfunction. There is a complex interaction of cells involved in this immune evasion (figure 2.1 and 2.2) and a change in the immune suppression as PAC progress from the pancreatic intraepithelial neoplasia (PanINs) to high grade PanINs and adenocarcinomas. There is an increase in immune cell activation and infiltrate leading to the sequential acquisition of mutations in pro-oncogene and tumour suppressor genes leading to pancreatic tumour progression[102]. Innate immune cells that stimulate cancer growth include neutrophils, M2 macrophages (tumour associated macrophages) and MDSCs, where dendritic cells and M1 macrophages inhibit growth[103]. Adaptive immune cells that stimulate cancer

growth include TH (T-helper) 2 $CD4^+$ T cells, T regulator cells (Tregs) and B lymphocytes where cytotoxic $CD8^+$ T cells, TH1 and TH17 $CD4^+$ T cells inhibit growth[103]. TH (T-helper) 2 $CD4^+$ T cells, T regulator cells (Tregs), B-lymphocytes all skew the immune response towards a T-helper 2 (TH2) response, promoting proliferation with the aid of interleukins and growth factors. Macrophages are a principal manufacturer of pro inflammatory cytokines. Tumour associated macrophages and MDSCs generate an environment rich in IL-4, IL-5, IL-6 and IL-10. This limits cytotoxic T lymphocyte (CTLs) proliferation and promotes a B cell response. T regulator cells are then recruited and secrete transforming growth factor-beta (TGF-β) further inhibiting CTLs.

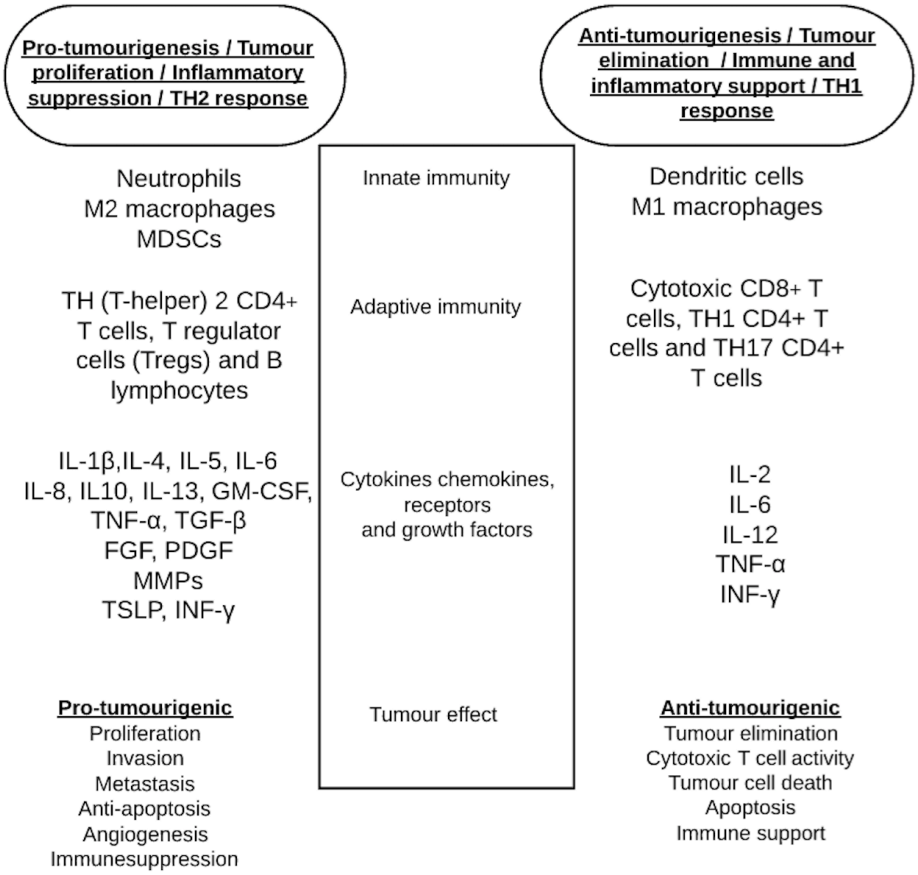

Table 2.1. Pro and anti-inflammatory cytokines that are predominantly involved in the TH1 and TH2 responses. MDSCs; Myeloid derived suppressor cells. M2 Macrophages; Type 2 or Tumour associated macrophages. M1 Macrophages; type 1 Macrophages. IL; Interleukin. GM-CSF; Granulocyte macrophage colony-stimulating factor. TNF-α; Tumour necrosis factor alpha. TGF-β; Transforming growth factor beta. FGF; fibroblast growth factor. PDGF; Platelet derived growth factor. MMPs; Matrix metalloproteinase. TSLP; Thymic stromal lymphopoietin. INF-γ; Interferon gamma.

Pancreatic cancer negatively expresses the major histocompatibility complex 1 (MCH-I)/human leukocyte antigen (HLA I) which results in a low density of tumour-infiltrating cytotoxic T cells and patients with a low number of cytotoxic cells have a poorer survival[104]. Pancreatic cancer cells also express non-functional FAS receptors allowing them to defy FAS mediated apoptosis and in addition to this they express the FAS-ligand (FAS–L), allowing them to counteract T-cells and natural killer cells (NK) by inducing apoptosis[105]. Indoleamine 2,3 dioxygenase (IDO) produced by PAC and MDSCs, catalyses the breakdown of tryptophan (TRP) to kynurenine (KYN), inhibiting T cells by limiting the amount of tryptophan available to them[106]. Pancreatic cancer, MDSCs and tumour associated macrophages all express programmed cell death ligand-1 (PDL-1) which bind programmed cell death protein-1 (PCD1), down regulating the immune system by preventing apoptosis[107]. Cytokines and growth factors are aberrantly expressed in PAC and interlukin-10 (IL-10) and transforming growth factor-beta (TGF-β) are produced by PAC, fork head FOX P3 T regulatory cells (TRegs / FOXP3) and tumour associated macrophages to suppress T cells and the immune response[93,108]. Intercellular adhesion molecule (ICAM2) is involved in facilitating the killing of PAC by $CD8^+$ T-cells, ICAM2 and is down-regulated in PAC permitting PAC immune evasion[97]. Toll-like receptors (TLR) are receptors that mediate interactions between the environmental stimuli and the immune system by triggering pro-inflammatory signaling cascades. Toll-like receptor-7 (TLR-7) is up regulated in PAC, driving stromal inflammation[109] and blockage of toll-like receptor-4 signaling results in recruitment of $CD4^+$ T-cells and increased pancreatic inflammation[109]. Pancreatic stromal cells (PSCs) are a major contributor to the PAC immunosuppressive microenvironment and produce various immune suppressive factors. In addition to CXC17, galectin-1 is produced by PSCs and promotes T-cell apoptosis[110]. Through these numerous mechanisms, cancer cells have a profound local and systemic immune modulating consequence which leads to general immune suppression and tumour progression[87]. This ongoing, dynamic and self-propagating infiltration and immune suppression contributes to the immune evasion seen in PAC.

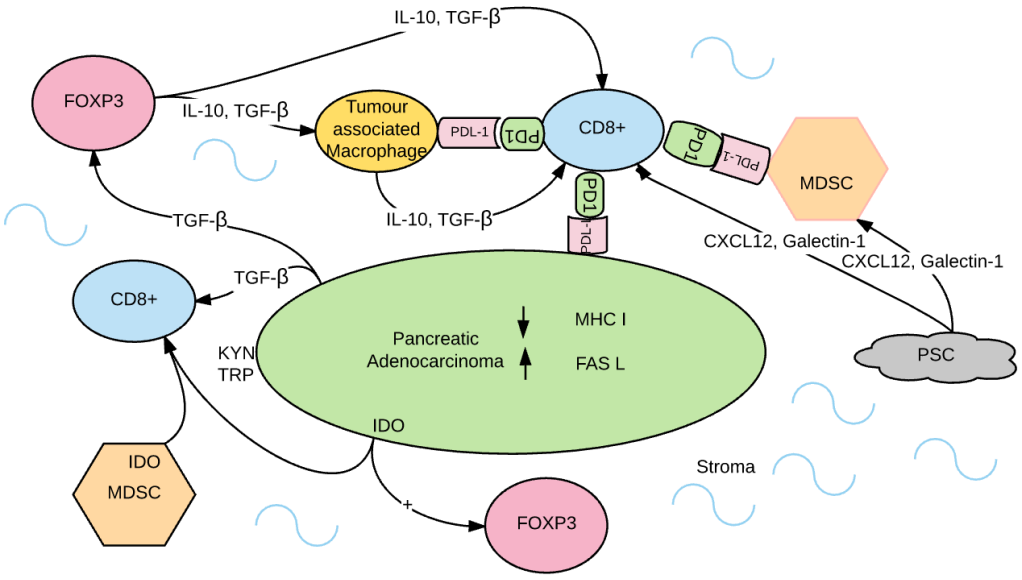

Figure 2.2. The interactions between cells in the pancreatic adenocarcinoma (PAC) microenvironment. PAC down regulates the expression of MHC-1 and over expresses the FAS ligand (FAS-L). Pancreatic adenocarcinoma and MDSCs supress $CD4^+$ and $CD8^+$ T cells with IDO which catalyses TRP to KYN. IDO has been shown to be associated with an increase FOXP3 cells. PAC inhibits FOXP3 and $CD8^+$ cells with TGF-β. FOXP3 cells inhibit $CD8^+$ cells and tumour associated macrophages by expressing IL-10 and TGF-β. Tumour associated macrophages also suppress CD8+ T cells with IL-10 and TGF-β. PAC, MDSCs and tumour associated macrophages produce PDL-1 inhibitory signal by binding to PD1 on $CD8^+$ T cells. PSC reduce $CD8^+$ T cell migration by producing CXCL12 and galectin-1. MHC-1; Major histocompatibility complex I, FAS-L; FAS ligand, PD1; Programmed cell death-1, PDL1; Programmed cell death ligand 1, TGF-β; Transforming growth factor-beta, IL; Interleukin, IDO; Indoleamine 2,3-dioxygenase, TRP; Tryptophan, KYN; Kynurenine, CXCL12; Chemokine ligand, MDSC; Myeloid derived suppressor cell, FOXP3; Foxp3 T cell / TRegs, PSC; Pancreatic stellate cell. Figure adapted from Chang et al[78].

3 Chapter Three: Myeloid Derived Suppressor Cells (MDSCs)

In the late 1970's an unknown population of cells that could induce immune tolerance were demonstrated in the bone marrows and spleens of neonatal or irradiated mice and termed natural suppressor cells (NS)[111]. These NS cells inhibited the proliferation responses of T-helper lymphocytes, antibody production by B lymphocytes and the generation of CTLs independent of antigen and MHC restriction[112]. These suppressive cells were difficult to define and various names were proposed including immature myeloid cells, myeloid suppressor cells and immature macrophages[111]. Subsequent research formally named these cells myeloid derived suppressor cells (MDSCs) reflecting their origin and function[113]. MDSCs are defined as a heterogeneous population of activated immature myeloid cells with immune suppressive functions characterised by a morphological mixture of granulocytic and monocytic cells, but they lack the expression of cell-surface markers that are specific to the fully differentiated monocytes, macrophages or dendritic cells[114]. These cells have been demonstrated to have immune suppressive functions in chronic infectious diseases, inflammation, autoimmunity, transplantation, sepsis and cancer[113,115,116]. Studies have demonstrated that in cancer they have important roles in angiogenesis, invasion and metastasis[117–119]. MDSCs are considered to be a major contributor to the overwhelming immune dysfunction in patients with sizable tumour burdens[120,121].

MDSCs arise from myeloid progenitor cells that have failed to terminally differentiate into mature granulocytes and macrophages[82]. The diverse heterogeneity of MDSCs has made their characterisation difficult. In humans MDSCs express CD11b (common myeloid marker, Mac-1) and macrophage markers such as CD14 and CD33 (common myeloid marker), or common granulocyte/neutrophil markers including CD15 (neutrophil marker, Lewis X antigen), often without exhibiting markers of terminal differentiation ($LIN1^{low/-}$)[122]. There are therefore two main subsets of MDSCs, granulocytic are predominantly $CD15^+$ and monocytic are predominantly $CD14^+$. Human MDSCs are traditionally defined as $CD14^-$, $CD11b^+$, $CD33^+$, $CD15^+$ cells or cells that express the CD33 marker but lack the expression of markers of mature myeloid

and lymphoid cells and the major histocompatibility complex (MHC) class II molecule HLADR[123,124]. The prevalence of each subset of MDSC depends on the cancer type and both monocytic and granulocytic MDSCs are present in PAC. In humans the granulocytic MDSCs represent the major subset of circulating and expanding MDSCs with approximately 75% granulocytic and 25% monocytic[125,126]. Granulocytic ($CD15^{+}$) MDSCs have been shown to be the predominant cell type in PAC[82,126–128]. In the PAC periphery granulocyte MDSCs are significantly more prevalent compared to controls [122]. There are also a subtype of MDSCs that expresses both CD14 and CD15 demonstrating the immature phenotype of MDSCs[122]. Granulocytic MDSCs express CD33, CD11b, IL-4Rα and CD15 and contain high levels of arginase[82]. Monocytic MDSCs express the same markers but predominantly express CD14 to CD15[82] and in addition to arginase, they also express inducible nitric oxide synthase (iNOS). The development and function of most MDSCs requires INF-γ[121] and both monocytic and granulocytic subtypes have been reported to be INF-γ dependent. However, INF-γ may not be crucial because MDSC from INF-γ-receptor-deficient mice are equally suppressive for T cell activation[121]. The variation in MDSC phenotype is consistent with the concept that that are a diverse family of cells in various stages of myeloid cell differentiation[121]. The specific phenotype will depend on the specific tumour type and the tumour factors secreted. Essentially this is a heterogeneous population of immature cells and results in a challenging population that no marker or combination of markers can definitely identify, and it may be that their immune suppressive activity is their defining characteristic[121].

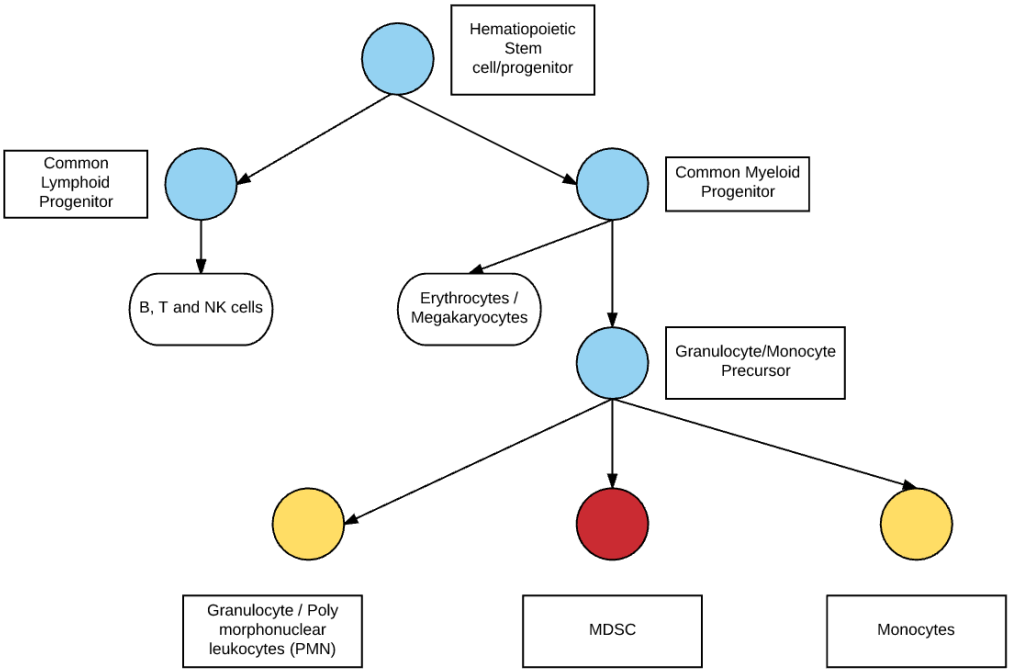

Figure 3.1. Simple schematic showing the development of mature peripheral blood cells and MDSCs from hematopoietic stem cells. Granulocyte / Monocyte precursors fail to differentiate into mature poly morphonuclear leukocytes and monocytes in a tumour bearing host and instead give rise to MDSCs that have the same markers as both poly morphonuclear leukocytes and monocytes. Figure adapted from Goedegebuure et al[122].

3.1 MDSCs in pancreatic cancer

MDSCs are significantly elevated in patients with PAC compared to healthy controls[82]. Immune suppressive cells increase in number as pancreas cancer develops and MDSCs have been shown to be increasing levels from PanIN to PAC[129] in a genetically engineered mouse model where there was a correlation between increased levels of MDSCs and decreased levels of $CD8^+$ cells. MDSCs are increased both in the circulation and the microenvironment of PAC[78,127] and their levels in the circulation also correlate with disease progression[130]. Lower levels of circulating MDSCs have been demonstrated in patients with stable PAC compared to those with progressive PAC prior to chemotherapy treatment[131], suggesting that MDSCs in peripheral blood may be a predictive biomarker of chemotherapy failure in PAC patients. Controversy still exists with the exact antibody signature of MDSCs and recent studies have investigated both a 4 and 3 antibody MDSC phenotype. Diaz-Montero et al[130] and Gabitass et al[82]

both used a 4 antibody stain to identify MDSCs: $Lin1^-$, $HLADR^-$, $CD33^+$and $CD11b^+$. Annels et al[128] utilised a 3 antibody stain comprising $Lin1^-$, $HLADR^-$, and $CD11b^+$. Khaled et al[127] recently utilised 6 antibodies ($CD14^+$, $CD15^+$, $Lin1^-$, $HLADR^-$, $CD33^+$and $CD11b^+$) to investigate a combination of MDSC subsets. They demonstrated that the amount of granulocytic MDSCs defined as $CD15^+$, $HLADR^-$, $Cd33^+$and $CD11b^+$ was significantly greater than monocytic MDSCs in the peripheral blood of patients with PAC. Bronte et al[132] recently recommended characterization standards for MDSC nomenclature and suggested a gating strategy for the identification of human MDSC subsets that included a $Lin1^-$, $HLADR^-$, $CD33^+$and $CD11b^+$ signature.

3.2 MDSCs and immune suppression in cancer

MDSCs supress both the innate and adaptive immune responses and they utilise a wide assortment of mechanisms to regulate anti-tumour immunity including the secretion of molecules and the expression of cell surface molecules. Production of harmful reactive oxidative species (ROS)[126] and peroxynitrate is particularly prominent, these molecules cause DNA mutations that contribute to genetic instability and the proliferation of malignant cells[133]. In addition they catalyse the nitration of the T cell receptor, preventing its interaction with peptide MHC complexes[134]. This renders the CD8+ cytotoxic T cells (CTLs) unresponsive to antigen specific stimulation[135]. Peroxynitrate damages proteins in a wide variety of processes in both tumour and immune cells. In addition it leads to the nitration of CCL2 chemokines inhibiting tumour-infiltrating lymphocytes trafficking into the tumour which results in the trapping of CTLs in the surrounding stroma[136]. MDSCs also reduce T cell mobility by expressing disitegrin and metalloproteinase domain 17 (ADAM) which decreased CD62 ligand expression on T cells[137]. L-arginine is an amino acid essential for the production of the T cell receptor signalling molecule zeta (TCRζ)[122]. The depletion of arginine from the tumour microenvironment is a well-documented mechanism of MDSCs[138]. Arginase 1 converts arginine into ornithine and urea, and iNOS converts arginine into nitric oxide (NO), all of which supress T cell activation and induce apoptosis[122,139]. MDSCs produce high levels of arginase 1 and iNOS, which degrade arginine and the TCRζ chain and result in the blocking of T cell activation and proliferation[140] and

prevents T cell-peptide-MHC interaction[135]. Specifically arginase 1 results in the down regulation of the surface expression of the TCRζ protein resulting in an arrest of T cells in the G0-G1 phase of the cell cycle. This phenomenon is reversible by replacing L-arginine in vitro[141] and by depleting MDSCs in vivo[142] demonstrating the importance of arginine depletion as a tool in the armament of MDSCs immune suppression. MDSCs also secrete pro-inflammatory cytokines into the immune microenvironment. For example MDSCs are activated by tumour-associated macrophages to increase production of IL-10, which down regulates IL-12[143]. TGF-β is an important immunosuppressive cytokine produced by MDSCs, which can block CTL activity and activate and expand Tregs[122]. Yan et al[144] demonstrated that MDSCs contribute to TGF-β mediated metastasis through enhancing tumour cell invasion and metastasis. They demonstrated increased levels of TGF-β in the tumour microenvironment where the tumour cells were deficient for the type II TGF-β receptor which resulted in increased C-X-C motif chemokine ligand 5 (CXCL5) which chemo-attracted CXCR2 expressing MDSCs. Cytokines including INF-γ, IL1β, TGF-β, IL-13, IL-4 in addition to NOS are known to activate the pathways of STAT1, STAT6, NFκB, STAT3 which are responsible for expansion and activation of MDSCs[120,145].

MDSCs can also promote tumour development by inducing angiogenesis[146] and by formation of distant metastasis[147]. Tumours secrete VEGF and granulocyte colony stimulating factor (G-CSF) which activate myeloid precursors in bone marrow[148]. The precursors enter the peripheral circulation and migrate to the primary tumour as well as sites of future metastases where they become activated MDSCs[122]. MDSCs participate in tumour angiogenesis through the expression of matrix metalloproteinases (MMPs)[149], which facilitate invasion and metastasis[144] and VEGF receptor 1 (VEGFR1)[150] which promote tissue neovascularisation[151]. In addition to this, some MDSCs differentiate into endothelial cells that encourage vasculogenesis[149]. The "seed and soil" hypothesis for metastasis describes a niche or microenvironment that is required for disseminating tumour cells to "seed" distant sites[152,153]. Select MDSCs migrate to distant sites where they express VEGFR1, MMP-9 and VLA-4 (very late anyigen-4 / integrin α4β1)[153], this allows them to prepare a site for the arrival of tumour cells where they can develop into metastasis[150,152,153].

3.3 MDSCs and inflammation

There is a strong correlation between inflammation and tumour initiation and progression. MDSCs are increased in inflammation and many of the factors described in inflammation also drive MDSC accumulation and activation. There is evidence that blocking inflammatory mediators and signalling pathways regulating inflammation reduces tumour incidence and delays tumour growth, and that elevated levels of pro-inflammatory mediators and cells increase tumour development[121,154]. Studies have demonstrated that pro inflammatory cytokines IL-1β, IL-6 and prostaglandin E2 (PGE_2), in addition to VEGF and G-CSF induce MDSCs[124,155–159].

Arachidonic acid (AA) is converted to PGE_2 by cyclooxygenase (COX)-2 and is a potent inflammatory mediator. PGE_2 is produced by tumours and tumour infiltrating macrophages contributing to the inflammatory microenvironment[160,161]. PGE_2 acts to expedite tumor growth through a variety of mechanisms including stimulating tumour growth and metastasis, promoting angiogenesis and protecting against apoptosis[162]. S100A8/A9 proteins are a family of pro and anti-inflammatory proteins that are calcium-binding proteins released from neutrophils and activated monocytes[163]. They chemo-attract leukocytes that produce pro-inflammatory mediators in inflammatory diseases[164] and they have been implicated in MDSCs accumulation in cancer models[165,166]. S100A8/A9 proteins block the differentiation of myeloid precursors into differentiated dendritic cells and macrophages through the signal transducer and activator of transcription 3 (STAT3) pathway[166] and in addition they chemo-attract MDSCs through a nuclear factor kappa-light-chain-enhancer of activated B cells(NFκB), that controls transcription of DNA, cytokine production and cell survival dependent pathways[167]. Interestingly MDSCs also produce S100A8/A9 proteins, enabling them to continue the accumulation of MDSCs whilst concomitantly chemo-attracting additional pro-inflammatory mediators[121]. The complement system is a key mechanism in the innate immunity to inflammation[168]. Both the classical and lectin pathways have C5 convertase (including C3a) that generates C5a from C5, both C5a and C3a are both chemo-attractants and localise to endothelial cells in tumours[168,169]. A model of C5a

receptor deficient mice demonstrated that C5a facilitates tumour progression through the binding of C5a receptors on MDSCs[170] and that this occurred through regulation of reactive oxygen and nitrogen species that resulted in MDSCs that were more suppressive for T cells.

High Mobility Group Box 1 (HMGB1) is the second most abundant protein within cells and elevated levels are associated with numerous cancers and are known to directly promote tumour growth[171]. HMBG1 can act in either a pro or anti-inflammatory manner depending on its redox state, and in inflammation reactive oxygen species (ROS) favor the anti-inflammatory state. However HMGB1 has been shown to stimulate the differentiation and expansion of MDSCs and inhibition of HMGB1 prevents the expansion of MDSCs from bone marrow progenitor cells in vitro[171]. In vivo inhibition of HMGB1 in mice reduces MDSC levels in the tumour, spleen and blood[171]. In addition HMGB1 increases pro tumour cytokine (IL-10 and IL-1β) secretion by MDSCs[172].

Mouse models have demonstrated that IL-1β induces MDSCs, tumours with higher levels of IL-1β develop significantly higher levels of MDSCs[158] and in addition IL-1β secreting tumours were more invasive and progressed longer than non IL-1β producing tumours[158,173]. MDSCs do not express IL-1 receptor but do express IL-6 receptor[174]; IL-6 is a downstream effector of IL-1β in the inflammatory response and the effects of IL-1β are likely a result of IL-6. IL-1β also heightens the cross talk between MDSCs and macrophages with IL-1β secreting tumours producing increased IL-10 and MDSCs produced from an IL-1β enriched microenvironment are down-regulators of macrophage produced IL-12[121]. These pathways are mediated through the lipopolysaccharide (LPS)- toll like receptor 4 (TLR4) pathway and MDSCs activated through this pathway demonstrate that TLR4 is critical for a MDSC mediated TH2 inflammatory response that favors tumour progression[175]. Therefore limiting inflammation, including IL-1β, can reduce MDSC immune suppressive activity, tumour growth and is a potential therapeutic strategy for inhibiting tumour inflammation.

In summary MDSCs are potent immune suppressors in cancer and they are activated by both tumour and the immune response. They are potent suppressors of both the innate and adaptive immune responses and also facilitate tumour progression, development and metastasis. MDSCs are induced by the pro inflammatory environment generated by both inflammation and cancer progression. The pro-inflammatory mediators are potential therapeutic targets that can suppress the inflammatory response and microenvironment present in pancreatic cancer. It is not known what pathway or pro-inflammatory factor induces MDSCs and equally distinguishing what pathway may be of therapeutic value. A therapeutic approach to reduce the pro-inflammatory response would be an ideal approach.

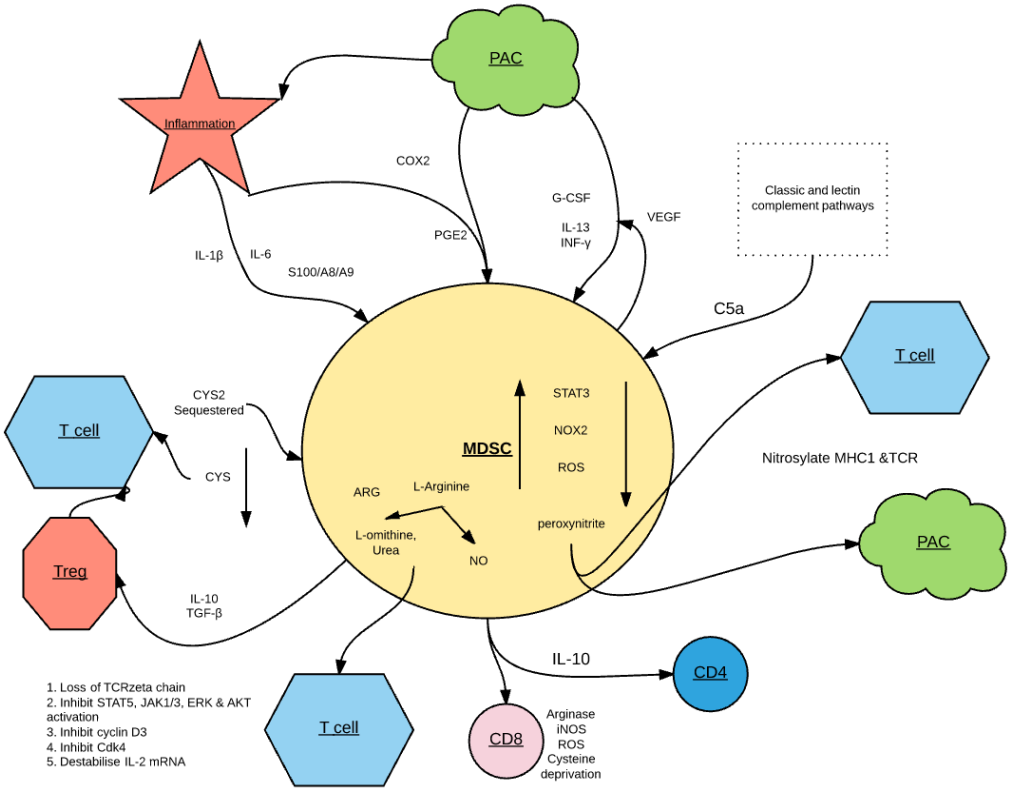

Figure 3.2. MDSC activation and effector pathways. MDSCs are sequestered and activated by pro inflammatory mediators and growth factors. Inflammation increases the production of IL-1β, IL-6, COX2, s100a8/a9 and complement component C5a. These mediators all drive MDSC accumulation by binding to their respective receptors. MDSCs do not express the IL-1β receptor and so IL-1β drives inflammation through its down-stream mediator, IL-6. Pancreatic cancer (PAC) produces COX2, PGE_2 and G-CSF which all stimulate MDSCs. MDSCs produce VEGF and S100A8/A9 which provide for autocrine cell growth regulation. Other factors such as INF-γ and IL-13 released by natural killer cells, effector T cells and MDSCs promote MDSC activation. MDSCs induce a pro-inflammatory response through various pathways. MDSCs supress T cells activation through the production of arginase, nitric oxide (NO) and reactive oxygen sepsis (ROS). L-arginine is degraded to urea, orthithine, NO and other metabolites. Arginase from MDSCs depletes T cells of arginine which has multiple actions including: down regulating the T cell receptor ζ chain that prevents T cells by proliferating by inhibiting cyclin D3 and cyclin-dependent kinase 4(CDK4). NO blocks T cell activation by destabilizing IL-2 messenger RNA (mRNA) and preventing signaling through the transcription factors janus kinase (JAK1/3), STAT5, Extra cellular signal-regulated kinases (ERK) and AKT (also known as protein kinase b) which are downstream of IL-2 receptor. MDSCs suppress T cells by sequestering cysteine (cys2) and limit the levels of cysteine (cys) available to T cells, resulting in the inhibition of their action and proliferation. T cell activation is suppressed by the production of arginase and ROS, the nitration of the T cell receptor (TCR), cysteine deprivation and the induction of Tregs.

4 Chapter Four: T cells

T cells are part of the adaptive immune system and as described can either stimulate or inhibit cancer growth. An adaptive T cell response requires antigen recognition and is comprised of both $CD4^+$ and $CD8^+$ T cells. T cells are also known as T-helper (TH) cells as they can secrete cytokines involved in the acute inflammatory response[103]. Tumours are predominantly eliminated by cytotoxic T lymphocytes (CTL), but the importance of CD4+ TH cells in enhancing or limiting CTLs has been increasingly demonstrated and understood[103]. It has been shown that pancreatic cancer patients generate B and T cells that recognise autologous pancreatic cells[176–178] and animal models have shown that mice deficient in genes associated with immunity are prone to developing cancer[179,180]. The principal immune infiltrates found in the stroma of PAC are $CD3^+$ T lymphocytes[181] and the major components of $CD3^+$ T lymphocytes are $CD4^+$ helper T (TH) cells, $CD8^+$ cytotoxic/effector T cells, and $CD4^+$, $CD25^+$, Forkhead P3 (FOXP3) T regulator cells (Tregs)[78].

4.1 $CD8^+$ cytotoxic T cells

Cytotoxic CD8+ T lymphocytes (CTL/killer T cells) are cells that can lyse target cells by recognising a specific antigen, for example a peptide produced by a tumour, presented by antigen presenting cells with the major histocompatibility complex class I (MHC-I) on their surface. CTLs are capable of eradicating tumour cells through a variety of mechanisms. An increase in CTL infiltrate has correlated with favourable clinical outcomes in pancreatic cancer[182–184] and several other cancers including oesophageal[185], colorectal[186,187], lung[188] and renal cancer[189]. $CD8^+$ T cell levels have been shown to be reduced in PAC compared to control[190,191]. Pancreatic cancer evades and diminishes cytotoxic $CD8^+$ T cells activity by a variety of mechanisms including the down regulation of adhesion molecule ligand E-cadherin[192], overexpression of TGF-β[193], promoting their aggregation in fibrous tissue away from PAC[182], down regulation of surface activation markers[182] and compromising the number and function of circulating cytotoxic $CD8^+$ T cells[194]. Pancreatic cancer cells also express PCDL1 that binds to PCD1 expressed on the surface of activated T cells and impairs their function

leading to death[195]. In addition PAC loses the expression of MHC-I that prevents $CD8^+$ T cells from employing a cytotoxic effect[104].

4.2 CD4+ T cells

Several CD4+ T cells are present in the PAC microenvironment (table2.1). CD4+ T cells activate innate immune cells and modulate the function of B cells and CD8+ T cells. Studies have shown that higher levels of tumour infiltrating CD4+ T cells correlate with favourable survival[183], however PAC, induces INF-γ and inhibits the proliferation and migration of CD4+ T cells[196]. CD4 T helper (TH) cells differentiate into TH1 and TH2 subsets of cells. TH1 cells induce cell mediated immune response via IL-2 and INF-γ where TH2 cells assist humoral immune responses by secreting IL-4, IL-5, IL-6, IL-9, IL-10 and IL-13[197]. TH2 T cells, TH2 CD4+ T cells and Tregs have profound pro tumorigenic effects and increased levels correlate with reduced prognosis and survival[198,199]. There is a TH2 immune deviation in PAC with a predominance of TH2 adaptive immune cells and cytokines[82,200]. The systemic TH1 response appears to be down regulated in response to the indirect action of several important mediators including TGF-β, IL-4, IL-10, and INF-γ[82,93]. $CD4^+$ T cells have functional plasticity and can interchange between TH2 and TH1[78]. Tassi et al demonstrated that carcinoembryonic antigen specific TH2 cells from PAC patients could be reverted to TH1 type with IL-12 and IL-27[200]. In addition Suzuki et al[197] modulated TH differentiation into TH1 rather than TH2 in patients undergoing pancreaticoduodenectomy with the pre-operative diet of supplemented omega-3 fatty acids (ω-3FAs), arginine and ribonucleotides, this diet was associated with significantly reduced infectious complications. Of all $CD4^+$ T cells the $CD4^+$, $CD25^+$, Forkhead P3 (FOXP3) T regulator cells (Tregs), that potently supresses the adaptive immune response, have gained particular interest and research.

4.3 T regulator cells (Tregs)

A population of CD4+ CD25+ T cells that prevented autoimmunity in mice was discovered by Sakaguchi et al[201] in 1995 and transformed T cell research. These T cells, now known as T regulatory cells (Tregs) are a subpopulation of $CD4^+$ T cells that have up regulated the forkhead/winged helix transcription factor Foxp3 (FOXP3) that enables them to supress inflammation and multiple immune pathways[202,203]. The FOXP3 factor is a key regulatory gene for the development and function of Tregs and may implicate a regulatory program for the development of Tregs[203]. Ectopic expression of FOXP3 in $CD4^+CD25^+$ T cells is able to confer suppressive ability[204,205]. Phenotypically Tregs are defined as $CD4^+CD25^+FOXP3^+$ cells[78,206]. Tregs include both thymus-derived natural Tregs (nTregs) and locally induced Tregs (iTregs). Naïve $CD4^+$, $CD25^-$ T cells can be converted into iTregs as a consequence of exposure to antigen in the presence of immunosuppressive conditions, including the presence of TGF-β and IL-10[207,208]. Tregs are critical for the maintenance of immune homeostasis and prevention of autoimmunity in healthy individuals, however mice with a loss of FOXP3 function die early from of autoimmunity and lymphoproliferative diseases[209]. In humans FOXP3 mutations have been shown to result in immune dysregulation, polyendocrinopathy, enteropathy and X-linked syndrome[210,211]. Although some pathways, mediators and cells are known to be responsible for inducing and maintaining Tregs in the PAC microenvironment, there is still a plethora of unanswered questions as to the exact mechanistic pathways.

Tregs are therefore important in normal immune homeostasis however their expansion results in immune suppression and dysregulation. Increased Treg levels have been reported in pancreatic cancer[212] as well as several other cancers including breast[212], gastrointestinal malignancies[213] (stomach, colon, oesophageal and liver) and hepatocellular carcinoma[214]. In addition Tregs have been shown to be increased in both the tumour microenvironment and peripheral blood[215]. Treg levels have also been shown to be increased in peripheral blood of patients with PAC with developing tumour stage[216]. An increase in T cell infiltrate, specifically Tregs has been shown to correlated with significantly reduced survival[76], more advanced presentation of

disease[206,216], a lower chance of surgical resection and a worse survival after resection[217], while a low number of Tregs in circulation one year post resection correlates with improved survival[217]. In addition levels of $CD8^+$ effector cells decrease as levels of Tregs increase[206]. Homma et al[218] demonstrated that the percentage and numbers of Tregs were significantly reduced in patients who received gemcitabine based chemotherapy compared to those who received best supportive care. This change did not correlate with a clinical response and the exact mechanism behind the Treg reduction is unknown but it has been hypothesised that may be due to the reduction of MDSCs.

4.4 Treg suppression of tumour immunity

Tregs suppress antitumour immunity, thereby facilitating tumour growth[219], and can supress both adaptive and innate immunity. The suppressive mechanism of Tregs can be divided into three categories; cell-cell contact, local competition for growth factors and local secretion for growth factors[220]. Tregs act to suppress the immune system through the expression of cytotoxic T-lymphocyte-associated protein 4 (CTLA-4), an immune checkpoint protein receptor, and the expression of TGF-β and IL-10 (figure 2.1). Tregs can also inhibit T cell production of INF-γ and IL-2 in response to tumour associated antigens[83]. Tregs use these mechanisms to suppress tumour specific CD4+ and CD8+ T cells, macrophages and natural killer (NK) cells[77,221,222]. T cells inhibit generation and expansion of the adaptive immune response, resulting in decreased frequencies of T and B effector lymphocytes[223]. Tregs suppress the proliferation of $CD4^+$ and $CD8^+$ T cells in a contact dependent manner[223] and suppression of IL-2 production by Tregs is thought to be play a key role in the suppression of CD4 proliferation[224] which also inhibits the proliferation of CD8 cells[225]. Tregs can also stimulate metastatic progression through receptor activation of nuclear factor kappa-B (RANK) signalling[226].

α-Enolase (ENO1) is an enzyme expressed on the surface of pancreatic cancer cells and able to induce a immune response, promote cell migration and cancer metastatis[227]. ENO1 specific Tregs in PAC have been demonstrated to inhibit antigen-specific effect T

cells (TH17 and TH1 T cells) and patients with low ENO1 specific Tregs/T effector ratio survived more than 10 months compared to those with a high ratio[227]. Tregs are also potent inhibitors of immune trafficking and have been shown to inhibit CD8 cell infiltration of tumours in vivo and in vitro[228,229]. In addition Tregs have also been shown to inhibit the cytolytic actions of CD8 T cells, NK cells and NK T cells[223].

PAC and Tregs interact via specific tumour chemokines that encourage Treg migration into the microenvironment. PAC up-regulates ligands for chemokine receptor type 5 (CCR5) and Tregs preferentially express CCR5[230], and when CCR5 is inhibited, Treg migration to tumours is reduced and tumours are smaller[230]. This demonstrates that blockade of Treg migration may inhibit tumour growth. TGF-β is produced by PAC and acts to induce Tregs[231], however Tregs secrete TGF-β to suppress other immune cells. In a mouse model TGF-β converted $CD4^+$, $CD25^-$ naïve T cells into Tregs and administration of neutralizing anti- TGF-β antibody blocked the induction of Tregs[231]. Tumour derived endothelial cells express higher levels of addressins, ligands to the homing receptors of lymphocytes, including mucosal adressin cell adhesion molecule-1, vascular cell adhesion molecule-1, CD62-E and CD166, than endothelial cells from normal tissues[232]. These addressins allow selective Tregs to migrate from peripheral blood to the pancreatic cancer microenvironment[232].

4.5 Treg immune therapy

It can therefore be hypothesised that modulating Treg function or decreasing the levels of Tregs in PAC may improve immune dysregulation and antitumour immunity. There have been several immune therapy studies looking at supressing Treg function. Viehl et al [233] showed that depletion of Tregs alone or in combination with an anti-CD25 monoclonal antibody promoted a tumour-specific immune response in a mouse model resulting in smaller pancreatic tumours and longer survival. Aida et al[234] recently demonstrated that administration of an anti-glucocorticoid induced TNF receptor monoclonal antibody suppressed Treg infiltration in PAC with down regulation of CCR5 leading to an enhanced antitumour immunity of INF-α gene therapy in a murine pancreas cancer model. Ipilimumab is an anti-CTLA-4 monoclonal antibody

that blocks CTLA-4, which produces an inhibitory signal on target tissues and antigen-presenting cells, and acts to reduce this inhibitory signal and induce apoptosis of Tregs[78]. A phase II trial using single agent Ipilimumab in APC demonstrated disappointing results with no responses to treatment[235]. Another approach that had been investigated involved targeting the PD1 receptor on activated T cells. PDL-1 ligands are also expressed on MDSCs and tumour infiltrating lymphocytes. Brahmer et al[236] demonstrated that blocking the PD1 with anti PD1 (MX-1106) was well tolerated with disease stabilisation and tumour regression seen. Interestingly there was a sustained mean occupancy of greater than 70% of PD1 molecules on circulating T cells seen at over 2 months following treatment.

Denileukin toxin, comprised of IL-2 and diphtheria toxin, is a drug that selectively kills cells that express the high affinity IL-2 receptor and its effect on depleting CD4+, CD25+ cells is currently being investigated[223]. Two anti-human IL-2 receptor antibodies, daclizumab and basiliximab, that block the binding of IL-2 to its receptor, have been approved for clinical use[223]. Data has shown that basiliximab does not affect the suppressive activity of CD4+, CD25+ cells in vitro[237], however daclizumab may alter FOXP3 expression in Treg cells both in vitro and in vivo[238]. The best Treg blockage medication currently available is cyclophosphamide and fludarabine, which have been shown to inhibit the function and number of CD4+, CD25+ Treg cells[239,240]. Although suppression and depletion of Tregs remains an interesting research avenue, more studies are required to fully explore the therapeutic potential.

4.6 T cells, Tregs and MDSC crosstalk

MDSCs have been implicated in the recruitment and maintenance of Tregs[129,205,241] and are significantly elevated in patients with PAC with levels correlating with Treg levels[78]. MDSCs supress T cells through a variety of mechanisms such as the use of reactive oxygen species (ROS), depletion of L-arginine, free radical peroxynitrate and down regulation of L-selectin[242–244]. MDSCs use arginase to catabolise L-arginine and therefore express high levels of arginase-depleted L-arginine in the tumour environment. MDSCs down regulate L-selectin levels on T cells, a plasma membrane

molecule necessary for the homing of naïve T cells to lymph nodes, which decreases their ability to home to sites where they could be activated[244].

Cysteine is an essential amino acid for T cell activation. T cells are dependent on antigen presenting cells (APCs) to export cysteine as they lack cystathionase, which converts methionine to cystine[245]. MDSCs sequester cysteine, limiting its availability and depriving T cells of the cysteine they require to synthesise the necessary proteins for activation and function[245]. In addition MDSCs suppress $CD8^+$ cell response by producing ROS through their interaction with antigen-specific T cells[125]. MDSCs also produce free radical peroxynitrate that can inhibit the binding of processed tumour peptides to tumour associated MHC molecules thereby mediating tumour resistance to cytotoxic T cells[246]. In the tumour microenvironment MDSCs equally suppress $CD4^+$ and $CD8^+$ T cells, and expand immunosuppressive Tregs[78]. MDSCs from tumour bearing mice have been reported to impair T cell function through a variety of mechanisms including inhibiting antigen-specific responses mediated by T cells[247], down regulation of the T cell receptor ζ chain, a key component of T cell receptor (TCR) signaling[248] and by eliciting apoptosis in T cells[83]. MDSCs can induce the development of Tregs [205], mouse studies in vivo suggest that MDSCs support the de novo development of Tregs through TGF-β dependent[205] and independent[249,250] pathways.

In a colon cancer mouse model, Huang et al[205] demonstrated INF-γ activated MDSCs increased IL-10 and TGF-β to mediate the development of tumour induced $CD4^+$, $CD25^+$ Tregs, however this study did not demonstrate the activation of FOXP3 Tregs. They also demonstrated that MDSC in mice can induce the development of Tregs in vitro and that it is regulated by INF-γ and IL-10. In an A20 B-cell lymphoma model, Serafini et al[249] showed that MDSCs acted as tolerogenic antigen presenting cells capable of antigen uptake and presentation to tumour specific Tregs and that inhibition of MDSC function abrogates Treg proliferation and tumour induced tolerance in antigen specific T cells. In an ovarian cancer mouse model Yang et al[251] reported that suppression of MDSCs was dependent on the presence of CD80 on MDSCs and involved $CD4^+$, $CD25^+$ Tregs, suggesting a relationship between MDSCs and Tregs. MDSCs and Tregs are therefore key contributors to the immune suppression

that occurs in the pancreatic microenvironment. Their intimate interaction involves the production and suppression of signaling molecules, ligands and receptors in a complex inflammatory cauldron that is the tumour microenvironment. Ultimately they are both masters and slaves to a stimulating and perpetuating tumour microenvironment. Targeting these cells has been proven difficult and reducing their number does have real theoretical benefit.

5 Chapter Five: Endothelial Progenitor Cells (EPCs)

Vasculogenesis is defined as "the differentiation of precursor cells (angioblasts) into endothelial cells and the de novo formation of a primitive vascular network". It is the process by which blood vessels are formed de novo and angiogenesis is the expansion and remodelling of the existing blood vessel network[252]. The process of angiogenesis is regulated by multiple pro and anti angiogenic mediators and growth factors including VEGF and FGF. The imbalance of these anti and pro angiogenic factors activates an "angiogenic switch"[253], and involves a wide variety of participating cells. Tumours can form vessels by "high jacking" neighbouring pre-existing vessels[254], however there is increasing evidence that vasculogenesis, through which bone marrow derived hematopoietic stem cells and endothelial progenitors home in to tumour sites[255], plays an important role. Cancer progression requires new vessel formation to deliver oxygen, nutrients and growth factors and tumours are therefore key promoters of vasculogenesis and angiogenesis. Tumours like PAC have a hypoxic environment and circulating endothelial cells (CECs) and bone marrow endothelial progenitor cells (EPCs) are mobilised in response to the tissue hypoxia where they promote angiogenesis. Studies have shown that EPCs have the ability to form colonies in vitro, demonstrating their involvement and role in angiogenesis[256], the maintenance of existing vascular structures[257] and tumour vasculogenesis[258].

In 1997 Asahara and colleagues isolated $CD34^+$ hematopoietic cells from human peripheral blood [259,260] which launched further studies looking for an endothelial progenitor cell. Piechev et al[261] incorporated CD133 and VEGFR-2 to distinguish circulating endothelial progenitors (CECs) from mature endothelial cells. However as the markers identifying EPCs are also expressed on CECs, identifying specific markers has been difficult and studies have demonstrated that defining the exact phenotypic identification is challenging (table 5.1). EPCs are a subtype of stem cells with a high proliferative potential that are capable of differentiating into mature endothelial cells and contributing to neovascularization[252,261]. EPCs have the ability to migrate, colonise, proliferate and ultimately, differentiate into endothelial lineage cells[262]. In patients

following a myocardial infarction, circulating EPCs have been shown to induce vasculogenesis and angiogenesis at the site of injury[263], suggesting an ischaemia driven mobilisation to these sites. EPCs are mainly found in the bone marrow of adults but are also present in peripheral blood in a state of transformation and can be considered to be in a developmental continuum. There are two types of EPCs, pro-angiogenic hematopoietic cells (early EPCs) and outgrowing endothelial cells (late EPCs)[259,264]. Early EPCs, located predominantly in the bone marrow are characterised by the cell markers CD133, CD34 and VEGF receptor 2. As they enter the circulation they start to loose CD133/CD34 and start to express CD31, vascular endothelial cadherin and Von Willebrand factor[265]. EPC recruitment and mobilisation has been shown to correlate with increased levels of angiogenic growth factors including VEGF[266]. Indeed, Willett et al[267] demonstrated that the VEGF specific antibody bevacizumab decreases CEC and EPC levels in rectal carcinoma patients. VEGF is responsible for the proliferation, differentiation and chemotaxis of EPCs[262,268] and is released from tumour cells, macrophages and platelets[269]. Other mediators and growth factors stimulating EPC recruitment include FGF, angiopoietin-1, stromal derived factor-1 and placental growth factor[270–272].

5.1 EPCs in cancer

The “cancer stem cell” hypothesis is a proposed model that attempts to explain the heterogeneity in solid tumours[273]. It proposes a hierarchical organisation of tumours, in which a subpopulation of stem cell-like cells sustains tumour growth, metastasis and resistance to therapy. Therefore, with the proposed importance of these cells research into their specific elimination and manipulation becomes clinically relevant. There is wide variety of stem and progenitor cells involved in tumorigenesis of pancreatic cancer including cancer stem cells, haematopoietic stem cells, very small embryonic/epiblast-like stem cells and endothelial stem/progenitor cells[274]. The possible mechanism(s) for the increase in EPCs in cancer may include the generalised activation of the endothelium, localised endothelial damage or an elevation in stimulating growth factors and mediators mobilising precursor cells[254]. In addition, pancreatic cancer is notoriously hypoxic with an inflammatory stromal cuff that results

in tumour release of mediators that result in EPC recruitment. However the mobilisation, recruitment and incorporation of EPCs into tumours is a complex and multifactorial process that involves the participation of numerous mediators and cells in the tumour microenvironment[255] and the details of the mechanisms are yet to be fully elucidated.

CECs and EPCs have been shown to be elevated in a variety of cancers (table 5.1), and there is a clear increase in EPC number in peripheral blood with increased tumour burden[275]. Beerepoot et al[276] found a significant rise of CECs in patients with progressive cancer but patients with stable disease had levels equal to those in healthy subjects. Vizio et al[254] demonstrated that levels of CECs and EPCs were between 10 and 26 times higher in APC patients compered to healthy controls[254]. They further demonstrated that increased EPC levels were significantly correlated with an increased TMN stage, a deteriorating prognosis and a poorer overall survival[254]. In addition Ko et al[277] also demonstrated that the baseline EPC concentration was inversely associated with overall survival in patients treated with bevacizumab plus erlotinib for gemcitabine refractory APC. There have not been many studies into the effect of chemotherapy regimens on EPCs in APC although there have been studies in other cancers. In immunodeficient mice bearing human lymphoma cells, Bertolini et al[278] demonstrated that the frequent administration of cyclophosphamide at low doses suppressed EPC numbers and viability with concurrent inhibition of tumour growth which may be a result of the anti-vasculogenic effect from reduced EPC mobilisation. A phase II study administering celecoxib and low dose cyclophosphamide in patients with non-Hodgkin's lymphoma demonstrated that EPCs declined and remained low in responders[279]. Additional studies in lymphoma administering endostatin, a naturally occurring anti-angiogenic agent derived from type XVIII collagen, compared to chemotherapy resulted in greater inhibition of EPCs, bone marrow neovascularisation and increased tumour suppression[280,281]. Several studies have demonstrated no significant rise in EPCs in human cancers, including lymphoma, breast cancer[282] and gastric cancer[283] although VEGF levels were elevated. It may be that VEGF and other mediator levels in these cancers are not sufficiently elevated to stimulate EPC production and recruitment. Within cancer, EPCs are incorporated into the neo-

endothelium and contribute to tumour vessel formation[284] and tumour growth[285]. EPCs have been shown to play an important role in the growth of tumours at both an early and late stage[286] although their exact role as either markers of altered vascular integrity or direct contributors to the neoplastic process remains unclear [262]. It is also not known if their increase is the result of a systemic endothelial activation in response to the cancer, a result of endothelial shedding, a response to cytotoxic chemotherapy or due to tumour induced mediators and growth factors. Gemcitabine treatment has been shown to affect VEGF-A and circulating CECs but not EPCs[254]. It is believed that EPCs may play an important role in tumour resistance, neo angiogenesis and also in facilitating metastasis by providing both instructive (release of pro angiogenic cytokines) and structural (vessel formation, incorporation and stabilisation) functions[254]. Pancreatic cancer is often diagnosed at an advanced stage and as previously discussed is highly resistant to chemotherapy treatment. As a therapeutic tool EPCs can potentially be used as a marker of anti-angiogenesis therapy, tumour burden and growth and angiogenesis. In addition EPCs may offer a marker to predict response to therapy, metastasis or recurrence. This potential make EPCs an interesting research aspect, particularly in APC.

5.2 EPC measurement

EPCs are rare cells and make up between 0.01% and 0.001% of mononuclear cells in normal peripheral blood[287]. The number of circulating $CD34^+$ positive cells is around 50-100/million WBC (0.005-0.001%), equal to about 350-700 cells per mL[259]. There are also some reports of co-expression of CD133 which could increase the specificity for EPCs as it is not expressed on mature endothelial cells[259,288]. This co-expression of CD34 and CD133 cells in peripheral blood is even lower and makes quantification more difficult and in an attempt to compensate for this researchers acquire large numbers of cells or events. Strict criteria for the separation of cells, tittering of antibodies, use of high-end flow cytometry machines and methods are essential. The lack of agreement on phenotypic identification and lack of methodological consensus compounds the variability in published literature. As a consequence there is wide variability in reported phenotypic subtypes that include a variety of markers (table

5.1). There are also inconsistencies in the reporting of results, with some studies reporting EPCs for a sample volume and EPCs for a defined number of mononuclear cells[289].

Study	Pathology	Subjects	Antibody					
			CD45-	CD31+	CD133+	CD34+	CD146-	VEGFR2
Vizio et al (2010)[254]	PAC	Human	Y	Y	Y	Y		
Sakamori et al (2012)[290]	NSCLC	Human	Y	Y	Y	Y		
Morita et al (2011)[291]	NSCLC	Human	Y	Y	Y	Y		
Steurer et al (2008)[292]	NSCLC	Human	Y	Y	Y	Y		
Roodhard et al (2010)[293]	Various*	Human	Y	Y	Y			
Li et al (2011)[294]	PAC	Mouse			Y	Y	Y	
Staringer et al (2011)[295]	PAC	Human	Y	Y			Y	
Kuo et al (2012)	Breast	Human	Y	Y	Y		Y	
Lin et al (2013)[296]	Rectal cancer	Human	Y	Y	Y			Y
Fuereder et al (2014)[297]	Prostate cancer	Human	Y	Y	Y		Y	
DuBois et al (2012)[298]	Osteosarcoma	Human	Y	Y	Y		Y	
Corsini et al (2012)[299]	Glioma	Human	Y		Y	Y		

Kim et al (2013)[300]	Gynaecological cancers	Human	Y		Y	Y		Y
Bhatt et al (2011)[301]	Renal cell carcinoma	Human	Y		Y	Y	Y	
Ha et al (2013)[302]	Gastric cancer	Human			Y	Y		
Marlicz et al (2016)[303]	Colorectal cancer	Human	Y		Y	Y		Y
Starzynske et al (2013)[274]	PAC	Human	Y	Y		Y		Y
Ko et al (2010)[277]	PAC	Human	Y	Y		Y		
Steurer et al (2008)[292]	NSCLC	Human	Y	Y		Y		Y
Shim et al (2015)[304]	Myocardial infarction	Human	Y	Y		Y	Y	
Mancuso et al (2011)	Breast cancer	Human	Y	Y		Y		

Table 5.1. Antibody phenotypes and characteristics from select studies. There is wide discrepancy in the antibody phenotypes used to identify EPCs. In PAC the antibody phenotype of $CD45^-$, $CD31^+$, $CD34^+$ & $CD133^{+254}$ and $CD45^-$, $CD31^+$ and $CD34^{+274,277}$. However the phenotype of $CD45^-$, $CD34^+$ & $CD133^+$ has been investigated in various other cancers as shown above. NSCLC: Non-small cell lung cancer. VEGFR2: Vascular endothelial growth factor receptor 2. PAC: Pancreatic adenocarcinoma. Various*: Cancers studied include breast, colorectal, ovarian, oesophagus, prostate, head and neck, sarcoma, cervical and others not described. CD45: A hematopoietic marker also known as the Leukocyte Common Antigen which is present on all human leucocytes, including lymphocytes, monocytes, granulocytes, eosinophils and thymocytes. It is absent from erythrocytes, platelets or mature erythroid cells of bone marrow and non-haemopoietic tissues. CD31: An endothelial cell marker also known as PECAM-1 (Platelet And Endothelial Cell Adhesion Molecule 1), It is implicated in angiogenesis [305], vascular wound healing and trans-endothelial migration of leukocytes in inflammatory processes. It is widely expressed on endothelial cells as well as platelets, monocytes and granulocytes. CD34: An endothelial cell marker also known as the hematopoietic progenitor cell antigen, it is expressed on hematopoietic progenitor cells, vascular endothelium and some tissue fibroblasts. CD133: An early hematopoietic stem cell marker, CD133 is expressed on circulating endothelial progenitor cells[261,288]. In the

hematopoietic system, CD133 expression is restricted to a subset of CD34 ^{bright} stem and progenitor cells in human foetal liver, bone marrow, cord blood and peripheral blood [306]. CD146: Also known as melanoma cell adhesion molecule or MCAM it belongs to the immunoglobulin superfamily. It is expressed in epithelial cells, activated T cells, endothelial cells and multipotent mesenchymal stromal cells[307]. VEGFR-2: An endothelial marker.

6 Chapter Six: Micro RNA (miRNA)

Micro RNAs (miRNAs, micro ribonucleic acids) are a group of single stranded, short (19-25) ribonucleotides. They are non-coding RNA transcripts that regulate gene expression by affecting the translation of messenger RNA (mRNA). MiRNAs function is to stabilise mRNA transcripts via post-transcriptional gene silencing through inhibition of the translational process or cleavage of their target mRNAs[308,309]. They represent approximately 1-3% of the human genome but are thought to be involved in the regulation expression at the post transcriptional level, of approximately 30% of all protein coding genes in mammals[310]. The international miRNA database has over 2588 distinct miRNAs listed for the human genome as of May 2017. MicroRNAs are formed and processed in the nucleus of the cell and released via small membrane vesicles known as exosomes, these exosomes transport circulating miRNA in human plasma thereby allowing miRNA to exist and function in peripheral blood. MiRNA can be isolated from plasma by isolating these exosomes and further amplification and quantification using real time PCR and microarray methods are used to identify and quantify these miRNAs.

The generation of miRNAs is a multistep process and initially miRNAs are transcribed into a longer transcript (pri-miRNA) of several kilobases in length by RNA polymerase II[311]. This transcript has a 5' 7-methyl guanylate (m7G) cap and a 3' poly (A) tail[312]. Mature RNA is produced as a result of two endonuclease reactions, the first in the nucleus by Drosha/DGCR8, a ribonuclease III endonuclease that cleaves the pri-miRNA. This is then transported to the cytoplasm where the pre-miRNA is processed to generate a mature 17-25 base pair RNA duplex by ribonuclease III endonuclease (Dicer/TRBP and argonaute (AGO2))[311]. The RNA duplex unwinds with helicase activity and a mature single stranded miRNA and enters into the RNA-induced silencing complex (RISC) and with the help of AGO protein it is directed to target mRNA[313]. This mature miRNA can then hybridise with it's "target mRNA" with either imperfect or perfect complementarity. Imperfect complementarity leads to translational repression,

while binding with high complementarity leads to either cleavage or degradation of the target mRNA[313].

MiRNAs are involved in a wide range of crucial biological processes, including development, differentiation, apoptosis and proliferation[314]. They were first identified in 1993 in a study into the development of C.elegans and miRNAs they were subsequently first associated with cancer following a genetic study into chronic lymphocytic leukaemia[315]. Increasing evidence demonstrates that the altered expression of miRNAs can be demonstrated in various cancers and may be associated with cancer pathogenesis, apoptosis and cell growth[311]. Studies have shown that while some miRNAs accompany tumour promotion and carcinogenesis (oncogenes) others inhibit tumours by reducing cell proliferation, survival and cellular differentiation (tumour suppressor)[316,317]. Aberrant expression of miRNAs has been described in almost all human cancers and evidence suggests that abnormally expressed miRNAs have a causative role in tumurogenesis[310]. MiRNAs are very stable in tissue, plasma and other fluids and can be quantified in extremely small samples making them an excellent marker (diagnostic, response to treatment or prognostic)[308].

6.1 Micro RNA and pancreatic cancer

Cancer cells often express mRNA isoforms in substantial amounts with shorter 3' untranslated regions (UTRs) and polyadenylation[318]. These shorter transcripts produce substantially more protein than their full-length counterparts, in part through escape of miRNA-mediated targeting[313] and this mechanism of oncogene activation directly links miRNAs to cancer risk[313]. MiRNAs have been shown to correlate with tumour location, the mutation status of several oncogenes/tumour suppressor genes and cancer disease stages[313].

Expression profiling studies have demonstrated deregulation of a number of miRNA expressions in pancreatic cancer[310,319–321]. These profiles have been examined in the hope that they may represent useful markers aiding the differentiation of pancreatic cancer from other tumours and chronic pancreatitis[322]. A number of studies have

demonstrated that eight up-regulated and down-regulated miRNAs can differentiate the pancreatic cancer from chronic pancreatitis with 93% accuracy[311]. Differentially expressed miRNAs have been shown to be involved in the malignant transformation of pancreatic cancer and six of the most widely studied miRNAs are discussed below.

Micro RNA-21 has been shown to be an oncogenic miRNA and high expression has been reported in numerous cancers including colon[323], breast[324] and pancreas[325–327]. Micro RNA-21 is expressed at high levels in pancreatic cancer, and through an inhibitory mechanism and negative expression of tumour suppressor and programmed cell death proteins, there is an inhibition of apoptosis and facilitation of invasive potential in progressively malignant transforming cells[311]. In addition miRNA-21 has been shown to contribute to the cell proliferation, invasion, and chemo resistance of pancreatic cancer[325]. MiRNA-21 has been shown to predict survival in patients with node-negative disease and may be an important biologic marker for outcome[326] and over expression of miRNA-21 has also been shown to be predictive of a poorer outcome in patients with PAC[326]. MiRNA-21 has been demonstrated to negatively regulate the expression of phosphatase and tensin homolog (PTEN), programmed cell death 4 protein, and tissue inhibitor of metalloproteinase 3 proteins, leading to inhibition of apoptosis as well as facilitating PACs invasive potential in cells[311].

Park et al[328] demonstrated that over expression of miRNA-21 and miRNA-221 enhances the malignant phenotype of pancreatic cancer cells and inhibition of these miRNAs using antisense oligonucleotides revealed decreased proliferation and increased apoptosis. In addition antisense to miRNA-21 and miRNA-221 sensitised tumours to the effects of gemcitabine, and the antisense-gemcitabine combinations were synergistic. MiRNA-21 may play a role in the gemcitabine resistance seen in PAC and miRNA-21 has been shown to significantly reduce the anti-proliferative effects of gemcitabine and reduce cell apoptosis[329] in a cell model. In addition gemcitabine exposure in cells transfected with anti-miRNA-21 significantly increased the apoptotic index up to 39%[329].

Micro RNA-146a is primarily involved in the regulation of inflammation and other processes that function in the innate immune system. MiRNA-146a has been shown to have a lower expression in PAC cells compared to normal pancreatic ductal epithelial cells[330,331]. Li et al (2010)[330] demonstrated that re-expression of miRNA-146a inhibits the invasive capacity of PAC cells with concomitant down regulation of EGFR and the NFκB regulatory kinase interleukin 1 receptor-associated kinase 1. MiRNA-196a, together with miRNA-217, has been shown to discriminate normal pancreas, chronic pancreatitis and cancerous tissue[332]. The expression of miRNA-196a has been shown to be specific to PAC cells and its expression parallels disease progression[322]. In addition overexpression of miRNA-196a has been shown to predict poor survival in PAC[333]. MiRNA-155 has been shown to be overexpressed in PAC[333] and over expression has been observed in PanIN, the most common non-invasive precursor to PAC[334], demonstrating early deregulation in PAC development. Furthermore miRNA-155 has been shown to down regulate tumour protein 53 (TP53) induced nuclear protein 1 gene accelerating pancreatic cancer development[335]. Elevated expression of miRNA-155 and miRNA-196a has been observed with the parallel progression of PAC in plasma samples[311]. In addition elevated levels of miRNA-155 and miRNA-210 expression in PAC have been shown to be significantly associated with a 6.2-fold increase risk of death compared to patients with tumours demonstrating reduced expression[336].

MiRNA-221 is significantly over expressed in PAC compared to normal pancreatic tissue[337] and high plasma concentrations have a significant correlation with distant metastasis and non-resectable status. MiRNA-21, miRNA-210 and miRNA-221 have been shown to play a role in regulating angiogenesis. MiRNA-221 has been demonstrated to block angiogenesis[338], whereas miRNA-210 has been shown to be promote angiogenesis[339]. PAC is characterised by an extremely hypoxic micro environment and miRNA-210 has been shown to be significantly increased in PAC compared to controls[340] and in addition miRNA-210 has been shown to be up-regulated in response to hypoxia[339]. In endothelial cells miRNA-210 expression is increased in response to hypoxia and leads to up-regulation of several angiogenic factors, inhibition of caspase activity and prevention of cell apoptosis[341]. Furthermore, miRNA-210 regulates the interaction between PAC cells and stellate cells, promoting

the progression of chemo resistance of cancer cells[342]. MiRNA-221 blocks angiogenesis by down regulating zinc finger E-box-binding homeobox 2 protein (ZEB2)[343], which usually modulates epithelial-mesenchymal transition[344]. This down regulation of ZEB2 leads to decreased angiogenesis through the inhibition of NFκB[345] by maintaining endothelial cells in G0/G1 cell cycle arrest. Hundreds of miRNA have been profiled in pancreatic cancer but to date none have been studied in peripheral blood samples of patients undergoing chemotherapy and intravenous ω-3 treatment and dysregulation of the six miRNAs discussed (miRNA-21, 146a, 155, 196a, 210 and 221) are examined in this study.

Micro RNA	Expression profile	Role	Study
21	Up	• Proliferation, invasion and chemoresistance • Diagnostic • Survival • Deregulated	Moriyama et al[325] Bloomston et al[333], Wang et al[346] Dillhoff et al[326], Liu et al[347], Giovannetti et al[329] Lee et al[319], Bloomston et al[333], Zhang et al[320]
146a	Up/Down	• Deregulated	Szafranska et al[332], Bloomston et al[333]
155	Up	• Survival • Diagnostic • Deregulated	Greither et al[336] Bloomston et al[333], Wang et al[346], Ryu et al[334] Lee et al[319], Bloomston et al[333], Zhang et al[320], Szafranska et al[332]
196a	Up	• Diagnosis • Survival • Deregulated	Szafranska et al[332] Wang et al[346] Bloomston et al[333] Zhang et al[320], Szafranska et al[332]
210	Up	• Survival • Diagnosis • Deregulated	Greither et al[336] Wang et al[346] Ho et al[340] Bloomston et al[333], Zhang et al[320], Szafranska et al[332]
221	Up	• Diagnostic • Metastasis • Deregulated	Bloomston et al[333] Kawaguchi et al[337] Lee et al[319], Bloomston et al[333], Zhang et al[320], Szafranska et al[332]

Table 6.1. Common miRNAs deregulated in PAC.

6.2 Micro RNAs and MDSCs

MiRNAs can both enhance and inhibit MDSC accumulation and suppressive potency[171]. MiRNAs contribute to normal and dysregulated myelopoiesis and alterations in myelopoiesis underlie MDSC expansion, with recent studies implicating miRNAs in MDSC expansion[348]. Several miRNAs have been implicated in MDSC accumulation and function including miRNA-17-5p, miRNA-20a, miRNA-21, miRNA-101, miRNA-155, miRNA-223 and miRNA-690[349]. MiRNA-146a has been shown to prevent inflammation, MDSC proliferation and oncogenic transformation[350]. MiRNA-155 and miRNA-21 facilitate the accumulation of MDSCs by activating STAT3, which contributes to MDSC accumulation and suppressive potency[351]. Furthermore miRNA-155 plays an important role in immunosuppression and tumour promotion. Chen et al[352] demonstrated that genetic ablation of miRNA-155 renders mice resistant to chemical carcinogenesis and the growth of several transplanted tumours. MiRNA-155 acts to increase MDSCs and therefore facilitate tumour growth. MiRNA-155 may also be required for MDSC-dependent tumour angiogenesis as miRNA-155 deficient MDSCs produce decreased levels of MMP-9 and VEGF[349]. MDSCs are not only stimulated by miRNAs they also use miRNAs to influence cancer growth. Cui et al[353] demonstrated that MDSCs in patients with ovarian cancer, triggered miRNA-101 expression. MiRNA-101 subsequently repressed the co-repressor gene C-terminal binding protein-2 which directly targeted stem cell core genes resulting in increased cancer “stemness” and increasing metastatic and tumorigenic potential[353]. MDSC targeted therapy is an important avenue in cancer research and targeting miRNAs may offer an alternative therapeutic strategy.

7 Chapter Seven: Omega 3 Fatty Acids (ω-3FAs)

The first evidence that fish oil may benefit health derived from epidemiological data that demonstrated Greenland Inuits (who consumed large amounts of oily fish, containing a high quantity of ω-3FAs) had a lower incidence of diseases such as asthma, psoriasis, diabetes and myocardial infarction than a matched population[354]. In saturated fatty acids, all of the carbons are connected by single bonds, whereas unsaturated fatty acids have some carbons connected by double bonds[355]. ω-3FAs have the first double bond 3 carbons from the methyl end and omega 6 fatty acids (ω-6FAs) have the first double bond 6 carbons from the methyl end. ω-3FAs are not synthesised in meaningful quantities by human metabolism, and are effectively only available from dietary intake, mainly from oily fish, vegetable oil, soybean oil and green leafy vegetables making them essential fatty acids. Oily fish have a particularly high concentration of ω-3FAs. The principle constituents in ω-3FAs are eicosapentaenoic acid (EPA, C20:5 n-3) and docosahexaenoic acid (DHA, C22:6 n-3). ω-3 is a structural descriptor for a family of polyunsaturated fatty acids (PUFA)[356]. The simplest ω-3FA is α-linoleic acid (C18:3 n-3) which is synthesized from linoleic acid by desaturation, catalysed by Δ-5 desaturase[357], humans do not possess this enzyme making α-linoleic acid an essential fatty acid. Humans can metabolise α-linoleic acid to steridonic acid (C18:4 n-3) by Δ-6 desaturase[357], which can then be elongated to eicosatetraenoic acid (C20:4 n-3). Eicosatetraenoic acid can then be converted to eicosapentaenoic acid (EPA, C20:5 n-3) by Δ-5 desaturase. Eicosapentaenoic acid (EPA, C20:5 n-3) can then be converted to docosahexanoic acid (DHA, C22:6 n-3) by elongase and Δ-6 desaturase, although not in meaningful quantities, meaning dietary intake is essential. DHA and EPA can supress the production of arachidonic acid (AA), a ω-6FA, from linoleic acid by competing for the desaturases[355].

PUFAs are important components of the phospholipids of all cell membranes. ω-3FAs are incorporated into cellular membranes where their functions include the modulation of pro and anti-inflammatory cytokine and eicosanoid synthesis. Eicosanoids and cytokines play a central role in the inflammation of PAC. The

incorporation of ω-3FAs into the cell membrane alters its composition and they play an important role in membrane protein function and intracellular fatty acid receptors[358]. They maintain membrane fluidity[359], influence lipid raft formation[360] and importantly are metabolised to secondary messengers and metabolites[361]. Both ω-3FAs and ω-6FAs are incorporated into the cell membrane and human immune and inflammatory cell membranes are rich in PUFAs, particularly ω-6FAs which comprise approximately 30% of the fatty acids present[362]. This is a major component of the cell membrane and the composition can be significantly altered by dietary intake, with Yaqoob et al[362] demonstrating that with oral supplementation (approximately 3.2g of EPA/DHA) the proportion of ω-3FAs, EPA in this case, in plasma phospholipids was increased 10 fold after 4 weeks of treatment.

The ratio of ω-3FAs/ω-6FAs in the cell membrane, in the western world, is approximately 1:15 when studies have shown the optimum ratio to be 1:2-1:4[363]. Increasing the amount of ω-3FAs reduces the amount of ω-6FAs, particularly AA, present in the cell membrane and therefore the amount available for downstream eicosanoid production. Increasing the ω-3 profile will therefore improve the ω-3/ω-6 balance, the inflammatory profile and the potential anti-cancer effect. Dietary supplementation results in the modification of fatty acid profiles in the cell membrane and the incorporation of EPA and DHA occurs in a dose-response fashion [364,365]. High dose supplementation therefore increases cell membrane ω-3FAs however oral supplementation has some limitations in that there is a maximum dose tolerable before side effects such as abdominal cramps and diarrhoea occur and in addition there is a delay before ω-3 FAs are incorporated into cell membrane and the ω-3 FAs/ω-6FAs is reduced. An alternative method of administration is intravenously, which would allow higher doses to be administered, eliminate the side effects from oral administration and allow rapid uptake into the cell membrane.

7.1 Anti-inflammatory actions of ω-3FAs

Activation of the immune system and the subsequent inflammation which ensues creates an environment characterised by oxidative stress. This may be in response to insult of endogenous pathogens and aids the body to create an environment hostile to these insults. However, persistent and unregulated inflammation, such as that found in cancer, can result in the inappropriate, unregulated and excessive production of inflammatory mediators to the detriment of the host. As discussed PUFAs constitute up to 30% of the cell membrane. An important anti-inflammatory role is their mobilisation from the cell membrane to produce down-stream inflammatory mediators. ω-3FA (EPA) and AA (ω-6FAs) are cleaved from the cell membrane by phospholipase A2 and then metabolised by lipoxygenase (LOX) to produce leukotrienes and cyclooxygenase (COX) to produce thromboxanes and prostaglandins, collectively known as eicosanoids (Figure 7.1). COX has two isoenzymes, COX1 and COX2, with COX2 being induced in inflammation and not normally detectable in normal tissue[355] and COX2 is increased in several cancers including PAC[366]. LOX and COX activity on AA produces pro inflammatory and pro proliferative mediators in contrast to their activity on EPA and DHA which produces less inflammatory and proliferative mediators[355] (Figure 7.1). The ability of ω-3FAs to compete with ω-6FAs for eicosanoid synthesis constitutes a key ability of its anti-inflammatory properties[367].

The eicosanoids produced by EPA include the 3 series prostaglandins (PGE3) and thromboxanes (A3) and the 5 series leukotrienes (LT)[368], and ω-3FA supplementation has been demonstrated to increase production of these mediators by inflammatory cells[369–371]. The mediators formed from EPA are much less potent that those formed from AA, for example leukotriene B_5 is 10 to 30 times less potent as a neutrophil chemotactic agent that leukotriene B_4[372]. The eicosanoids produced by AA are pro-inflammatory and include PGE2, thromboxane A2 and the 4 series leukotrienes[368]. ω-3FAs can influence pro inflammatory cytokine production at the gene level through peroxisome proliferator-activated receptor (PPAR) activation[373]. PPARs bind proteins that participate in controlling a wide variety of genes involved in the inflammatory and immune response[374]. Poynter et al[375] demonstrated that activation of the alpha

isoform of PPAR antagonised signalling pathways of NFκB, a key component of the inflammatory microenvironment. In addition EPA prevents NFκB activation by tumour necrosis factor-α (TNFα) in cultured pancreatic cells[376]. In other cancer cell lines EPA and DHA reduce production of pro inflammatory cytokines including TNFα, interleukin 1α, interleukin 1β, interleukin 8 and interleukin 6 (IL6)[377–379]. Supplementation of ω-3FAs in healthy volunteers demonstrated decreased production of TNFα, interleukin 1β and IL-6[380,381]. In addition to downstream eicosanoids produced from ω-3FAs, recent studies have identified a novel group of anti-inflammatory mediators termed resolvins and protectins[382]. Both have been shown to have potent anti-inflammatory actions with resolvins having a role in the resolution phase of inflammation and protectins having a wider anti-inflammatory role.

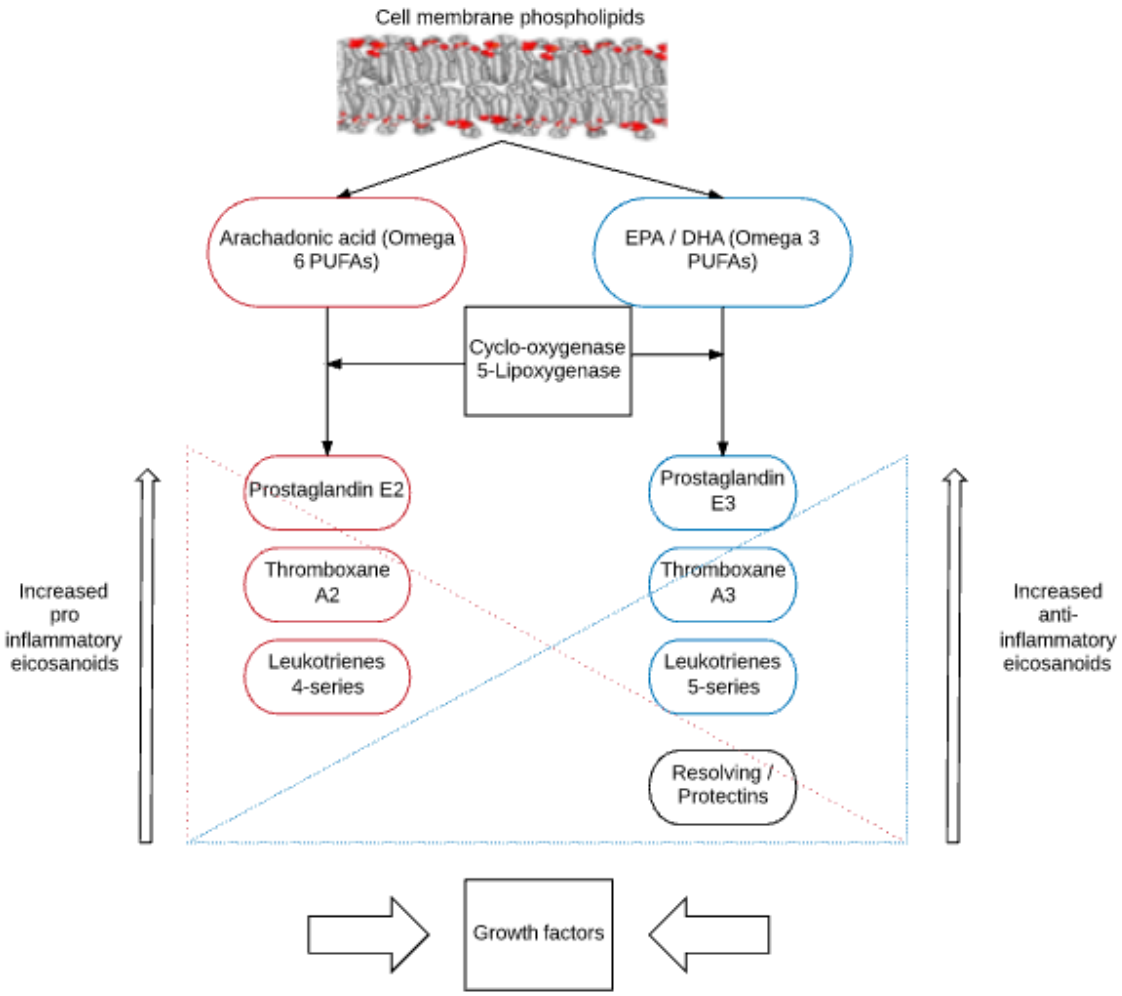

Figure 7.1. Eicosanoids derived from ω-3 FAs (EPA and DHA) and ω-6FAs (AA). They are metabolised by cyclooxygenase and Lipoxygenase. The anti-inflammatory eicosanoids produced by ω-3FAs include the 3 series prostaglandins and thromboxanes and the 5 series leukotrienes. The pro inflammatory eicosanoids produced by ω-6FAs include the 2 series prostaglandins and thromboxanes and the 4 series leukotrienes. Increasing the amount of ω-3FAs improves the ω-3 FAs/ω-6FAs ratio and reduces the amount of ω-6FAs, particularly AA, present in the cell membrane and therefore the amount available for downstream pro inflammatory eicosanoid production. ω-3 FAs also produce anti-inflammatory resolvins and protectins. All these secondary mediators have either a general suppressive, or enhancing effect on growth factors and various cells in the inflammatory microenvironment.

7.2 ω-3FAs and cancer

An uncontrolled pro-inflammatory response is a pathognomonic feature of cancer and when unregulated, perpetuating and persistent can result in irreversible damage to the host. Epidemiological data suggest that ω-3FAs exert protective effects against several common malignancies, including breast, colon and prostate cancer[383]. Evidence has demonstrated that ω-3FAs suppress the development of various cancers including colon[384–386] and breast cancer[387], by modifying gene expression and signalling pathways[313]. Various human studies have demonstrated that ω-3FAs are protective in colon cancer[388]. Hall et al[388] demonstrated that ω-3 intake was inversely associated with colorectal cancer risk in a 22 year follow up study, demonstrating their potential long term protective benefit. In contrast, ω-6FAs enhance both the initiation and promotion of colon cancer[389]. There are several mechanisms through which ω-3FAs affect carcinogenesis.

1. Improvement of the ω-3 FA:ω-6FA cell membrane ratio, reduction in ω-6FAs driven pro-inflammatory eicosanoid production resulting in modulation of inflammation, cell proliferation, apoptosis, metastasis and angiogenesis[390].
2. Effects on transcription factor activity, gene expression and signal transduction, leading to changes in metabolism, cell growth and diffrentiation[390].

As discussed above ω-3FAs are incorporated into the cell membrane, reducing the amount of ω-6FAs available for the production of pro inflammatory eicosanoids. ω-6FAs promote colon and breast cancer by upregulating the expression of cyclooxygenase-2 (COX2)[391]. By increasing ω-3FAs and decreasing ω-6FAs in the cell membrane, COX2 expression is reduced, providing an indirect mechanism by which ω-3FAs exert one of their anti-tumour effects. Nitric oxide (NO) and its reactive products are mutagenic and excessive production of NO causes DNA damage, impaired DNA repair and eventually cancer[392]. Tumour produced NO enhances the angiogenic and invasive ability of tumour cells promoting growth and metastasis[392,393]. ω-3FAs have been shown to suppress NO production in a macrophage cell line in a dose dependent fashion[394], and in contrast there was no suppression of NO with ω-6FAs. ω-3FAs influence transcription factor activity, gene expression and signal transduction through

their effect on PPAR and NFκB as discussed above. In addition to this, rats fed a diet of ω-3FAs have been shown to have decreased levels of protein kinase C β2 that promotes carcinogenesis in intestinal epithelial cells[395]. Cockbain et al[396] recently demonstrated that patients with colorectal liver metastasis administered 2 g of oral EPC daily demonstrated reduced vascularity of liver metastasis in ω-3FA naïve patients which translated into an overall survival benefit compared with placebo. In addition they demonstrated that there was a significant increase in red blood cell EPA compared to placebo, and that patients with elevated post treatment levels had improved overall survival[397].

7.3 ω-3FAs and pancreatic cancer

There is a wealth of research demonstrating the benefit of ω-3FAs in PAC, from cell culture models, animal models and human clinical trials. ω-3FAs PUFAs have been shown to inhibit the growth of human pancreatic adenocarcinoma cell lines in a dose-dependent manner, with EPA being the most potent[398,399]. In addition EPA and DHA has been shown to induce apoptosis of pancreatic cancer cell lines in a concentration-dependent manner[399]. ω-3FAs also decrease pancreatic cell proliferation and result in time dependent cell-cycle arrest resulting in apoptosis[400]. ω-3FAs can also inhibit the proliferation of pancreatic cell lines irrespective of the varied gemcitabine resistance, and the co-administration of ω-3FAs with gemcitabine inhibited gemcitabine induced NFκB activation and restored apoptosis in a gemcitabine resistant cell line[401].

In vitro ω-3FAs have also been shown to inhibit the growth of human pancreatic cancer, augment the effect of gemcitabine, induce apoptosis, and inhibit the proliferation and invasion of PAC[399,401]. In a xenograft model, ω-3FAs decreased the growth of cyclooxygenase-2 (COX2) positive and negative pancreatic cancer cells, which was accompanied by a decrease in prostaglandin E2 and an increase in prostaglandin E3[402]. In contrast ω-6FAs stimulated the growth of COX2 positive pancreatic cancer cells, which was mediated through prostaglandin E2. In an animal model, rats administered a ω-3FA rich diet were shown to develop significantly less pre-neoplastic pancreatic lesions (atypical acinar cell nodules) than those with a ω-6FA

diet[403]. In addition the ω-3FA mice had significantly decreased serum levels of thromboxane B2 and prostaglandin E2. In another animal model where N-nitrosobis-2-oxopropylamine was used to induce ductal pancreatic cancer, Heukamp et al[404] demonstrated that hamsters fed a diet high in ω-3FAs had a reduced incidence of liver metastasis and hepatic lipid peroxidation compared to those fed a diet high in ω-6FAs or a combination of ω-3, ω-6, and ω-9FAs.

Clinical data have demonstrated that ω-3FAs in PAC augments functional status and reduces treatment related consequences, improves patients quality of life, resulting in weight gain and also limits or reverses the profound cachexia seen in PAC[405–407]. Wigmore et al[406] demonstrated that patients with APC who were administered high dose oral fish oil had a significant reversal of weight loss which persisted at 3 months and there was an associated reduction in the acute phase protein response. Barber et al[408] showed that 2 g of oral EPA daily increased the body weight of PAC patients compared to healthy controls after 3 weeks and in addition they had increased energy and normalisation of the metabolic response although high dose oral preparations are limited by compliance, side effects, previous diet, age, sex, variability in individual metabolism and bioavailability. Arshad et al[409] recently demonstrated that patients with APC treated with high dose intravenous ω-3 and gemcitabine had improved activity and quality of life. In addition patients has significantly reduced PDGF and FGF concentrations during treatment and low baseline IL-6 and IL8 levels which correlated with improved survival[410]. Intravenous ω-3 was both safe and well tolerated and resulted in rapid and sustained cellular uptake with a reduction in ω-6FA within the cell membrane and an improvement in the ω-3 FAs/ω-6FAs ratio[411]. The benefit of intravenous ω-3 FAs was further demonstrated by Eltweri et al[412] in patients with oesophagogastric cancer. Intravenous ω-3 FAs resulted in increased EPA and DHA in plasma non-esterified fatty acids and repeated infusion increased the EPA content of red blood cell membranes.

7.4 ω-3FAs, MDSCs and Tregs

ω-3FAs are known to have significant anti-inflammatory properties and inflammation plays a key role in cancer development, growth, invasion and metastasis. ω-3FAs have been shown to inhibit key mediators in the inflammatory microenvironment including IL1β, IL6, PGE2 and C5a (figure 7.2). Targeting these inflammatory pathways and mediators may reduce MDSC and Treg accumulation (the pro inflammatory mediators), and indirectly ameliorate the tumour directed inflammatory stimulus. Irregular haematopoiesis in cancer involves the abnormal expansion of immature myeloid cells such as MDSCs. ω-3 FAs have been shown to promote differentiation of cells and they may have a therapeutic role[413]. Varney et al[414] demonstrated that mice fed ω-3FAs rich diets had a significantly reduced myeloid progenitor cell frequency and ω-3FAs promoted differentiation of specific progenitor cell types in bone marrow. This result suggests that ω-3FAs may be used to slow progression of haematopoietic dysregulation seen in cancer by increasing differentiation of myeloid progenitor cells. ω-3 PUFAs have however also been shown to promote the expansion of MDSCs. Yan et al[415] showed that PUFAs enhance the accumulation of MDSCs both in cultured mouse bone marrow cells in vitro and in vivo in mice fed diets enriched with PUFAs, effects which were further confirmed in tumour bearing mice (Lewis lung carcinoma). They further determined that PUFAs mediate its effects through the JAK-STAT3 signalling pathway, by administering a JAK inhibitor (JSI-124), which by affecting STAT3 phosphorylation, abrogated the effects of PUFAs on MDSCs. Further to this Xia et al[416] showed that mice fed a high ω-3 PUFA diet demonstrated higher levels of MDSCs in their spleen at 4 weeks. They subsequently transplanted the mice with B16 melanoma cells subcutaneously and saw that the mice with a high ω-3 PUFA diet had a more pronounced tumour growth. The exact molecular mechanism underlying this is unclear and there have been no replicated studies in human cancer patients. PUFAs, in particular DHA has been reported to reduce the suppressive and migratory functions of Tregs in a dose dependent manner[417] and DHA reduced the migration of Tregs towards chemokines but also down regulated SMAD 7 levels and messenger RNA expression of CXCR-4 in Tregs. The evidence behind ω-3FAs effect on MDSCs and Tregs requires further investigation to fully understand their effect in a clinical setting.

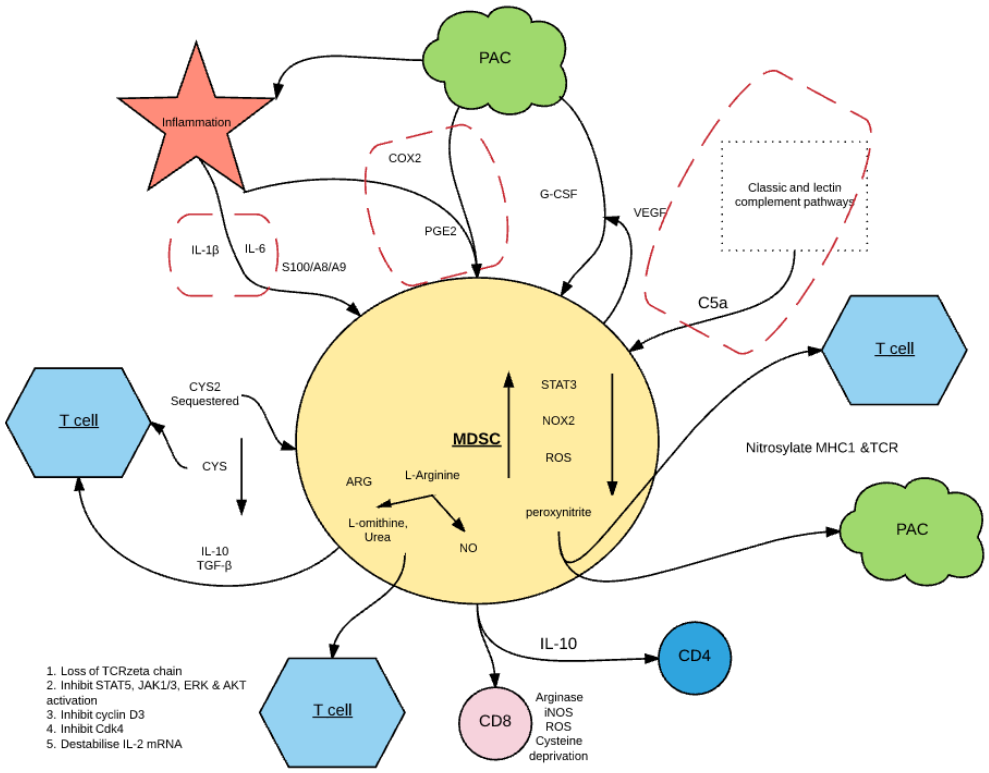

Figure 7.2. (Adapted from figure 3.2). Potential mechanisms in the ω-3FA suppression of PAC. ω-3 FAs have been shown to inhibit key mediators in the inflammatory microenvironment including IL1β, IL6, PGE_2 and C5a (red interrupted line).

7.5 ω-3FAs and EPCs

Angiogenesis is increased in cancer and regulated by a wide range of pro and anti-inflammatory mediators and in cancer there is propensity to induce and sustain angiogenesis by activating an "angiogenic switch"[253]. ω-3FAs have been demonstrated to have a anti-angiogenic effect by inhibiting the production of angiogenic mediators including, VEGF, PDGF, COX-2, NFκB, PGE_2, nitric oxide and MMPs[418–422]. There are no studies reporting the effect of ω-3FAs supplementation on EPC levels in cancer and APC. However, There has been several studies exploring the benefits of ω-3FAs on EPCs in cardiovascular disease[423–425], and even though a recent meta-analysis demonstrated no benefit of supplementation to major cardiovascular end points[426], there has been some interesting results from numerous studies. The mechanisms suggested through which ω-3FA mediate their beneficial effects on cardiovascular

function include improvement in endothelial function and anti-inflammatory effects[427]. Theoretically increasing the number of EPCs would benefit patients with cardiovascular disease by improving endothelial dysfunction, promoting endothelial repair and reducing the effects on atherosclerosis. It has been shown that ω-3FA improve EPC number and functionality in vitro[428]. Spigoni et al[429] demonstrated that circulating EPC numbers significantly increased in patients following 6 weeks of a diet high in ω-3FAs and returned to baseline after a 6 week diet free from ω-3FAs. In addition in a randomised, double blind, placebo controlled 8 week crossover trial administering 1.5g of ω-3FAs a day, Wu et al[430] demonstrated a significant increase in EPCs in patients administered ω-3FAs. The increase in EPCs has been postulated to reduce vascular cell adhesion molecules and pro-inflammatory cytokine expression[429]. The underlying molecular mechanisms for the increase in EPCs by ω-3FAs in cardiovascular disease however remain unclear. Theoretically if ω-3FAs reduce the numerous pro-angiogenic mediators as discussed there would be a reduction in EPCs over treatment with ω-3FAs. There must be additional factors influencing EPC mobilisation in the studies above and the effect of ω-3FAs is on cancer EPCs remain to be clearly elucidated.

7.6 ω-3FAs and Micro RNAs

PUFAs anti-oncogenic and chemo protective actions may be mediated through miRNAs. Davidson et al[323] demonstrated that let-7d, miR-15b, miR-107, miR-191 and miR-324-5p were significantly dysregulated in rats administered diets high in ω-3FAs and injected with azoxymethane (a colon carcinogen). They observed that a non-fish oil diet (corn oil) in the presence of azoxymethane compared to a ω-3FAs diet increased the expression of miR-16, miR-19B, miR-21, miR-26b, miR-27b, miR-93, miR200C and miR203, while reducing the expression of some of their targets including insulin growth factor-1[313]. Farago et al[431] evaluated the cytotoxic action of γ-linolenic acid (GLA), arachidonic acid (AA) and docosahexaenoic acid (DHA) on glioma cells. Specifically with DHA they found miR-143 was down regulated and miR-20b was up regulated compared to control cells. They further demonstrated that miR-143 targeted the gene of COX2, which plays a role in triggering apoptosis. Vinciguerra et al[432] demonstrated that unsaturated fatty acids (e.g. linoleic acid) reduced phosphatase and

tensin homolog (PTEN), a regulator of phosphoinositide 3-kinase signaling and an important tumor suppressor mutated/deleted in human cancers, by up-regulating miRNA-21 synthesis. This demonstrated a novel mechanism by which fatty acids affect PTEN expression and consequently their actions on human cancers. Mandal et al[433] showed that DHA inhibits expression of colony stimulating factor 1 (CSF1) and its expression from human breast cancer cell lines. DHA also significantly inhibited the expression miRNA-21 (which has been shown to contribute to cancer growth and metastasis), which was associated with increased PTEN protein levels and attenuated CSF1 expression.

8 Chapter Eight: Aim and Hypothesis

8.1 Aims

This study aims to assess the effects of administering intravenous ω-3FAs in combination with gemcitabine chemotherapy on specific circulating immunological cells and miRNAs, compared to patients receiving gemcitabine chemotherapy alone in patients with advanced pancreatic cancer.

8.2 Hypothesis

The hypothesis tested will be that intravenous ω-3FA infusion reduces the quantities of the cell populations and miRNA levels, and the change will correlate with clinical outcome, particularly progression free survival and overall survival between the two cohorts.

8.3 Null hypothesis

The null hypothesis is that parenteral ω-3FAs will have no effect on the levels of immune regulatory cells and targeted miRNAs in the trial cohort compared to control patients.

8.4 Primary objective

To study the levels of immune modulatory cells and specific microRNAs in patients receiving gemcitabine plus parenteral ω-3FAs compared to gemcitabine alone.

8.5 Secondary objectives

To analyse how the changes in the immune modulatory cells and micro RNAs correlate with clinical outcome, particularly progression free survival and overall survival between the two cohorts.

8.6 Study design

This was a single centre comparative pilot study. Trial patients were recruited as part of a phase II trial investigating the administration of intravenous ω-3FAs and gemcitabine chemotherapy in patients with APC. Control patients were recruited separately and only received gemcitabine chemotherapy.

9 Chapter Nine: Methods

Twenty-seven patients were recruited. Eighteen patients were recruited in a non-randomised manner as part of a phase II, single arm, and single-centre study of gemcitabine plus parenteral ω-3FAs in patients with chemotherapy-naïve advanced pancreatic cancer. Nine subsequent control patients were recruited in a non-randomised manner, in which they receive standard gemcitabine treatment without parenteral ω-3FAs. The local Ethics Committee and the Medicines and Healthcare Products Regulatory Agency (MHRA) approved both studies. All patients had a diagnosis of advanced pancreatic adenocarcinoma that was confirmed either histologically or cytologically. All patients were discussed at the local multi-disciplinary team meeting and a consultant oncologist assessed them as suitable to receive gemcitabine chemotherapy. All patients were assessed against trial protocol inclusion/exclusion criteria. The trial was registered with clinicaltrials.gov (Number: NCT01019382)

9.1 Inclusion criteria

Patients with histologically or cytologically confirmed pancreatic adenocarcinoma, in whom the disease is assessed as unresectable, either due to metastatic or locally advanced disease, and deemed suitable to receive gemcitabine chemotherapy were eligible for the study. Both trial and control patients had to fulfil the same selection criteria. The inclusion criteria are detailed below:

- Aged >18 years.
- Able to give informed written consent.
- ECOG performance status of 0 or 1.
- Life expectancy > twelve weeks.
- Adequate hepatic and renal function documented within fourteen days prior to treatment.
- AST and ALT ≤2.5x upper limit of normal (ULN), unless liver metastases present, in which case ≤5.0xULN.
- Total bilirubin ≤2.5xULN.

- Serum creatinine ≤1.5xULN or calculated creatinine clearance ≥60ml/min.
- Urinary protein <1+ by urine dipstick. If ≥1+, then 24-hour urine collection should be done and may only be enrolled if urine protein is <2g/24hours.
- Adequate bone marrow function.
- Haemoglobin ≥9g/dL (can have transfusion or growth factors).
- Platelets ≥100,000 cells/mm^3.
- Neutrophil count ≥1500cells/mm^3.
- No significant hyperlipidaemia.
- Patients without severe blood coagulation disorders (anticoagulants allowed)
- Women of childbearing age must have a negative pregnancy test (urine or serum) at commencement of treatment.
- Willingness to comply with scheduled visits, treatment, laboratory test, and other aspects of the trial.

9.2 Exclusion criteria

The exclusion criteria are detailed below:

- Prior treatment with any systemic chemotherapy for metastatic disease.
- Prior adjuvant radio- or chemotherapy within four weeks of starting the study.
- Previous treatment with gemcitabine.
- Hypersensitivity to fish, egg, or soy protein, or to any of the active substances or constituents in the lipid emulsion.
- Any general contra-indications to infusion therapy; pulmonary oedema, hyper hydration, decompensated cardiac insufficiency.
- Any unstable medical conditions; uncontrolled diabetes mellitus, acute myocardial infarction, stroke, embolic disease, metabolic acidosis, sepsis, pancreatitis.
- Known HIV or AIDS.
- Dementia or significantly altered mental status that would prohibit the understanding or rendering of informed consent and compliance with requirements of the protocol.

- History of malignancy other than pancreatic cancer, with the exception of curative treatment for skin cancer (other than melanoma) or in situ breast or cervical carcinoma, or those treated with curative intent for any other cancer with no evidence of disease for five years.
- Major surgical procedure or significant traumatic injury within four weeks of treatment.
- Female patients must be surgically sterilised or postmenopausal or agree to use two adequate contraception measures during the period of therapy to continue for six months after the last dose of gemcitabine. Male patients must be surgically sterilised or agree to use adequate contraception for the same period.
- Patients deemed unsuitable for gemcitabine chemotherapy.

9.3 Treatment protocol

Patients receive a standard dose of gemcitabine (1000mg/m^2) administered as a thirty minute infusion once weekly for three weeks, followed by a one week break from treatment up to a maximum of six months. Immediately following every administration of gemcitabine patients received up to 500mL of a lipid emulsion intravenously (Lipidem, BBraun) containing 10g ω-3 fatty acids (0.5-1g ALA and 4.3-8.6g EPA/DHA) over four hours. Patients were administered their gemcitabine chemotherapy in the chemotherapy treatment suite and then transferred to a bespoke trials unit (HOPE treatment facility) within the same building. New intravenous access was obtained and the infusion of Lipidem commenced. This resulted in a washout period of 30 minutes from gemcitabine treatment. Lipidem was infused at a rate of 125mls/hr. Control patients received gemcitabine treatment alone. Patients received gemcitabine at a standard dose prescribed weekly by an oncologist, dose adjustments were allowed as per standard clinical practice. Patients were included in the study until progression of disease, death or serious adverse events necessitating withdrawal or patients requested trial cessation.

A CT scan was performed at baseline, and at any stage if disease progression was suspected, or every eight weeks. Patients continued in the trial as long as their tumour did not show progression as defined by modified RECIST (Response Evaluation Criteria in Solid Tumours – Appendix 1) criteria and assessed by a radiologist blinded to the clinical findings and independent of the clinical team, reporting in real time according to an agreed protocol. Blood samples were obtained at each treatment time point and kept on ice prior to sample processing. All samples were processed immediately following collection.

9.4 Lipidem

All patients were screened to ensure they did not have any contraindication to treatment as per manufacturer guidelines. Lipidem (200mg/ml) was supplied by BBraun Melsungen. Lipidem was administered intravenously and patients received up to 500mls over 4 hours immediately following gemcitabine treatment on days 1, 8 and 15 of each cycle followed by a rest week. The active substances in 1000ml of Lipidem are: Medium-chain triglycerides -100g, Soya-bean oil – 80g, omega-3-acid triglycerides – 20g (Alpha-linolenic acid (4-8.8g), Eicosapentaenoic acid and Docosahexaenoic acid (8.6-17.2g)). Lipidem also contains Linoleic acid (omega-6) – 38.4-46.4g, glycerol, egg lecithin, all rac-α-tocopherol, ascorbyl palmitata, sodium oleate, sodium hydroxide and water. Lipidem is a safe and tolerable treatment however patients were monitored closely during treatment for any side effects including fat overload syndrome, anaphylaxis or hypersensitivity reactions, metabolic disturbances including hypoglycemia, hypo and hypertension, dyspnoea, and nausea and vomiting. The same batch of Lipidem was utilized throughout the trial and verification of Lipidem content was not undertaken as this was performed by the manufacturer and listed with the product.

9.5 Sample processing

Cell samples were batch processed during one-week time frames over the course of the trial. This was the result of processing the samples around on-going clinical commitments, patient recruitment; time available using the flow cytometer and the

specialised scientific assistance available. Micro RNA samples were transported to Taiwan and processed as a separate batch.

9.5.1 Buffers, Reagents and Solutions

All chemicals were supplied by Sigma-Aldrich life sciences unless stated.

- Dulbecco's Phosphate Buffered Saline (PBS, without Calcium Chloride and Magnesium Chloride), Sigma-Aldrich, St Louis, USA.
- Storage Solution:
  Mixture of one mL Dimethyl sulfoxide (99.5% GC, Sigma-Aldrich, Steinheim, Germany) and 9 ml of Foetal Bovine Serum (heat inactivated), GIBCO, NY, USA.
- Ficoll-paque^{TM} PREMIUM 1.084 (GE Healthcare, Uppsala, Sweden). Ficoll-Paque^{TM} contains Ficoll PM400, sodium diatrizoate and edatate calcium dissolved in water.

A balanced salt solution containing a 1: 9 ratio of solution A and B was used as a diluent and washing solution during the isolation of mononuclear cells (Figure 9.1). 5mL of Solution A was added to 45mL of solution B. The solutions were prepared regularly and autoclaved prior to storage to ensure sterility.

Sample	**Concentration** **Molarity (M=moles/litre), normality=N**	**Concentration (g/L)**
Anhydrous D-glucose	0.1%	1.0
$CaCl_2 \times 2H_2O$	5.0×10^{-5} M	0.0074
$MgCl_2 \times 6H_2O$	9.8×10^{-4} M	0.1992
KCL	5.4×10^{-3} M	0.4026
Tris $(HOCH_2)_3CNH_2$	0.145 M	17.565
Conc. HCL	10 N	To Ph 7.6
Distilled Water		To 1000 mL

Table 9.1. Stock solution A (1 litre distilled water and add 10N HCL until pH is 7.6).

Sample	Concentration	Concentration (g/L)
NaCl	0.14 M	8.19

Table 9.2. Stock solution B (add to 1 litre of distilled water).

9.5.2 PMBC separation and storage

Blood samples were collected from each patient at each treatment point and post treatment. A sample of 19.6mL of whole blood was collected in 4 x 4.9mL Ethylenediaminetetraacetic acid (EDTA) bottles. Samples were centrifuged at 400g for five minutes to separate blood from plasma. Four mL of plasma was transferred into 4 x 2mL Eppendorf ® safe-locking micro-centrifuge tubes and stored in -80˚C for further analysis. Three mL of balanced salt solution was added to 3mL whole blood and layered on 3mL ficoll-Paque™ PREMIUM 1.084 (density gradient separation solution). Care was taken when adding the blood/buffer mixture to density gradient separation solution so as to not mix the two and to layer it carefully on top to ensure maximum separation of cells. Samples were centrifuged at 400g for thirty minutes at 15°C to separate out the individual layers. The mononuclear layer containing peripheral blood mononuclear cells (PBMCs) was removed and washed with 6mL of balanced salt solution. The samples were centrifuged at 400g for ten minutes at 15 °C. The supernatant was then discarded. The mononuclear pellet was further washed with 6mL of buffer solution. The samples were centrifuged at 400g for ten minutes at 15 °C. The excess supernatant was discarded and the mononuclear pellet was then suspended in 1mL of Dimethyl sulfoxide (DMSO) (1%)/Foetal Bovine Serum (9%) solution and added to thermo scientific™ Nalgene™ general long-term storage cryogenic tubes (cryo vials). Cryo vials were transferred to a Nalgene® Mr. Frosty freezing container, suspended in isopropyl alcohol, and transferred to a -80°C freezer. These freezing containers provide a repeatable 1°C/min cooling rate for successful cryopreservation of cells.

9.5.3 Thawing and processing samples for flow cytometry (FACS) analysis

Samples were removed from -80°C storage and snap-thawed at 37°C in a temperature controlled water bath. The samples were transferred to 15mL conical centrifuge tube. Ten mL of calcium and magnesium free phosphate buffered solution (PBS) was added and cells washed. Samples were centrifuged at 400g for ten minutes at 4°C. The supernatant was removed and the pellet washed further in 10mL of calcium and magnesium free PBS. Samples were centrifuged at 400g for ten minutes at 4°C. The supernatant was removed and the cells suspended in 1mL of PBS. The cell number and percentage of viable cells was then determined prior to antibody staining using the cell counting protocol.

9.5.4 Cell count and concentration

PBMCs were counted following thawing and prior to antibody staining. PBMCs were suspended in 1mL of PBS. Viable PBMCs were counted per mL. 10µL of PBMC suspension was pipetted into a 0.5mL micro centrifuge tube. 90µL of 0.4% Trypan blue stain was added. The cell mixture was loaded on to a haemocytometer. Viable PBMCs number was calculated per mL using a standard equation.

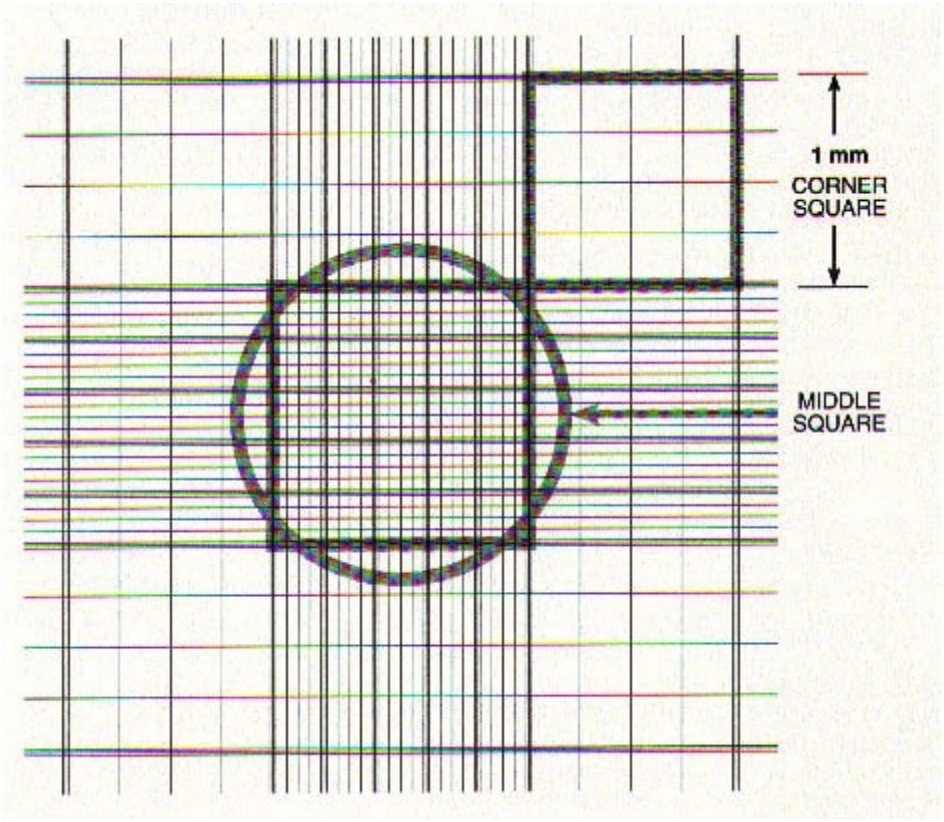

Figure 9.1. Haemocytometer used to count cell concentration prior to antibody staining. The cell suspension was allowed to settle and PBMCs were counted in on four large squares and the average calculated (viable PBMCs were clear, nonviable PBMCs were blue). Cells touching the top and left line were included; cells touching the bottom and right were excluded.

9.6 Antibody selection and validation

A review of the literature was conducted and antibodies for specific cell phenotypes were selected based on recent peer reviewed studies of selected mononuclear cells in pancreatic cancer. The selected antibodies for each cell have undergone independent validation and verification as discussed previously. MDSCs were identified following staining with HLADR, CD33, CD11b and LIN-1 antibodies. Tregs were identified following staining with CD4, CD25 and FOXP3 antibodies. EPCs were identified following staining with CD34, CD31, CD133 and CD45 antibodies.

9.7 Immune modulatory cell staining

9.7.1 Staining protocol for MDSCs.

Samples were counted and number of cells per mL determined. The volume of antibody used was titrated to the volume required to stain the appropriate number of cells. 1mL of sample was divided into five 15mL conical centrifuge tubes as detailed below

Sample and antibody	Sample volume	Antibody concentration
Unstained cells	0.1mL	
HLADR (HLADR APC Mouse Anti-Human. BD Pharmingen®)	0.1mL	20µL – 1 million cells, 2µL – validation
CD33 (CD33 V450 Mouse Anti-Human Cat. BD Pharmingen®)	0.1mL	5µL – 1 million cells, 500nL – validation
CD11b (CD11b/Mac-1 PE-Cy7 Mouse Anti-Human. BD Pharmingen®)	0.1ml	5µL – 1 million cells, 500nL – validation
Lin1 (Lin-1 FITC (Lineage Cocktail (CD3, CD14, CD16, CD19, CD20, CD56). Becton Dickinson Immunocytometry Systems®)	0.1mL	20µL – 1 million cells, 2µL – validation
Combination stain (HLADR, CD33, CD11b, Lin1)	0.5ml	Appropriate volume of antibody to cell concentration

Table 9.3. Preparation of MDSC sample tubes for flow cytometry analysis.

An appropriate volume of antibody was added to the samples and incubated on ice for 30 minutes. One mL of calcium and magnesium free PBS was added to the sample. The samples were centrifuged at 500G for five minutes at 20°C and supernatant removed. Samples were re-suspended in 0.5ml of calcium and magnesium free PBS and analysed.

9.7.2 Staining protocol for Tregs.

Samples were counted and number of cells per mL determined. The volume of antibody used was titrated to the volume required to stain the appropriate number of cells and 1mL of sample divided into five 15mL conical centrifuge tubes as detailed below. All tubes were as per full FOXP3 protocol and exposure to light kept to a minimum once stained. For each individual sample the following tubes were prepared; unstained cells, CD4, CD25, FOXP3, combination stain (CD4, CD25, FOXP3).

Sample and antibody	Sample volume	Antibody concentration
Unstained cells	0.1mL	
CD4 (CD4 FITC Mouse Anti-Human. BD Pharmingen®)	0.1mL	20µL – 1 million cells, 1µL – validation
CD25 (CD25 APC Mouse Anti-Human. BD Pharmingen®)	0.1mL	5µL – 1 million, 500nL – validation
FOXP3 (FOXP3 PE Mouse Anti-Human. BD Pharmingen®)	0.1ml	5µL – 1 million, 500nL– validation
CD4, CD25, FOXP3	0.6ml	Appropriate volume of antibody to cell concentration

Table 9.4. Preparation of Treg sample tubes for flow cytometry analysis.

The appropriate amount of CD4/CD25 antibody was added to the respective sample tube and incubated on ice in the dark for 30 minutes. One mL of calcium and magnesium free PBS was added to the sample and the samples centrifuged at 250g for ten minutes at 20°C. Samples were suspended in 1mL of diluted FOXP3 buffer A (diluted 1:10 with deionised water). Samples were incubated for ten minutes in the dark at room temperature then centrifuged at 500g for five minutes at 20°C and supernatant removed. One mL of calcium and magnesium free PBS was added to the samples, the samples centrifuged at 500g for five minutes at 20°C and supernatant removed following which 0.25mL of FOXP3 buffer C was added to each tube and incubated at room temperature in the dark for thirty minutes. To make buffer C:

FOXP3 buffer B was diluted into FOXP3 buffer A at a ratio of 1:50 (buffer B: buffer A). One mL of calcium and magnesium free PBS was added to the samples which were then centrifuged at 500g for five minutes at 20°C and the supernatant removed. This step was repeated and FOXP3 antibody at appropriate concentrations was added to the samples and incubated at room temperature in the dark for thirty minutes. One mL of calcium and magnesium free PBS was added to the samples. The samples were centrifuged at 500g for five minutes at 20°C and supernatant removed. Samples were re-suspended in 0.5ml of PBS and analysed.

9.7.3 Staining protocol for EPCs.

Samples were counted and number of cells/mL determined. The volume of antibody used was titrated to the volume required to stain the appropriate number of cells. One mL of sample was divided into five 15mL conical centrifuge tubes.

Sample and antibody	Sample volume	Antibody concentration
Unstained cells	0.1mL	
CD31 (CD31 FITC Mouse Anti-Human. BD Pharmingen®)	0.1mL	20µL – 1 million cells, 2µL – validation
CD45 (CD45 R/B220 Pacific Blue Mouse Anti-Human. BD Pharmingen®)	0.1mL	5µL – 1 million cells, 1µL – validation
CD34 (CD34 PE Mouse Anti-Human. BD Pharmingen®)	0.1ml	20µL – 1 million cells, 2µL – validation
CD133 (CD133 APC. Miltenyi Biotec®)	0.1mL	5µL – 1 million cells, 1µL – validation
Combination stain (CD31, CD45, CD34, CD133)	0.5ml	Appropriate volume of antibody to cell concentration

Table 9.5. Preparation of EPC samples for flow cytometry analysis.

An appropriate volume of antibody was added to the samples and incubated on ice for 30 minutes. One mL of calcium and magnesium free PBS was added to the sample. The samples centrifuged at 500G for 5 minutes at 20°C and supernatant removed. Samples were re-suspended in 0.5ml of PBS and analysed.

9.8 Flow Cytometry (FACS) analysis

Samples were analysed with the FACS Aria II flow cytometer (Becton Dickinson, BD Biosciences, San Jose, USA). The FACS Aria II is a specialized flow cytometer and has five lasers allowing complex analysis of rare cell populations utilizing multiple antibody staining. The five lasers include ultraviolet (wavelength - 355 nm), violet (wavelength - 405 nm), blue (wavelength - 488 nm), yellow/green (wavelength - 561 nm) and red (wavelength - 640 nm).

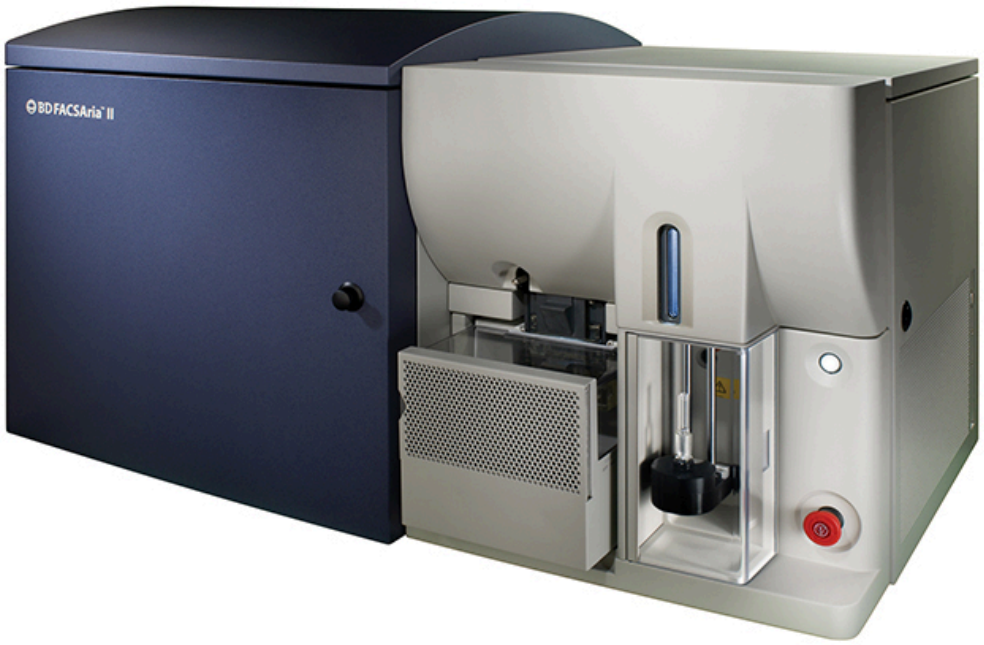

Figure 9.2. FACS Aria II flow cytometer (Becton Dickinson, BD Biosciences, San Jose, USA).

Flow cytometry allows the simultaneous measurement of multiple cell characteristics such as, size, various internal characteristics and fluorescence. Cells suspended in fluid are arranged into a fast flowing single stream and passes through a beam of light (utilising multiple lasers) that allows multiple analyses to take place. As the cell passes though the beam of light, it scatters the laser and fluorescent light emitted. The light scattered is detected on two axis. The forward scattered light (FSC) is proportional to the cell size or surface area. The side-scattered light (SSC) is collected at 90 degrees to the laser and is a measurement of refracted and reflected light. It is proportional to the

granularity of the cell. A specialised detector then collects the emitted light through specific filters and this optical data is converted into electronic signals and analysed.

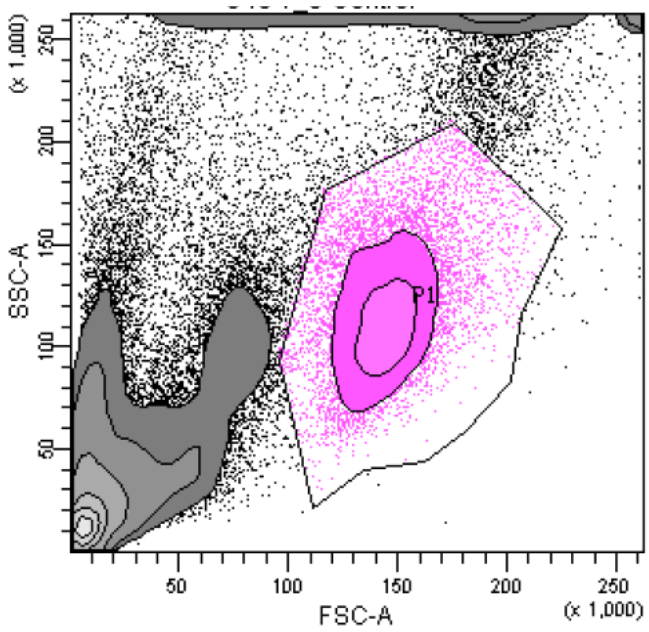

Figure 9.3. FACS schematic showing cell population following forward (FSC) and side scatter (SSC) analysis. Forward scatter is shown on the x-axis and side scatter on the y-axis. There is often a degree of debris that is seen in the bottom left hand corner of the figure. The debris is gated out and the cell population of interest is seen as P1.

Antibodies were selected from recently validated and verified studies as described previously. Together with a specialized flow cytometer scientist antibodies and their appropriate fluorophores were selected. Fluorophores are chemical compounds that are excited by a particular light wavelength. The wavelength excites an electron in the fluorophore and raises it to a higher energy wavelength. The electron quickly returns to its resting state, emitting energy as a photon of light. The transition of energy is called fluorescence. An antibody is conjugated to a specific fluorophore and following laser stimulation the re-emitted light is measured. A fluorochrome is conjugated to a monoclonal antibody and is used to identify specific antigenic surface markers on the cell. Specific fluorochromes, combined with FSC and SSC data can identify specific cell populations (with a specific antibody signature) and their relative percentages relative to the parent population. Validation of all staining protocols and antibodies was conducted on three patient samples on three separate occasions for each immune

modulatory cell investigated, to ensure reproducibility and repeatability of the method.

Fluorochrome	Max. Excitation (nm)	Max. Emission (nm)	Laser wavelengths (nm)
V450	404	448	405
Pacific Blue	405	455	405, 407
Fluorescein (FITC)	495	520	488
Phycoerythrin (PE)	565	575	488, 514, 568
PE-Cyanine-7 (PE-Cy7)	565	770	488, 514
Allophycocyanin (APC)	650	660	633, 635, 647

Table 9.6. List of Fluorochromes used for immunophenotyping. The fluorochrome and its max excitation and emission laser wavelength in nano meters are shown. Figure modified from Macey and Perry, 2007 [434].

MDSC antibody	Fluorochrome	Laser used	Laser wavelength filter
CD33	V450	Violet	450/50-A
LIN1	FITC	Blue	530/30-A
CD11b/Mac-1	PE–Cy7	Yellow/green	780/60-A
HLADR	APC	Red	670/14-A
Treg antibody	**Fluorochrome**	**Laser used**	**Laser wavelength filter**
CD4	FITC	Blue	530/30
CD25	APC	Red	670/14
FOX-P3	PE–Cy7	Yellow/green	582/15
EPC antibody	**Fluorochrome**	**Laser used**	**Laser wavelength filter**
CD31	FITC	Blue	530/30
CD45	Pacific Blue	Violet	450/50
CD133	APC	Red	670/14
CD34	PE	Yellow/green	582/15

Table 9.7. Antibodies used to identify MDSCs, Tregs and EPCs, their conjugated Fluorochrome and the wavelength utilised. The laser wavelength describes the filter used, for example the filter used in from of the FITC detector is 530/30. This number refers to the spectral band transmitted: 530 ± 15nm, so wavelengths between 515nm and 545nm.

9.9 MDSC FACS analysis

PBMC were analysed for MDSCs. One hundred and thirty four samples were analysed from eighteen trial patients and nine control patients. MDSCs with two antibody phenotypes were analysed:

1. Lin1$^-$, HLA-DR$^-$, CD33$^+$ and CD11b$^+$
2. Lin1$^-$, HLA-DR$^-$ and CD11b$^+$.

Samples were analysed for the unstained cells, each individual antibody and a combination stain.

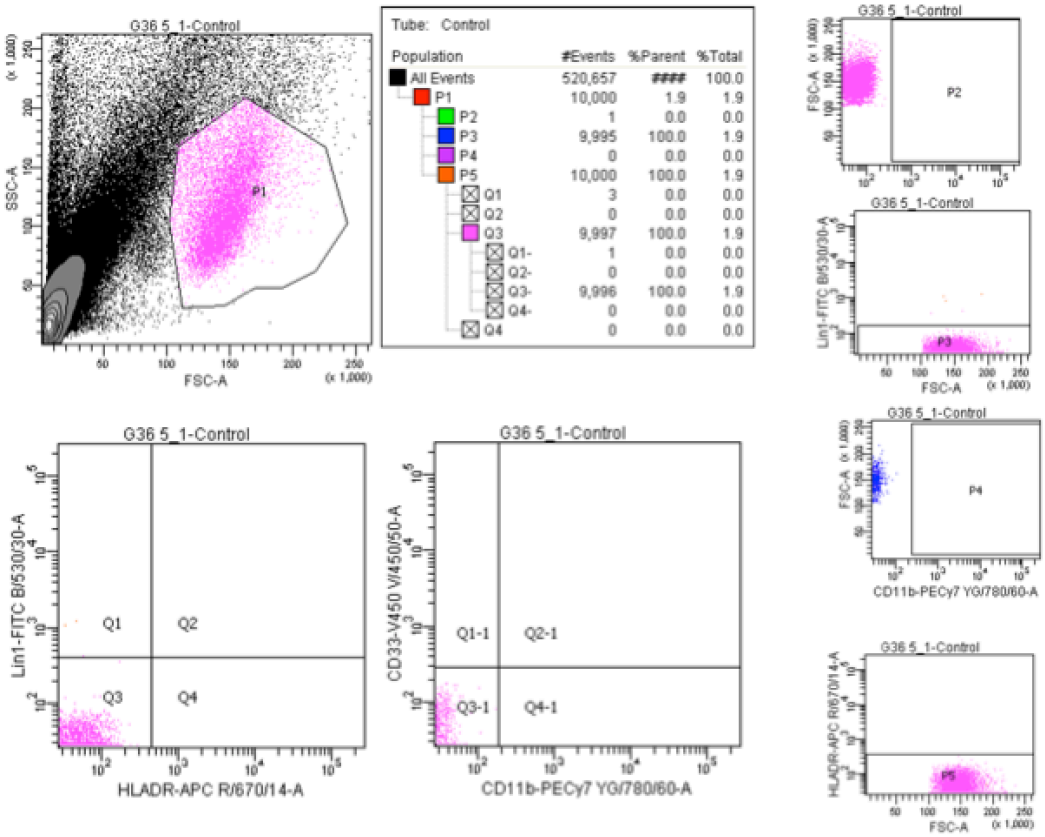

Figure 9.4. FACS schematic of unstained MDSCs. All samples had an unstained sample analysed to ensure sample were not compromised and cell separation was standard and valid. Ten thousand cells were analysed in the target population (P1).

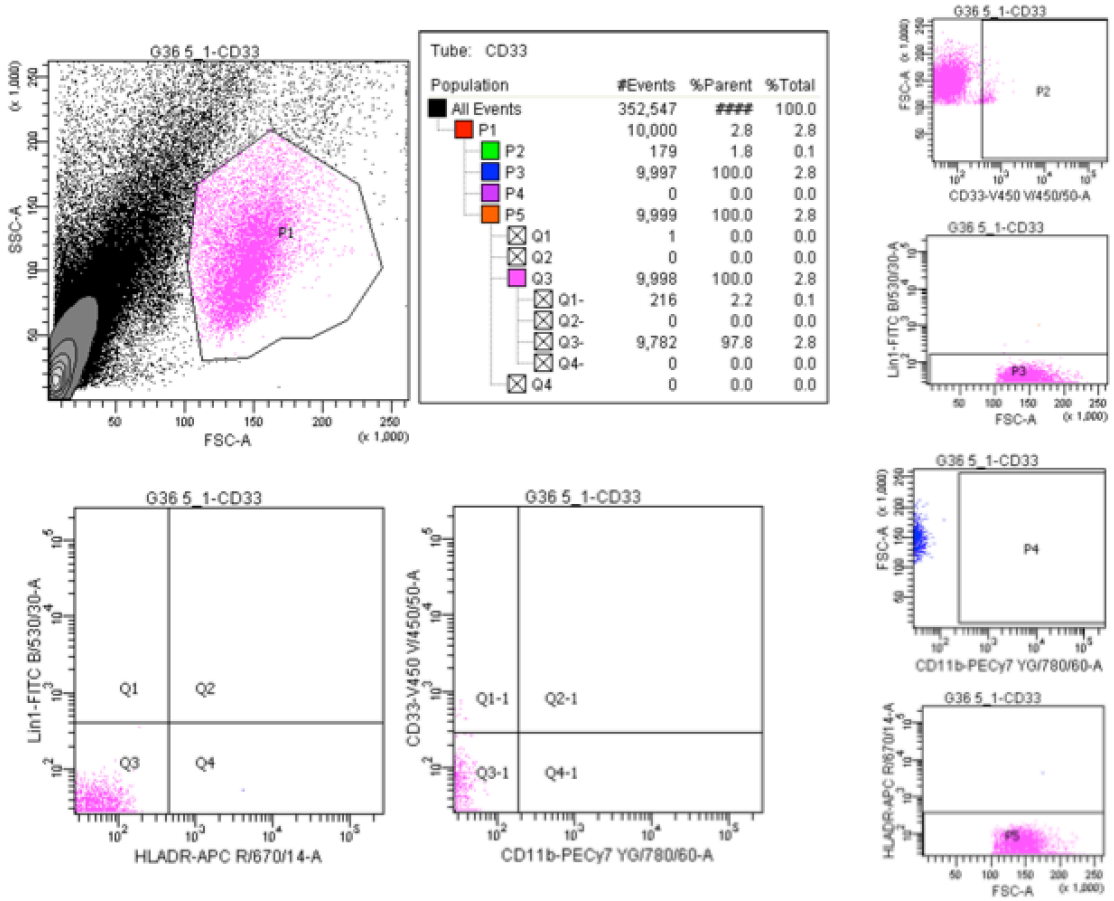

Figure 9.5. FACS schematic of MDSCs stained with only CD33 antibody (CD33 V450 Mouse Anti-Human Cat, BD Pharmingen®). All samples had a CD33 stained sample analysed to ensure samples were not compromised and cell separation was standard and valid. Ten thousand cells were analysed in the target population (P1). The violet laser was used with a filter set at 450/50 nm. The $CD33^{+}$ cell population was gated as shown in the figure as P2.

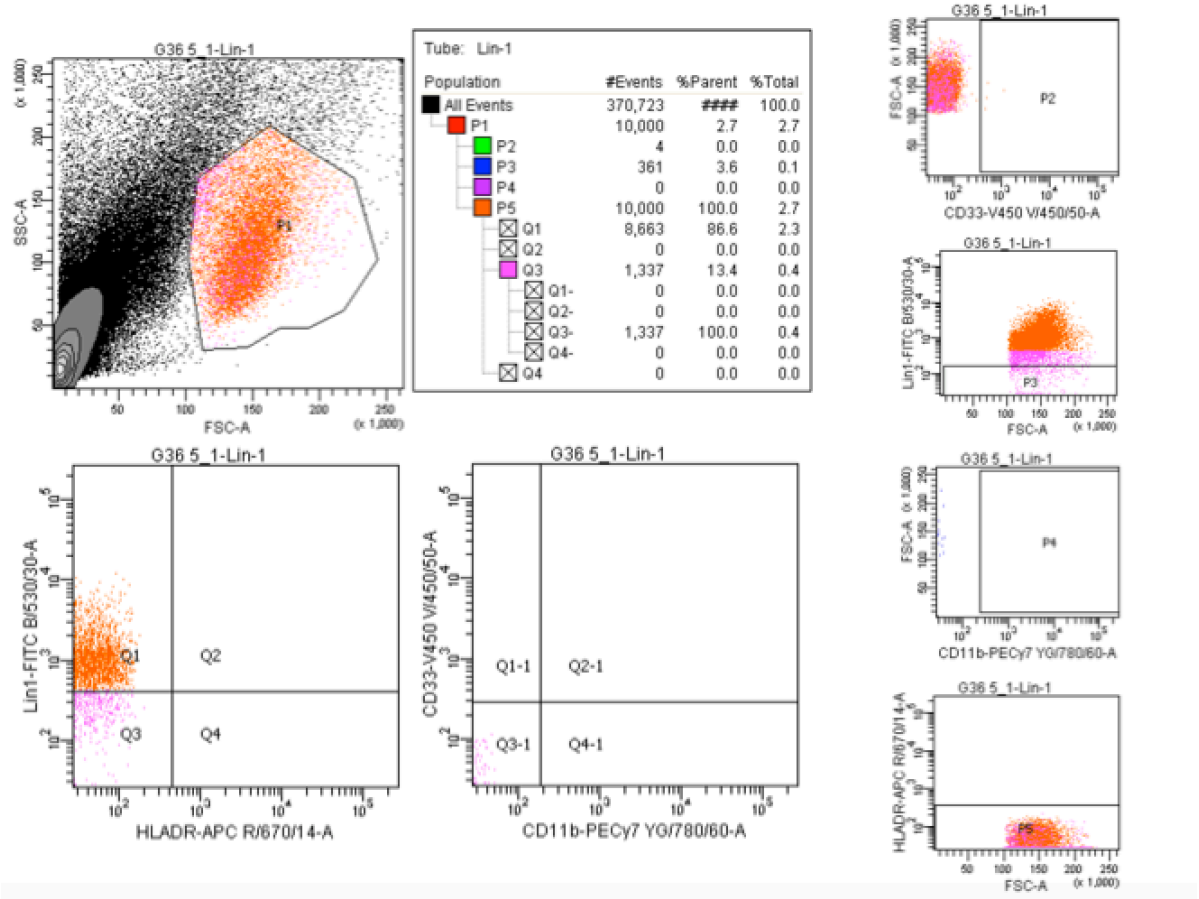

Figure 9.6. FACS schematic of MDSCs stained with only Lin1 antibody (Lin-1 FITC (Lineage Cocktail (CD3, CD14, CD16, CD19, CD20, and CD56), Becton Dickinson Immunocytometry Systems®). All samples had a Lin1 stained sample analysed to ensure samples were not compromised and cell separation was standard and valid. Ten thousand cells were analysed in the target population (P1). The blue laser was used with a filter set at 530/30 nm. The $Lin1^-$ cell population was gated as shown in the figure as P3.

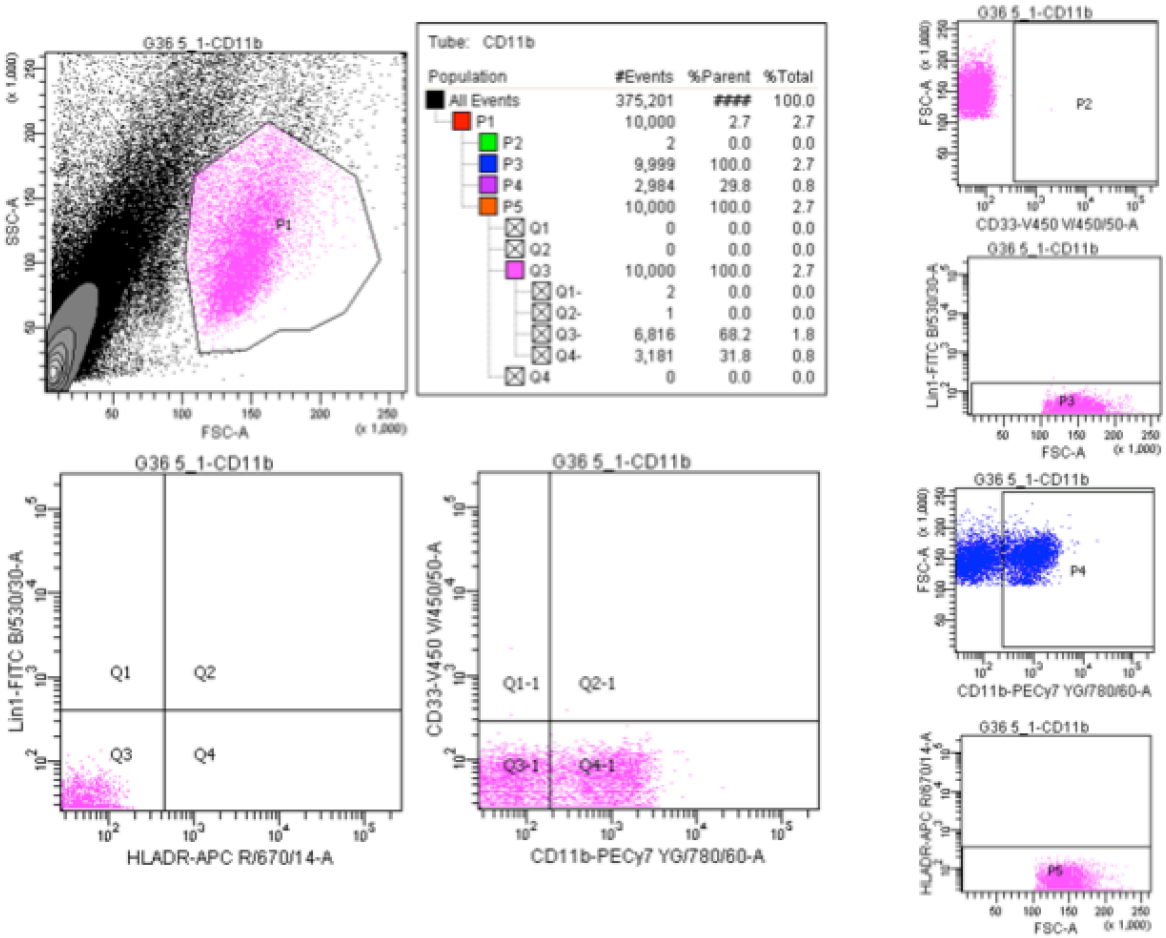

Figure 9.7. FACS schematic of MDSCs stained with only CD11b antibody (CD11b/Mac-1 PE Cy7 Mouse Anti-Human, BD Pharmingen®). All samples had a CD11b stained sample analysed to ensure samples were not compromised and cell separation was standard and valid. Ten thousand cells were analysed in the target population (P1). The yellow green laser was used with a filter set at 760/60 nm. The $CD11b^{+}$ cell population was gated as shown in the figure as P4.

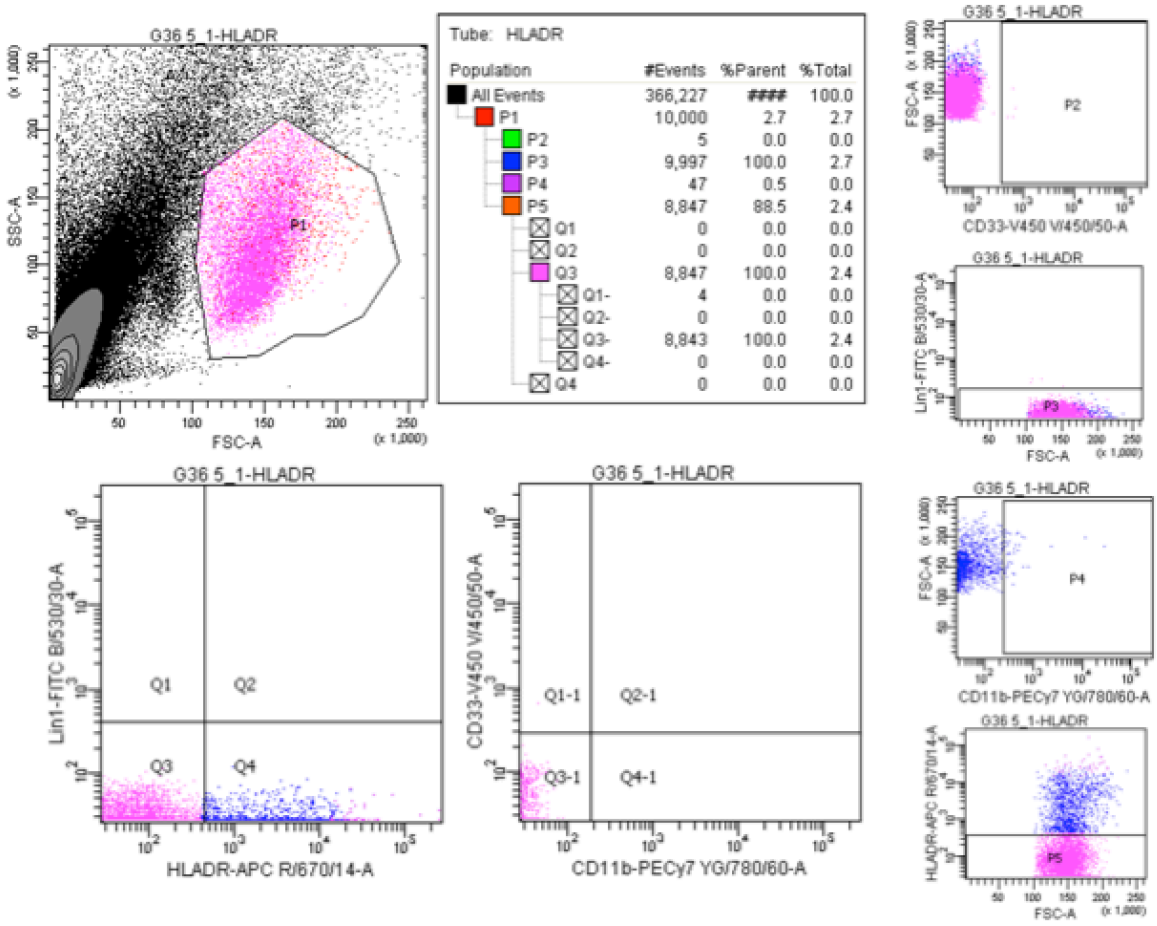

Figure 9.8. FACS schematic of MDSCs stained with only HLA-DR antibody (HLA-DR APC Mouse Anti-Human, BD Pharmingen®.) All samples had a HLA-DR stained sample analysed to ensure samples were not compromised and cell separation was standard and valid. Ten thousand cells were analysed in the target population (P1). The red laser was used with a filter set at 670/14 nm. The HLA-DR$^-$ cell population was gated as shown in the figure as P5.

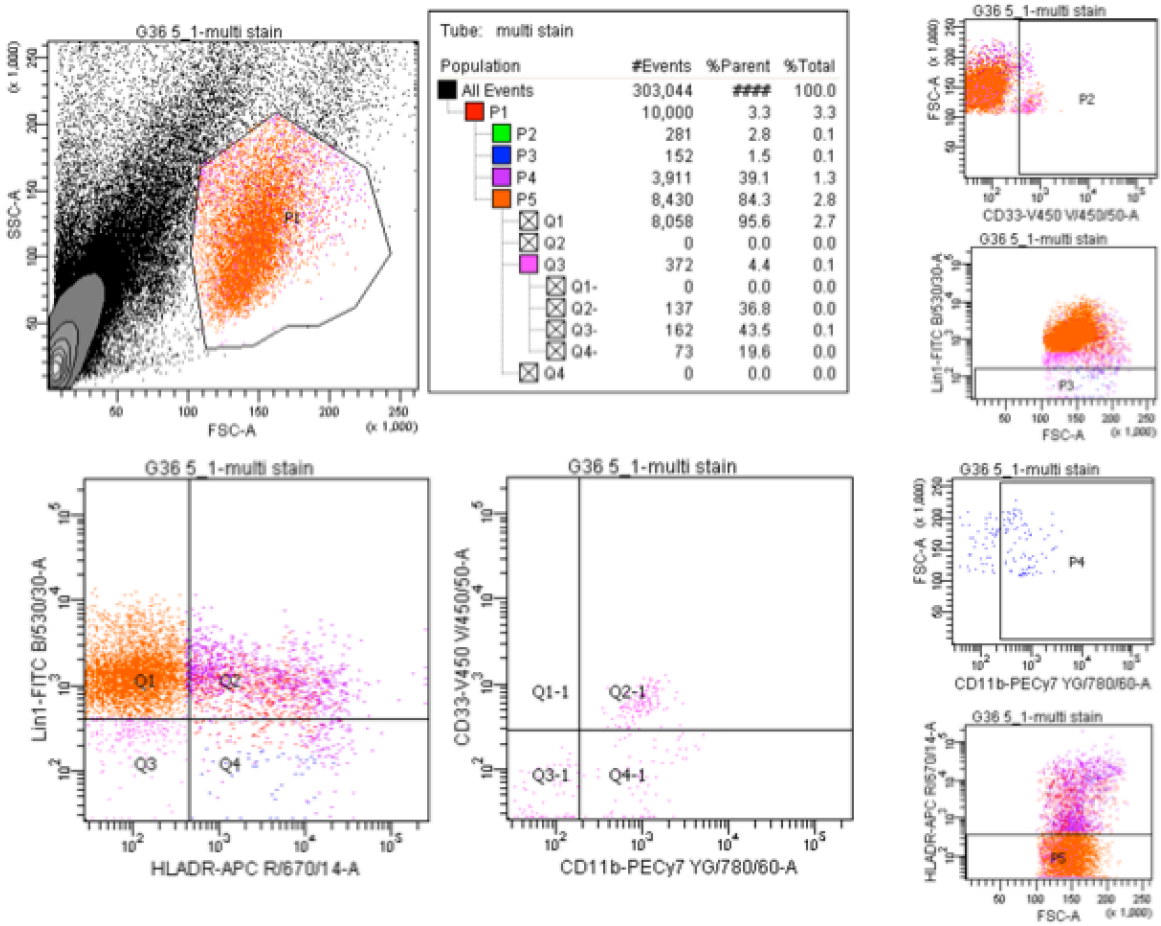

Figure 9.9. FACS schematic of MDSCs with a quadruple stain for HLA-DR$^-$, Lin1$^-$, CD33$^+$ and CD11b$^+$ antibodies. Prior to analysing a complete quadruple stain sample an initial analysis of ten thousand cells in the target population (P1) was conducted to ensure appropriate staining of cells. A quadruple stained sample was analysed to ensure samples were not compromised and cell separation was standard and valid. MDSCs were gated off P5 (HLA-DR$^-$) as Q3 (HLA-DR$^-$ & Lin1$^-$) and further gated as CD33$^+$ and CD11b$^+$ in Q2.1, or CD11b$^+$ in Q2.1 and Q4.1. HLA-DR$^-$, Lin1$^-$, CD33$^+$ and CD11b$^+$ MDSCs are seen as a distinct population in Q2.1. Lin1$^-$, HLA-DR$^-$, CD11b$^+$ MDSCs are seen in Q2.1 & Q4.1.

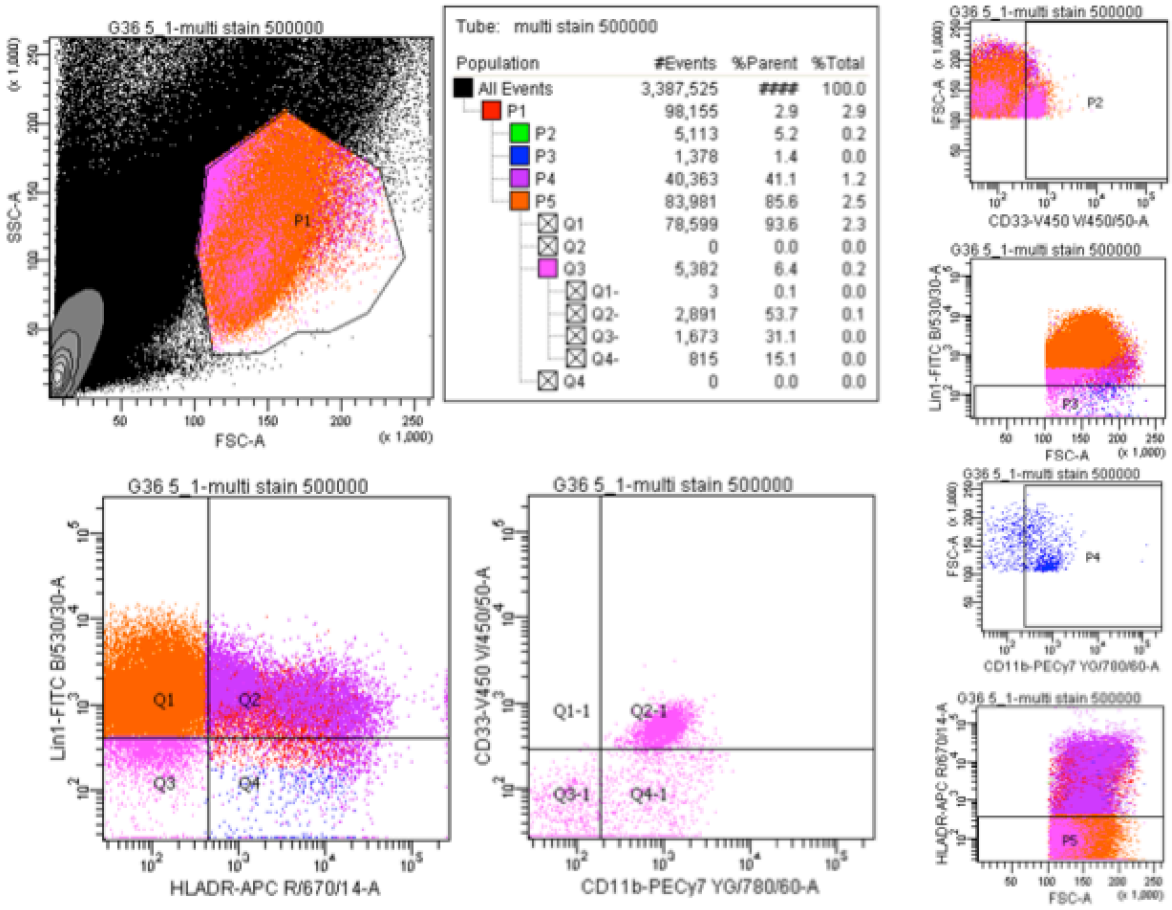

Figure 9.10. FACS schematic of MDSCs with a quadruple stain for HLA-DR$^-$, Lin1$^-$, CD33$^+$ and CD11b$^+$ antibodies. The samples were analysed until the entire sample was completed. An average of 328,851 cells in the target population were analysed over the one hundred and sixty-one samples investigated. MDSCs were gated off P5 (HLA-DR$^-$) as Q3 (HLA-DR$^-$ & Lin1$^-$) and further gated as CD33$^+$ and CD11b$^+$ in Q2.1, or CD11b$^+$ in Q2.1 and Q4.1. HLA-DR$^-$, Lin1$^-$, CD33$^+$ and CD11b$^+$ MDSCs are seen as a distinct population in Q2.1. Lin1$^-$, HLA-DR$^-$, CD11b$^+$ MDSCs are seen in Q2.1 & Q4.1. MDSCs were then calculated as a percentage of the target population (P1).

9.10 Tregs FACS analysis

PBMCs were analysed for Tregs. One hundred and thirty six samples were analysed from eighteen trial patients and nine control patients. Tregs were identified as triple positive for CD4, CD25 and Fox-P3 antibodies. Samples were analysed for the unstained cells, each individual antibody and a combination stain.

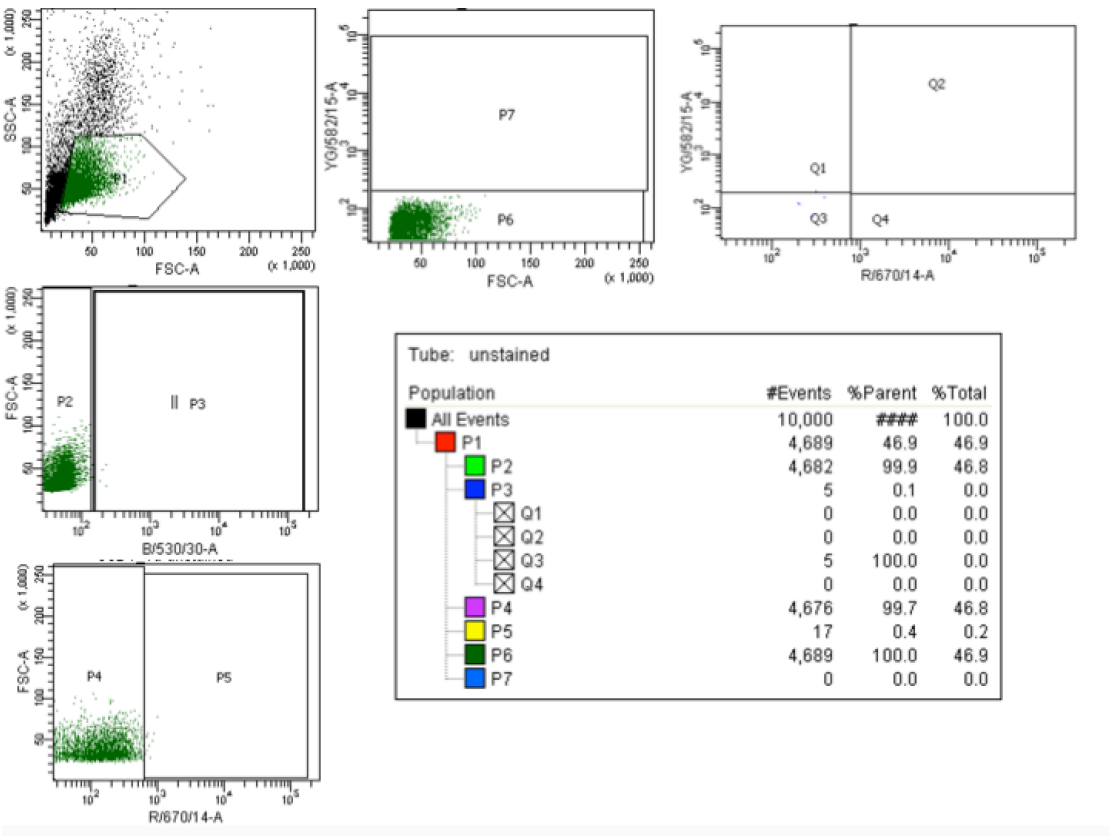

Figure 9.11. FACS schematic of unstained T regulator cells. All samples had an unstained sample analysed to ensure sample were not compromised and cell separation was standard and valid. Ten thousand cells were analysed in the target population (P1).

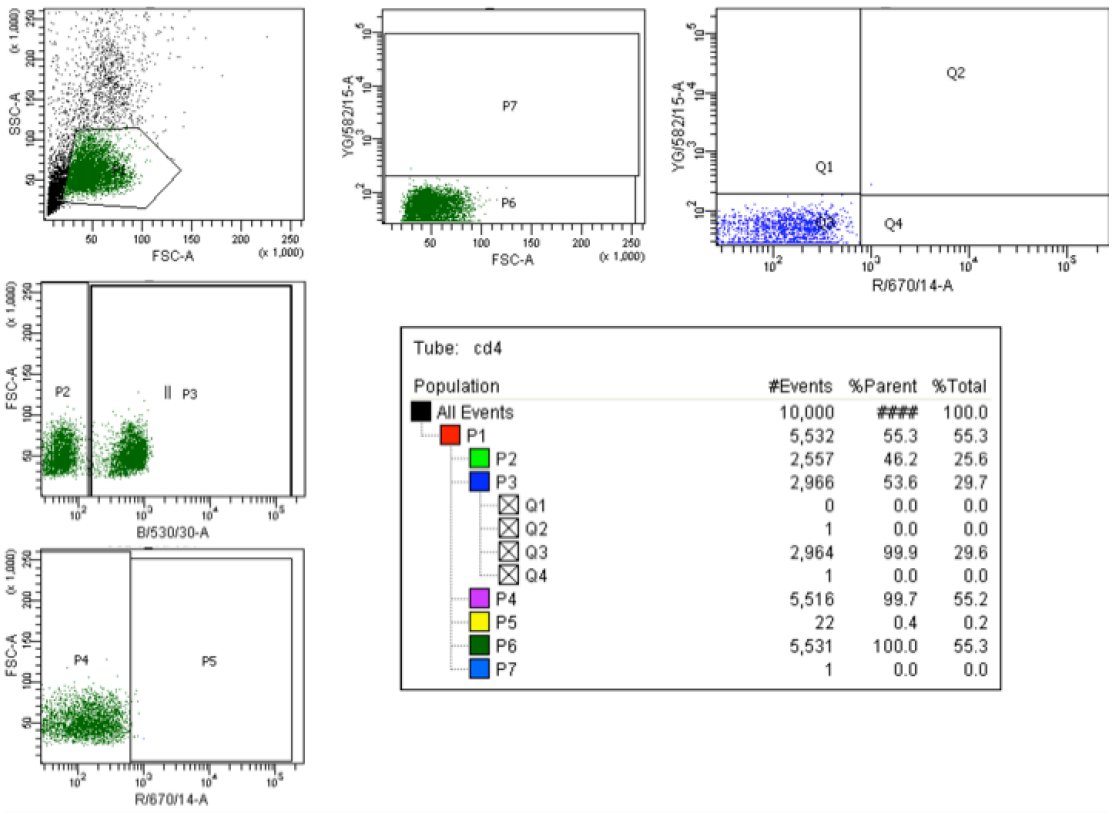

Figure 9.12. FACS schematic of T regulator cells stained with only CD4 antibody (CD4 FITC Mouse Anti-Human, BD Pharmingen®). All samples had a CD4 stained sample analysed to ensure samples were not compromised and cell separation was standard and valid. Ten thousand cells were analysed in the target population (P1). The blue laser was used with a filter set at 530/30 nm. The $CD4^+$ cell population was gated as shown in the figure as P3.

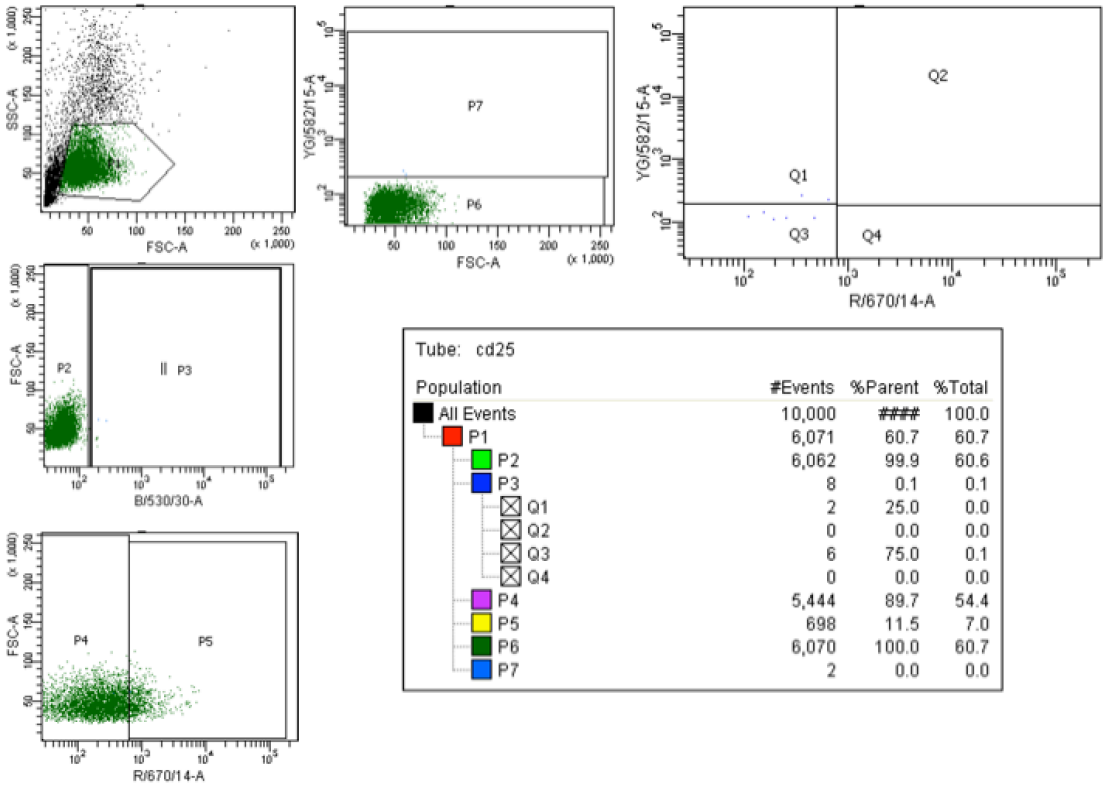

Figure 9.13. FACS schematic of T regulator cells stained with only CD25 antibody (CD25 APC Mouse Anti-Human, BD Pharmingen). All samples had a CD25 stained sample analysed to ensure samples were not compromised and cell separation was standard and valid. Ten thousand cells were analysed in the target population (P1). The red laser was used with a filter set at 670/14 nm. The $CD25^{+}$ cell population was gated as shown in the figure as P5.

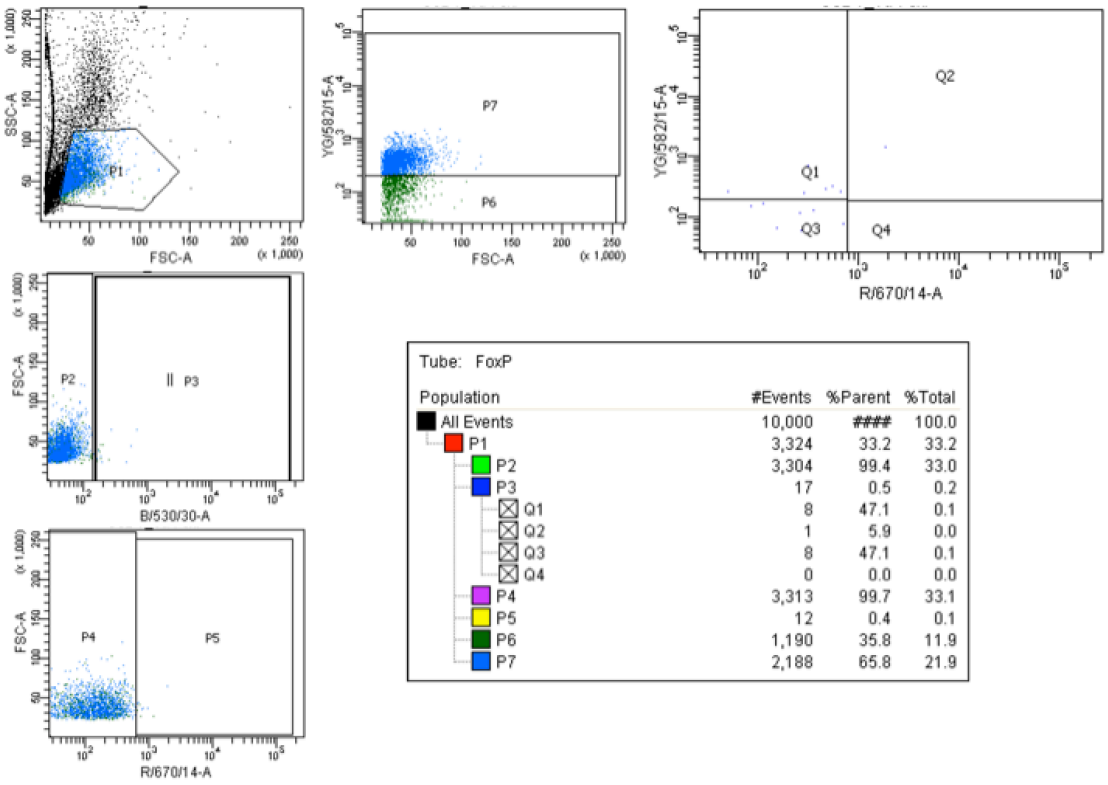

Figure 9.14. FACS schematic of T regulator cells stained with only Fox-P3 antibody (Fox-P3 PE Mouse Anti-Human, BD Pharmingen®). All samples had a Fox-P3 stained sample analysed to ensure samples were not compromised and cell separation was standard and valid. Ten thousand cells were analysed in the target population (P1). The yellow green laser was used with a filter set at 582/15 nm. The Fox-P3^{+} cell population was gated as shown in the figure as P7.

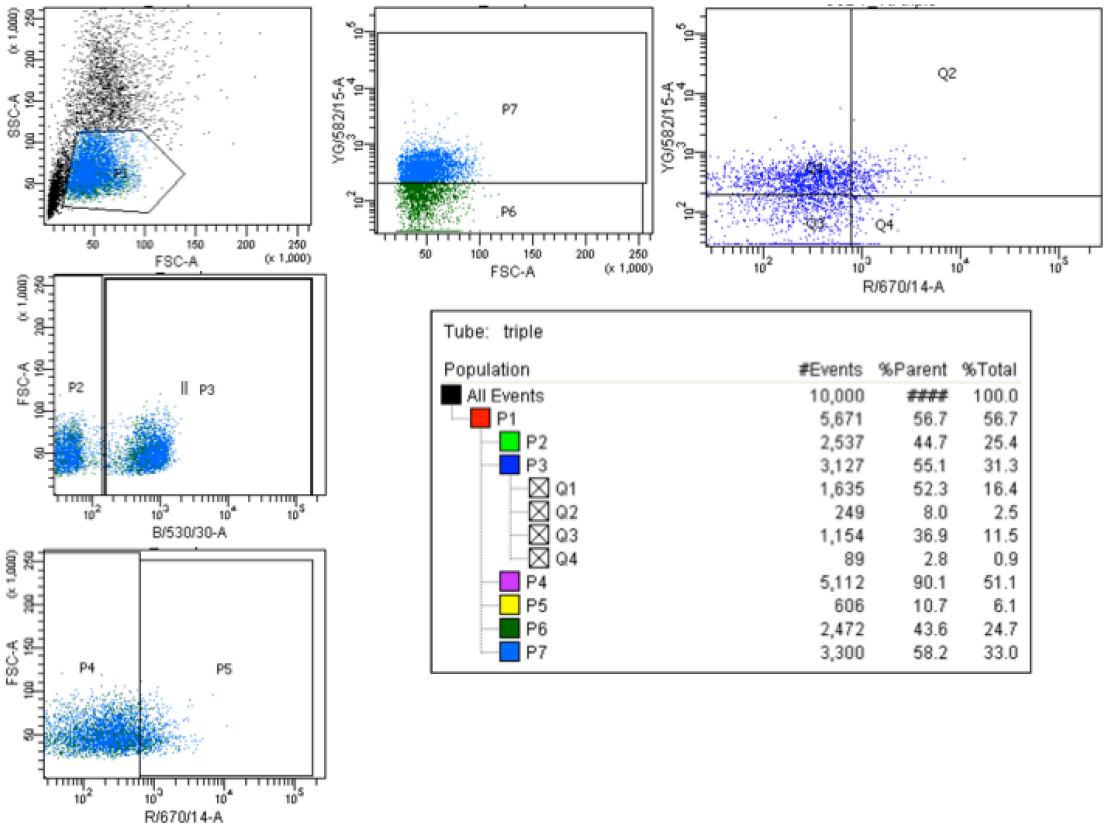

Figure 9.15. FACS schematic of T regulator cells with a triple stain for $CD4^+$, $CD25^+$ and Fox-$P3^+$ antibodies. Prior to analysing a complete triple stain sample an initial analysis of ten thousand cells in the target population (P1) was conducted to ensure appropriate staining of cells. A triple stained sample was analysed to ensure samples were not compromised and cell separation was standard and valid. T regulator cells were gated off P3 ($CD4^+$), as $CD4^+$, $CD25^+$ and Fox-$P3^+$ and can be seen as Q2 in the diagram.

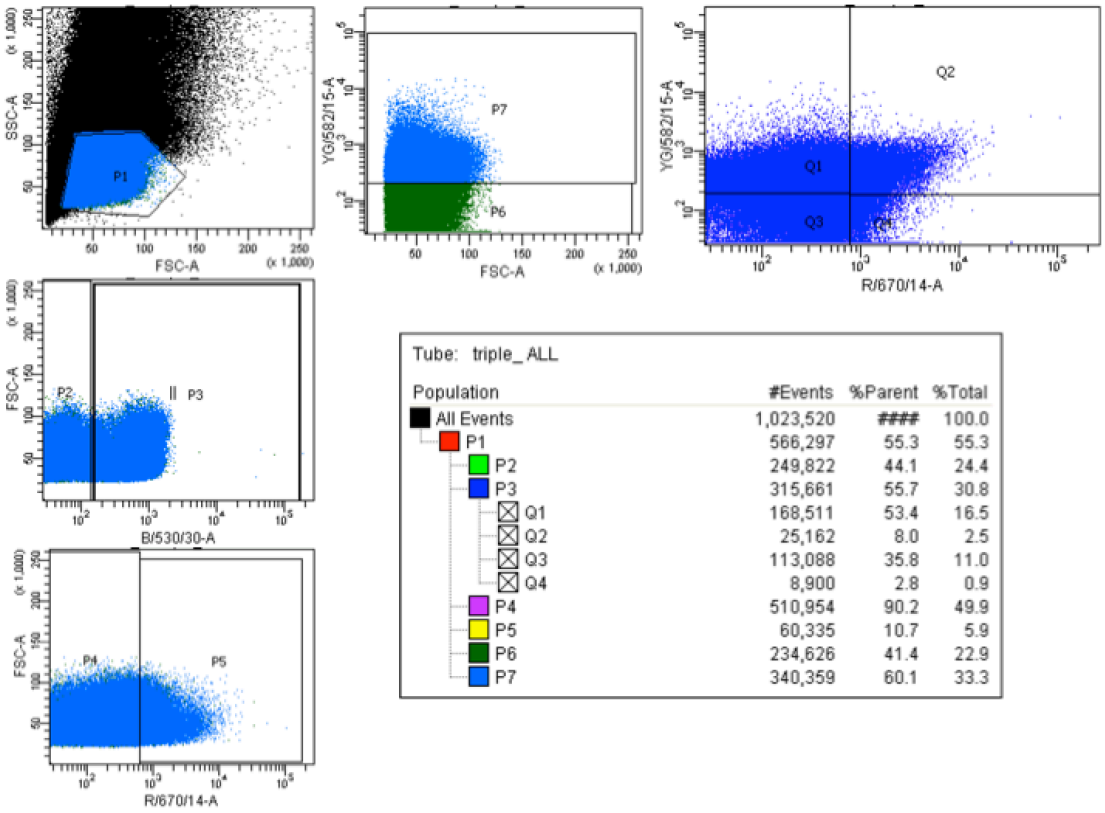

Figure 9.16. FACS schematic of T regulator cells with a triple stain for CD4, CD25 and Fox-P3 antibodies. The samples were analysed until the entire sample was completed. An average of 366,626 cells in the target population were analysed over the one hundred and thirty-six samples investigated. T regulator cells were gated off P3 ($CD4^+$), as $CD4^+$, $CD25^+$ and Fox-$P3^+$ and can be seen as Q2 in the diagram. T regulator cells were then calculated as a percentage of the target population.

9.11 EPC FACS output

PBMC were analysed for EPCs. EPCs with three antibody phenotypes were analysed:

1. $CD45^-$, $CD31^+$ and $CD133^+$.

2. $CD45^-$, $CD31^+$ and $CD34^+$.

3. $CD45^-$, $CD31^+$, $CD133^+$ and $CD34^+$.

Samples were analysed for the unstained cells, each individual antibody and a combination stain.

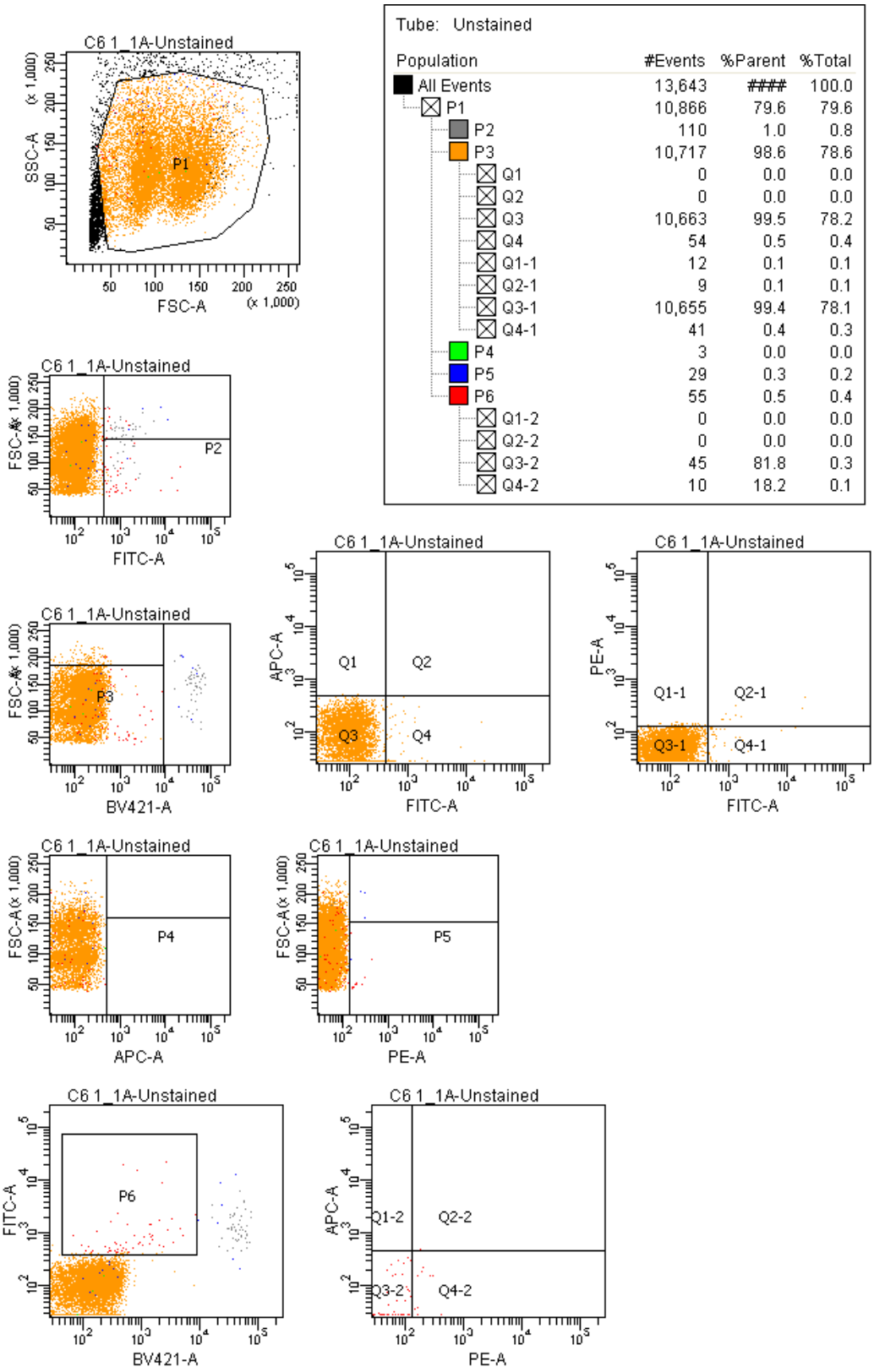

Figure 9.17. FACS schematic of unstained EPCs. All samples had an unstained sample analysed to ensure sample were not compromised and cell separation was standard and valid. Ten thousand cells were analysed in the target population (P1).

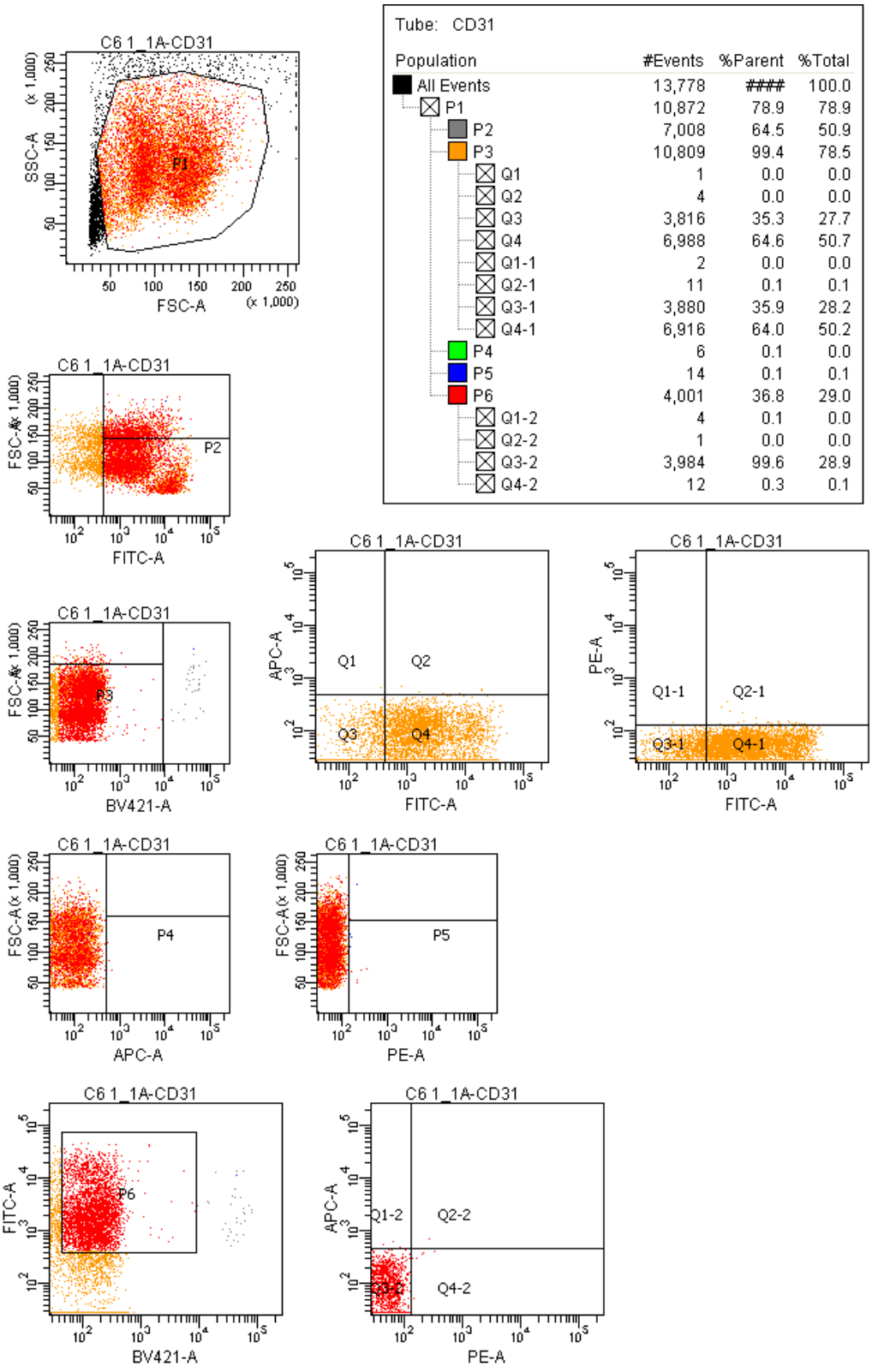

Figure 9.18. FACS schematic of EPCs stained with only CD31 antibody (CD31 FITC Mouse Anti-Human, BD Pharmingen®). All samples had a CD31 stained sample analysed to ensure samples were not compromised and cell separation was standard and valid. Ten thousand cells were analysed in the target population (P1). The blue laser was used with a filter set at 530/30 nm. The $CD31^{+}$ cell population was gated as shown in the figure as P2.

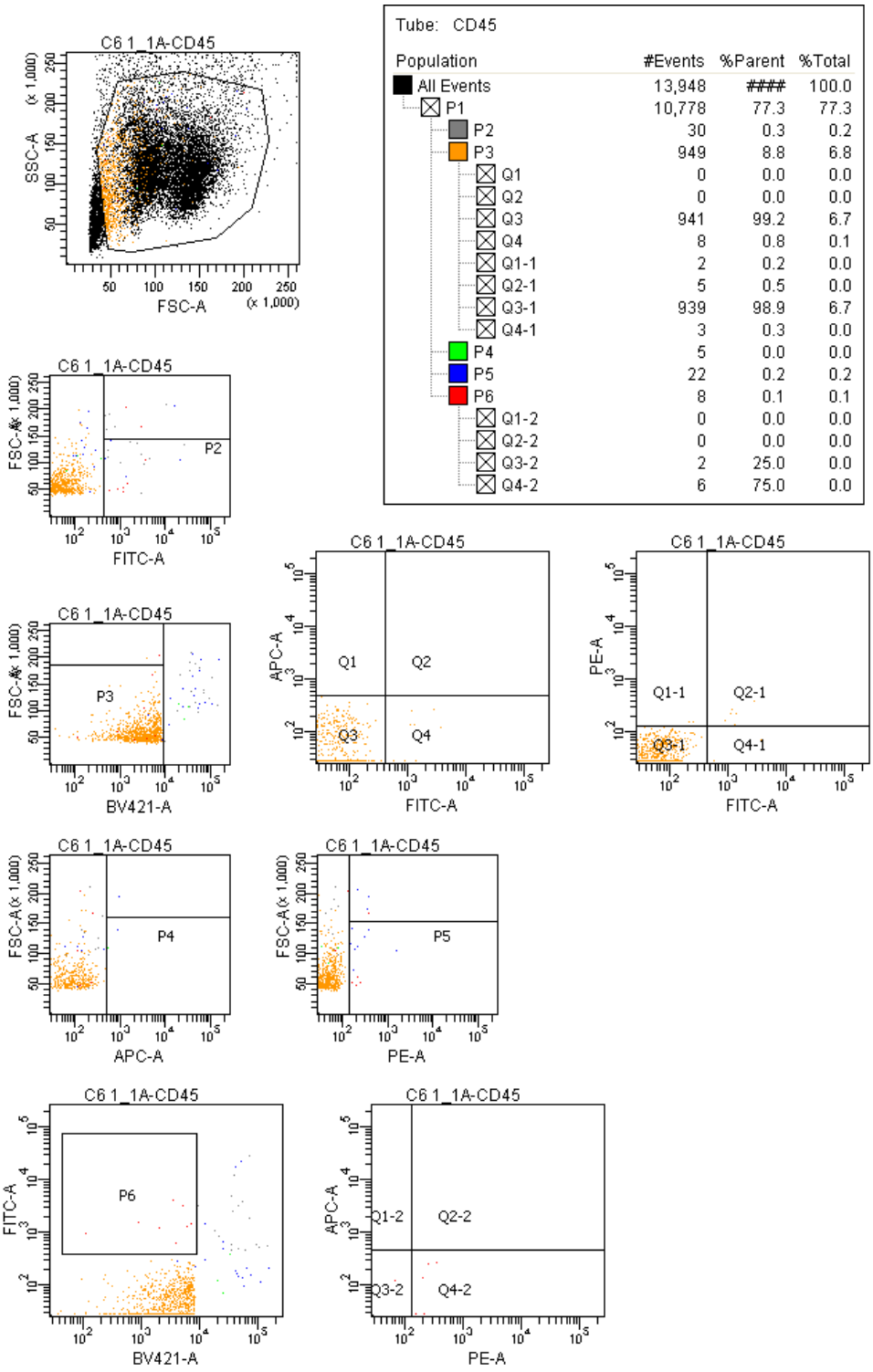

Figure 9.19. FACS schematic of EPCs stained with only CD45 antibody (CD45 R/B220 Pacific Blue Mouse Anti-Human, BD Pharmingen®). All samples had a $CD45^-$ stained sample analysed to ensure samples were not compromised and cell separation was standard and valid. Ten thousand cells were analysed in the target population (P1). The violet laser was used with a filter set at 450/50 nm. The $CD45^-$ cell population was gated as shown in the figure as P3.

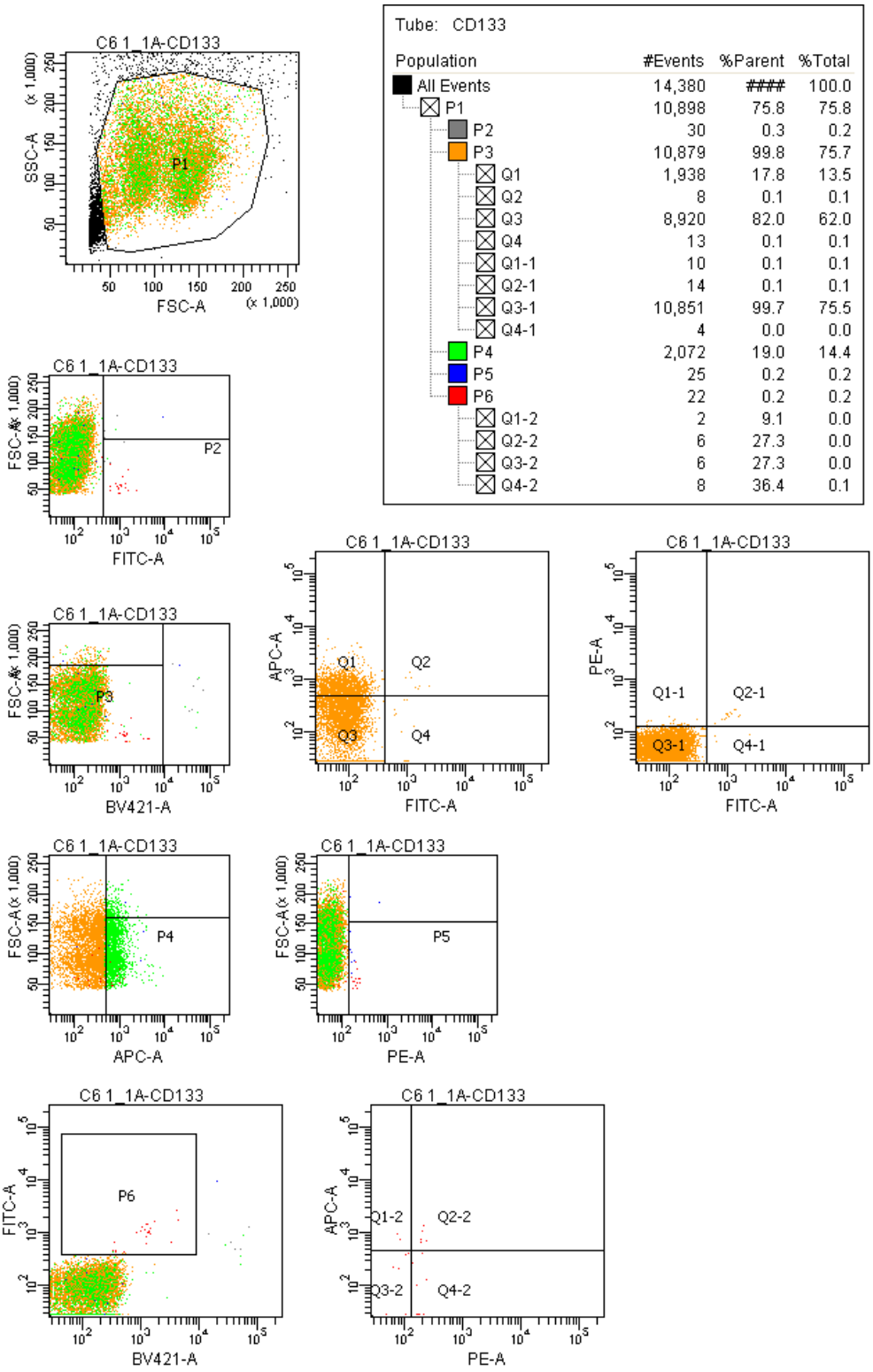

Figure 9.20. FACS schematic of EPCs stained with only CD133 antibody (CD133 APC, Miltenyi Biotec®). All samples had a CD133 stained sample analysed to ensure samples were not compromised and cell separation was standard and valid. Ten thousand cells were analysed in the target population (P1). The red laser was used with a filter set at 670/14 nm. The $CD133^{+}$ cell population was gated as shown in the figure as P4.

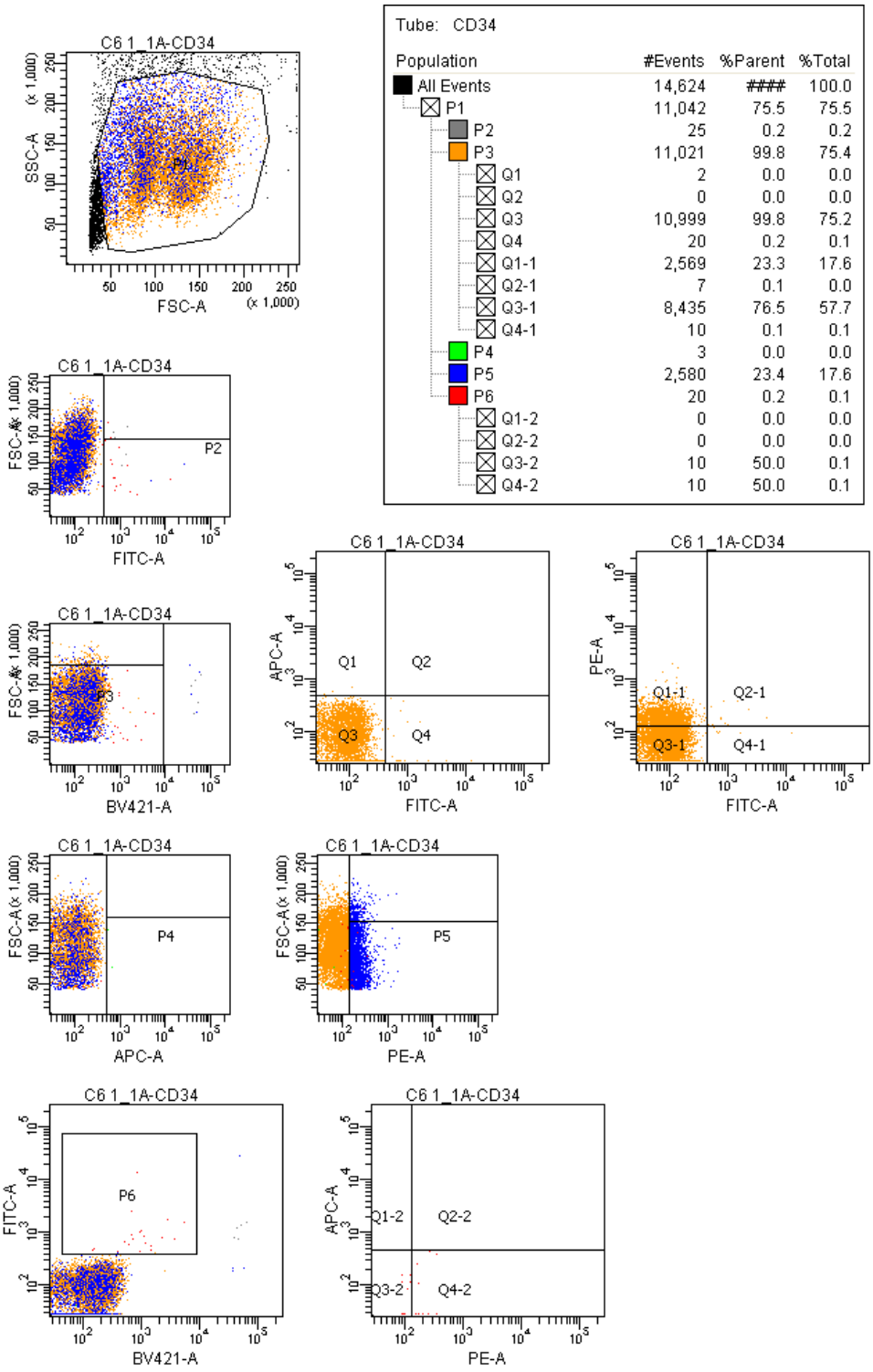

Figure 9.21. FACS schematic of EPCs stained with only CD34 antibody (CD34 PE Mouse Anti-Human, BD Pharmingen®). All samples had a CD34 stained sample analysed to ensure samples were not compromised and cell separation was standard and valid. Ten thousand cells were analysed in the target population (P1). The yellow green laser was used with a filter set at 582/15 nm. The $CD34^{+}$ cell population was gated as shown in the figure as P5.

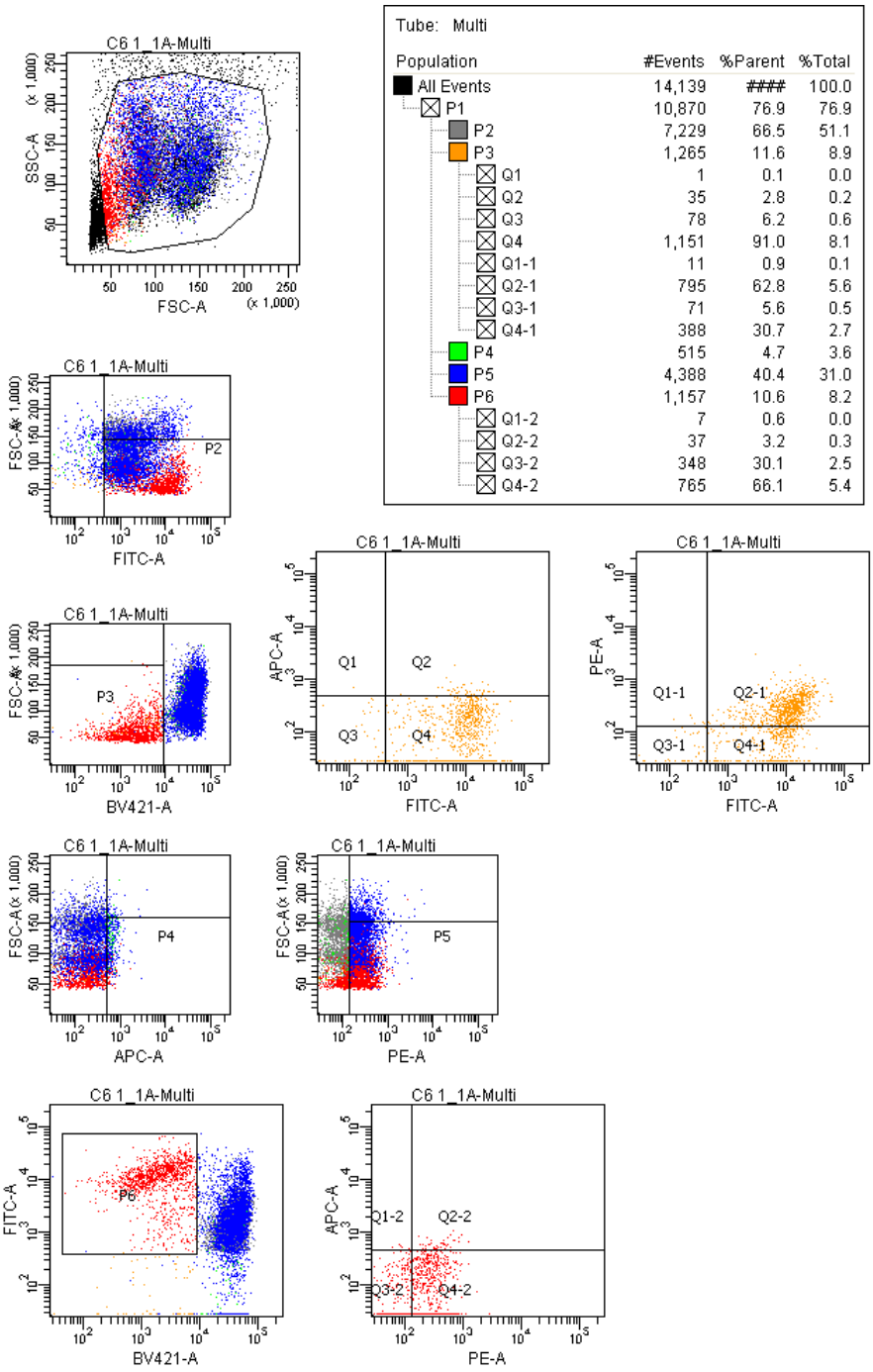

Figure 9.22. FACS schematic of EPCs with a quadruple stain for $CD45^-$, $CD31^+$, $CD133^+$ and $CD34^+$ antibodies. Prior to analysing a complete quadruple stain sample an initial analysis of ten thousand cells in the target population (P1) was conducted to ensure appropriate staining of cells. A trial quadruple stained sample was analysed to ensure samples were not compromised and cell separation was standard and valid. Three populations of EPCs were analysed. EPCs with a $CD45^-$, $CD31^+$, $CD133^+$ and $CD34^+$ phenotype are seen in Q2.2 ($CD133^+$ (APC) and $CD34^+$ (PE)), gated off P6 ($CD31^+$ (FITC) and $CD45^-$ (R/B220 pacific blue). EPCs with a $CD45^-$, $CD31^+$and $CD34^+$ phenotype are seen in Q2.1 ($CD34^+$ (PE) and $CD31^+$ (FITC)), gated off P3 ($CD45^-$ (R/B220 pacific blue). EPCs with a $CD45^-$, $CD31^+$and $CD133^+$ phenotype are seen in Q2 (CD31+ (FITC) and CD133+ (APC)), gated P3 ($CD45^-$ (R/B220 pacific blue).

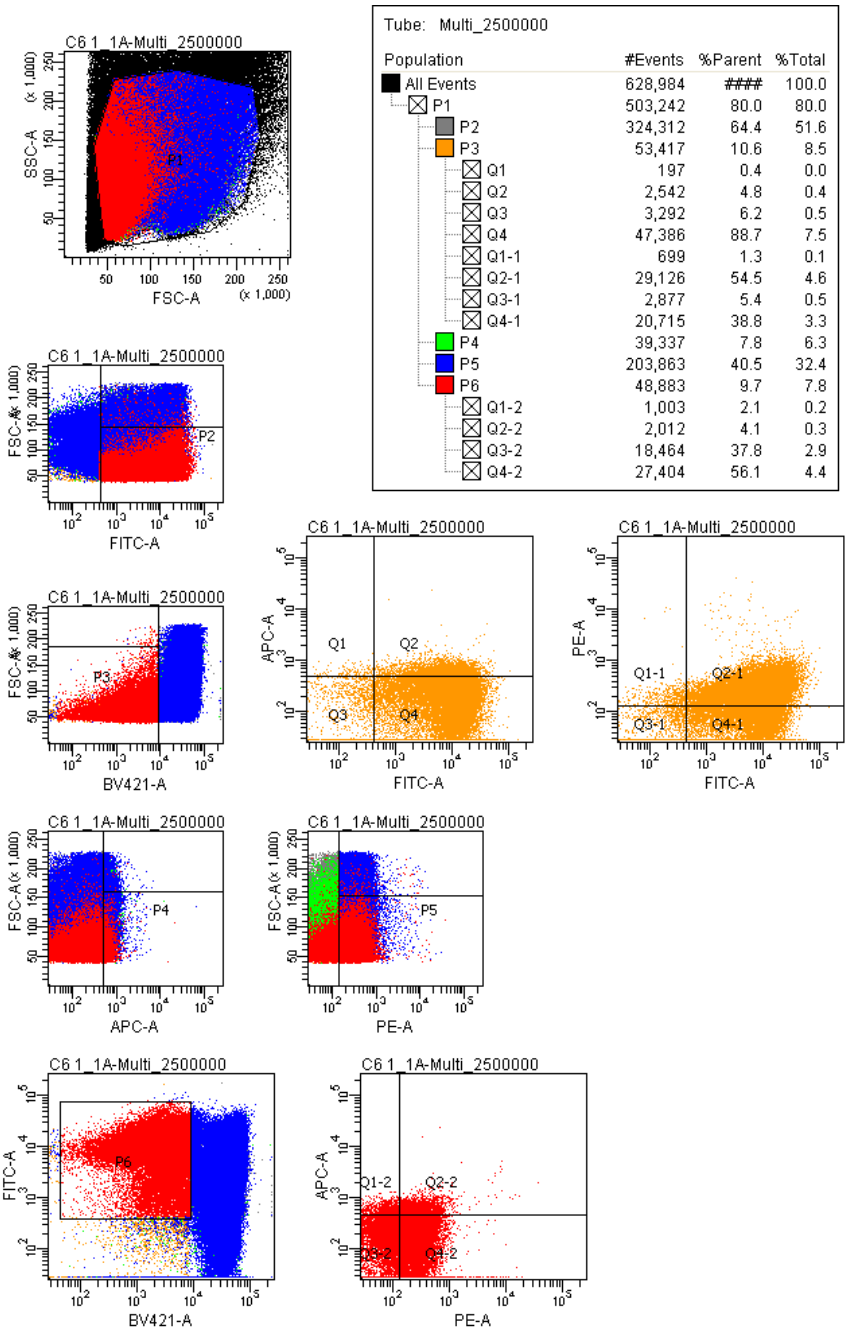

Figure 9.23. FACS schematic of EPCs with a quadruple stain for $CD45^-$, $CD31^+$, $CD133^+$ and $CD34^+$ antibodies. The samples were analysed until the entire sample was completed. An average of 374,796 cells in the target population were analysed over the one hundred and thirty-four samples investigated. Three populations of EPCs were analysed. EPCs with a $CD45^-$, $CD31^+$, $CD133^+$ and $CD34^+$ phenotype are seen in Q2.2 ($CD133^+$ (APC) and $CD34^+$ (PE)), gated off P6 ($CD31^+$ (FITC) & $CD45^-$ (R/B220 pacific blue). EPCs with a $CD45^-$, $CD31^+$and $CD34^+$ phenotype are seen in Q2.1 ($CD34^+$ (PE) and $CD31^+$ (FITC)), gated off P3 ($CD45^-$ (R/B220 pacific blue). EPCs with a $CD45^-$, $CD31^+$and $CD133^+$ phenotype are seen in Q2 (CD31+ (FITC) and CD133+ (APC)), gated P3 ($CD45^-$ (R/B220 pacific blue).

9.12 MicroRNA analysis

Blood samples were collected from each patient at each treatment point and post treatment. Each 19.6mL of whole blood was collected in 4 x 4.9mL Ethylenediaminetetraacetic acid (EDTA) bottles. Samples were centrifuged at 400g for five minutes to separate blood from plasma. Four mL of plasma was transferred into 4 x 2mL Eppendorf ® safe-locking micro-centrifuge tubes and stored in -80˚C. One hundred and thirty-nine samples were processed in twenty-six patients (seventeen trial and nine control patients [T1 was excluded as patient's samples were misplaced].

MiRNA analysis was conducted in collaboration with professor Chang's laboratory in the Molecular Medicine Research Center, Chang Gung University, Taipei, Taiwan. Samples were transferred to Taiwan by international courier with dry ice maintaining a temperature of -80˚C. This was ensured and checked regularly by the international courier. I did not process the samples myself but traveled to the laboratory to review all techniques and results with the department in Taiwan.

9.12.1 RNA preparation and reverse transcription

Candidate miRNAs were confirmed prior to analysis as discussed previously and samples checked for haemolysis prior to processing.

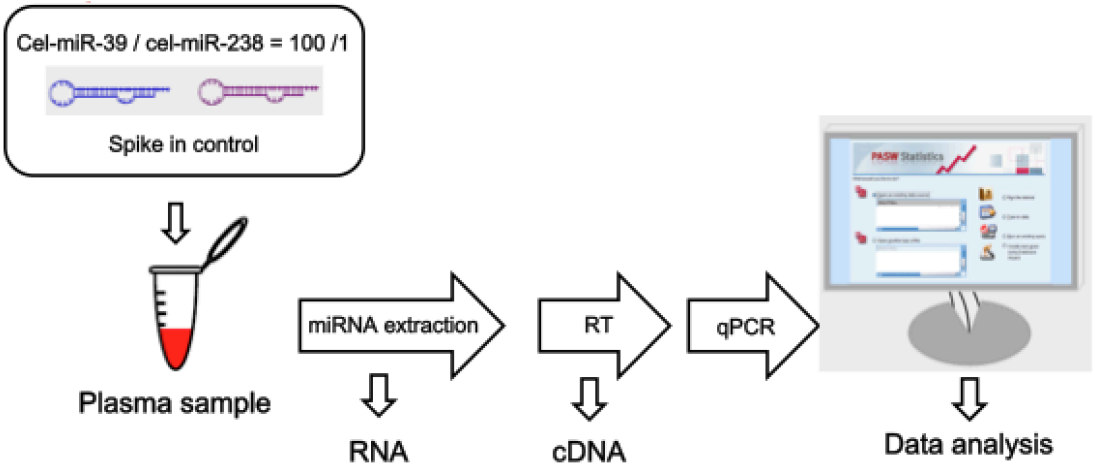

Figure 9.24. Figure showing overview of workflow method for microRNA analysis. A spike in control is an RNA transcript used to calibrate measurements (Cel-miR-39 and cel-miR-238). MiRNA was extracted from 300µl of plasma sample. Complementary DNA (cDNA) was made by reverse transcriptase (RT), which underwent quantitative PCR (qPCR) before data analysis.

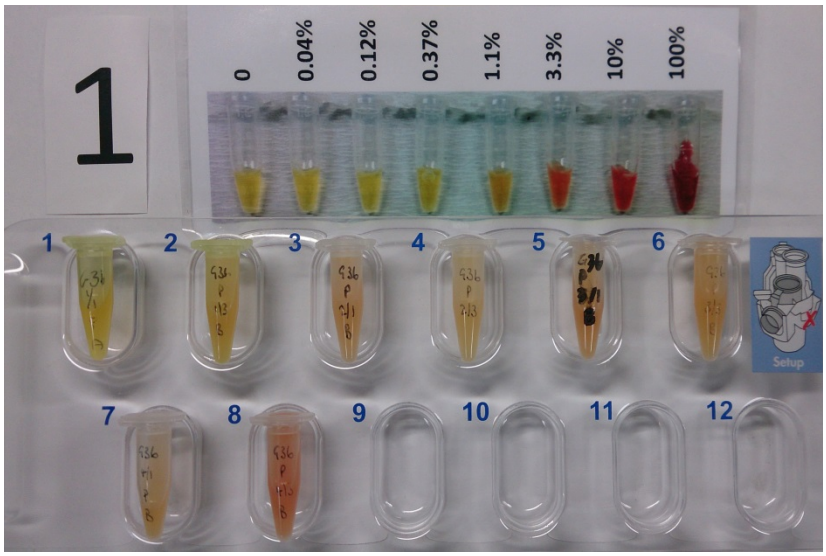

Figure 9.25. Test samples were analysed for their haemolysis level against a haemolysis measurement scale. Haemolysis can cause aberrant results of miRNA levels. Samples with a haemolysis over 10% were excluded (n=0).

A sensitivity and specificity assay was conducted prior to processing. The sensitivity assay was conducted to check for PCR efficiency and copy number transformation. The specificity assay was conducted to ensure the specificity between the primers/probe

and its own candidate miRNA. A standard curve and formula for each candidate was calculated.

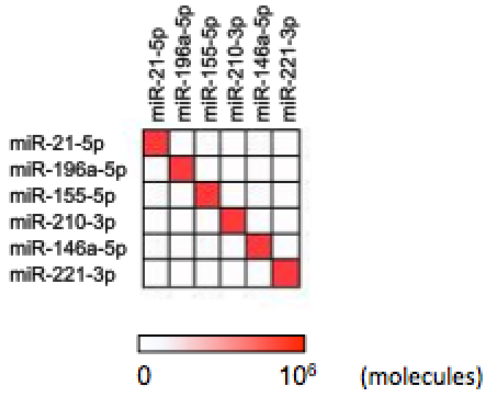

Figure 9.26. Specificity assay measured the specificity of the primer/probe to the candidate miRNA. It was important to ensure that there was no overlap between primer /probe and other miRNAs.

MiRNA extraction was conducted by extracting the total RNA using 300µl of plasma sample with miRNeasy® minikit (QIAGEN, Germany). 700µL of QUIzol® lysis reagent (QIAGEN, Germany) was added to the plasma sample, and the sample stood at room temperature for 5 minutes. 1nM of synthetic cel-miRNA-39 RNA (with a nucleotide signature of: 5'-CGAUGGGCAGCUAUAUUCACCUUG-3' (A=adenine, C=cytosine, G=Guanine, T=thiamine)) was added into the mixture as the spike-in control. 140µl of chloroform (Merck Millipore, USA) was added into the sample and mixed well for 15 seconds. This was allowed to stand for 3 minutes at room temperature.

550µl of the upper layer of the sample was aspirated and centrifuged at 15,000g at 4˚C for 15 minutes. The sample was then well mixed with 825µl of ethanol and then eluted through the micro-column and washed with RWP and RPE buffer (Qiagen Ltd. Crawley, UK). The total RNA was dissolved in 30 µl of RNase free water (QIAGEN, Germany). To convert detected miRNA into its corresponding complementary DNA (cDNA), 5.4µL of total RNA was added to 75nM of 20 miRNA primers mix, 0.5mM deoxynucleotide (dNTP, ThermoFisher Scientific, USA), 2 units RNaseOUT™ (ThermoFisher Scientific, USA: RNaseOUT™ recombinant ribonuclease Inhibitor is a potent non-competitive inhibitor of pancreatic-type ribonucleases such as RNase A, and is used to avoid RNA

degradation, and 120 units (200units/µL) of Superscript III (Invitrogen, CA) were used for reverse transcription reaction in a total reaction mixture of 12µl. Using the miRNeasy® minikit the processing program was set at 16°C for 30 minutes, followed by 49 cycles of 20°C for 30 seconds, 42°C for 30 seconds and 50°C for 1 second, and then kept at 72°C for 10 minutes. Reverse transcription products were stored at -20°C.

9.12.2 Quantitative real-time polymerase chain reaction (qPCR) assay

To 8 ml of miRNA qPCR assay, 0.5 µl of 5-folds diluted reverse transcriptase product was used as a template, and mixed together with4 µl 2 X master mix (Applied Biosystems, Foster City, CA), 0.25 mM universal reverse primer, 0.2 mM gene specific primers before being subjected to qPCR. This was performed using QuantStudio™ 12K Flex Real-time PCR System (Applied Biosystems, Foster City, CA). The qPCR protocol included: 95˚C for 10 minutes, followed 45 cycles at 95˚C for 15 seconds, and then at 60˚C for 30 seconds and a dissociation stage.

Data was processed using standard calculations. The cycle threshold (CT) was calculated and calibrated from the spike-ins. The degree of hybridization between the spike-ins and the control probes is then used to normalize the hybridization of the sample miRNA. The normalized data is adjusted for the copy number transformation and analysed.

9.13 Statistical analysis

Statistical advice was taken from Professor John Thompson (Professor of Genetic Epidemiology, University of Leicester). Changes in immune suppressor cells were analysed with Paired Students t-test to assess the differences in each study group and Unpaired Students t-test to assess the difference between study groups. Overall and progression free survival data was analysed with Kaplan-Meier curves with the log-rank (Mantel-Cox) test used. Clinical outcomes were correlated with changes in mediators and survival curves analysed with a log-rank (Mantel-Cox) test. Changes in mediators over the trial in both trial and control patients and between groups were analysed with two bespoke statistical models using STATA software (StataCorp, 4905 Lakeway Dr, College Station, TX 77845, Version 14.0 for Mac). A mixed effects regression model was utilised that generated regression analysis lines which allowed for random variation. These models were chosen as clinical trial data varies in length depending on individual treatment in addition to missing time points for various reasons, both patients and investigator. Professor John Thompson designed both of the bespoke STATA models specifically for this analysis.

Analysis of samples around a 6-month time frame was selected for several reasons.

1. Six months is a commonly utilised time frame in peer-reviewed journals.

2. Six months was the treatment course for this trial and completion of the trial at six months was deemed suitable for analysis.

Survival analysis was therefore performed at six months. Additional analysis was performed at one month as the majority of patients completed one cycle and additional sample time points were available for analysis. This was necessary due to the limited survival of both cohorts.

10 Chapter Ten: Clinical Results

Patients that were eligible for trial treatment were recruited between 21/01/12 and 06/03/13 (Figure 10.1). During this period there were one hundred and thirty seven patients discussed at MDT with advanced pancreatic cancer. Eighteen patients were enrolled as trial patients. Twenty-one patients passed away prior to any treatment assessment. Six patients declined any treatment. Seventy-five patients were assessed and treated with best supportive care. One patient was enrolled in the SCALOP trial[435] (a multicentre randomised phase two trial with either gemcitabine or capecitabine based chemo radiotherapy). One Patient was treated with FOLFIRINOX. One patient was treated with gemcitabine and capecitabine, one with gemcitabine and cisplatin and one with capecitabine only. One patient was deemed to have rapidly progressive disease and it was decided at MDT that they should be only eligible for gemcitabine treatment. Twelve patients were treated with gemcitabine only and not enrolled in the trial. This was decided at consultant oncology review and the patients were not deemed eligible for trial treatment based on performance status. All patients who were approached to participate in the trial were subsequently recruited.

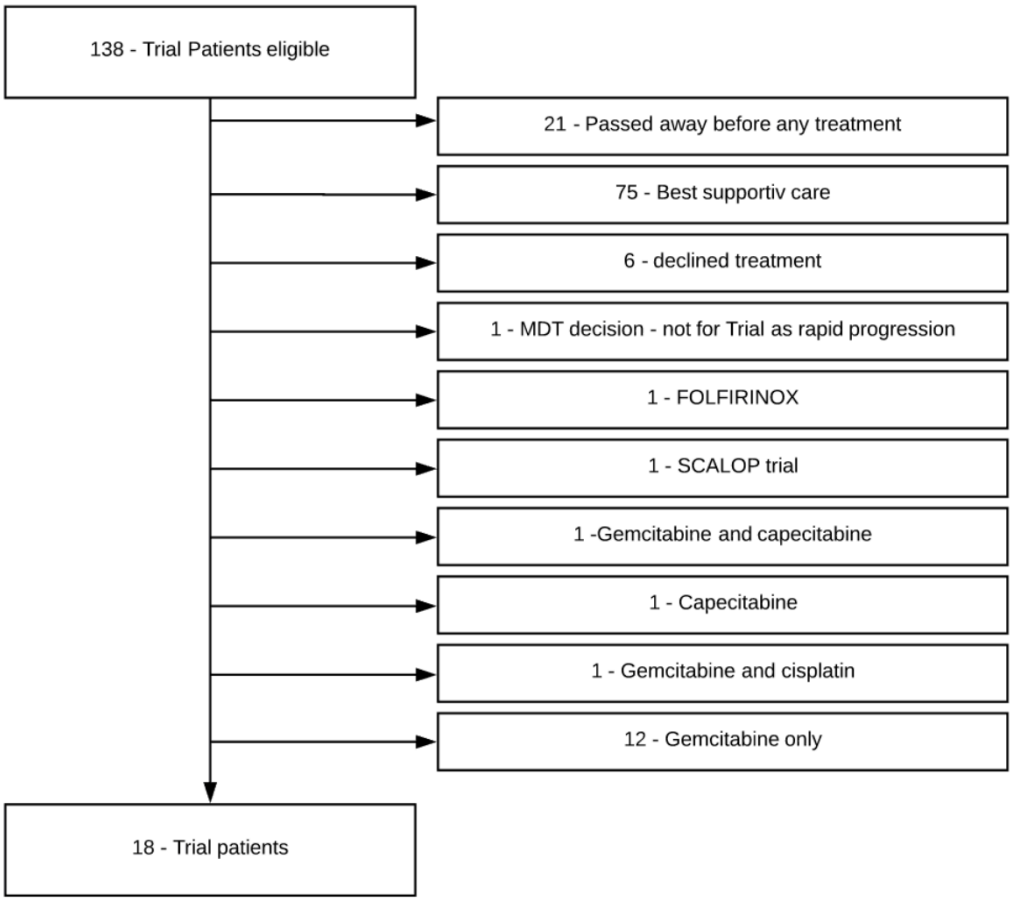

Figure 10.1. Diagram showing patient recruitment to the trial cohort.

Between 06/03/2013 and 04/11/2013 no patients were recruited as either trial or control. The Phase II trial that the trial patients were recruited had been completed and the control trial arm had not been received research and development approval. In between this time fifty-four patients were discussed at MDT. Fifteen patients were assessed and treated with best supportive care. One patient declined any treatment. Twelve patients passed away prior to any treatment. Twenty-six patients were treated with chemotherapy during this period.

Recruitment of control patients took place between 04/11/2013 and 14/05/2014. Twenty-one patients were discussed at the MDT. Seven patients passed away prior to any treatment. Two patients declined any treatment. Five were treated with best supportive care. One patient was referred for off trial radiotherapy at MDT. One patient was treated with FOLFIRINOX and one with gemcitabine and capecitabine. Four patients were treated with gemcitabine and not recruited as control patients.

This was the result of the oncologist decision, as patients were not deemed suitable based on performance status.

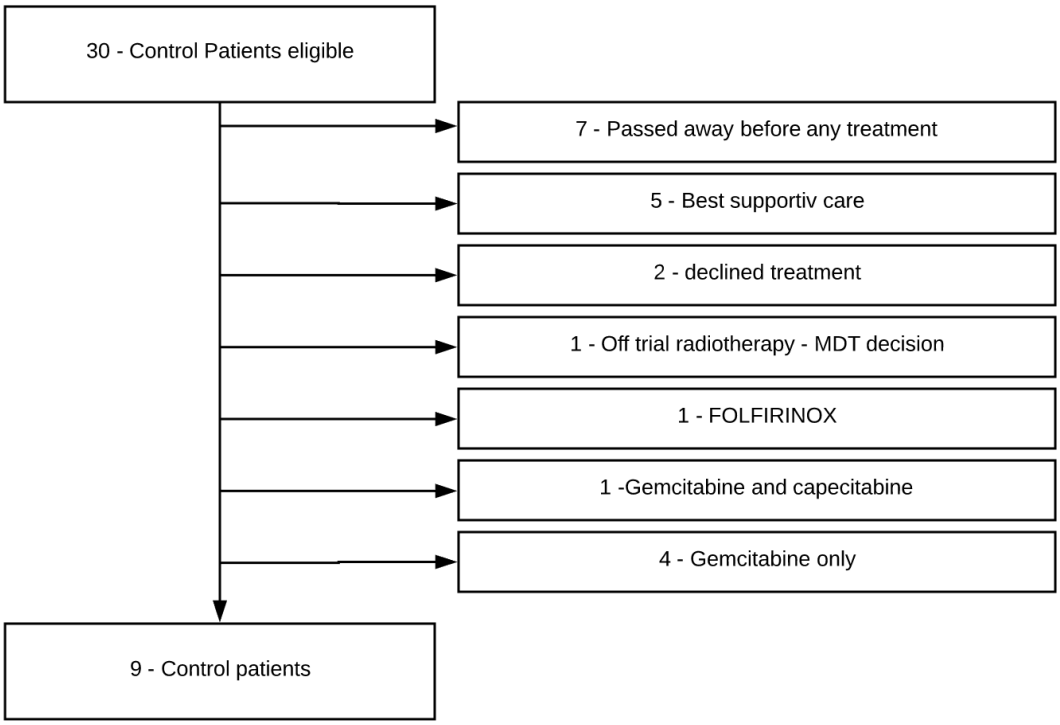

Figure 10.2. Diagram showing patient recruitment to the control cohort.

A total of twenty-seven patients were recruited into this study, eighteen trial and nine control patients. Patient's demographic data is seen in table 10.1 and 10.2.

Demographics		**Trial patients N=18**	**Control Patients N=9**
Gender	**Male** **Female**	10 8	7 2
Age	**Median age (range)** **>70 years** **<70 years**	70 (59-83) 8 10	64 (50-75) 2 8
Ethnicity	**White British** **Asian**	16 2	8 1
Baseline Weight	**Mean weight in Kilograms (range)**	62 (48-81)	69 (54-86)

Stage	**Stage 3** **Stage 4**	7 11	5 4
Total number of treatment time points (mean)		146 (6.5)	38 (3)
Number of patients completed 1 cycle (%)		14 (78%)	5 (63%)
Number of patients completed 2 cycles (%)		11 (61%)	2 (25%)
Number of patients completed 4 cycles (%)		7 (39%)	1 (12.5%)
Number of patients completed 6 cycles (%)		4 (22%)	1 (12.5%)

Table 10.1. Demographic characteristics of the study participants and the number of treatment time points and completed cycles per group. A treatment cycle included three treatment points (each week) and a rest week.

Patient: Trial-T, Control=C	ECOG	Date of first treatment	Stage	CA19.9	HB	Plt	Alb	ALT	Bil
T1	0	25/01/2012	4	12	11.0	120	40	14	6
T2	0	07/02/2012	3	8651	13.8	313	40	20	13
T3	0	28/03/2012	4	10	12.0	167	44	10	6
T4	1	23/05/2012	4	>14,000	10.7	466	34	35	20
T5	0	04/07/2012	3	32	11.2	282	43	78	4
T6	0	08/08/2012	4	>700	11.9	583	39	38	8
T7	0	22/08/2012	4	45730	12.9	334	40	33	17
T8	0	07/11/2012	3	2064	14.2	400	37	29	13
T9	1	07/11/2012	3	1382	10.8	434	39	14	4
T10	0	07/11/2012	3	398	12.7	303	44	23	10
T11	1	21/11/2012	4	50597	13.5	472	46	69	9
T12	0	12/02/2012	4	6	13.7	406	35	49	41
T13	0	12/12/2012	4	66770	11.2	352	35	47	27
T14	1	02/01/2013	3	338	12.7	510	34	33	5
T15	0	16/01/2013	3	124	12.5	281	38	33	14
T16	0	23/01/2013	4	16	11.8	307	39	18	16
T17	0	20/02/2013	4	1783	11.2	297	44	33	5
T18	1	06/03/2013	4	1586	10.3	554	47	53	25
C1	1	17/11/2013	4	72064	12.6	415	31	66	13
C2	1	08/04/2013	4	60	11.6	490	42	65	19

C3	0	11/09/2013	3	2784	71	612	41	10	7
C4	0	09/10/2013	3	206	13.2	298	43	24	8
C5	1	09/10/2013	4	<3	10.6	429	41	52	10
C6	0	16/10/2013	3	1432	12.5	306	39	19	17
C7	1	12/02/2014	3	1318	11.7	207	37	31	20
C8	0	19/02/2014	4	145	12.2	216	40	20	4
C9	1	19/03/2014	3	417	11.7	330	42	18	8

Table 10.2. Baseline performance status, Stage, Ca19.9 and blood tests for trial and control patients. Alb = Albumin – g/L (35-50); ALT = Alanine transaminase – iu/L (2-53); Bil= Bilirubin – umol/L (0-21); Hb = Haemoglobin – g/dL (13.0-18.0); Plt = Platelets – x10^9/L (140-400); Ca19.9 - Ku/L (0-37)

10.1 Lipidem administration, uptake and safety profile

All patients received 250mL of Lipidem infusion administered over 2 hours. Patients were generally unwilling to have 4 hours of treatment following their chemotherapy for various reasons but tolerated a 2-hour infusion. Patients tolerated 250mls of Lipidem well with no serious adverse events during administration. Occasionally patents reported nausea and were treated with an antiemetic. There were 8 treatment points in 4 patients where less then 250mls was administered (3 from patient request secondary to nausea, 4 at patient request (no symptoms) and 1 secondary to elevated bilirubin reported on recent bloods). The patient was admitted for an ERCP and stent change.

10.1.1 Lipidem uptake

Lipidem treatment within the same trial protocol had been demonstrated resulting in significant omega-3 uptake in plasma phospholipids with a concurrent decrease in omega-6 levels. In previous experiments within the same trial protocol Arshad et al [411] used gas chromatography to demonstrated that there was a rapid and significant uptake of EPA and DHA fatty acid methyl esters into non-esterified fatty acids and EPA into erythrocyte cell membrane pellets in post-treatment samples (median increase of 1.06%, 0.65% and 0.05% respectively). In addition there was a significant reduction in omega-6 fatty acid fatty acid methyl esters and DHA into erythrocyte cell membrane

pellets (decrease of 0.31% and 0.8% respectively – p=0.031 for all). They reported a sustained uptake of DHA and EPA into erythrocyte cell membrane pellets over the treatment course with corresponding reduction in the omega 6:3 ratio.

10.1.2 Treatment Interruptions

Patients were included in the study until progression of disease, death or serious adverse events necessitating withdrawal or patients requested trial cessation. There were 10 treatment interruptions in 5 patients as detailed in table 10.3.

Patient	Treatment point (cycle/week)	Reason
T3	2.2	Patient request
T4	1.2	Treatment deferred as inpatient
	1.3	Treatment deferred as inpatient
T10	4.2	Treatment deferred as inpatient
T17	2.1	Treatment deferred as inpatient
	3.3	Patient request (declined treatment point)
T18	1.3	Treatment deferred, elevated bilirubin
	2.2	Treatment deferred, elevated bilirubin
	2.3	Treatment deferred, elevated bilirubin
	4.3	Treatment deferred as inpatient

Table 10.3. Table showing interruptions to patient's treatment.

10.1.3 Serious adverse events (SAE)

Serious adverse events (SAE) were reported to Research and Development as per standard trial protocol. SAEs reported are shown in table 10.4. No SAE was attributable to the administration of omega-3 infusion. The majority of SAEs were due to blocked or infected biliary stents. There were no SAEs reported in the control patient's cohort.

Patient	Date of SAE	Aetiology
T4	25/05/12 (elevated temperature)	Blocked biliary stent
T4	16/08/12 (elevated temperature)	Blocked biliary stent
T5	03/10/12 (shortness of breath)	Myocardial Infarction secondary to atherosclerotic disease
T6	20/09/12 (neutropenic sepsis)	Gemcitabine side effect
T7	06/09/12 (elevated temperature)	Blocked biliary stent
T9	14/02/13 (pulmonary embolism)	Disease burden
T10	06/02/13 (elevated temperature)	Blocked biliary stent
T12	20/12/12 (jaundice)	Blocked biliary stent
T14	08/01/13 (respiratory infection)	Bacterial Infection secondary to immunosuppression (gemcitabine chemotherapy)
T15	31/01/13 (elevated temperature)	Blocked biliary stent
T17	21/03/13 (diarrhoea)	Viral infection
T17	08/04/13 (jaundice)	Blocked biliary stent
T18	14/06/13 (jaundice)	Blocked biliary stent
T18	15/07/13 (jaundice)	Blocked biliary stent

Table 10.4. Serious Adverse Events reported to Research and Development.

10.2 Patient survival

Progression free survival (PFS) is defined as time from start of treatment in a clinical trial to disease progression or death from any cause[436,437]. Time from assignment was defined as the time the patient commenced their first treatment. Disease progression required evidence of disease progression and was usually evidenced following a CT scan. Overall survival (OS) is defined as time from start of treatment to death from any cause.

Patient: Trial=T, Control=C	Progression free survival (Months)	Overall survival (Months)
T1	8	9.9
T2	5.3	7
T3	4.9	6
T4	3.2	3.2
T5	12.6	12.6
T6	1.9	1.9
T7	2.2	2.2
T8	11.1	11.1
T9	7.1	7.1
T10	20	26.6
T11	2.9	2.9
T12	1.5	1.5
T13	6.3	8.3
T14	3.2	3.2
T15	6	7
T16	4.2	4.8
T17	9	10.3
T18	11	13.3
C1	1	1
C2	1	1
C3	2	7
C4	6	10.1
C5	0.5	0.5
C6	2.9	2.9
C7	0.5	0.5
C8	1.8	6
C9	3	12.2

Table 10.5. Progression free and overall survival in trial and control patients. Trial patients are numbered T1-T18 and control patients are numbered C1-C9.

10.3 Progression free survival

Progression free survival analysis between trial and control patients was performed and Kaplan Meier plots drawn. Progression free survival curves are shown in figure 10.3 where there was a significant difference between cohorts.

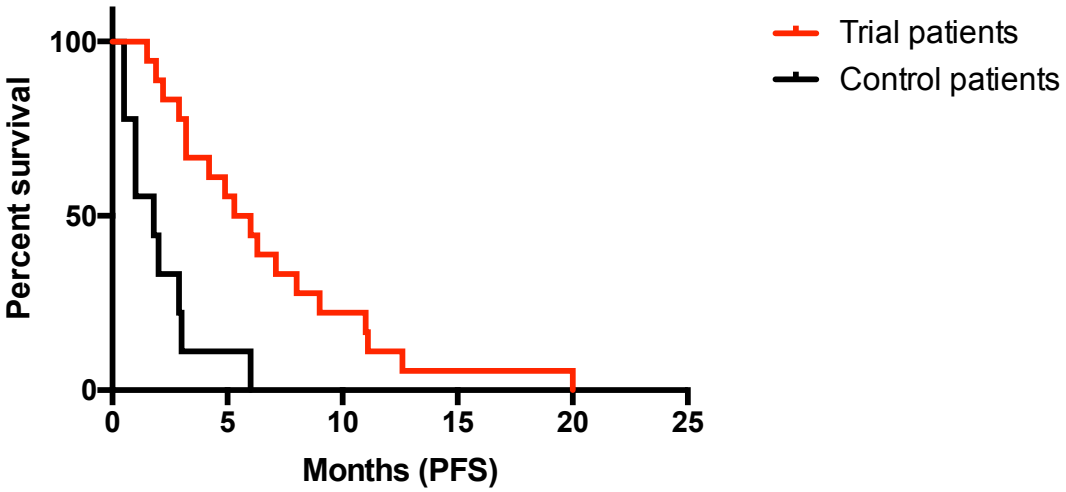

Figure 10.3. There was a significant benefit in progression free survival in trial compared to control patients (log-rank (Mantel-Cox) test, P=0.0003). Median survival in trial patients was 5.65 months. Median survival in control patients was 1.8 months. Patient T10 became operable following the trial and is seen as an outlier in the trial survival curve (PFS=20 months). Survival analysis excluding this patent demonstrated a significant benefit in PFS in trial compared to control patients (log-rank (Mantel-Cox) test, P=0.0005).

10.4 Overall survival

Overall survival analysis between trial and control patients were performed and Kaplan Meier plots drawn. Survival curves are shown in figure 10.4 where there was no significant difference between cohorts.

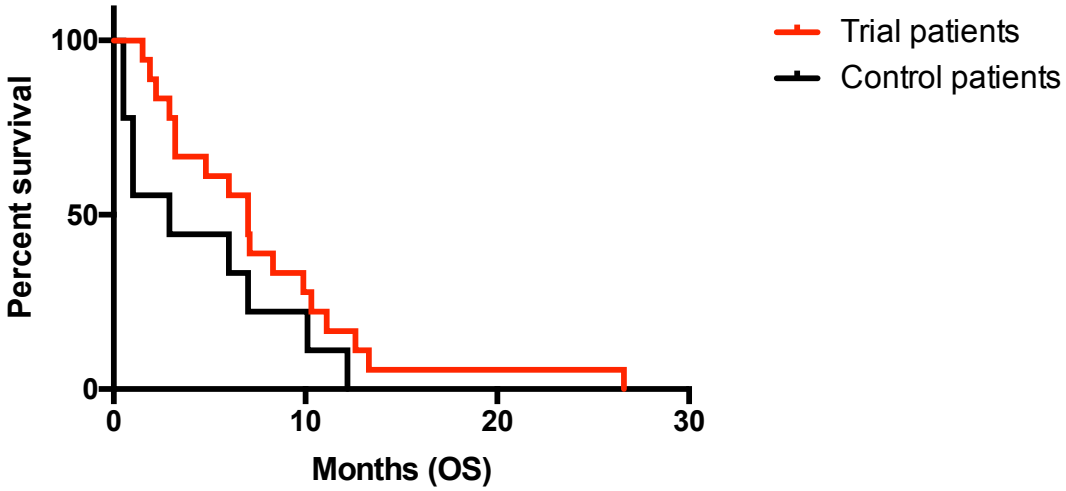

Figure 10.4. There was no significant benefit in overall survival in trial compared to control patients (log-rank (Mantel-Cox) test, P=0.13). Median survival in trial patients was 7 months. Median survival in control patients was 2.9 months.

10.5 Patient T10.

Patient T10 was diagnosed with stage three pancreatic cancer and was enrolled in the trial arm of this study. The CT scan following two months of treatment demonstrated stable disease with a reduction in in tumour size from 3.2cm (maximum diameter) to 2.6cm (-18.75%). The CT scan following four months of treatment demonstrated a partial response with a reduction in tumour size to 2cm (-37.5%) and this was also seen at the end of treatment at 6 months. Patient T10 was discussed at the multi-disciplinary team meeting where it was decided she had been down staged to stage two disease and was potentially operable. The patient underwent a successful pancreaticoduodenectomy (Whipple's procedure). The patient had a PFS of 20 months and an OS of 26.6 months. The patient is clearly an outlier and they were excluded from subsequent survival analysis but included in all other analysis.

11 Chapter Eleven: Myeloid derived suppressor cells (MDSCs) Results.

Two MDSC phenotypes were analysed.

1. Lin1$^-$, HLA-DR$^-$, CD33$^+$ and CD11b$^+$.

2. Lin1$^-$, HLA-DR$^-$, and CD11b.

11.1 MDSCs (Lin1$^-$, HLA-DR$^-$, CD33$^+$, CD11b$^+$): Trial patients

One hundred and fifteen samples were analysed from eighteen trial patients. MDSCs were identified as Lin1$^-$, HLA-DR$^-$, CD33$^+$ and CD11b$^+$. MDSCs were expressed as a percentage of the parent population analysed.

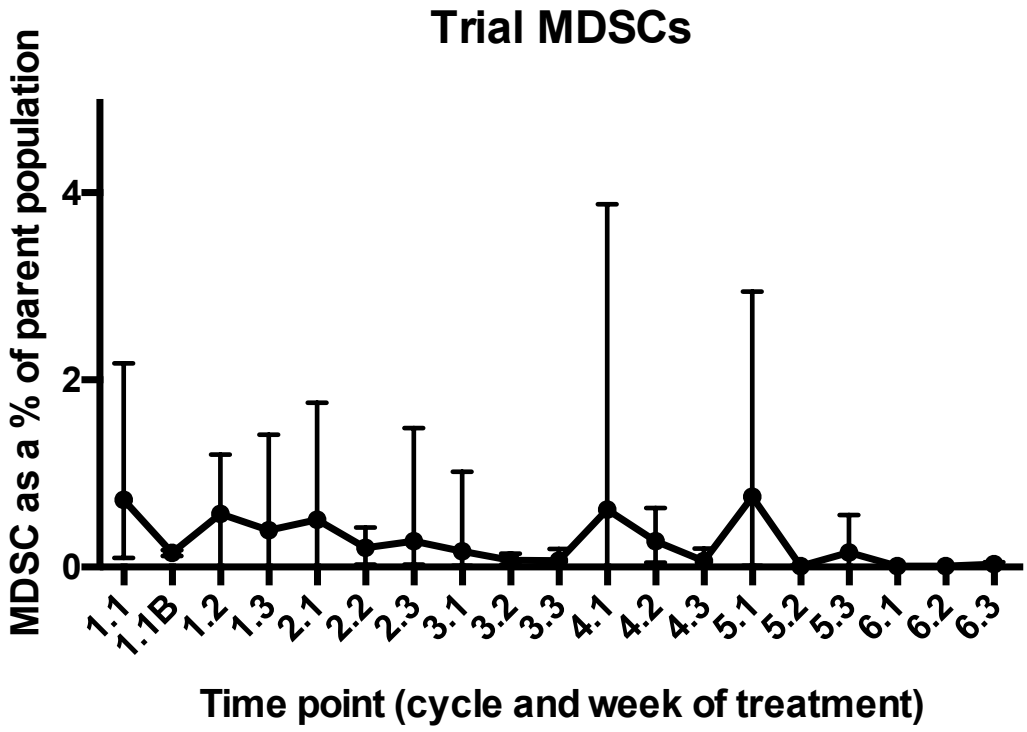

Figure 11.1. Figure showing mean trend line of trial MDSCs with range (minimum to maximum).

11.1.1 Baseline versus post treatment MDSCs at one month and trial end point.

MDSCs were analysed at baseline compared to one-month post treatment and trial end point. There was no significant change in MDSCs at one-month post treatment and at trial end point compared to baseline.

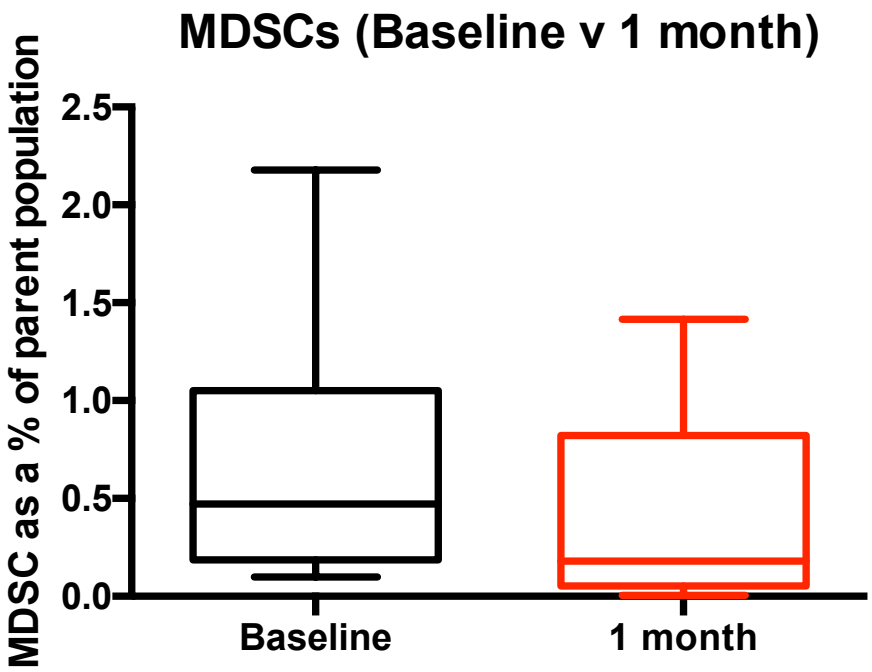

Figure 11.2. Box plot of baseline versus 1 month MDSCs in trial patients. Whiskers are minimum to maximum. There was no significant difference in MDSCs in trial patients at one month following treatment compared to baseline (P=0.149, 95% CI= -0.693 – 0.111).

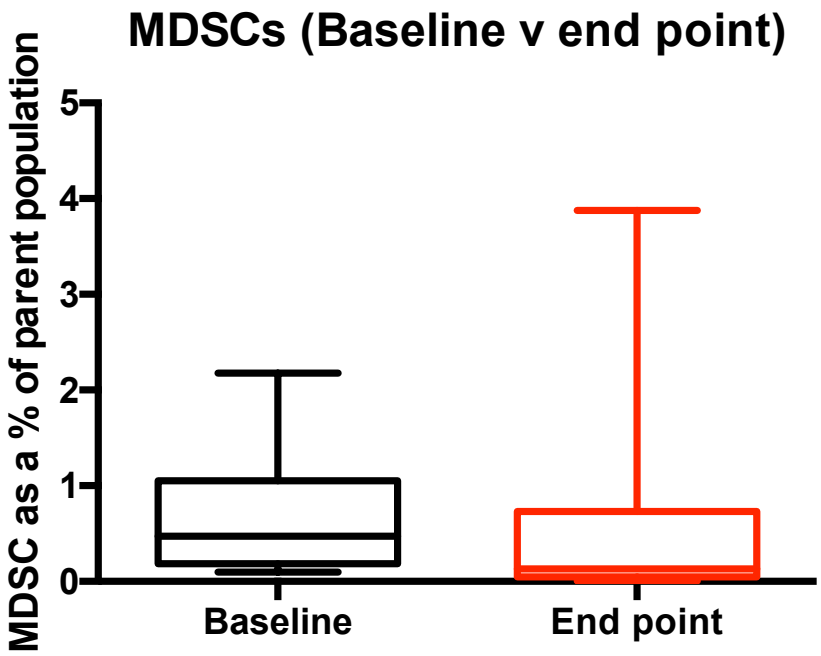

Figure 11.3. Box plot of baseline versus end point MDSCs in trial patients. Whiskers are minimum to maximum. There was no significant difference in MDSCs in trial patients at treatment end point compared to baseline (P=0.408, 95% CI= -0.741 – 0.316).

11.1.2 Baseline and end point MDSCs compared to patient overall survival.

Trial patients were divided into two groups around an overall survival of six months. MDSCs at baseline and end point were compared in these two groups. There was no significant difference in baseline or end point MDSCs in patients who survived less than 6 months compared to those who survived more than 6 months. There was no significant difference in MDSCs at treatment end point compared to baseline in patients who survived less or more than 6 months.

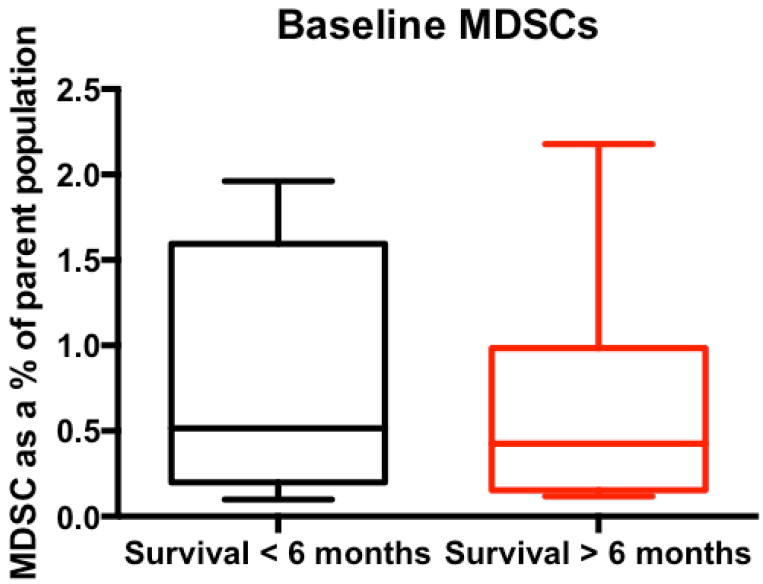

Figure 11.4. Box plot of baseline MDSCs in trial patients with an overall survival of less than or more than 6 months. Whiskers are minimum to maximum. There was no significant difference in baseline MDSCs in patients who survived less than 6 months compared to those who survived more than 6 months (P=0.705, 95% CI= -0.822 – 0.570).

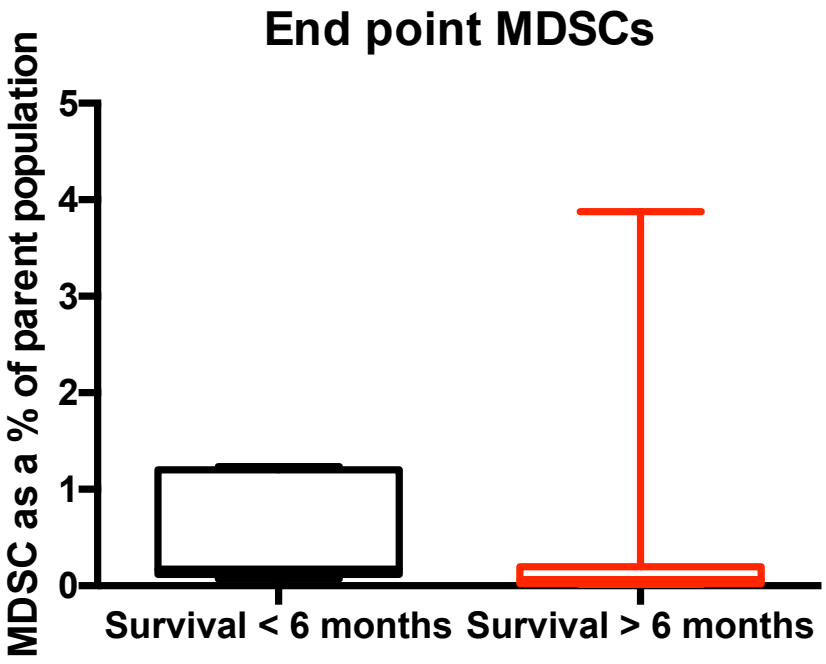

Figure 11.5. Box plot of end point MDSCs in trial patients with an overall survival of less than or more than 6 months. Whiskers are minimum to maximum. There was no significant difference in end point MDSCs in patients who survived less than 6 months compared to those who survived more than 6 months (P=0.827, 95% CI= -1.094 – 0.886).

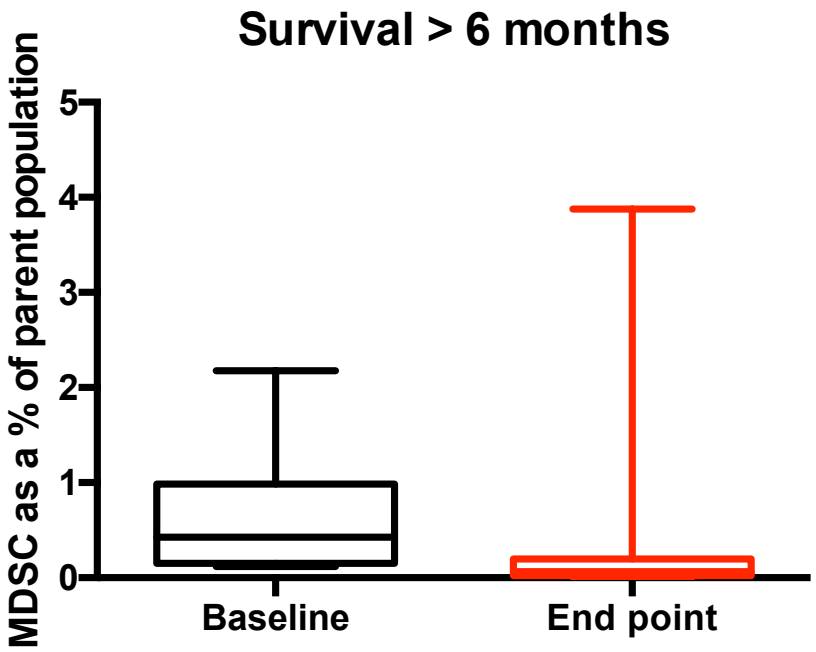

Figure 11.6. Box plot of MDSCs at baseline and trial end point in trial patients who had an overall survival of more than 6 months. Whiskers are minimum to maximum. There was no significant difference in MDSCs in trial patients with an overall survival over 6 months at treatment end point compared to baseline (P=0.591, 95% CI= -1.021 – 0.614).

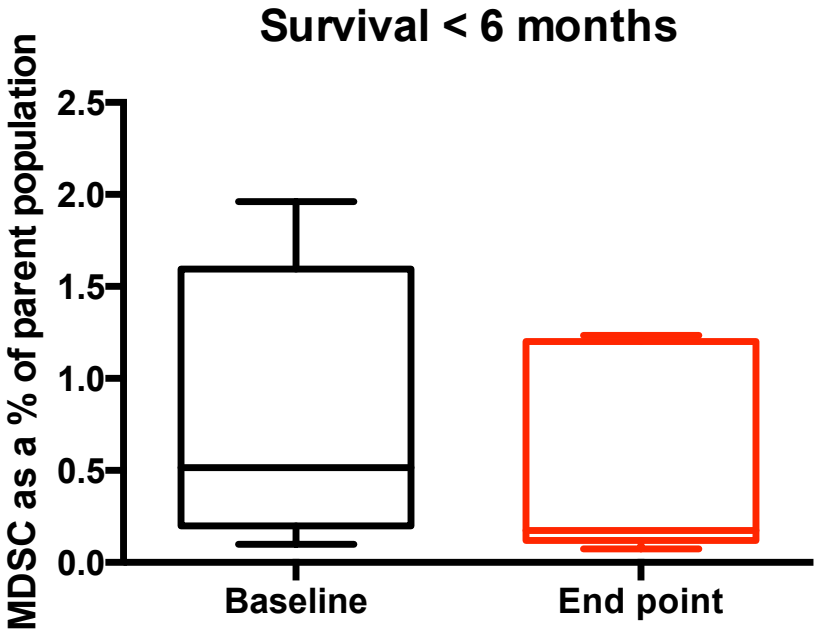

Figure 11.7. Box plot of MDSCs at baseline and trial end point in trial patients who had an overall survival of less than 6 months. Whiskers are minimum to maximum. There was no significant difference in MDSCs in trial patients with an overall survival under 6 months at treatment end point compared to baseline (P=0.511, 95% CI= -1.018 – 0.565).]

11.1.3 Trial patients: Regression analysis.

A mixed effects logistic regression analysis was performed on all trial patient samples using a bespoke regression model that allowed for random effects. There was a significant change in MDSCs over the trial treatment time course (P=0.0001).

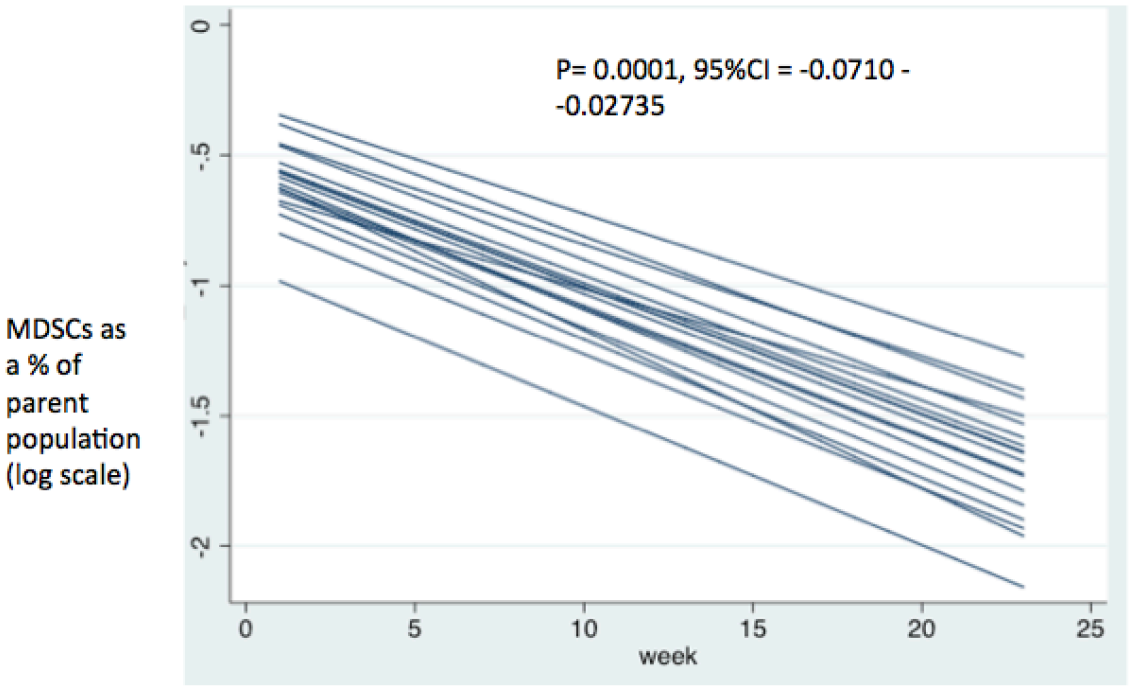

Figure 11.8. Output graph showing regression lines for individual patients plotted against time in weeks following mixed effects logistic regression analysis. MDSCs are shown on the y axis and are a calculated as a percentage of the parent population (log scale), time in weeks is shown on the x axis. Each regression line represents a patient. MDSCs are calculated as a percentage of the parent population and plotted on a log scale. One hundred and fifteen samples in eighteen patients were analysed. There is a highly significant decrease of MDSCs in trial patients during trial treatment (P=0.0001, 95% CI= -0.071- -0.027).

11.1.4 Trial patients: Survival analysis.

The percentage change of MDSCs at end point compared to baseline was calculated. Patients were divided into two groups, low and high MDSCs around the median value percentage change. Kaplan-Meier curves were drawn to examine the relationship of change in MDSCs and progression free survival (PFS) and overall survival (OS). Log rank analysis were used to evaluate the survival curves. 17 patients were eligible for analysis. Patient T10 was excluded from this analysis as the patient became operable and inclusion would bias the analysis. There was no difference in PFS or OS in patients who had a high or low change in MDSCs at trial end point.

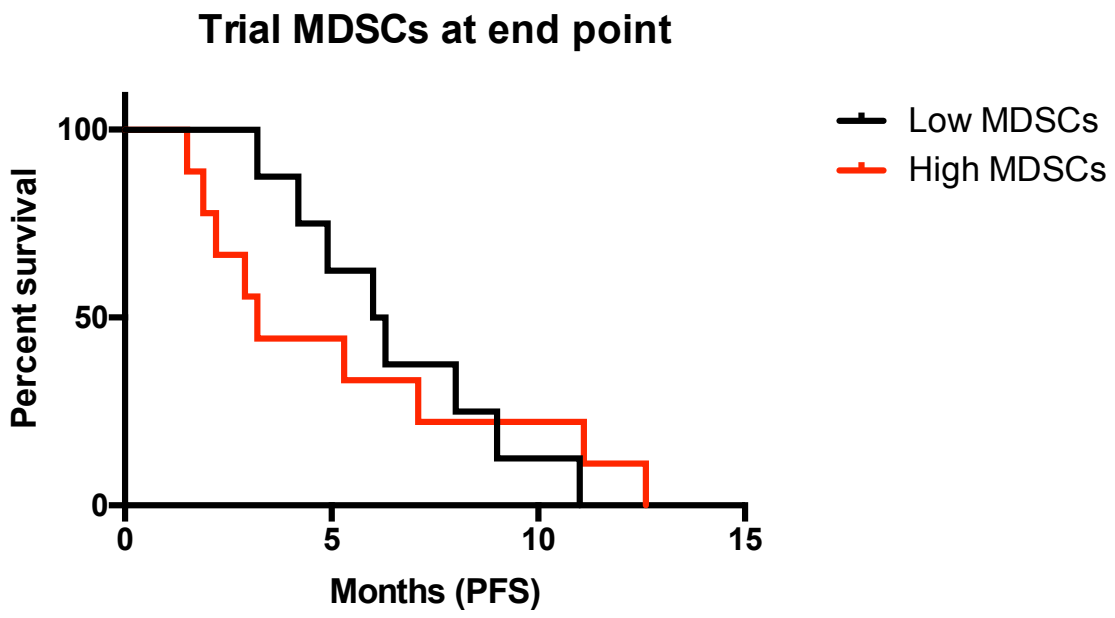

Figure 11.9. There was no benefit in progression free survival (PFS) in patients who had low MDSCs at treatment endpoint compared to baseline (log-rank (Mantel-Cox) test, P=0.904). Median survival in patients with low MDSCs was 6.15 months (N=8). Median survival in patients with high MDSCs was 3.2 months (N=9).

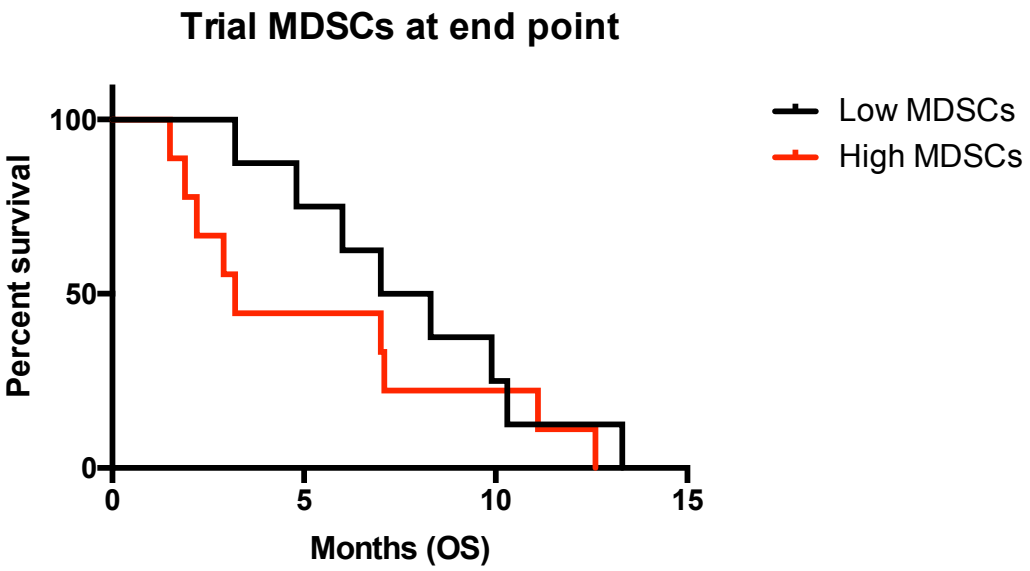

Figure 11.10. There was no benefit in overall survival (OS) in patients who had low MDSCs at treatment endpoint compared to baseline (log-rank (Mantel-Cox) test, P=0.34). Median survival in patients with low MDSCs was 7.65 months (N=8). Median survival in patients with high MDSC was 3.2 months (N=9).

11.2 MDSCs (Lin1$^-$, HLA-DR$^-$, CD33$^+$, CD11b$^+$): Control patients

Twenty-five samples were analysed from nine control patients. MDSCs were identified as Lin1$^-$, HLA-DR$^-$, CD33$^+$ and CD11b$^+$. MDSCs were expressed as a percentage of the parent population analysed.

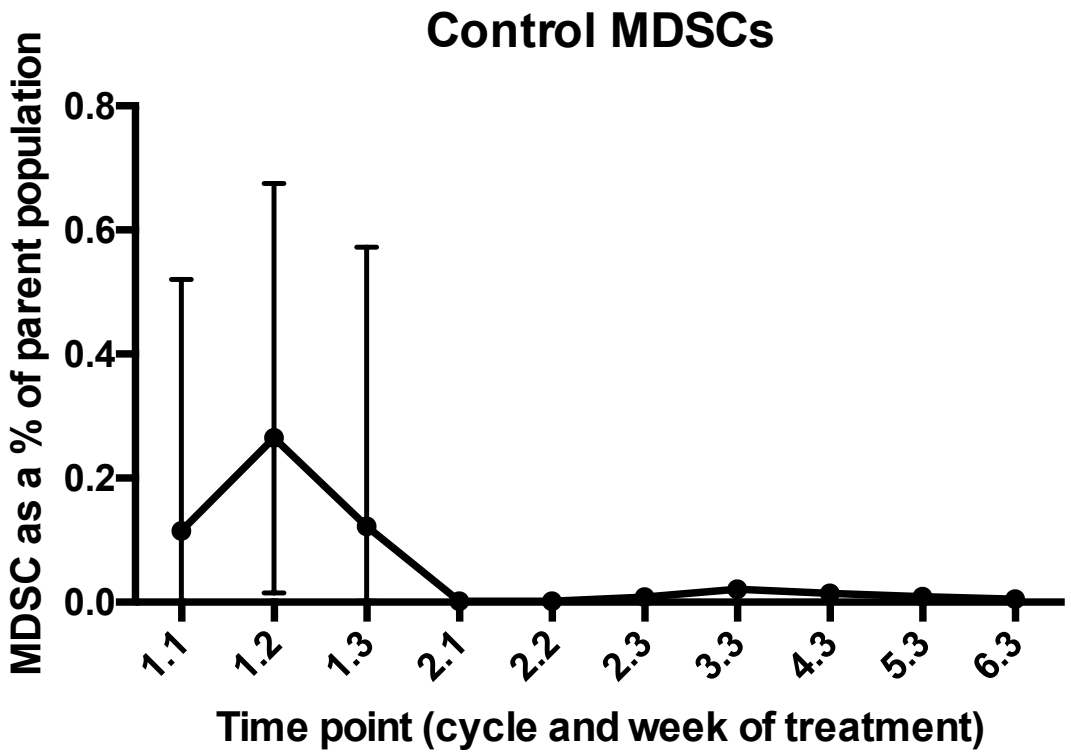

Figure 11.11. Figure showing mean trend line of control MDSCs with range (minimum to maximum).

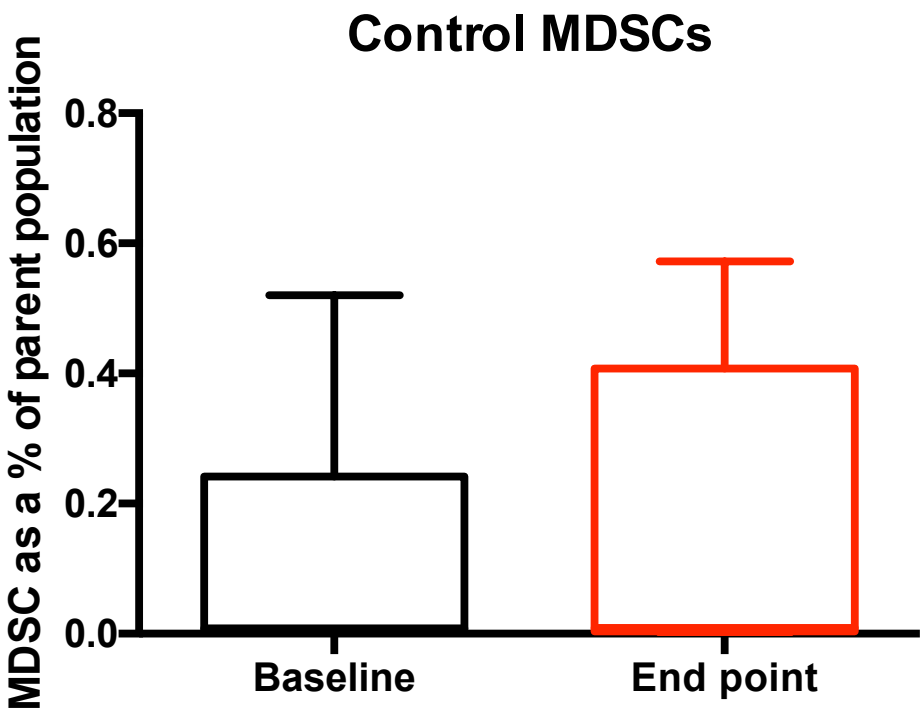

Figure 11.12. Box plot of baseline compared to end point MDSCs. Whiskers are minimum to maximum. There was no statistical difference when comparing levels at trial end point to baseline (P=0.72, 95% CI = -0.215– 0.301).

11.2.1 Control patients: Regression analysis

A bespoke mixed effects regression analysis was performed on all control patient samples using the previously described bespoke regression model that allowed for random effects. There was no significant change in MDSCs numbers over the trial treatment time course (P=0.901).

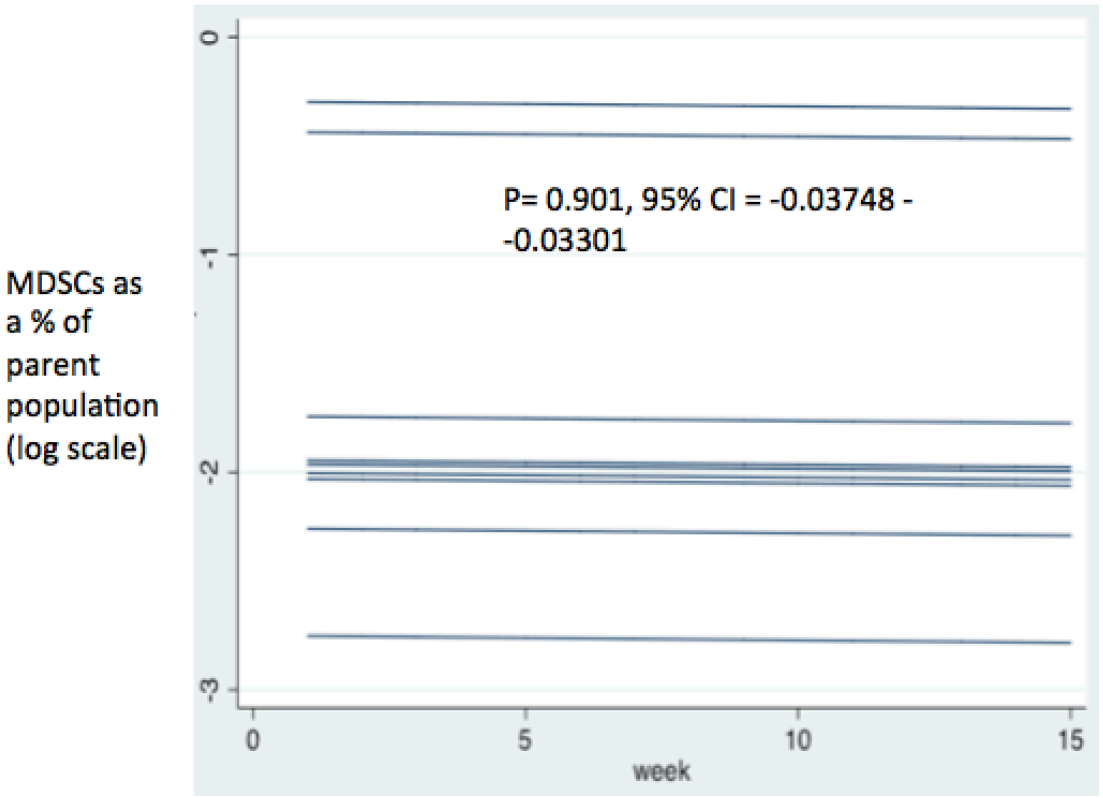

Figure 11.13. Output graph showing regression lines for individual patients plotted against time in weeks following multinomial logistic regression analysis. MDSC levels are shown on the y axis and are a calculated as a percentage of the parent population (log scale), time in weeks is shown on the x axis. Each regression line represents a patient. Twenty-five samples in nine patients were analysed. The regression lines are almost flat and show no significant change in MDSCs in the control patients (P=0.901, 95% CI= -0.037 - 0.033).

11.3 MDSCs: Comparison analysis

Trial patients were compared to the control cohort. There was a significant difference between baseline trial and control patient MDSCs (P=0.014), but no significant difference between end point trial and control patient MDSCs.

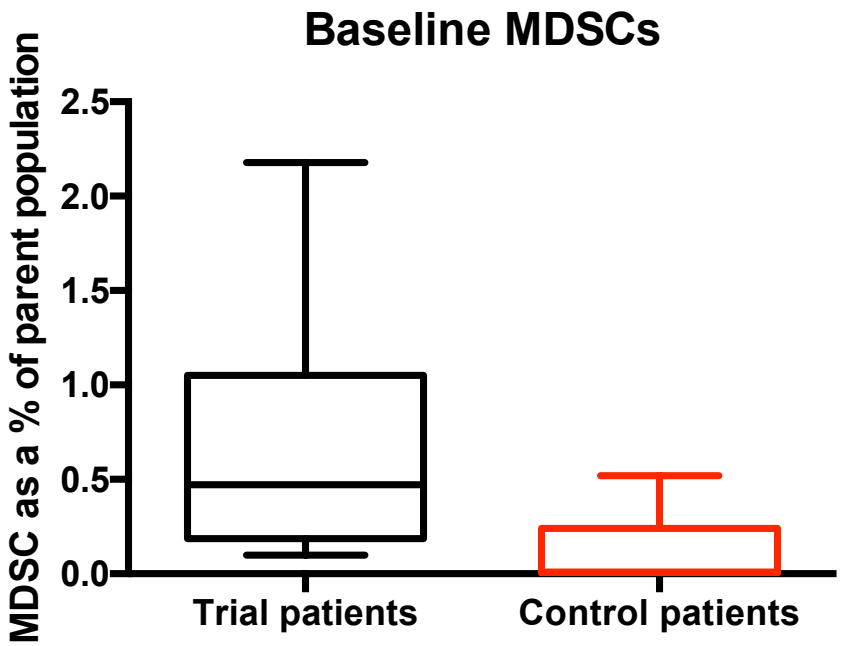

Figure 11.14. Box plot of baseline MDSCs in trial versus control patients. Whiskers are minimum to maximum. There was a significant difference between baseline trial and control patient MDSCs (P=0.014, 95 % CI= -1.074 – -0.133).

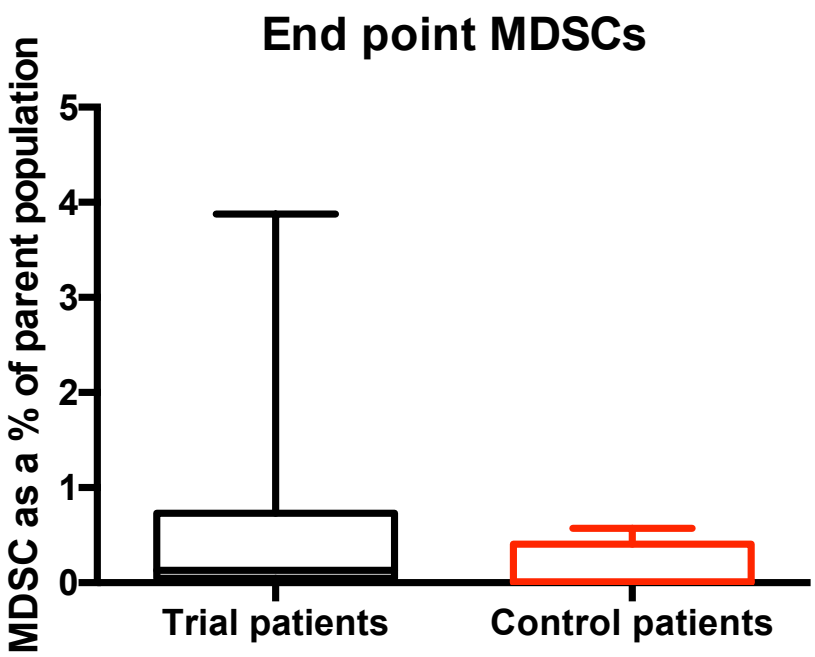

Figure 11.15. Box plot of end point MDSCs in trial versus control patients. Whiskers are minimum to maximum. There was no significant difference between end point trial and control patient MDSCs (P=0.384, 95 % CI= -1.163 – 0.466).

11.3.1 Comparison survival analysis

MDSCs in both trial and control patients were divided into two groups (low and high change groups) around the median percentage change of MDSCs between baseline and end point. Overall survival and progression free survival of trial and control patients was compared in the low and high change groups. Patient T10 was excluded from this analysis as the patient became operable and inclusion would have biased the analysis. Patients C5, C7 and C9 were excluded from this analysis, as they had no sample following a baseline measurement. There was no significant difference in progression free survival (PFS) in patients with a low change in MDSCs in trial versus control patients (log-rank [Mantel-Cox] test, P=0.057). In addition there was no significant difference in progression free survival (PFS) in patients with a high change in MDSCs in trial versus control patients (log-rank (Mantel-Cox) test, P=0.08). There was no significant difference in the OS of trial and control patients with a high or low change in MDSCs.

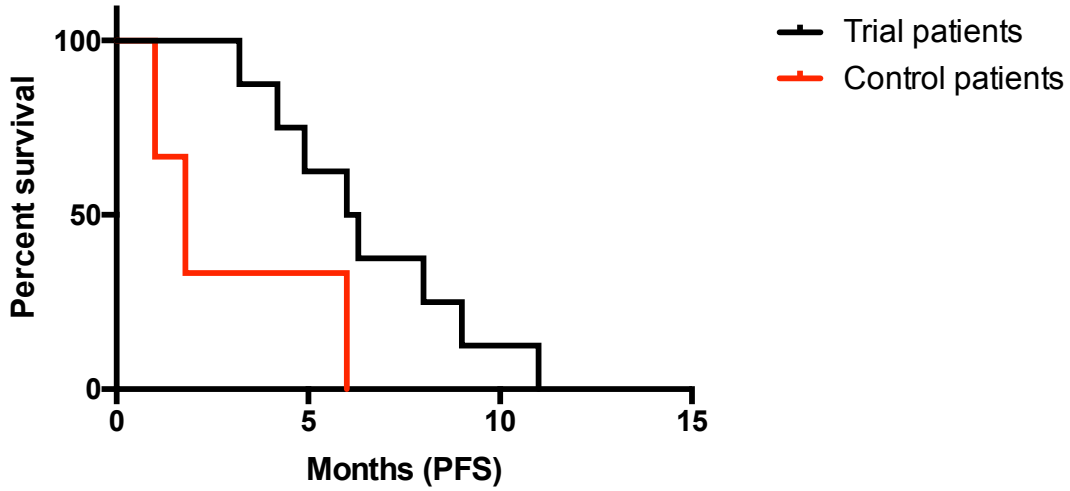

Figure 11.16. There was no significant difference in progression free survival (PFS) in patients with a low change in MDSCs in trial versus control patients (log-rank (Mantel-Cox) test, P=0.057). Median survival in trial patients (N=8) was 6.15 months. Median survival in control patients (N=3) was 1.8 months.

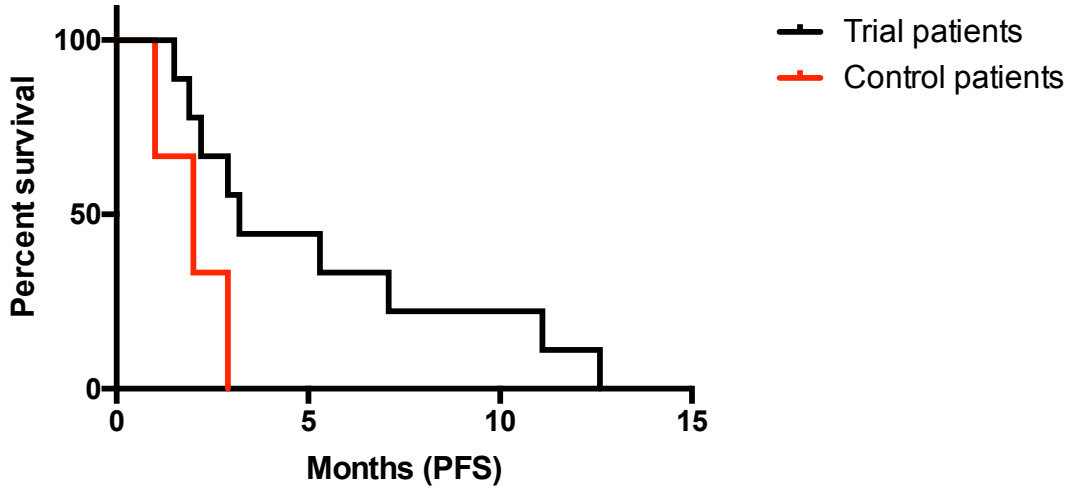

Figure 11.17. There was a significant difference in progression free survival (PFS) in patients with a high change in MDSCs in trial versus control patients (log-rank (Mantel-Cox) test, P=0.08). Median survival in trial patients (N=9) was 3.2 months. Median survival in control patients (N=3) was 1.6 months.

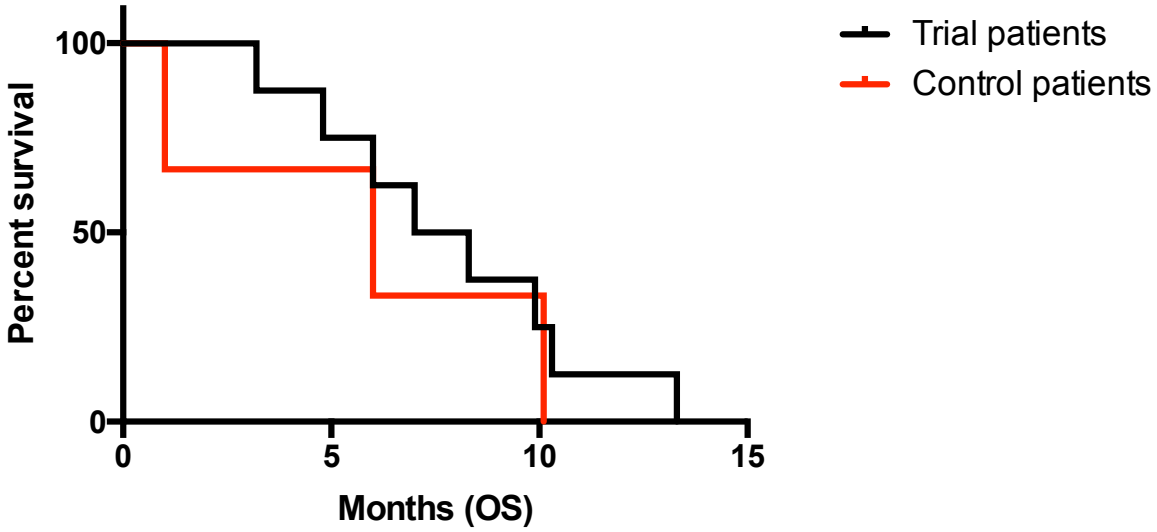

Figure 11.18. There was no significant difference in overall survival (OS) in patients with a low change in MDSCs in trial versus control patients (log-rank (Mantel-Cox) test, P=0.732). Median survival in trial patients (N=8) was 7.65 months. Median survival in control patients (N=3) was 6 months.

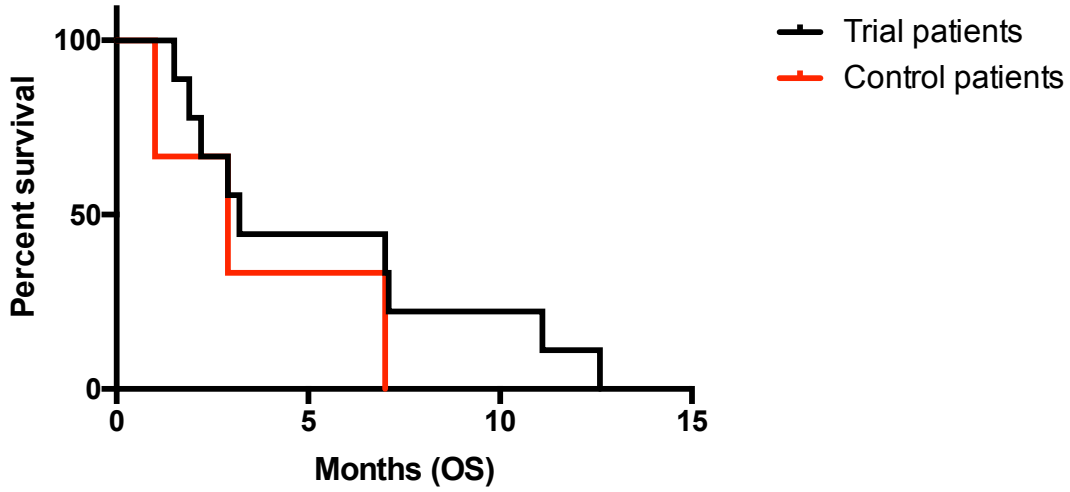

Figure 11.19. There was no significant difference in overall survival (OS) in patients with a high change in MDSCs in trial versus control patients (log-rank (Mantel-Cox) test, P=0.76). Median survival in trial patients (N=9) was 3.2 months. Median survival in control patients (N=3) was 2.9 month.

11.3.2 Regression analysis

A mixed effects regression model that allowed for random effects was used to compare MDSCs in the two groups. One hundred and thirty-six time points in twenty-seven patients were included for analysis. The effect of the cycle between trial and control patients was analysed. There was a significant difference seen in cycle one (P=0.01), cycle three (P=0.01) and cycle six (P=0.04). The effect of the week between trial and control groups was analysed in cycle one. There was a significant difference between week one (P=0.02, 95% CI=-0.034 – 0.467), and week three (P=0.025, 95% CI=-0.511 – 0.034), but not week two (P=0.12, 95% CI=-4.448 – 0.055). Overall there was no statistically significant difference between the trial and control patients over time (P=0.395).

11.4 MDSCs (Lin1$^-$, HLA-DR$^-$, CD11b$^+$): Trial patients

One hundred and fifteen samples were analysed from eighteen trial patients. MDSCs were identified as Lin1$^-$, HLA-DR$^-$ and CD11b$^+$ and expressed as a percentage of the parent population analysed.

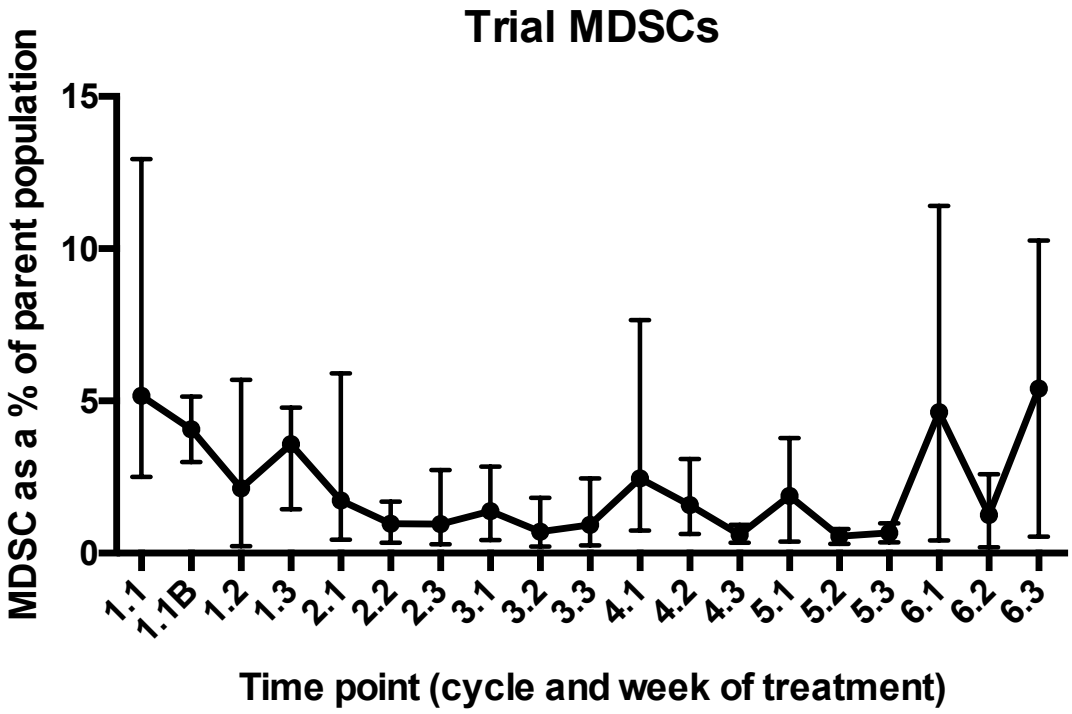

Figure 11.20. Figure showing mean trend line of trial MDSCs with range (minimum to maximum).

11.4.1 Baseline versus post treatment MDSCs at one month and trial end point

MDSCs were analysed at baseline compared to one-month post treatment and trial end point. There was a significant difference in MDSCs in trial patients at one month following treatment compared to baseline (P=0.014), and at treatment end point compared to baseline (P=0.006).

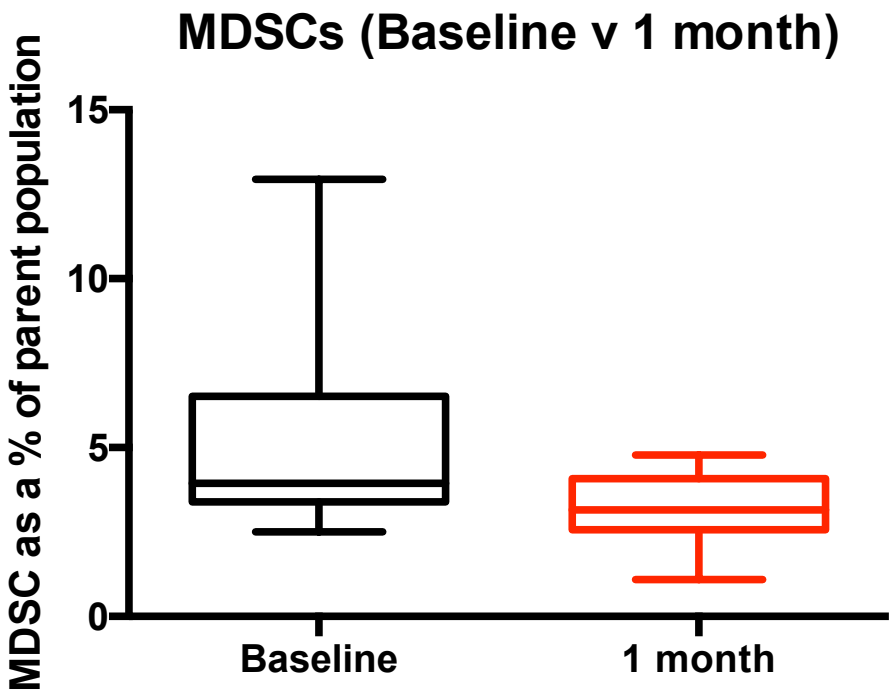

Figure 11.21. Box plot of baseline versus 1 month MDSCs in trial patients. Whiskers are minimum to maximum. There was a significant difference in MDSCs in trial patients at one month following treatment compared to baseline (P=0.014, 95% CI= -3.734 – -0.487).

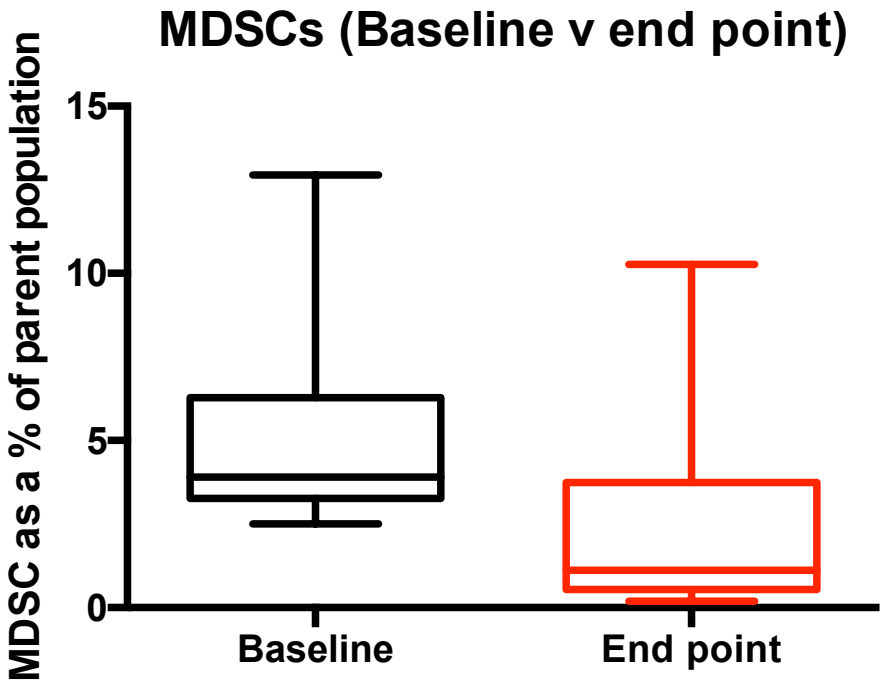

Figure 11.22. Box plot of baseline versus end point MDSCs in trial patients. Whiskers are minimum to maximum. There was a significant difference in MDSCs in trial patients at treatment end point compared to baseline (P=0.006, 95% CI= -4.419 – 0.835).

11.4.2 Baseline and end point MDSCs compared to patient overall survival.

Trial patients were divided into two groups around an overall survival of six months. MDSCs at baseline and end point were compared in these two groups. There was no significant difference in baseline or endpoint MDSCs in patients who survived less than 6 months compared to those who survived more than 6 months. There was a significant decrease in MDSCs in trial patients with an overall survival over 6 months at treatment end point compared to baseline (P=0.019). There was no significant difference in MDSCs in trial patients with an overall survival under 6 months at treatment end point compared to baseline.

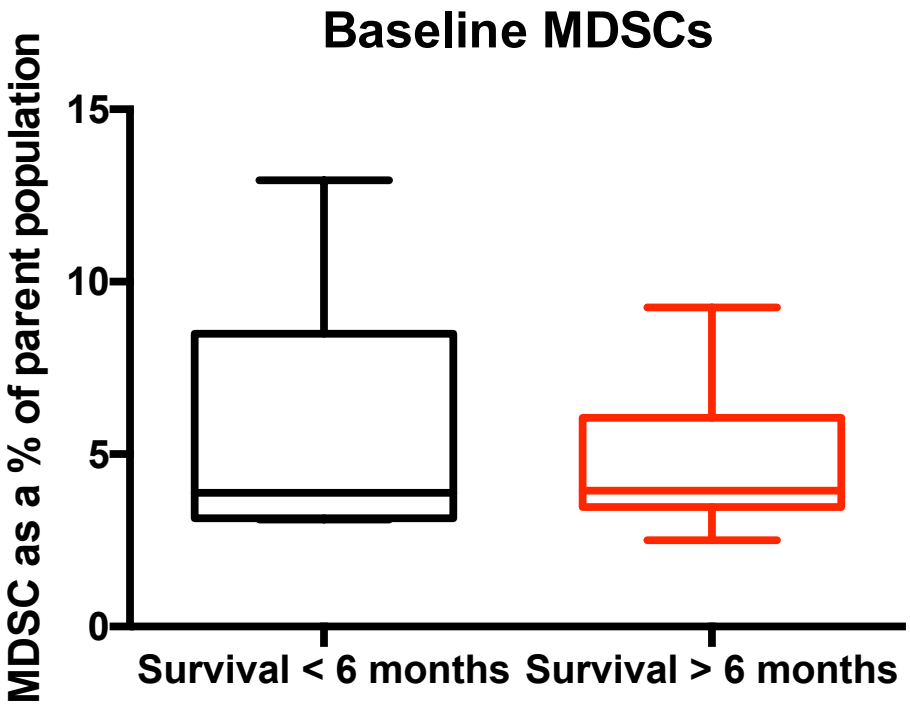

Figure 11.23. Box plot of baseline MDSCs in trial patients with an overall survival of less than or more than 6 months. Whiskers are minimum to maximum. There was no significant difference in baseline MDSCs in patients who survived less than 6 months compared to those who survived more than 6 months (P=0.536, 95% CI= -3.724 – 2.015).

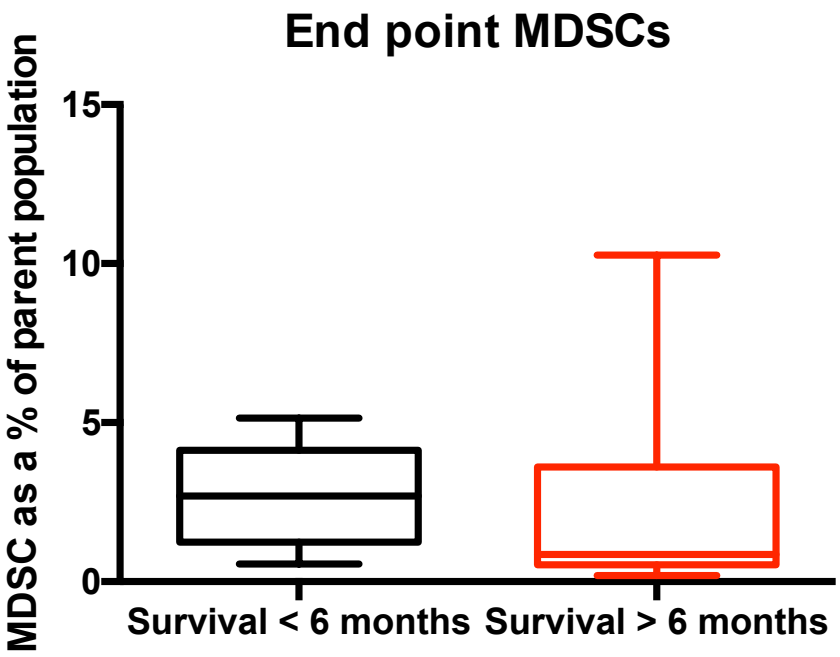

Figure 11.24. Box plot of endpoint MDSCs in trial patients with an overall survival of less than or more than 6 months. Whiskers are minimum to maximum. There was no significant difference in end point MDSCs in patients who survived less than 6 months compared to those who survived more than 6 months (P=0.836, 95% CI= -3.226 – 2.644).

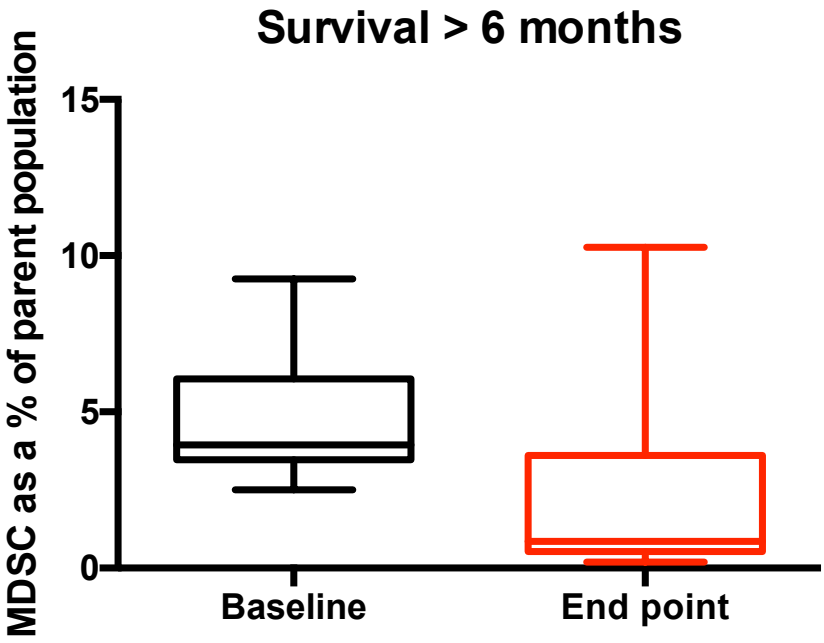

Figure 11.25. Box plot of baseline versus end point MDSCs in trial patients whose overall survival was over 6 months. Whiskers are minimum to maximum. There was a significant decrease in MDSCs in trial patients with an overall survival over 6 months at treatment end point compared to baseline (P=0.019, 95% CI= -4.346 – -0.469).

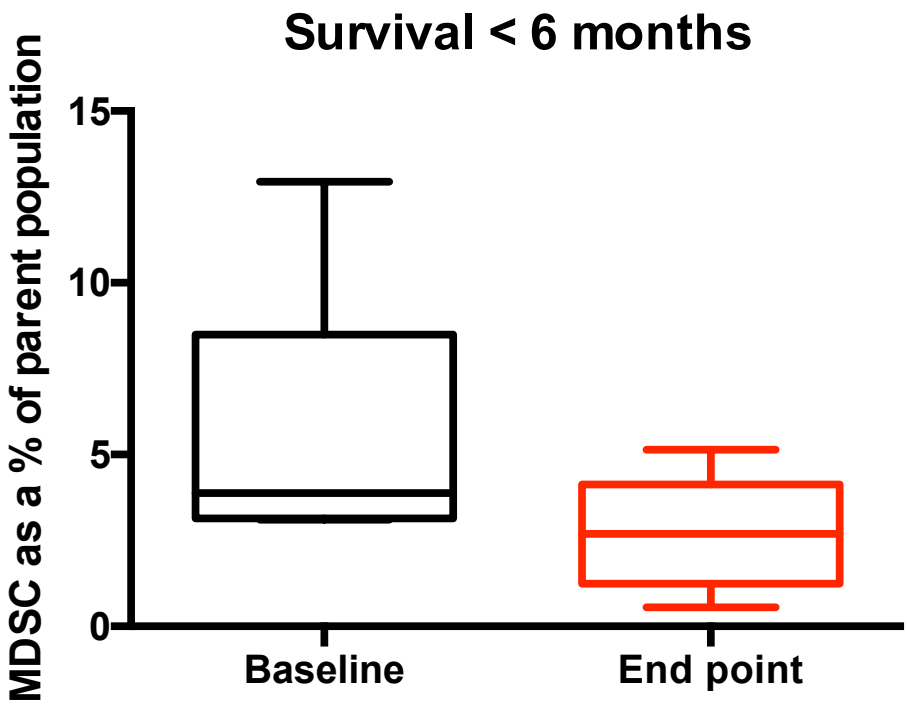

Figure 11.26. Box plot of baseline versus end point MDSCs in trial patients whose overall survival was under 6 months. Whiskers are minimum to maximum. There was no significant difference in MDSCs in trial patients with an overall survival under 6 months at treatment end point compared to baseline (P=0.149, 95% CI= -7.376 – 1.432).

11.4.3 Trial patients: Regression analysis

A mixed effects logistic regression analysis was performed on all trial patient samples using a bespoke regression model, as previously described, which allowed for random effects. There was a significant change in MDSCs over the treatment time course (P=0.0001).

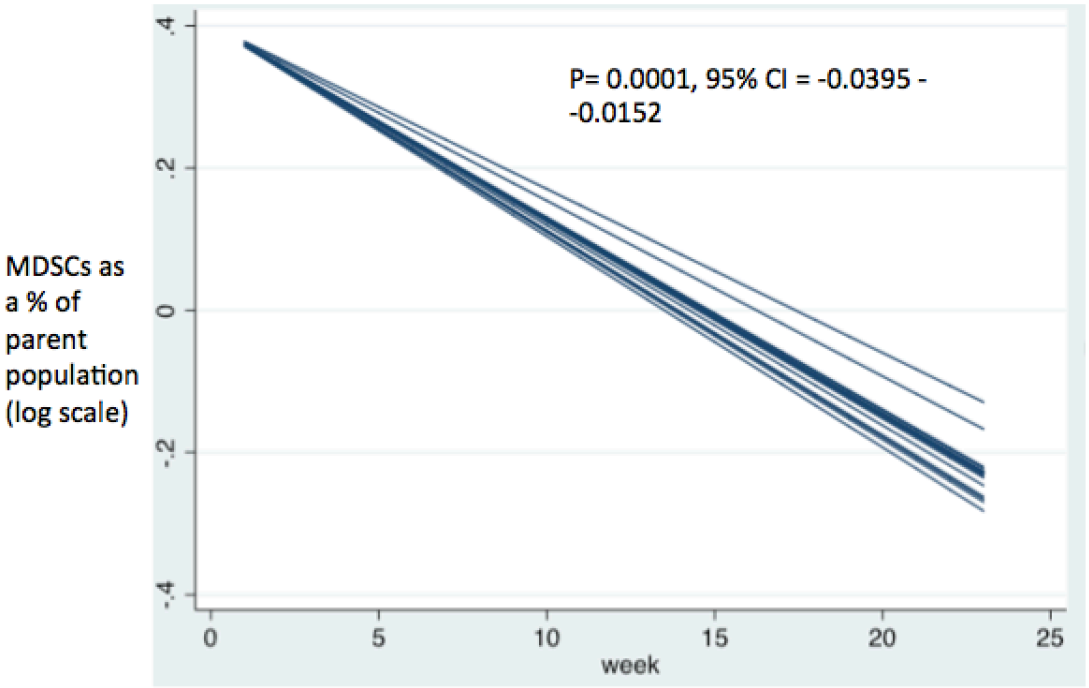

Figure 11.27. Output graph showing regression lines for individual patients plotted against time in weeks following mixed effects logistic regression analysis. MDSCs are shown on the y axis and are a calculated as a percentage of the parent population (log scale), time in weeks is shown on the x axis. Each regression line represents a patient. MDSCs are calculated as a percentage of the parent population and plotted on a log scale. One hundred and fifteen samples in eighteen patients were analysed. There is a highly significant decrease of MDSCs in trial patients during treatment (P=0.0001, 95% CI= -0.0395 - -0.0152).

11.4.4 Trial patients: Survival analysis

The percentage change of MDSCs at trial end point compared to baseline was calculated. Patients were divided into two groups, low and high MDSCs around the median value percentage change. Kaplan-Meier curves were drawn to examine the relationship of change in MDSCs and progression free survival (PFS) and overall survival (OS). Log rank analysis were used to evaluate the survival curves. 17 patients were eligible for analysis. Patient T10 was excluded from this analysis as the patient became operable and inclusion would bias the analysis. There was no difference in PFS or OS in patients who had a high or low change in MDSCs at trial end point.

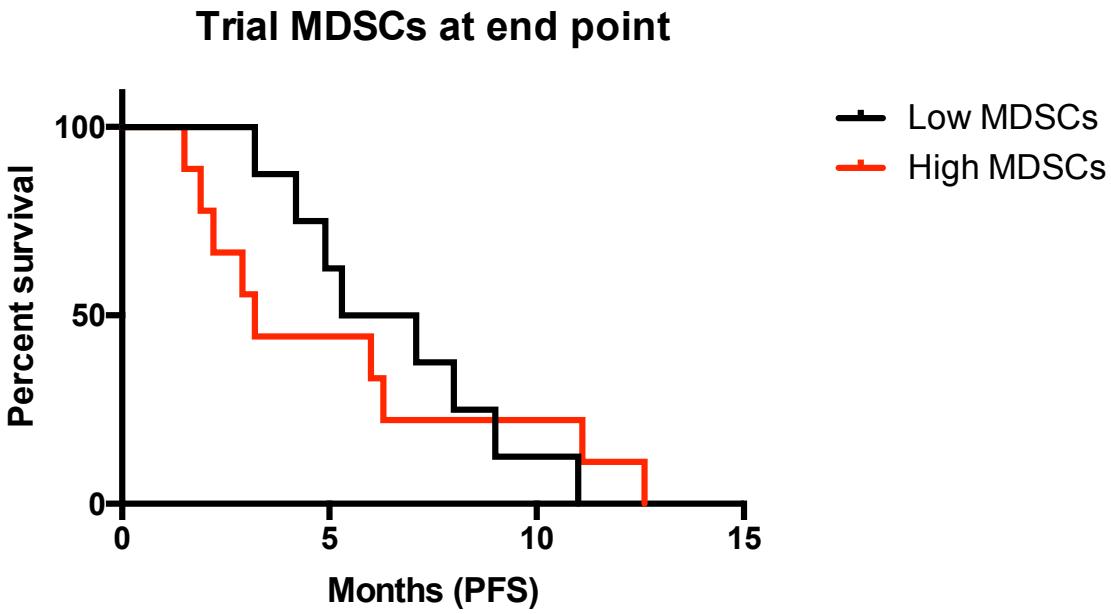

Figure 11.28. There was no benefit in progression free survival (PFS) in patients who had low MDSCs at treatment endpoint compared to baseline (log-rank (Mantel-Cox) test, P=0.88). Median survival in patients with low MDSCs was 6.2 months (N=8). Median survival in patients with high MDSCs was 3.2 months (N=9).

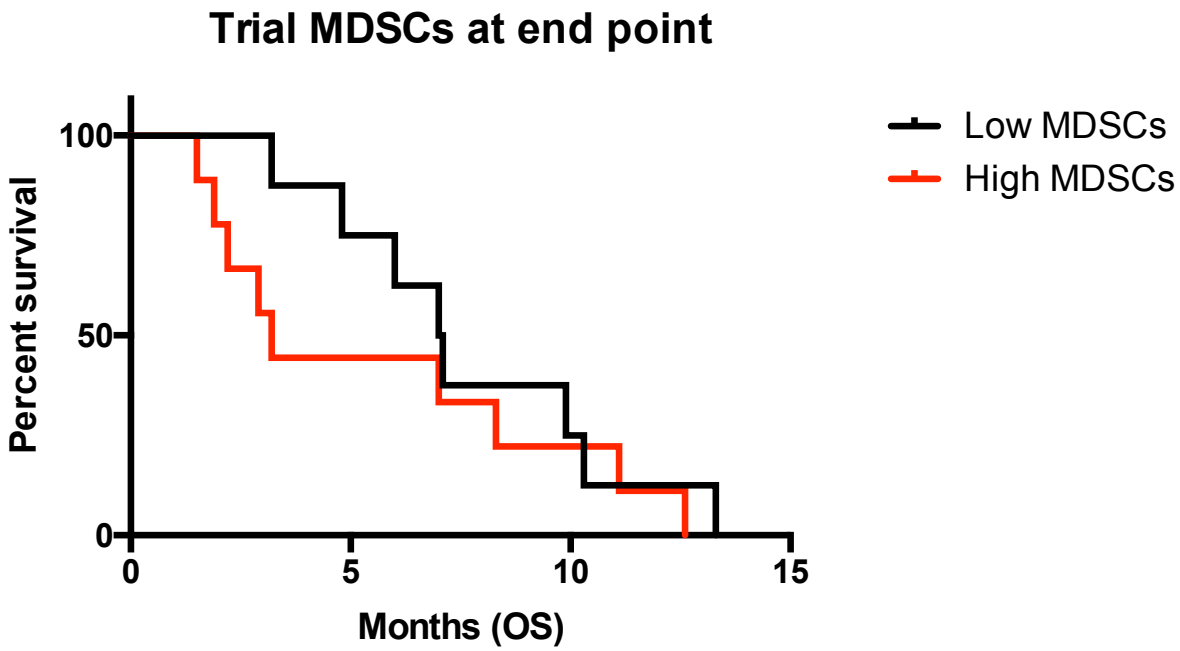

Figure 11.29. There was no benefit in overall survival (PFS) in patients who had low MDSCs at treatment endpoint compared to baseline (log-rank (Mantel-Cox) test, P=0.39). Median survival in patients with low MDSCs was 7.05 months (N=8). Median survival in patients with high MDSC was 3.2 months (N=9).

11.5 MDSCs (Lin1$^-$, HLA-DR$^-$, CD11b$^+$): Control patients

Twenty-five samples were analysed from nine control patients. MDSCs were identified as Lin1$^-$, HLA-DR$^-$, and CD11b$^+$. MDSCs were expressed as a percentage of the parent population analysed.

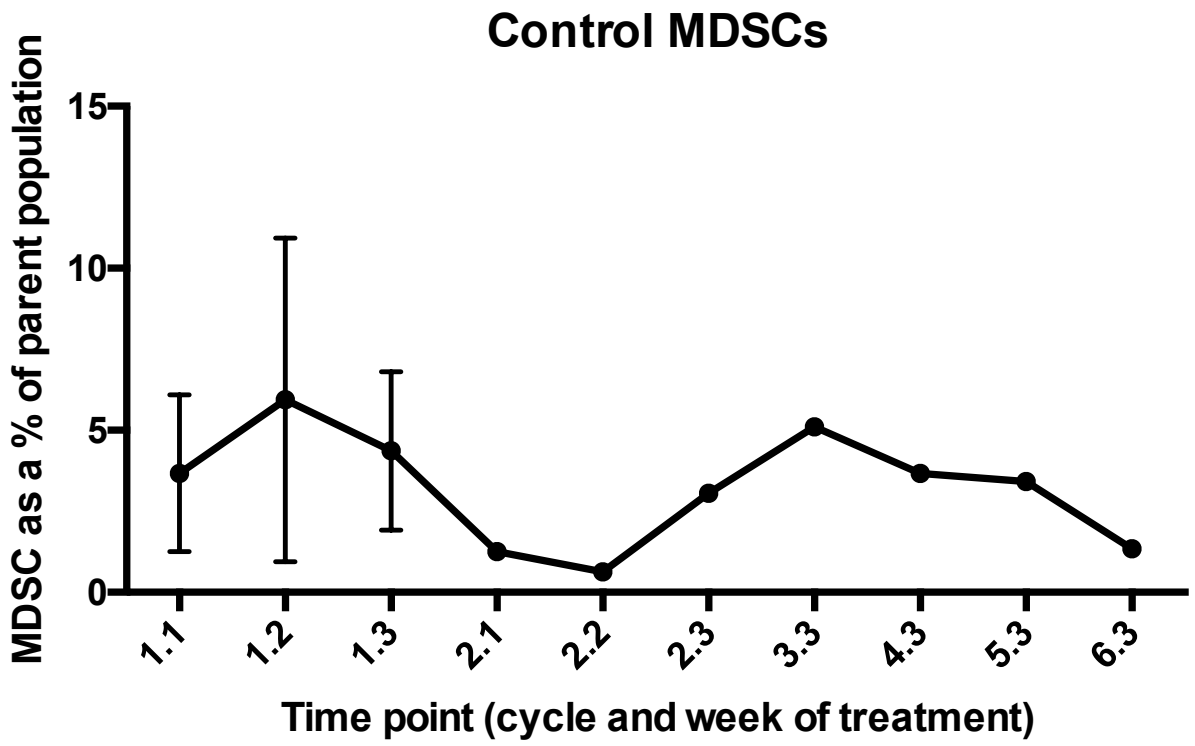

Figure 11.30. Figure showing mean trend line of control MDSCs with range (minimum to maximum).

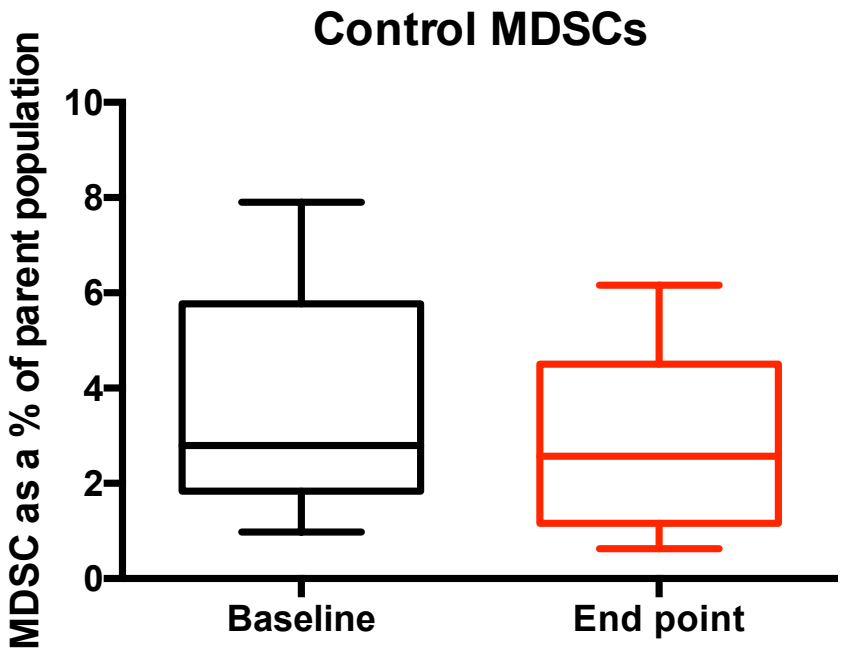

Figure 11.31. Box plot of baseline compared to end point MDSCs. Whiskers are minimum to maximum. There was no statistical significance when comparing levels at trial end point to baseline (P=0.51, 95% CI = -3.382– 1.776).

11.5.1 Control patients: Regression analysis.

A mixed effects regression analysis was performed on all control patient samples. There was no significant change in MDSCs (P=0.3).

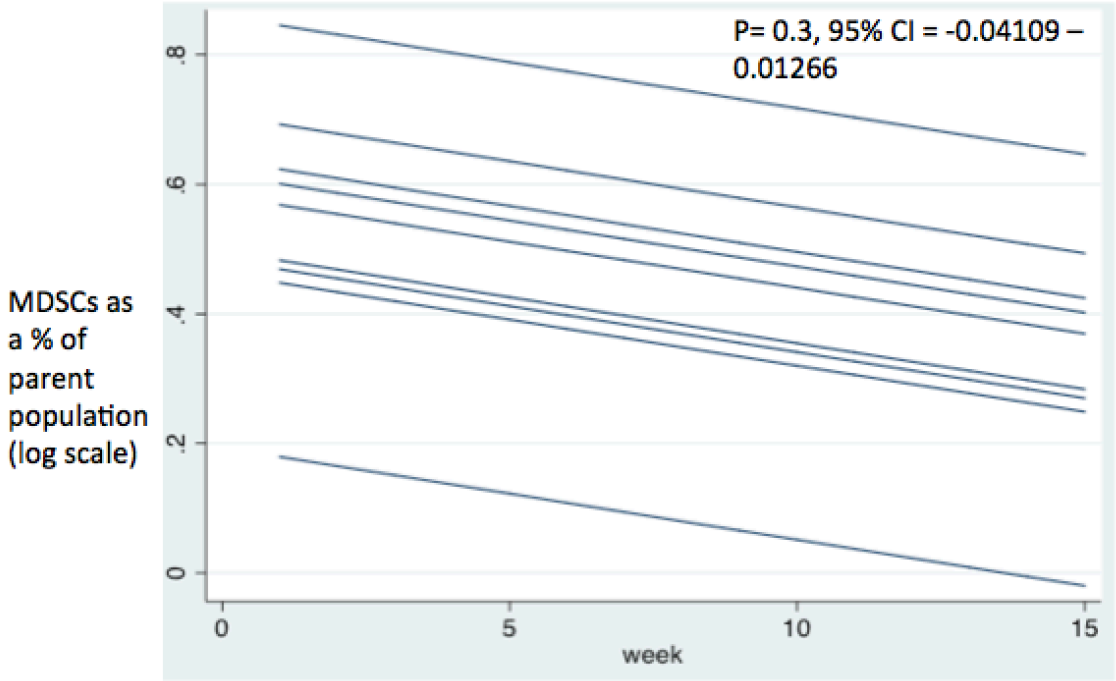

Figure 11.32. Output graph showing regression lines for individual patients plotted against time in weeks following multinomial logistic regression analysis. MDSC levels are shown on the y axis and are a calculated as a percentage of the parent population (log scale), time in weeks is shown on the x axis. Each regression line represents a patient. Twenty-five samples in nine patients were analysed. The regression lines have a downward trend but there is no significant change in MDSCs in the control patients (P=0.3, 95% CI= -0.04109 - 0.01266).

11.6 MDSCs: Comparison analysis

Trial patients were compared to the control cohort. There was no significant difference between baseline and end point trial and control patient MDSCs.

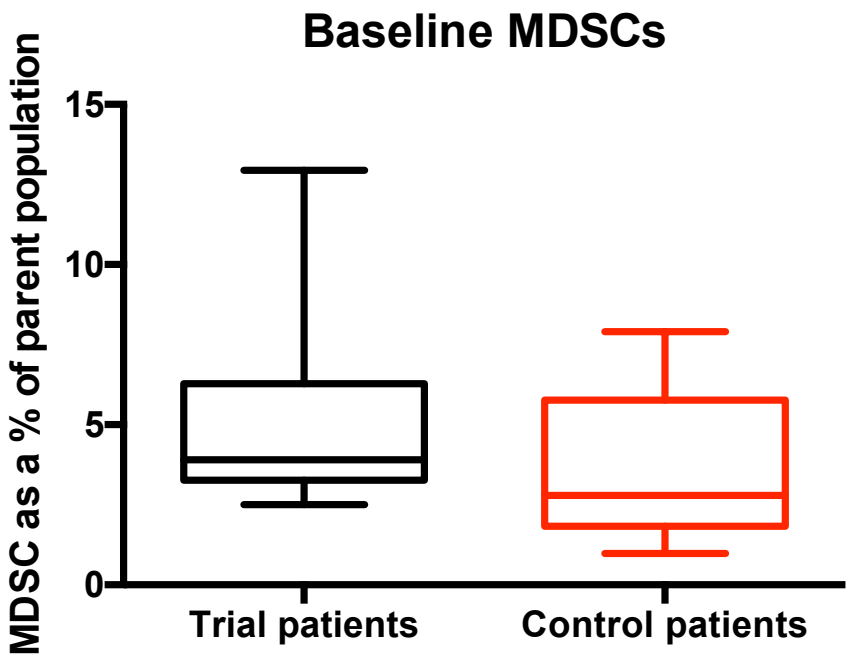

Figure 11.33. Box plot of baseline MDSCs in trial and control patients. Whiskers are minimum to maximum. There was no significant difference between baseline trial and control patient MDSCs (P=0.18, 95 % CI= -3.717 – 0.7369).

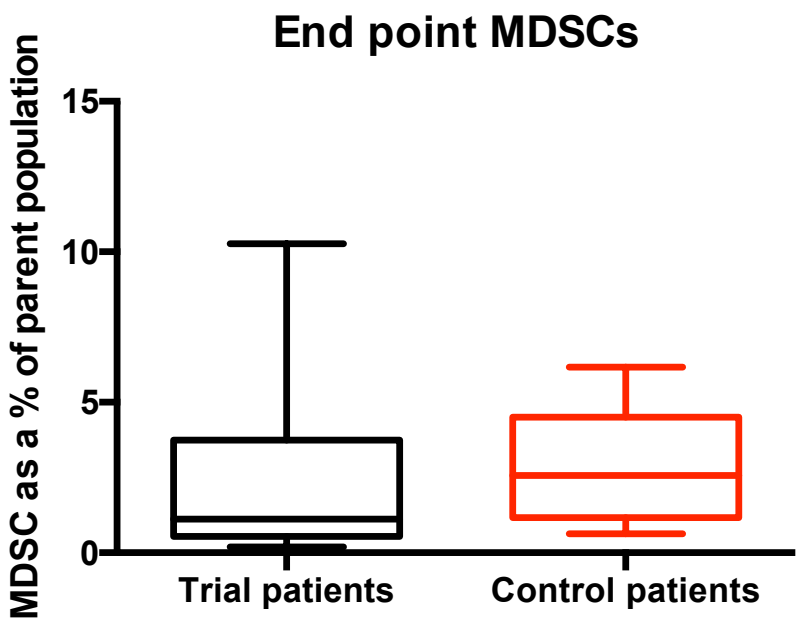

Figure 11.34. Box plot of end point MDSCs in trial and control patients. Whiskers are minimum to maximum. There was no significant difference between endpoint trial and control patient MDSCs (P=0.789, 95 % CI= -2.231– 2.900).

11.6.1 Comparison survival analysis

MDSCs in both trial and control patients were divided into two groups (low and high change groups) around the median percentage change of MDSCs between baseline and end point. Overall survival and progression free survival of trial and control patients was compared in the low and high change groups. Patient T10 was excluded from this analysis as the patient became operable and inclusion would have biased the analysis. Patients C5, C7 & C9 were excluded from this analysis, as they had no sample following a baseline measurement. There was no significant difference in the PFS or OS of trial and control patients with a high or low change in MDSCs.

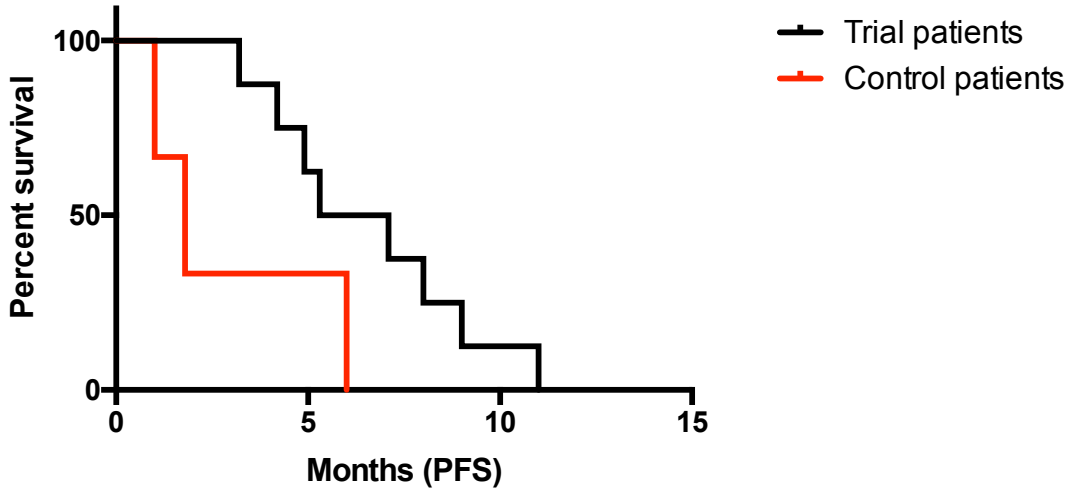

Figure 11.35. There was no significant difference in progression free survival (PFS) in patients with a low change in MDSCs in trial versus control patients (log-rank (Mantel-Cox) test, P=0.073). Median survival in trial patients (N=8) was 6.2 months. Median survival in control patients (N=3) was 1.8 months.

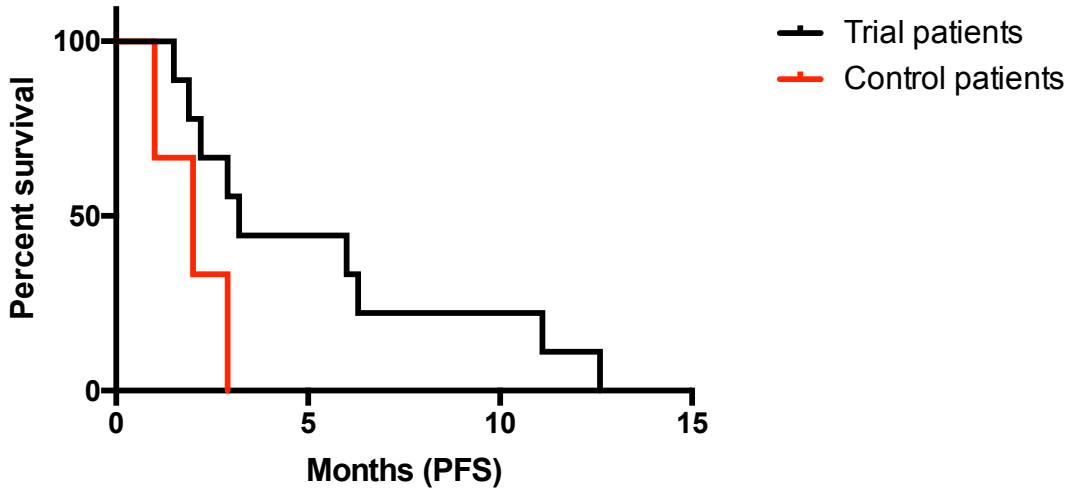

Figure 11.36. There was no significant difference in progression free survival (PFS) in patients with a high change in MDSCs in trial versus control patients (log-rank (Mantel-Cox) test, P=0.08). Median survival in trial patients (N=9) was 3.2 months. Median survival in control patients (N=3) was 2 months.

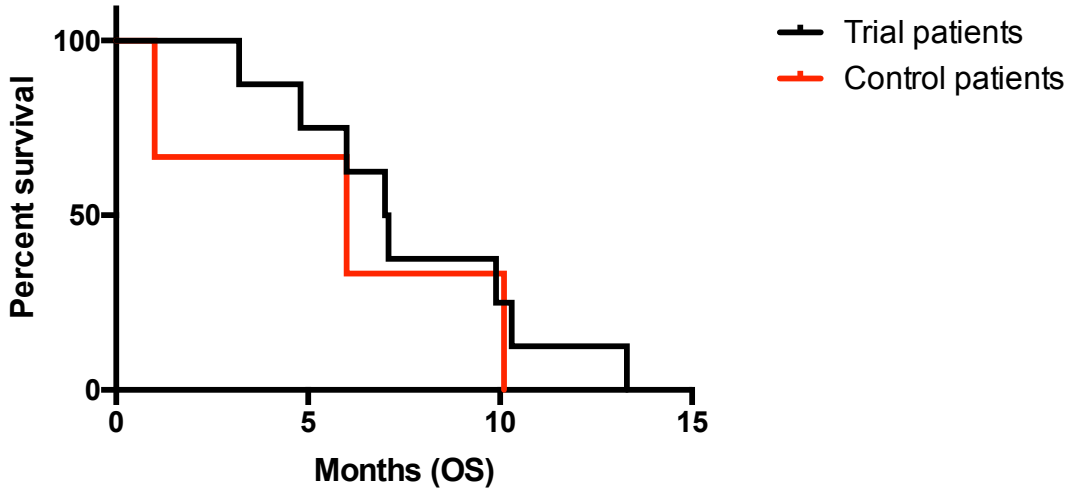

Figure 11.37. There was no significant difference in overall survival (PFS) in patients with a low change in MDSCs in trial versus control patients (log-rank (Mantel-Cox) test, P=0.493). Median survival in trial patients (N=8) was 7.05 months. Median survival in control patients (N=3) was 6 months.

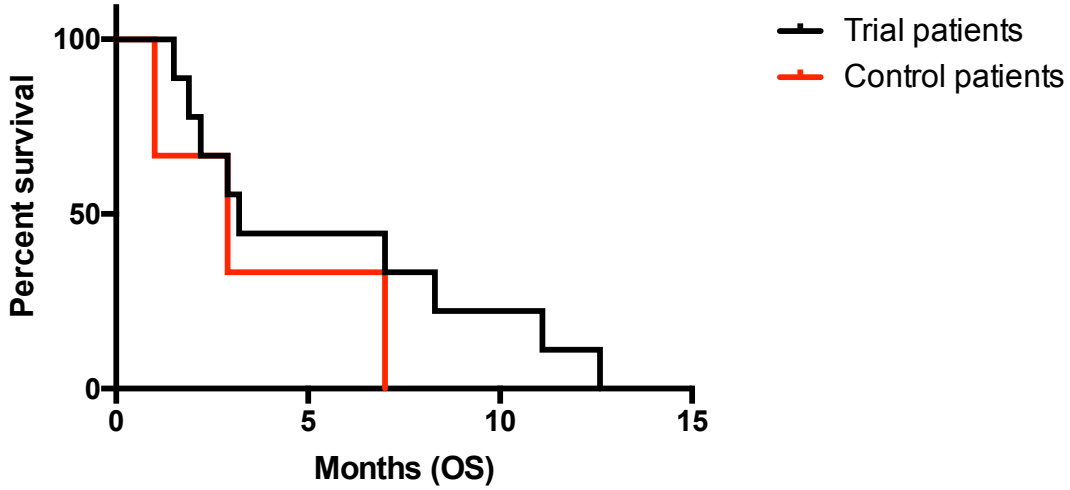

Figure 11.38. There was no significant difference in overall survival (PFS) in patients with a high change in MDSCs in trial versus control patients (log-rank (Mantel-Cox) test, P=0.356). Median survival in trial patients (N=9) was 3.2 months. Median survival in control patients (N=3) was 2.9 months.

11.6.2 Regression analysis.

A mixed effects regression model that allowed for random effects was utilised to compare MDSCs in the two groups. One hundred and thirty-six time points in twenty-seven patients were included for analysis. The effect of the cycle between trial and control patients was analysed. There was a significant difference seen in cycle two (P=0.0001), cycle three (P=0.0001), cycle four (P=0.0001) and cycle five (P=0.0001). The effect of the week between trial and control groups was analysed in cycle one. There was a significant difference between week one (P=0.0001, 95% CI=1.567 – 3.106), week two (P=0.012, 95% CI= -2.0263 – 0.249) but not week three (P=0.079, 95% CI=-1.532 – 0.076). Overall there was a significant difference in MDSCs between the trial and control patients over time (P=0.01).

12 Chapter Twelve: T Regulator Cells (Tregs) Results

12.1 T regulator cells: Trial patients

PBMC were analysed for Tregs. One hundred and nine samples were analysed from eighteen trial patients. Tregs were identified as triple positive for CD4, CD25 and Fox-P3 antibodies. Tregs were expressed as a percentage of the parent population analysed.

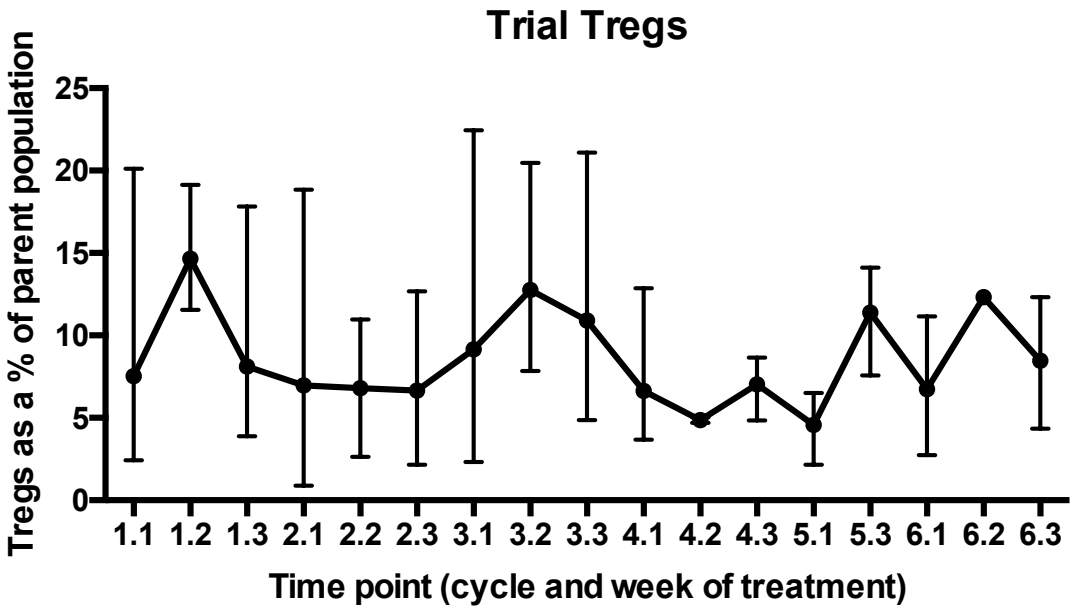

Figure 12.1. Figure showing mean trend line of trial T regulator cells with range (minimum to maximum).

12.1.1 Baseline versus post treatment Tregs at one month and trial end point

Tregs were analysed at baseline compared to one-month post treatment and trial end point. There was no significant change in Tregs at one-month post treatment and at trial end point compared to baseline.

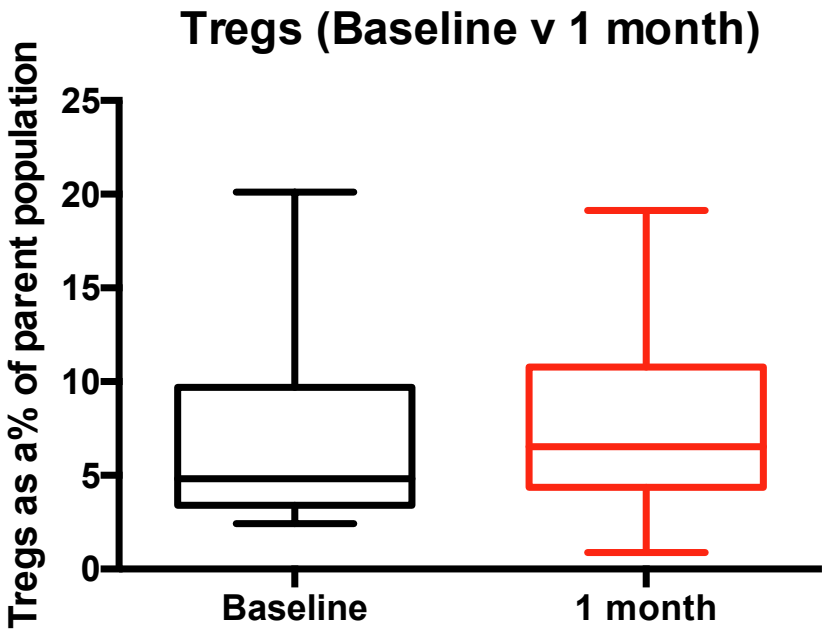

Figure 12.2. Box plot of Tregs at baseline and following 1 month of treatment. Whiskers are from minimum to maximum. There was no significant difference in Tregs in trial patients at one month following treatment compared to baseline (P=0.92, 95% CI= -2.621 - 2.871).

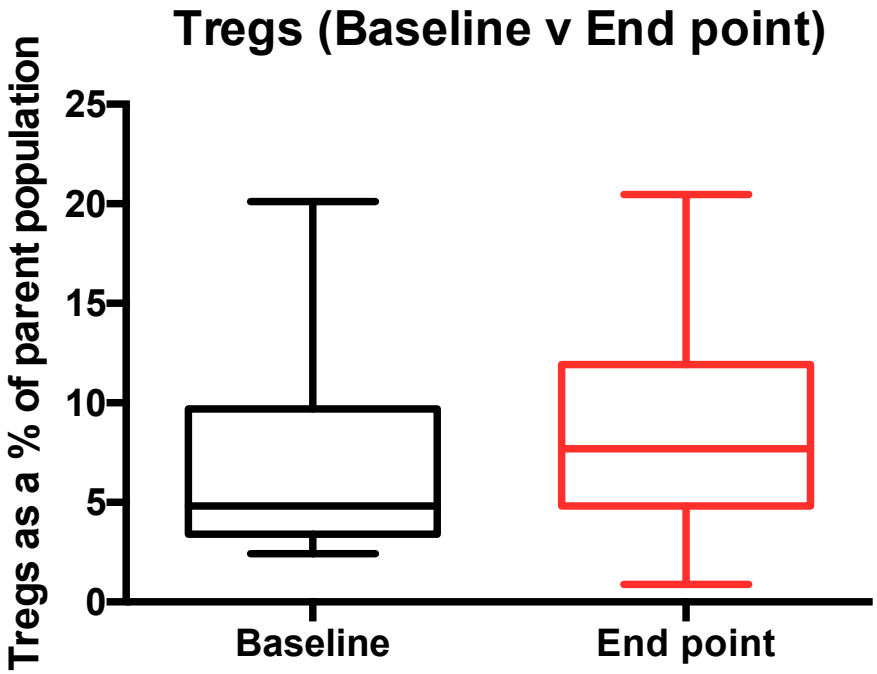

Figure 12.3. Box plot of Tregs at baseline and treatment end point. Whiskers are from minimum to maximum. There was no significant difference in Tregs in trial patients at treatment end point compared to baseline (P=0.36, 95% CI= -1.722 - 4.410).

12.1.2 Baseline and end point Tregs compared to patient overall survival

Trial patients were divided into two groups around an overall survival of six months. Tregs at baseline and end point were compared in these two groups. There was no significant difference in patients Tregs at baseline and end point in patients who survived more or less than 6 months. There was no significant change in Tregs at end point compared to baseline in patients who survived more than 6 months. There was a significant increase in Tregs in trial patients with a survival less than 6 months at treatment end point compared to baseline (P=0.03).

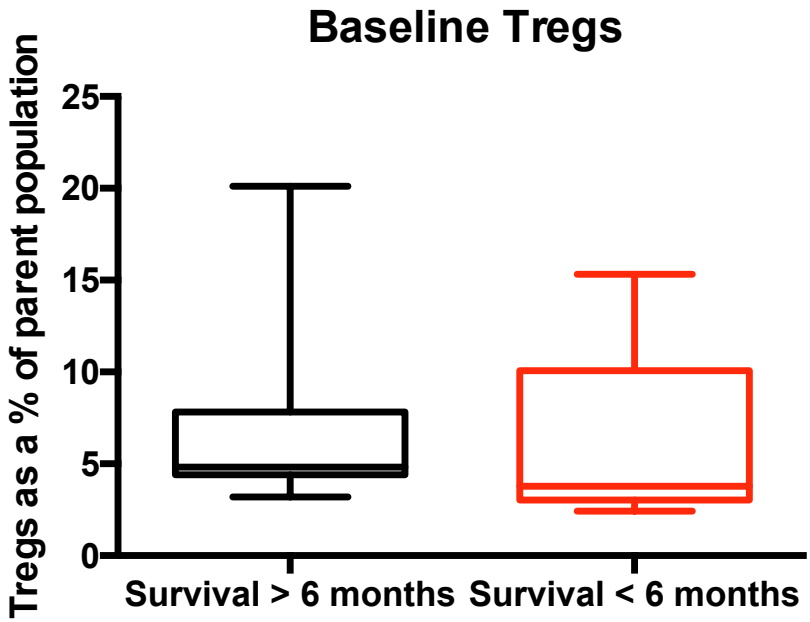

Figure 12.4. Box plot of baseline Tregs in trial patients who had an overall survival of less or more than 6 months. Whiskers are from minimum to maximum. There was no significant difference in baseline Tregs in patients who survived less than 6 months compared to those who survived more than 6 months (P=0.74, 95% CI= -4.319 - 5.918).

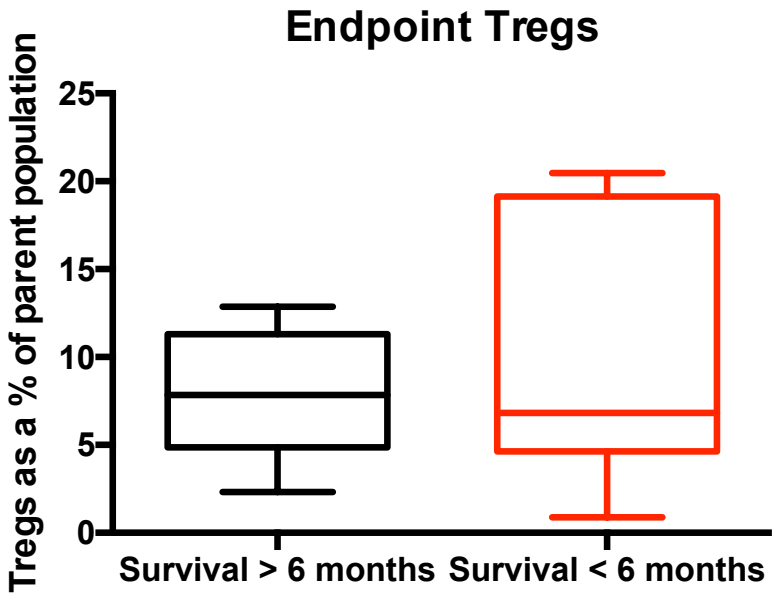

Figure 12.5. Box plot of end point Tregs in trial patients who had an overall survival of less or more than 6 months. Whiskers are from minimum to maximum. There was no significant difference in end point Tregs in patients who survived less than 6 months compared to those who survived more than 6 months (P=0.4865, 95% CI= -3.778 – 7.579).

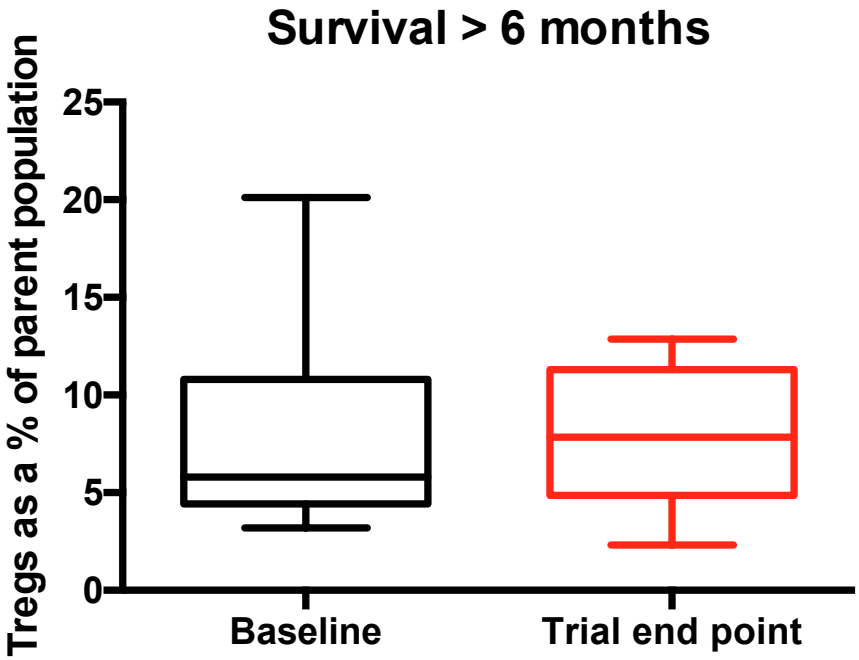

Figure 12.6. Box plot of Tregs at baseline and trial end point in trial patients who had an overall survival of more than 6 months. Whiskers are from minimum to maximum. There was no significant difference in Tregs in trial patients with a survival over 6 months at treatment end point compared to baseline (P=0.78, 95% CI= 5.636 - 7.205).

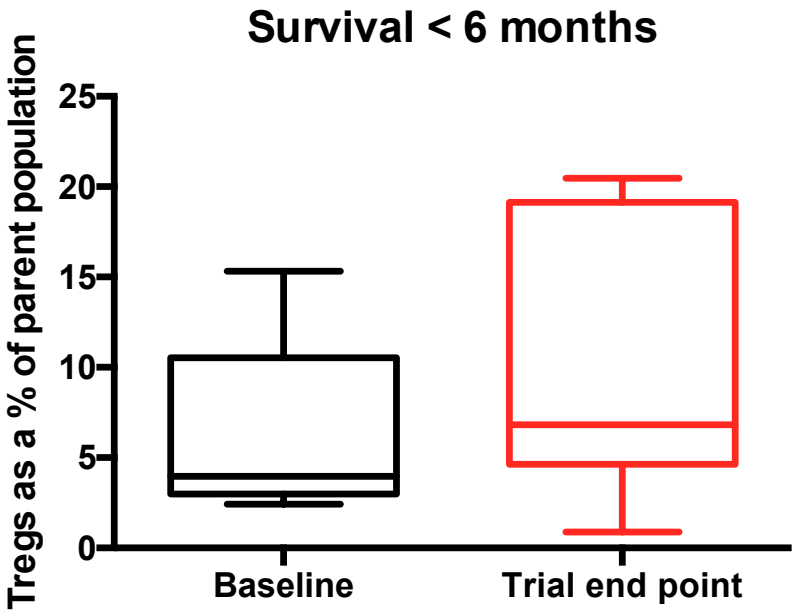

Figure 12.7. Box plot of Tregs at baseline and trial end point in trial patients who had an overall survival of less than 6 months. Whiskers are from minimum to maximum. There was a significant increase in Tregs in trial patients with a survival less than 6 months at treatment end point compared to baseline (P=0.03, 95% CI= -6.309 - -0.266).

12.1.3 Trial patients: Regression analysis

A mixed effects logistic regression analysis was performed on all trial patient samples using a bespoke regression model, as previously described, which allowed for random effects. There was no significant change in Tregs over the trial treatment time course.

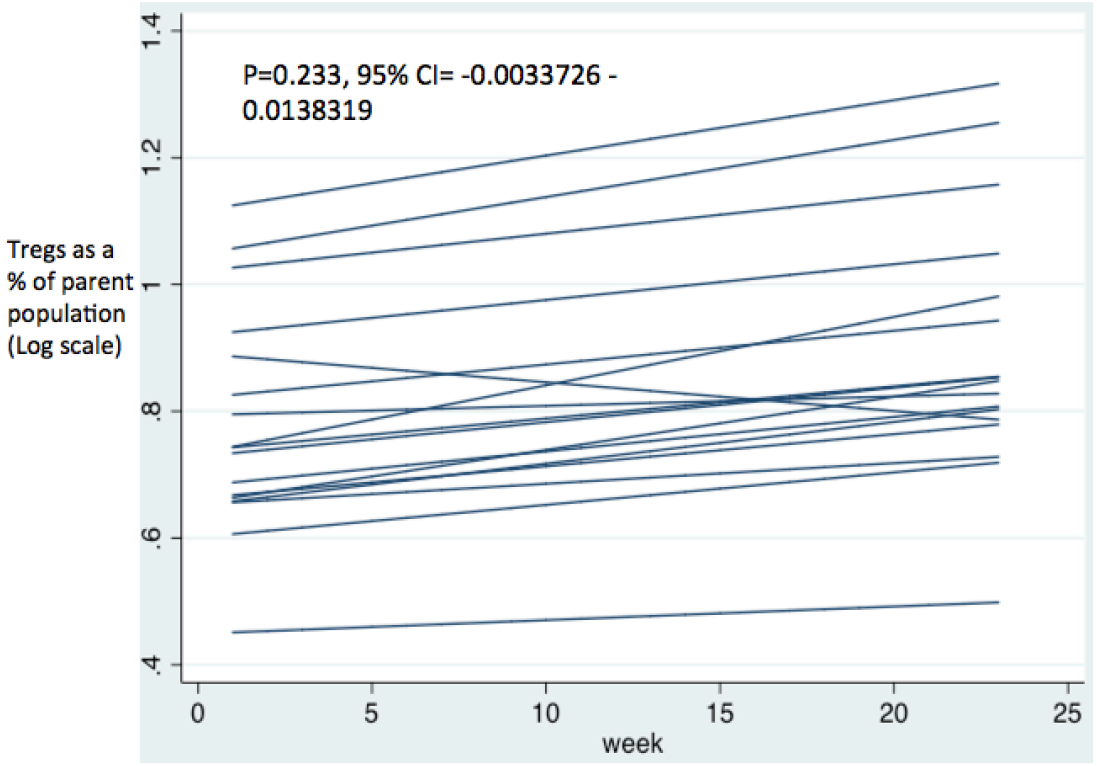

Figure 12.8. Output graph showing regression lines for individual patients plotted against time in weeks following mixed effects logistic regression analysis. Treg levels are shown on the y axis and are a calculated as a percentage of the parent population (log scale), time in weeks is shown on the x axis. Each regression line represents a patient. One hundred and five time points in eighteen patients were analysed. There is an increasing trend in Tregs over time but this was not significant (P=0.23, 95% CI= -0.003 - 0.014).

12.1.4 Trial patients: Survival analysis

The percentage change of Tregs at trial end point compared to baseline was calculated. Patients were divided into two groups, low and high Tregs around the median value percentage change. Kaplan-Meier curves were drawn to examine the relationship of change in Tregs and patients PFS and OS. Log rank analysis were used to evaluate the survival curves. 16 patients were eligible for analysis. Patient T10 was excluded from this analysis as the patient became operable and inclusion would have biased the analysis. Patient T14 was excluded from this analysis, as they had no sample following a baseline measurement. There was no difference in PFS or OS in patients who had a high or low change in Tregs at trial end point.

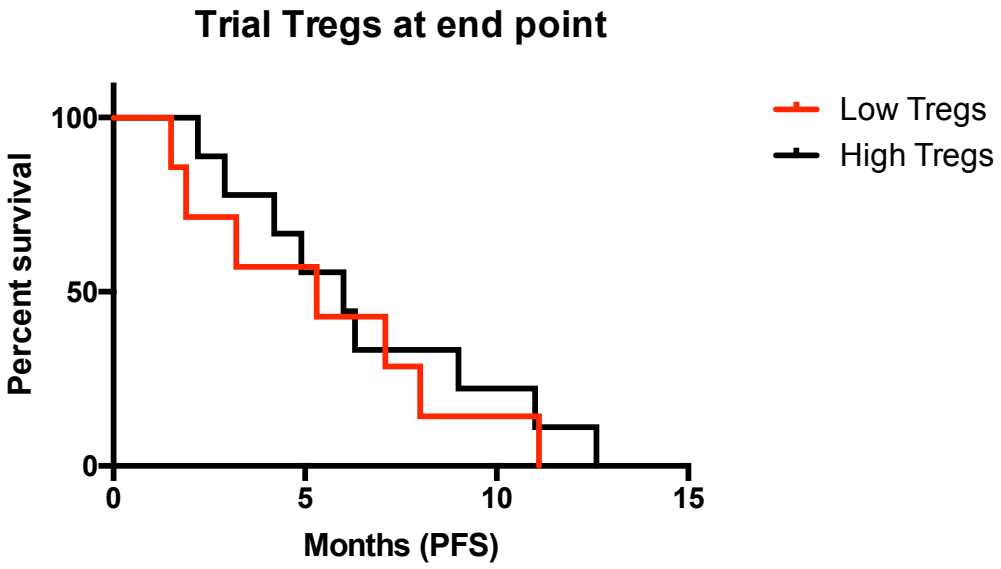

Figure 12.9. There was no benefit in progression free survival (PFS) in patients with either a low or high change in Tregs at treatment endpoint compared to baseline (log-rank (Mantel-Cox) test, P=0.69). Median survival in patients with low Tregs was 5.3 months (N=8). Median survival in patients with high Tregs was 6 months (N=8).

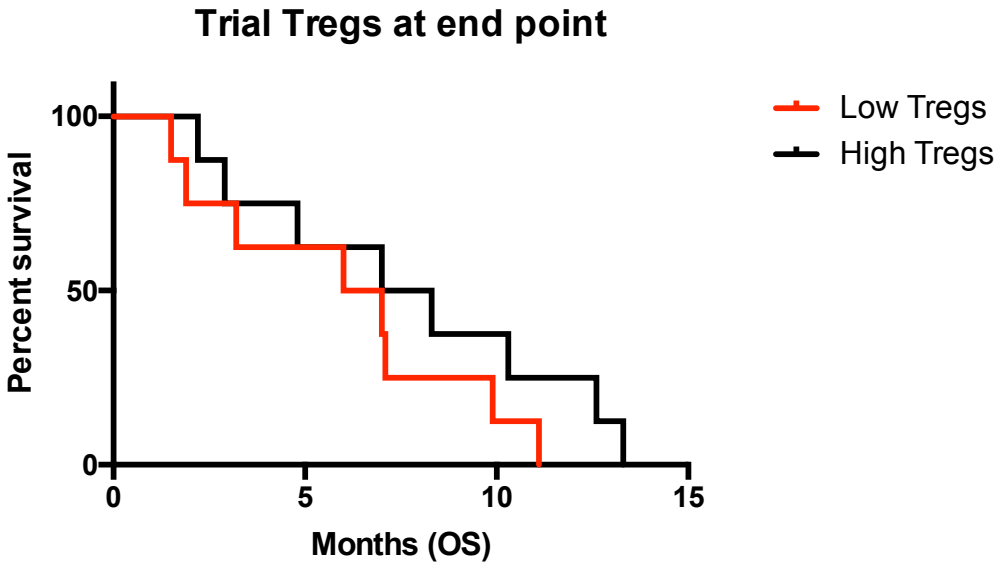

Figure 12.10. There was no benefit in overall survival (OS) in patients with either a low or high change in Tregs at treatment endpoint compared to baseline (log-rank (Mantel-Cox) test, P=0.25). Median survival in patients with low Tregs was 6.5 months (N=8). Median survival in patients with high Tregs was 7.65 months (N=8).

12.2 T regulator cells: Control patients

Twenty-seven samples were analysed from nine control patients. Tregs were identified as triple positive for CD4, CD25 and Fox-P3 antibodies. Tregs were expressed as a percentage of the parent population analysed. There was no significant increase in Tregs at trial end point compared to baseline.

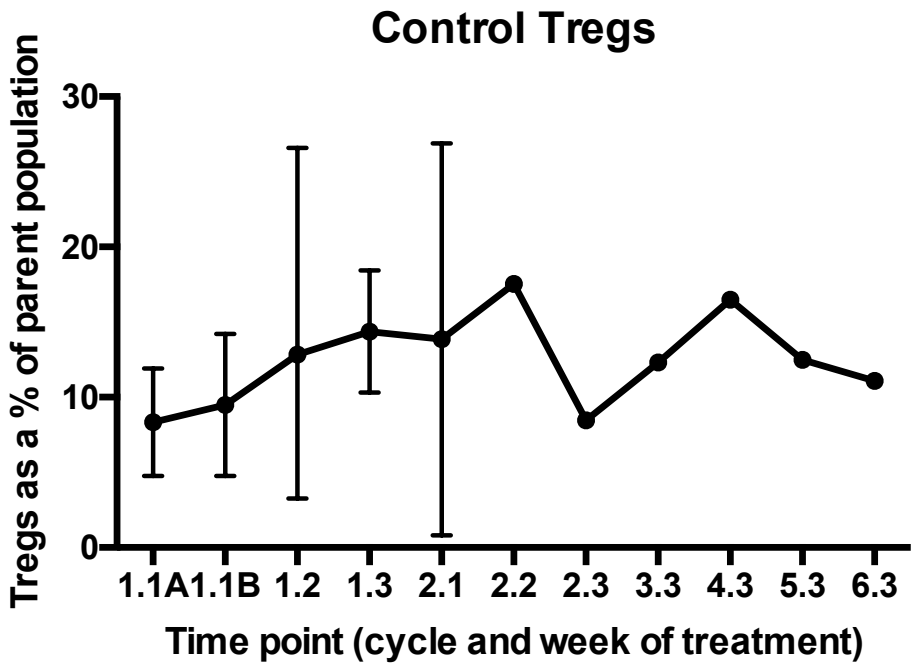

Figure 12.11. Figure showing mean trend line of control Tregs with range (minimum to maximum). Time point 1.1A is the baseline pre-treatment time point. Time point 1.1B is the post treatment time point.

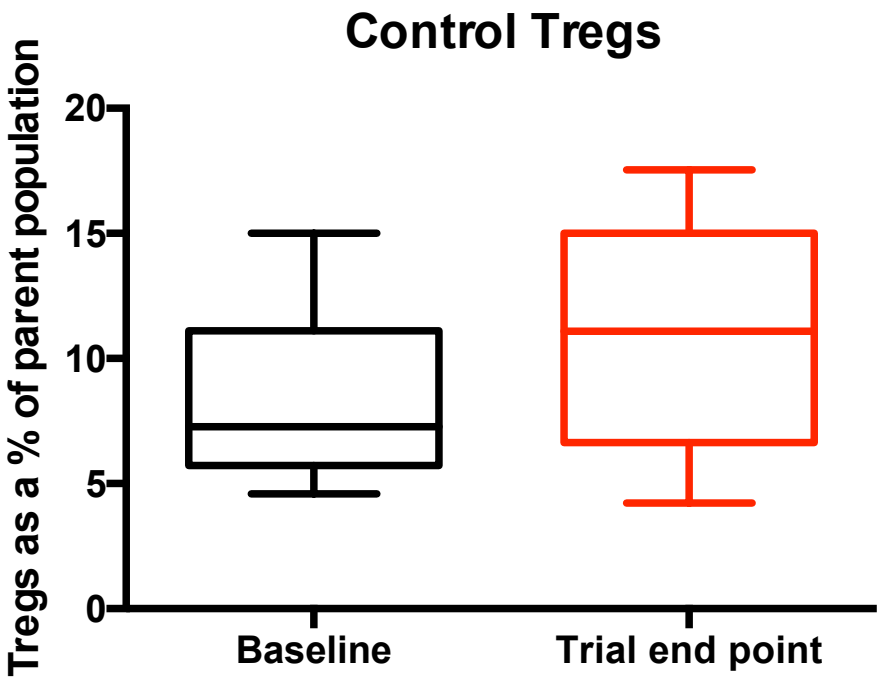

Figure 12.12. Box plot of Tregs at baseline and treatment end point. Whiskers are from minimum to maximum. There was no statistical significance when comparing levels at trial end point to baseline (P=0.09, 95% CI = -0.5184 – 5.750).

12.2.1 Control patients: Regression analysis

A bespoke mixed effects regression analysis was performed on all control patient samples. There was a significant increase in Tregs over the trial treatment time course (P=0.005).

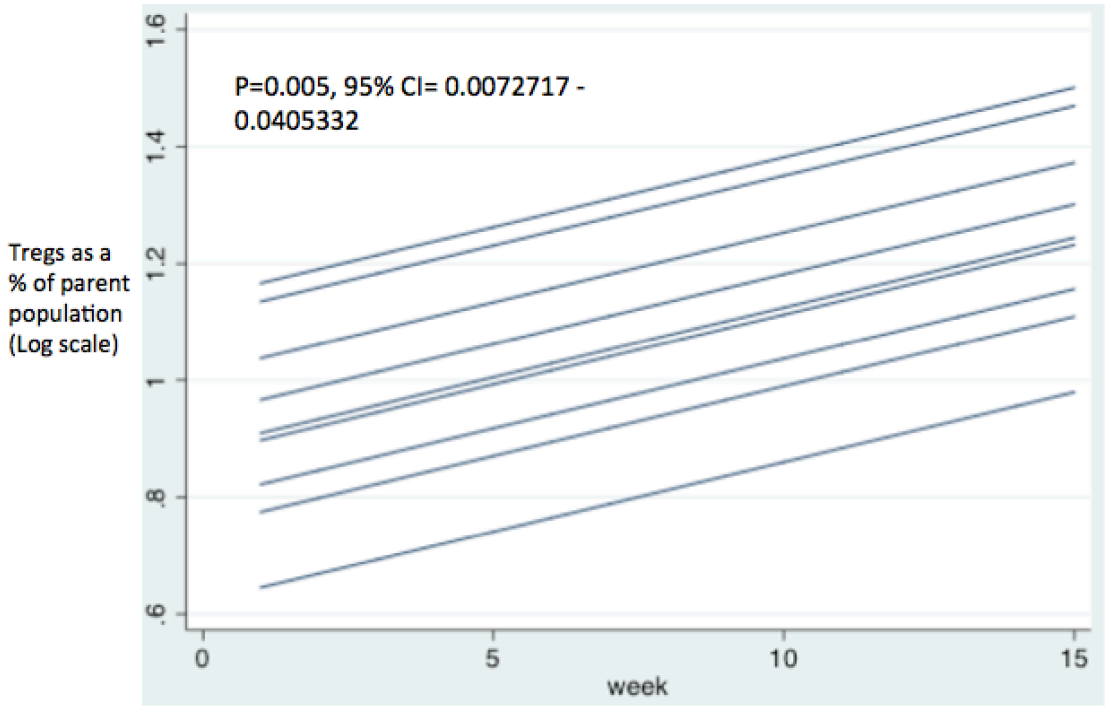

Figure 12.13. Output graph showing regression lines for individual patients plotted against time in weeks following multinomial logistic regression analysis. Treg levels are shown on the y axis and are a calculated as a percentage of the parent population (log scale), time in weeks is shown on the x axis. Each regression line represents a patient. Twenty-seven samples in nine patients were analysed. There is a significant increase in Tregs (P=0.005, 95% CI = 0.007 - 0.040).

12.3 T regulator cells: Comparison analysis

Trial patients were compared to the control cohort. There was no significant difference in baseline and end point Tregs in trial compared to control patients.

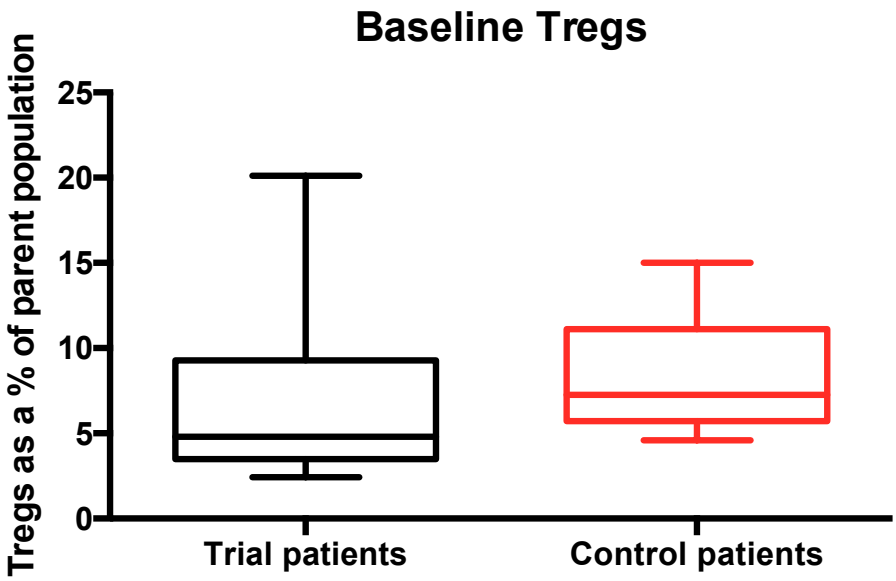

Figure 12.14. Box plot of baseline Tregs in trial and control patients. Whiskers are from minimum to maximum. There was no significant difference between baseline trial and control patient Tregs (P=0.601, 95 % CI= -2.966 – 5.015).

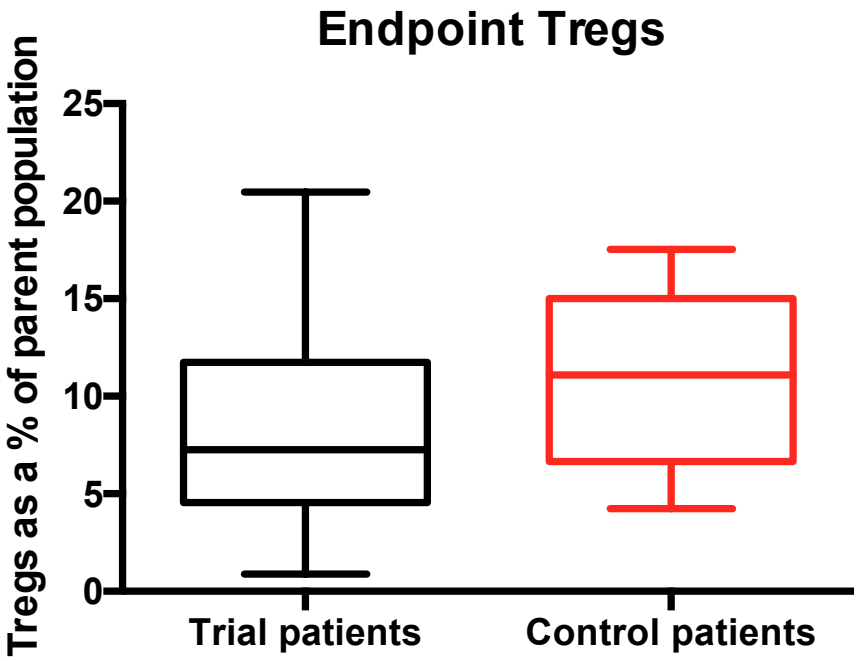

Figure 12.15. Box plot of end point Tregs in trial and control patients. Whiskers are from minimum to maximum. There was no significant difference between end point trial and control patient Tregs (P=0.26, 95 % CI= -1.908 - 6.694).

12.3.1 Comparison survival analysis

Tregs in both trial and control patients were divided into two groups (low and high change groups) around the median percentage change in Tregs between baseline and end point. Overall survival and progression free survival of trial and control patients was compared in the low and high change groups. Patient T10 was excluded from this analysis as the patient became operable and inclusion would bias the analysis. Patient T14 was excluded from this analysis, as they had no sample following a baseline measurement. In patients with a low change in Tregs, there was a significant difference in progression free survival in trial versus control patients (log-rank (Mantel-Cox) test, P=0.007). There was no difference in the PFS of trial and control patients with a high change in Tregs. There was no significant difference in the OS of trial and control patients with a high or low change in Tregs.

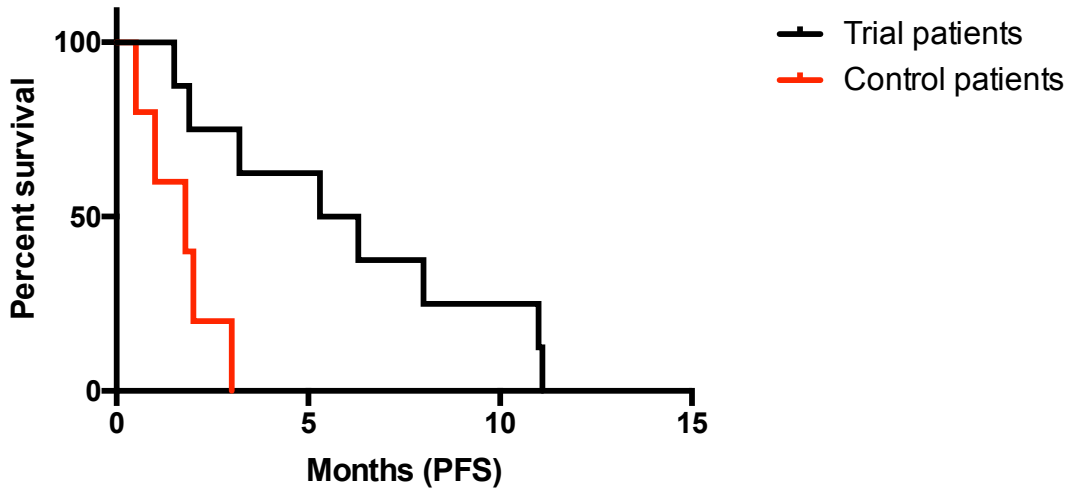

Figure 12.16. There was a significant difference in progression free survival (PFS) in patients with a low change in Tregs in trial versus control patients (log-rank (Mantel-Cox) test, P=0.007). Median survival in trial patients (N=8) was 5.8 months. Median survival in control patients (N=5) was 1.8 months.

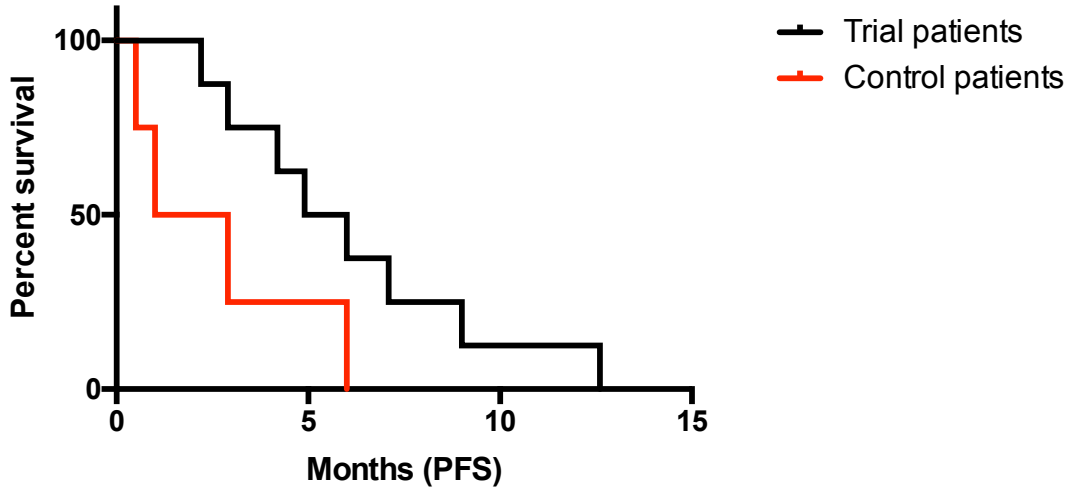

Figure 12.17. There was no significant difference in progression free survival (PFS) in patients with a high change in Tregs in trial versus control patients (log-rank (Mantel-Cox) test, P=0.083). Median survival in trial patients (N=8) was 5.45 months. Median survival in control patients (N=4) was 1.95 months.

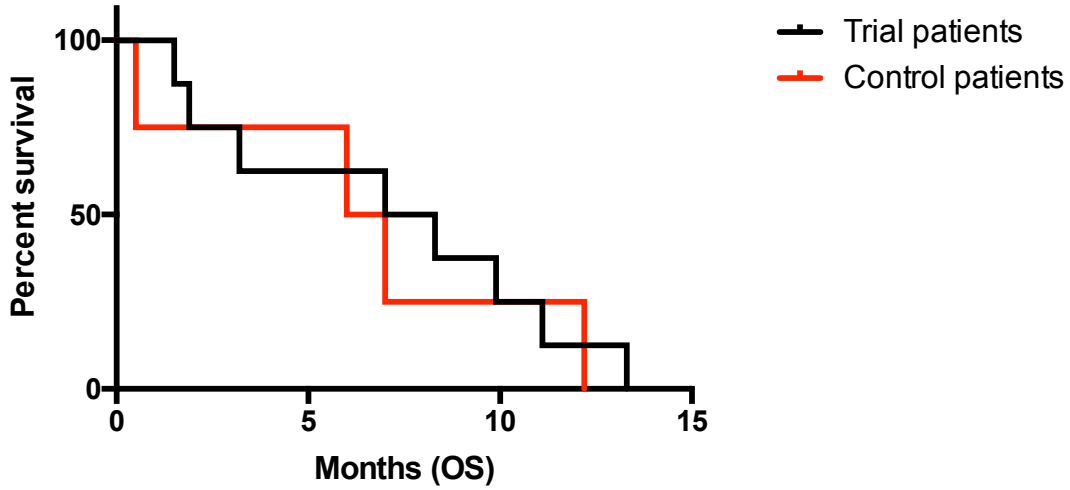

Figure 12.18. There was no significant difference in overall survival (OS) in patients with a low change in Tregs in trial versus control patients (log-rank (Mantel-Cox) test, P=0.732). Median survival in trial patients (N=8) was 7.65 months. Median survival in control patients (N=4) was 6.5 months.

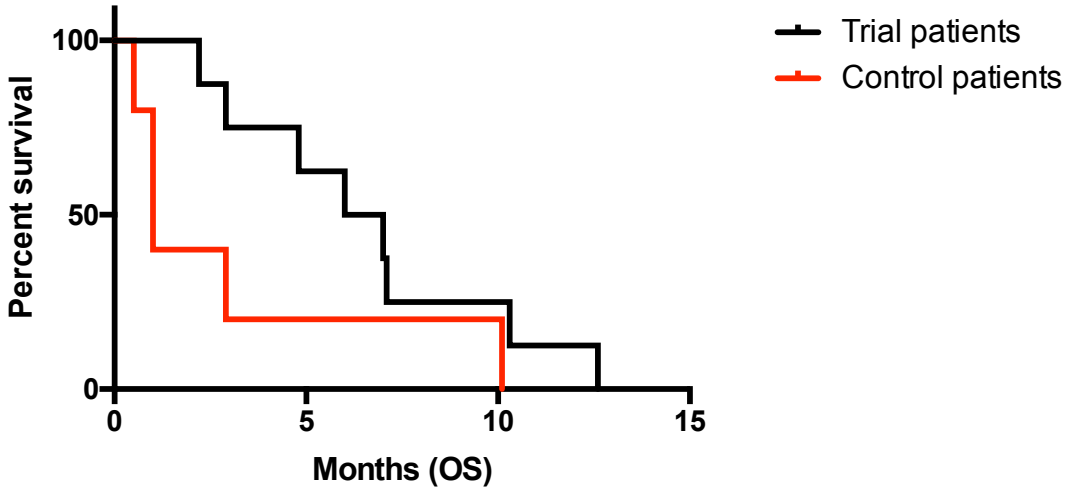

Figure 12.19. There was no significant difference in overall survival (OS) in patients with a high change in Tregs in trial versus control patients (log-rank (Mantel-Cox) test, P=0.1118). Median survival in trial patients (N=8) was 6.5 months. Median survival in control patients (N=5) was 1 month.

12.3.2 Regression analysis

A mixed effects regression model that allowed for random effects was used to compare Tregs in the two groups. One hundred and thirty-six time points in twenty-seven patients were included for analysis. There was no significance between the two groups at each cycle. The effect of the week between trial and control groups was analysed in cycle one. There was no significance between week one (P=0.99, 95% CI=-5.7354 – 1.8893), week two (P=0.07, 95% CI=-4.0107 – 4.2897), and week three (P=0.32, 95% CI=-6.2096 – 2.0285). Overall there was no statistically significant difference between the trial and control patients over time (P=0.586).

13 Chapter Thirteen: Endothelial Progenitor Cells (EPCs) Results

PBMC were analysed for EPCs. As discussed there is controversy defining a specific EPC phenotype and therefore EPCs with three antibody phenotypes were analysed.

1. $CD45^-$, $CD31^+$ and $CD133^+$.
2. $CD45^-$, $CD31^+$and $CD34^+$.
3. $CD45^-$, $CD31^+$, $CD133^+$ and $CD34^+$.

13.1 EPCs ($CD45^-$, $CD31^+$ and $CD133^+$ EPCs): Trial patients

One hundred and three samples were analysed from eighteen trial patients. EPCs were identified as having a $CD45^-$, $CD31^+$and $CD133^+$ phenotypes. EPCs were expressed as a percentage of the patient population analysed.

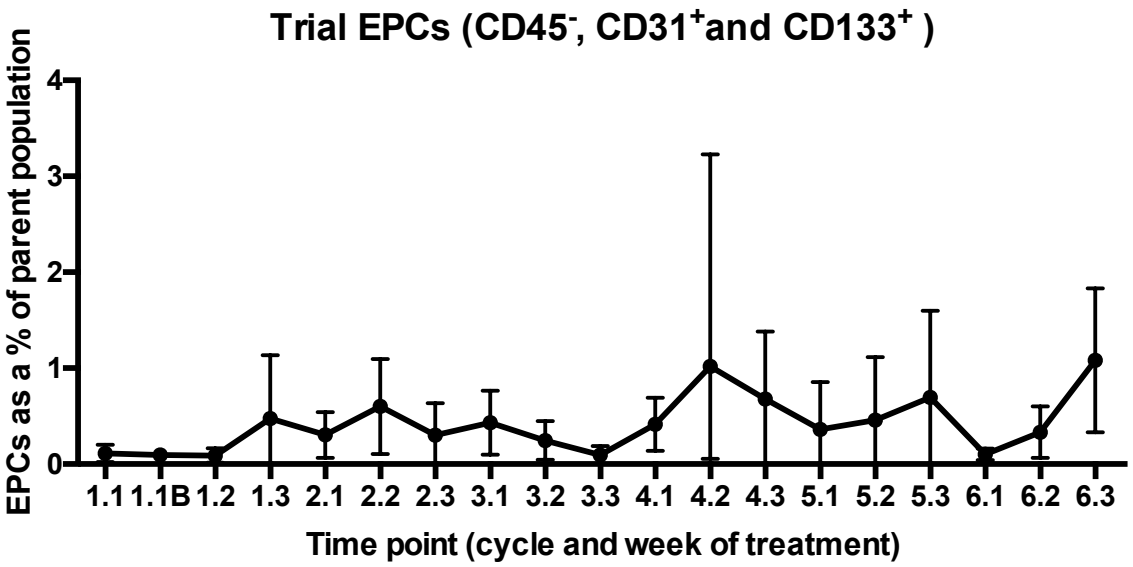

Figure 13.1. Figure showing mean trend line of trial EPCs with a $CD45^-$, $CD31^+$ and $CD133^+$ phenotype, with range (minimum to maximum).

13.1.1 Baseline versus post treatment EPCs at one month and trial end point

EPCs were analysed at baseline compared to one-month post treatment and trial end point. There was a significant increase in EPCs at one-month post treatment compared to baseline (P=0.02), and at end point compared to baseline (P=0.029).

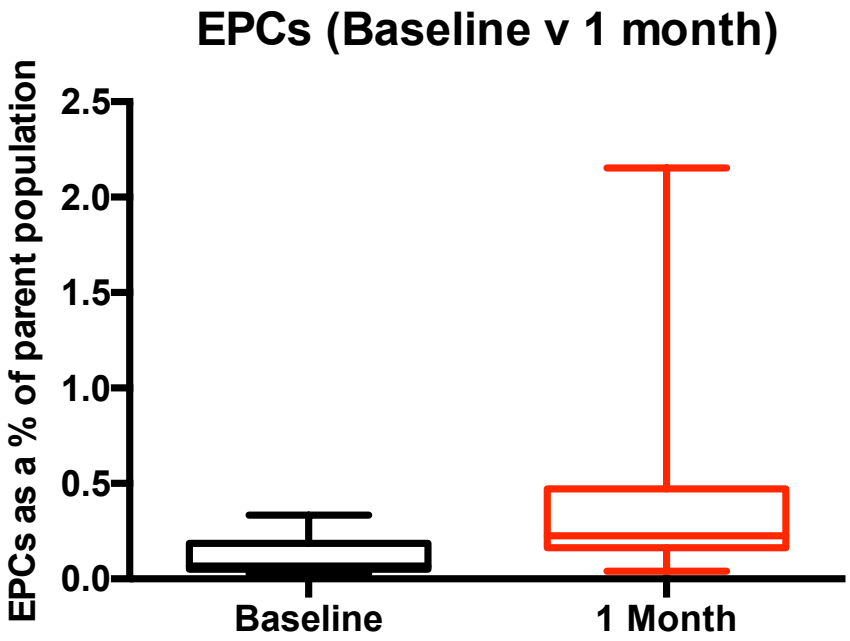

Figure 13.2. Box plot of EPCs at baseline and following 1 month of treatment. Whiskers are from minimum to maximum. There was a significant difference in EPCs in trial patients at one month following treatment compared to baseline (P=0.02, 95% CI= 0.052 – 0.614).

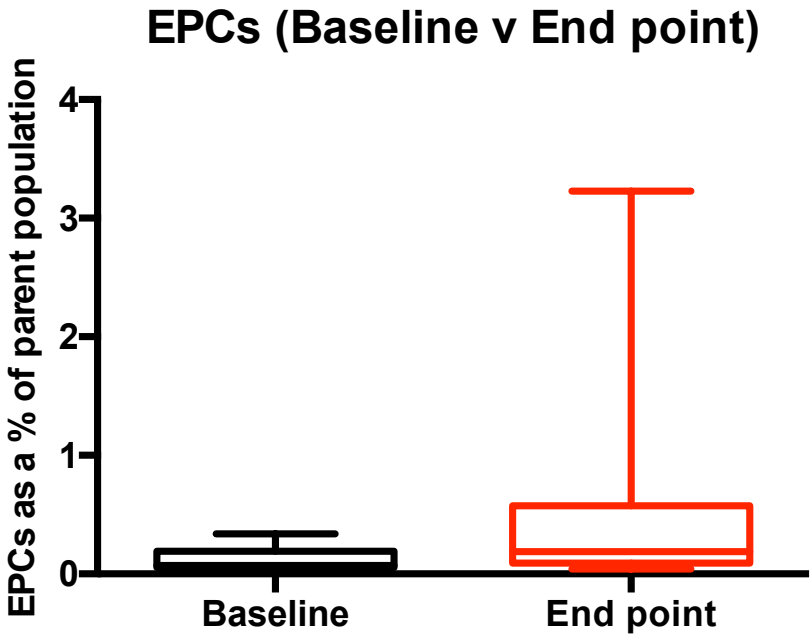

Figure 13.3. Box plot of EPCs at baseline and treatment end point. Whiskers are from minimum to maximum. There was a significant difference in EPCs in trial patients at end point following treatment compared to baseline (P=0.029, 95% CI= 0.0497 – 0.8720).

13.1.2 Baseline and end point EPCs compared to patient overall survival

Trial patients were divided into two groups around an OS of six months. EPCs at baseline and end point were compared in these two groups. There was a significant difference in baseline EPCs in patients who survived less than 6 months compared to patient who survived more than 6 months (P=0.008). This difference was not seen at end point EPCs (P=0.25). There was a significant increase in EPCs in trial patients with a survival over 6 months at treatment end point compared to baseline (P=0.048). There was no difference in EPCs in trial patients with a survival under 6 months at treatment end point compared to baseline (P=0.76).

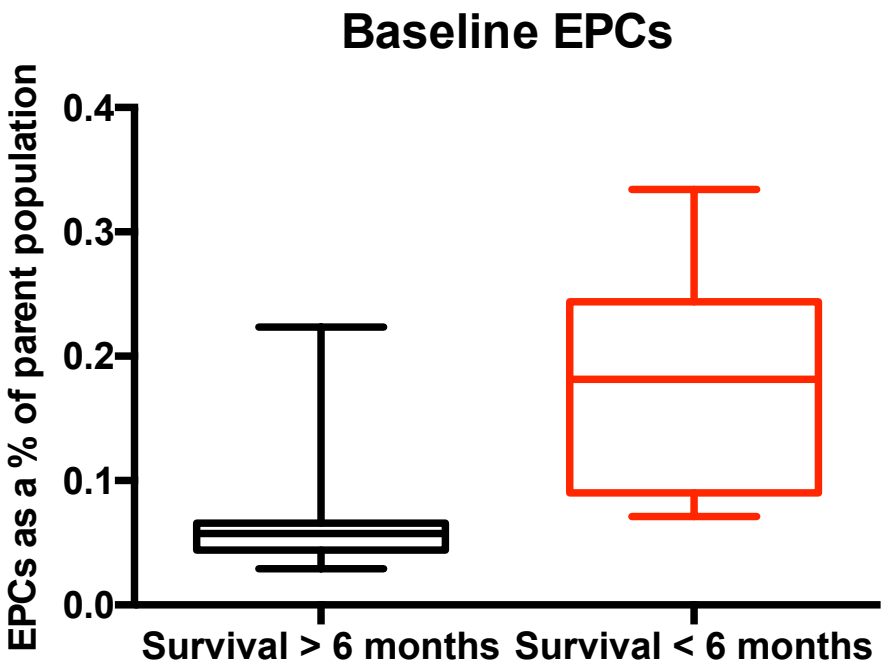

Figure 13.4. Box plot of baseline EPCs in trial patients who had an OS of less or more than 6 months. Whiskers are from minimum to maximum. There was a significant increase in baseline EPCs in patients who survived less than 6 months compared to those who survived more than 6 months (P=0.008, 95% CI= 0.0312- 0.1803).

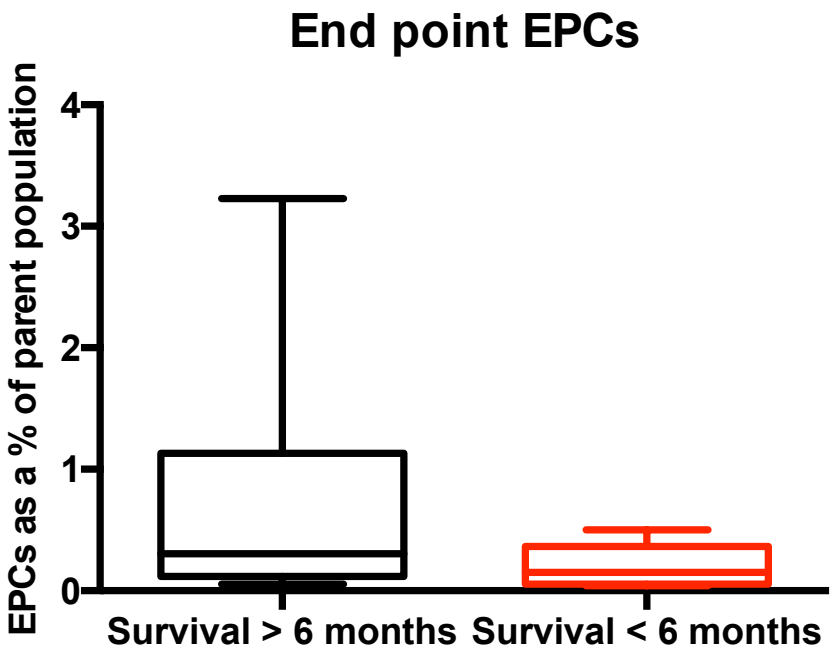

Figure 13.5. Box plot of end point EPCs in trial patients who had an OS of less or more than 6 months. Whiskers are from minimum to maximum. There was no significant difference in end point EPCs in patients who survived less than 6 months compared to those who survived more than 6 months (P=0.25, 95% CI= -1.513 – 0.432).

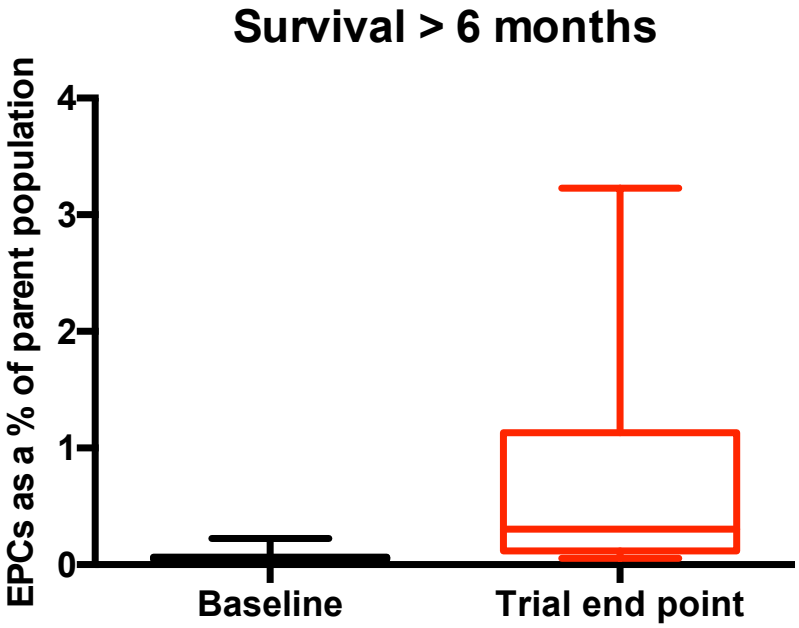

Figure 13.6. Box plot of EPCs at baseline and trial end point in trial patients who had an OS of more than 6 months. Whiskers are from minimum to maximum. There was a significant increase in EPCs in trial patients with a survival over 6 months at treatment end point compared to baseline (P=0.048, 95% CI= 0.006 – 1.335).

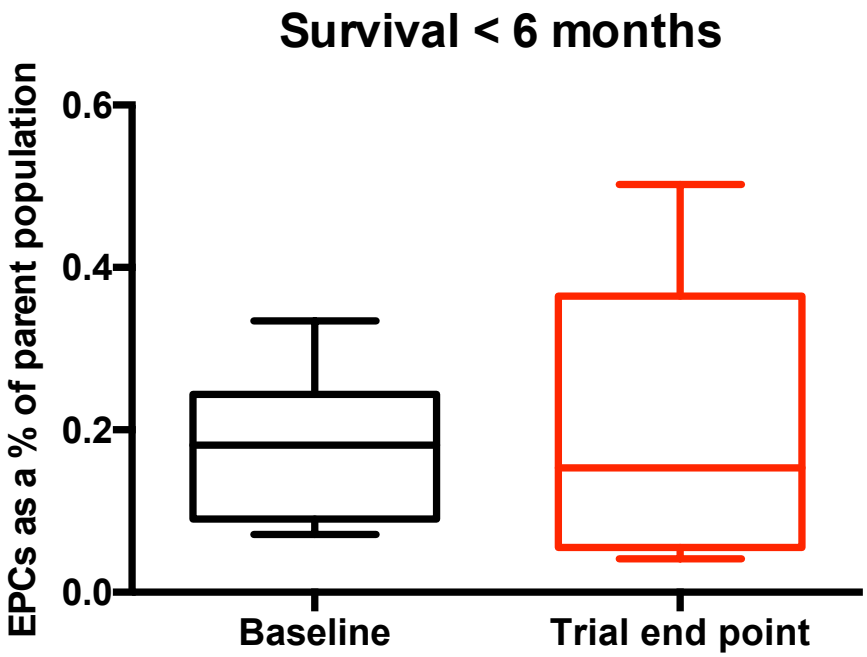

Figure 13.7. Box plot of EPCs at baseline and trial end point in trial patients who had an OS of less than 6 months. Whiskers are from minimum to maximum. There was no significant difference in EPCs in trial patients with a survival under 6 months at treatment end point compared to baseline (P=0.76, 95% CI= -0.156 – 0.206).

13.1.3 Trial patients: Regression analysis

Mixed effects logistic regression analysis was performed on all trial patient samples. There was a significant increase in EPC numbers over treatment (P=0.042).

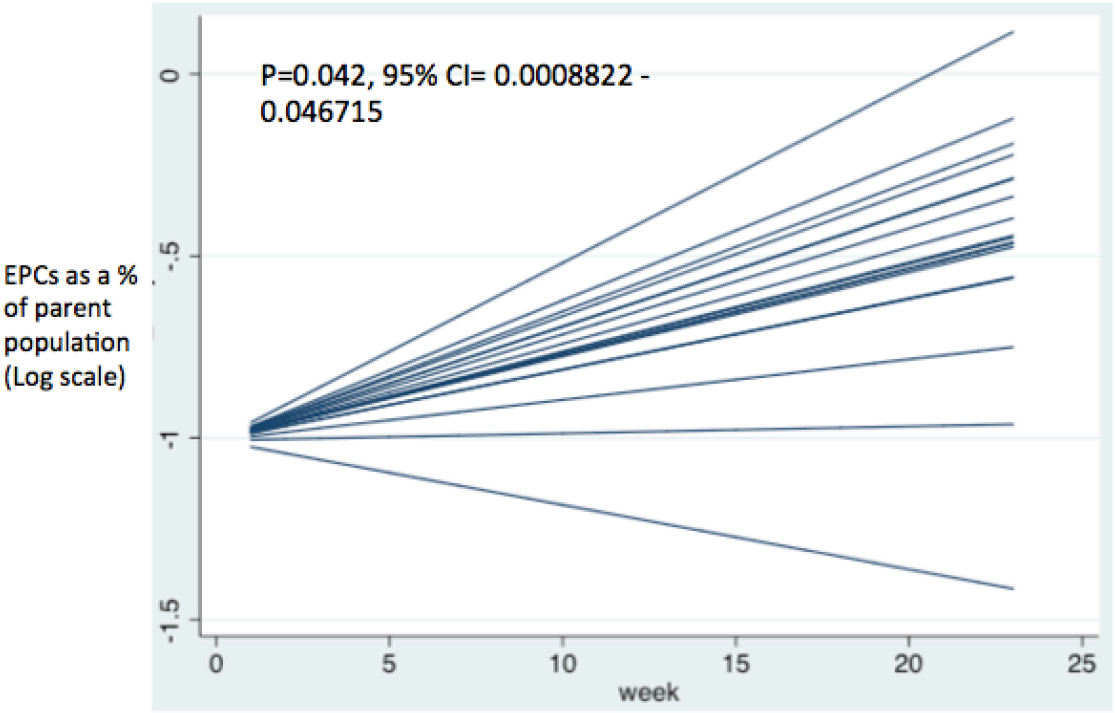

Figure 13.8. Output graph showing regression lines for individual patients plotted against time in weeks following mixed effects logistic regression analysis. EPCs levels are shown on the y axis and are a calculated as a percentage of the parent population (log scale), time in weeks is shown on the x axis. Each regression line represents a patient. One hundred and three time points in eighteen patients were analysed. There was a significant increase in EPCs over treatment (P=0.042, 95% CI= 0.0008 - 0.046).

13.1.4 Trial patients: Survival analysis

The percentage change of EPCs at trial end point compared to baseline was calculated. Patients were divided into two groups, low and high EPCs around the median value percentage change. Kaplan-Meier curves were drawn to examine the relationship of change in EPCs and patients PFS and OS. Log rank analysis were used to evaluate the survival curves. 15 patients were eligible for analysis. Patient T10 was excluded from this analysis as the patient became operable and inclusion would bias the analysis. Patients T7 and T14 were excluded from this analysis, as they had no sample following a baseline measurement. There was no difference in PFS or OS in patients who had a high or low change in EPCs at trial end point compared to baseline.

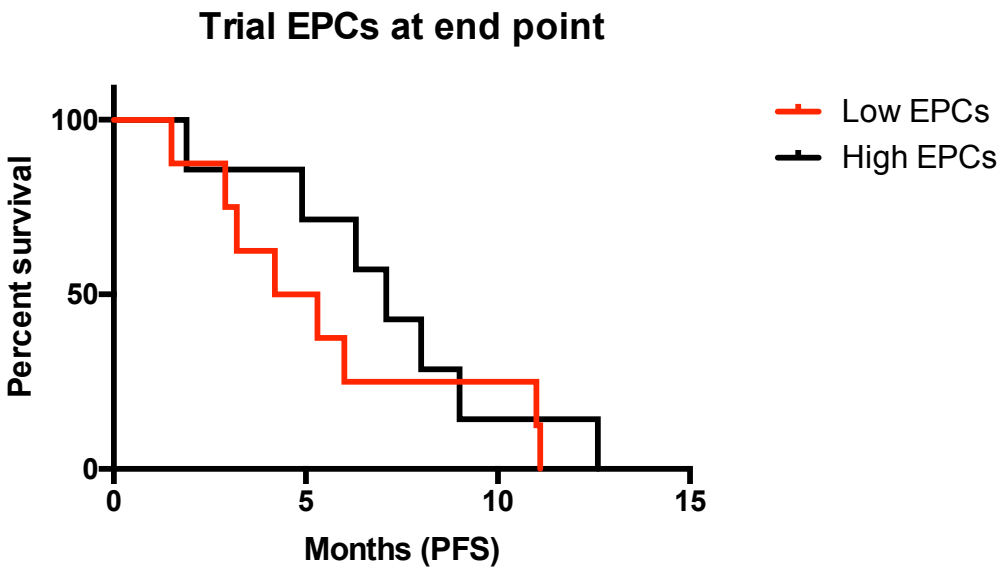

Figure 13.9. There was no significant difference in PFS in patients with a high change in EPCs at treatment end point compared to baseline (log-rank (Mantel-Cox) test, P=0.392). Median survival in patients with low EPCs (N=8) was 4.75 months. Median survival in patients with high EPCs (N=7) was 7.1 months

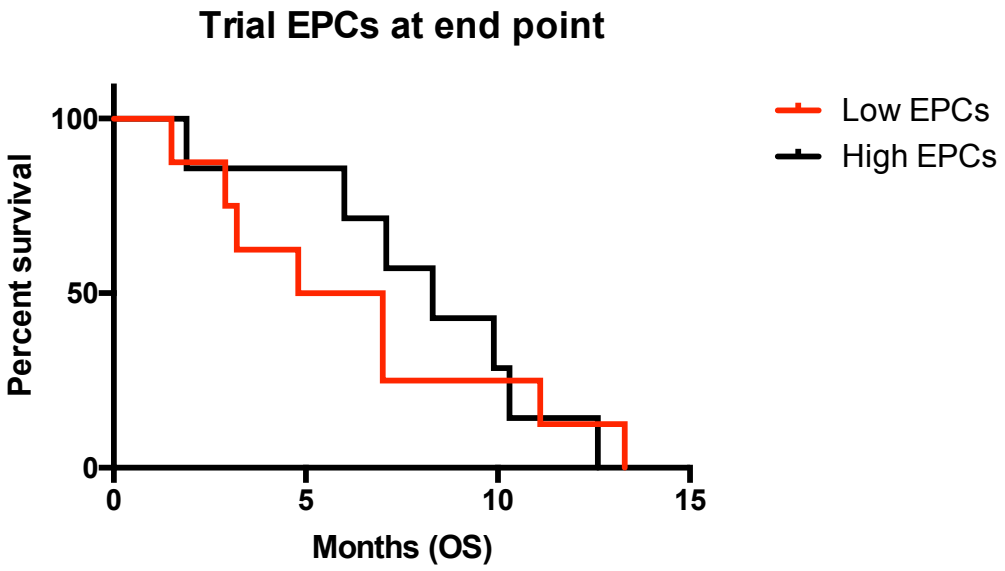

Figure 13.10. There was no significant difference in OS in patients with a high change in EPCs at treatment end point compared to baseline (log-rank (Mantel-Cox) test, P=0.78). Median survival in patients with low EPCs (N=8) was 5.9 months. Median survival in patients with high EPCs (N=7) was 8.3 months.

13.2 EPCs ($CD45^-$, $CD31^+$and $CD133^+$ EPCs): Control patients

Twenty-four samples were analysed from nine control patients. EPCs were identified as having a $CD45^-$, $CD31^+$and $CD133^+$ phenotype. EPCs were expressed as a percentage of the patient population analysed.

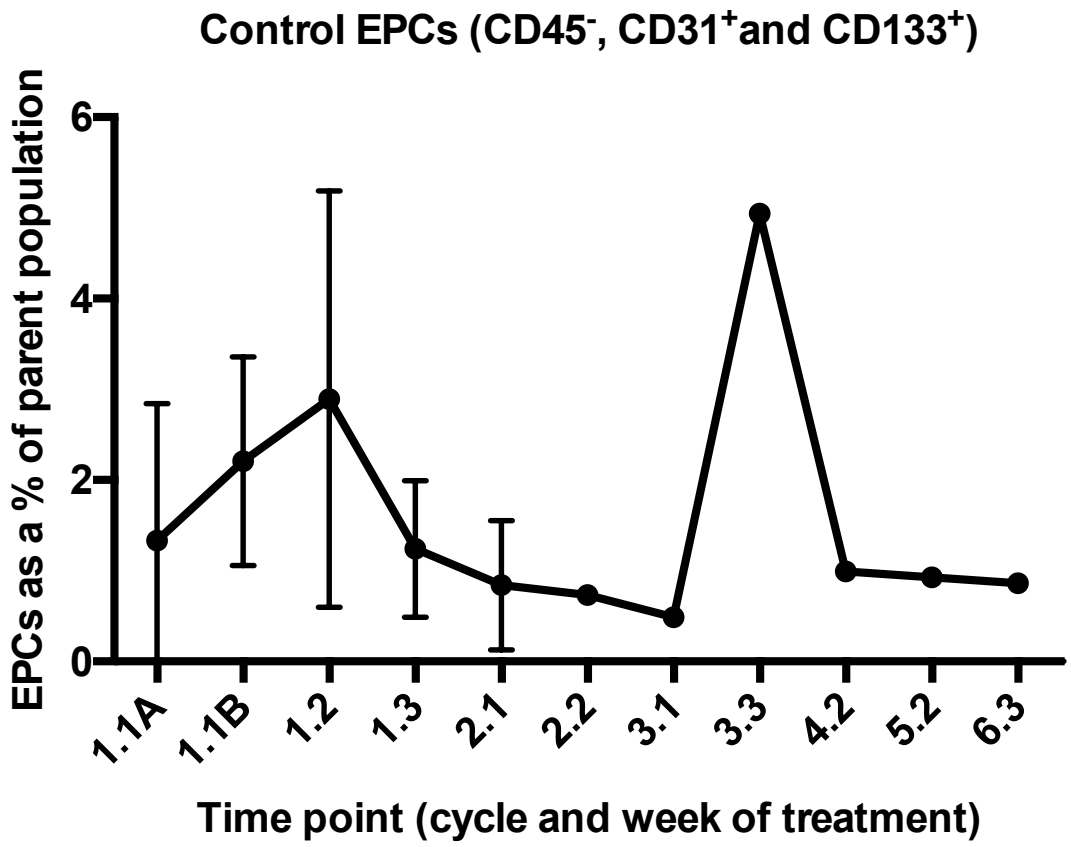

Figure 13.11. Figure showing mean trend line of trial EPCs with range (minimum to maximum). Time point 1.1A is the baseline pre-treatment time point. Time point 1.1B is the post treatment time point.

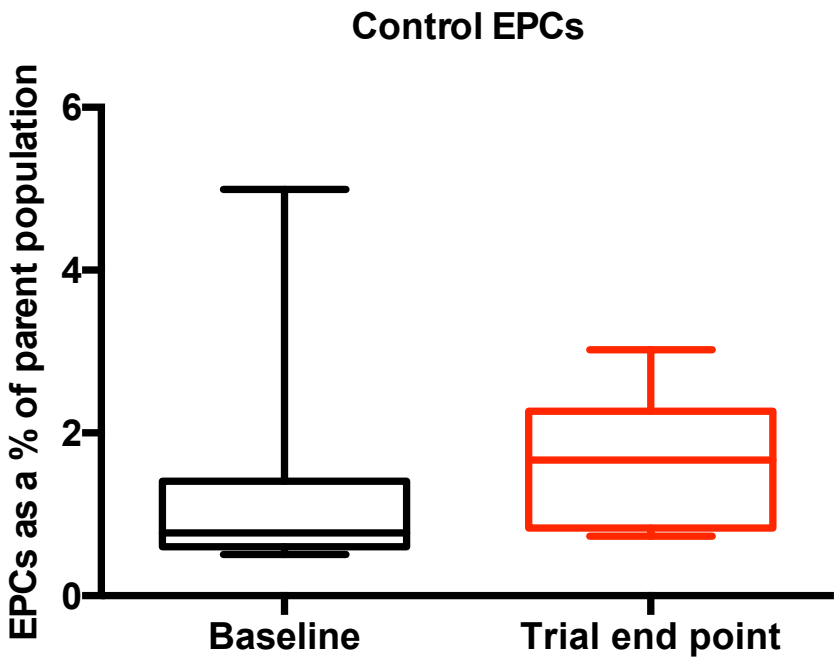

Figure 13.12. Box plot of baseline versus trial end point EPCs in control patients. Whiskers are from minimum to maximum values. There was no significant difference between baseline and trial end point EPCs (P=0.625, 95% CI= -01.072 – 1.717).

13.2.1 Control patients: Regression analysis

A mixed effects regression analysis was performed on all control patient samples. There was a non-significant increasing trend in EPCs over the trial treatment time course (P=0.705).

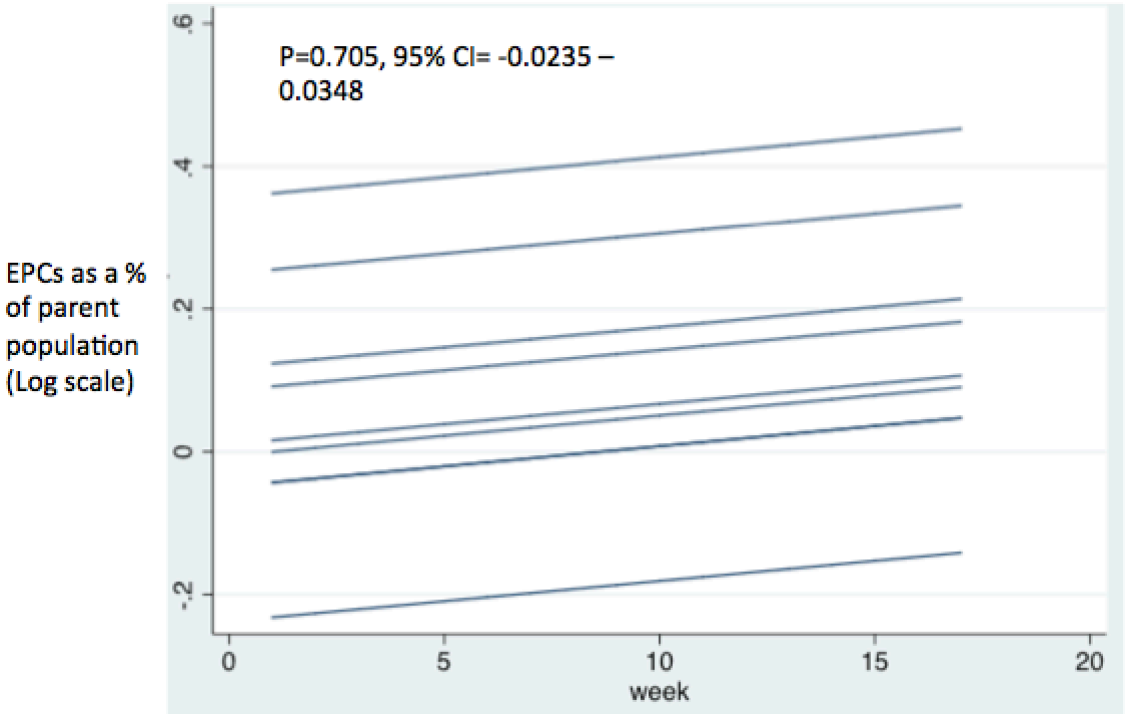

Figure 13.13. Output graph showing regression lines for individual patients plotted against time in weeks following mixed effects logistic regression analysis. EPCs levels are shown on the y axis and are a calculated as a percentage of the parent population (log scale), time in weeks is shown on the x axis. Each regression line represents a patient. Twenty-seven samples in nine patients were analysed. EPCs are calculated as a percentage of the parent population and plotted on a log scale. Twenty-four points in nine patients were analysed. There is an upward trend in EPCs over time, however this was not significant (P=0.705, 95% CI= -0.023 - 0.034).

13.3 EPCs ($CD45^-$, $CD31^+$ and $CD133^+$ EPCs): Comparative analysis

Trial patients EPCs were compared to the control cohort. There was a significant increase in control versus trial patients baseline EPCs (P=0.0009). This difference was not demonstrated between end point EPCs in trial and control patients (P=0.077).

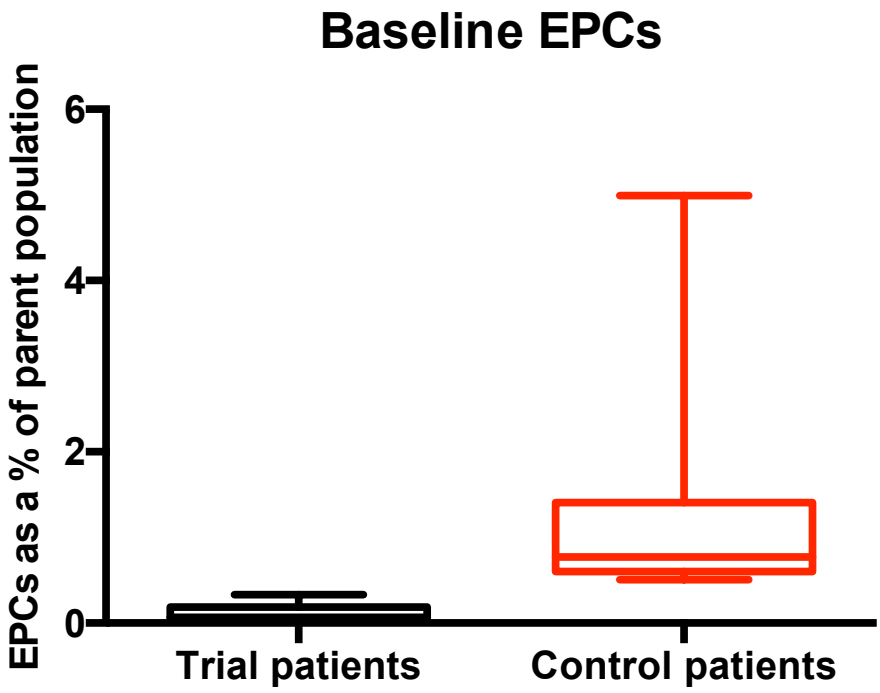

Figure 13.14. Box plot of baseline trial versus control patients EPCs. Whiskers are from minimum to maximum values. There was a significant increase in control versus trial patients baseline EPCs (P=0.0009, 95% CI = 0.554 – 1.905).

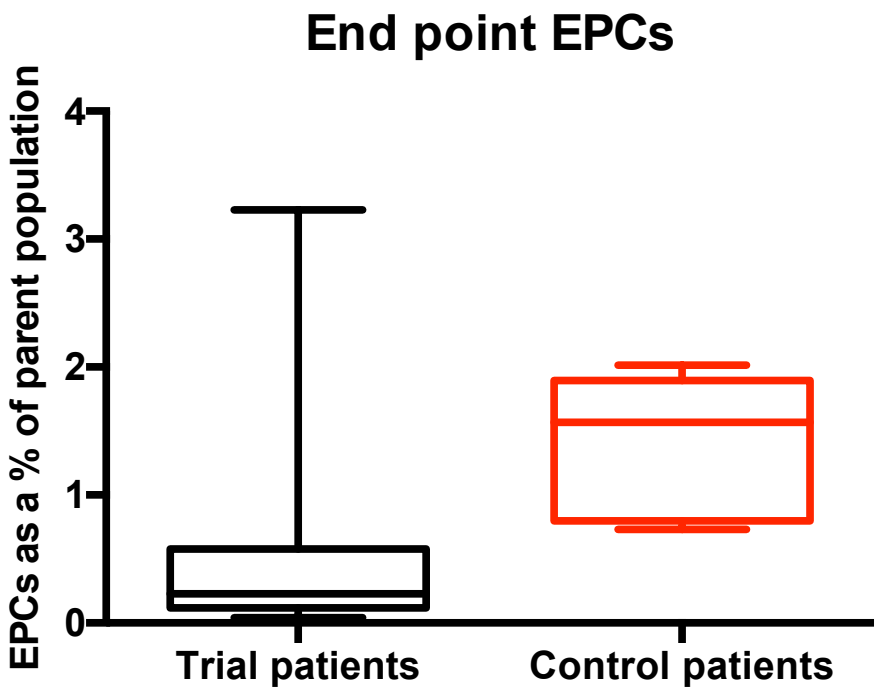

Figure 13.15. Box plot of endpoint trial versus control patients EPCs. Whiskers are from minimum to maximum values. There was no significant difference between endpoint EPCs in trial and control patients (P=0.077, 95% CI = -0.096 – 1.668).

13.3.1 Comparison survival analysis

EPCs in both trial and control patients were divided into two groups (low and high change groups) around the median percentage change in EPCs between baseline and end point. OS and PFS of trial and control patients were compared in the low and high change groups. Patient T10 was excluded from this analysis as the patient became operable and inclusion would bias the analysis. Patients C5, C7, C9, T7, T12 and T14 were excluded from this analysis as they had no sample following a baseline measurement. There was a significant PFS benefit in trial patients with a high change in EPCs versus control patients (P=0.0023). There was also a significant OS benefit seen in trial patients with a high change in EPCs versus control patients (P=0.019). This suggests a survival benefit in patients with an increase in EPCs. There was no difference in PFS or OS in patients with a low change in EPCs.

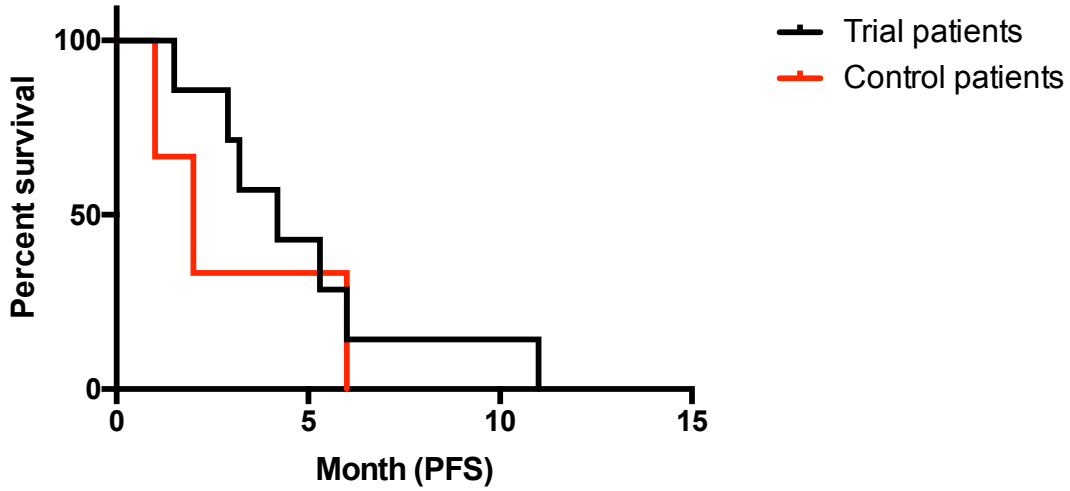

Figure 13.16. There was no significant difference in PFS in patients with a low change in EPCs in trial versus control patients (log-rank (Mantel-Cox) test, P=0.49). Median survival in trial patients (N=7) was 4.2 months. Median survival in control patients (N=3) was 2 months.

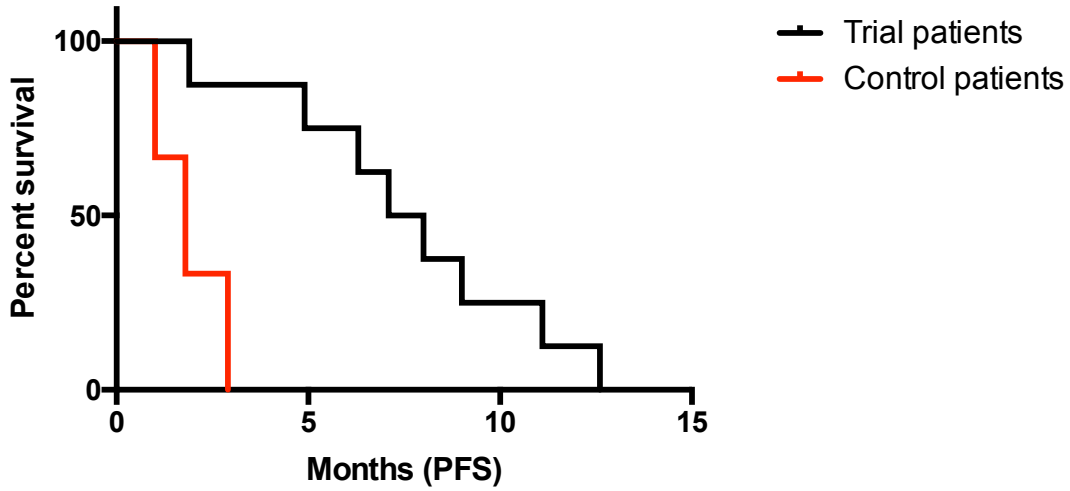

Figure 13.17. There was a significant difference in PFS in patients with a high change in EPCs in trial versus control patients (log-rank (Mantel-Cox) test, P=0.0023). Median survival in trial patients (N=8) was 7.55 months. Median survival in control patients (N=3) was 1.8 months.

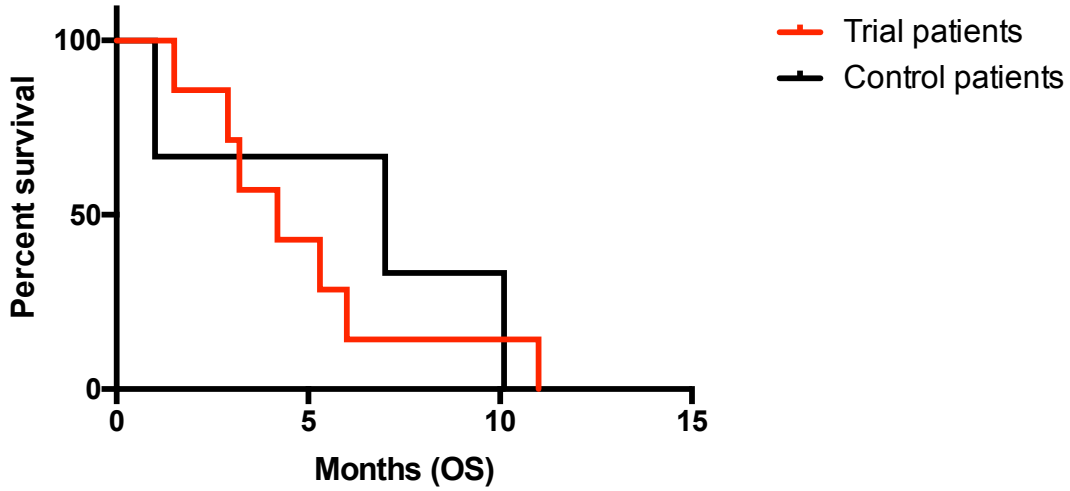

Figure 13.18. There was no significant difference in OS in patients with a low change in EPCs in trial versus control patients (log-rank (Mantel-Cox) test, P=0.74). Median survival in trial patients (N=7) was 4.2 months. Median survival in control patients (N=3) was 7 months.

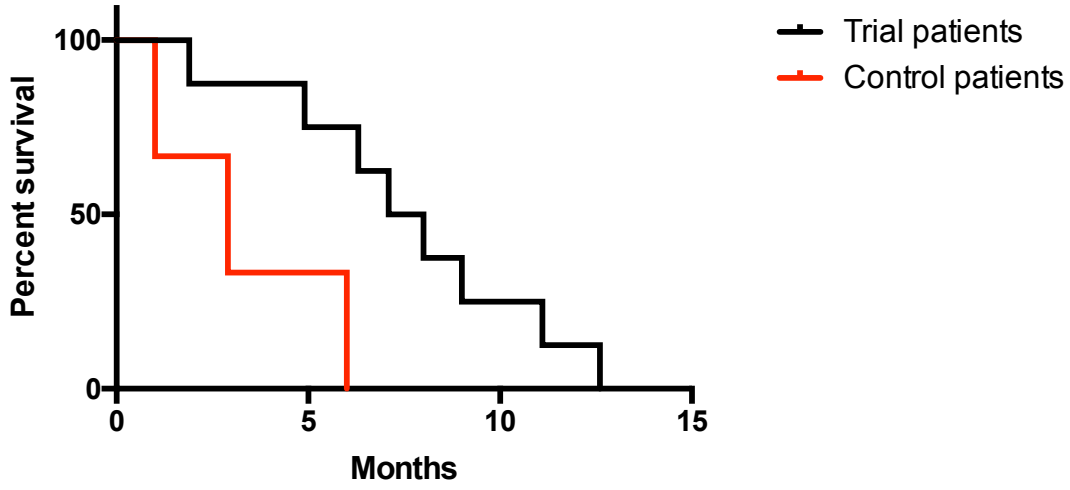

Figure 13.19. There was a significant difference in OS in patients with a high change in EPCs in trial versus control patients (log-rank (Mantel-Cox) test, P=0.019). Median survival in trial patients (N=8) was 7.5 months. Median survival in control patients (N=3) was 2.9 months.

13.3.2 Regression analysis

Mixed effects logistic regression analysis was used to examine EPCs between trial and control patients. One hundred and twenty-nine time points in twenty-seven patients were included for analysis. The effect of the week between trial and control groups was analysed in cycle one. There was no significance between week one (P=0.720, 95% CI= -07439 – 1.0767), week two (P=0.187, 95% CI= -1.4034 – 0.2733), and week three (P=0.272, 95% CI= -1.3806 – 0.3888). The effect of the cycle between the two groups was analysed, there was no significant difference between the two groups per cycle. Overall there was no significant difference between the trial and control patients over time (P=0.332).

13.4 EPCs ($CD45^-$, $CD31^+$ and $CD34^+$ EPCs): Trial patients

One hundred and two samples were analysed from eighteen trial patients. EPCs were identified as having a $CD45^-$, $CD31^+$ and $CD34^+$ phenotype. EPCs were expressed as a percentage of the patient population analysed.

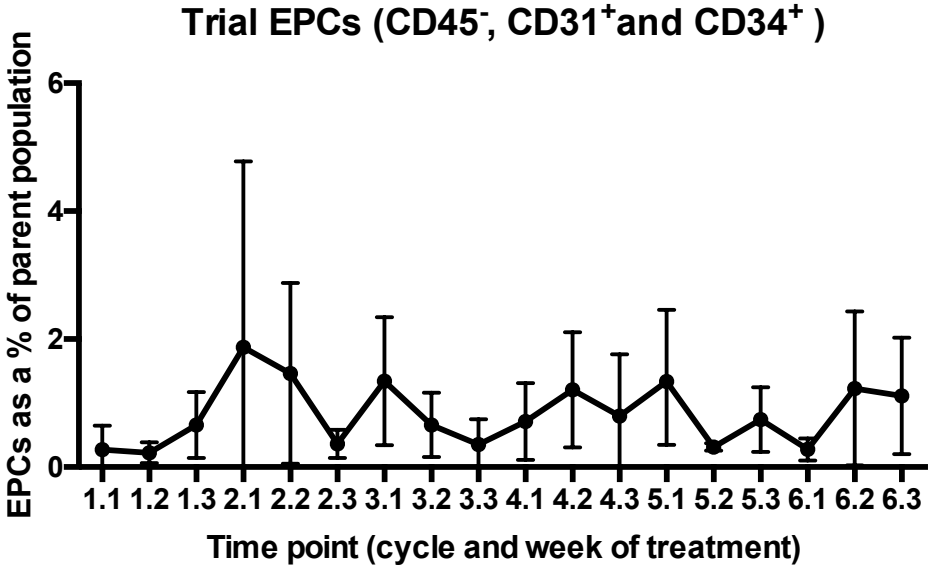

Figure 13.20. Figure showing mean trend line of trial EPCs with a $CD45^-$, $CD31^+$ and $CD34^+$ phenotype, with trend (minimum to maximum).

13.4.1 Baseline versus post treatment EPCs at one month and trial end point

EPCs were analysed at baseline compared to one-month post treatment and trial end point. There was a significant increase in EPCs at one-month post treatment compared to baseline (P=0.018), and at end point compared to baseline (P=0.045).

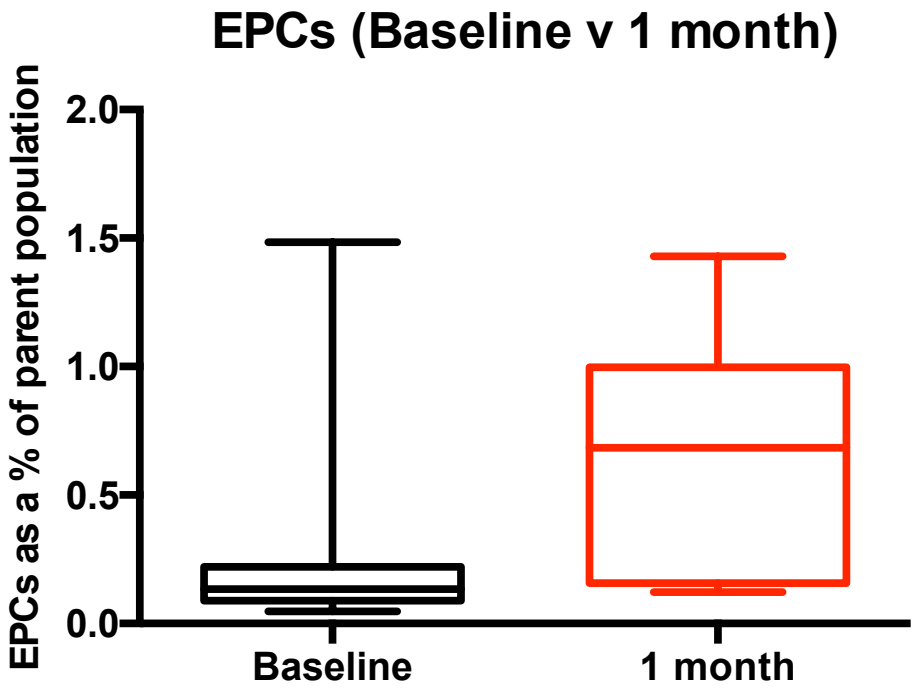

Figure 13.21. Box plot of EPCs at baseline and following 1 month of treatment. Whiskers are from minimum to maximum. There was a significant difference in EPCs in trial patients at one month following treatment compared to baseline (P=0.018, 95% CI= 0.073 – 0.734).

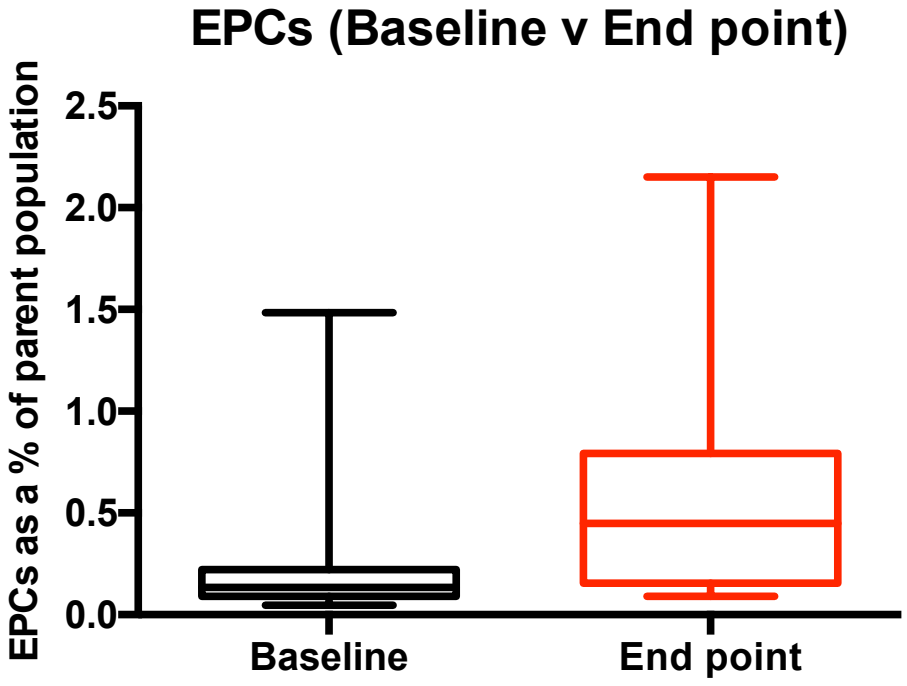

Figure 13.22. Box plot of EPCs at baseline and treatment end point. Whiskers are from minimum to maximum. There was a significant difference in EPCs in trial patients at end point following treatment compared to baseline (P=0.045, 95% CI= 0.008 – 0.687).

13.4.2 Baseline and end point EPCs compared to patient overall survival

Trial patients were divided into two groups around an OS of six months and EPCs at baseline and end point were compared in these two groups. There was no significant difference in baseline (P=0.1) or end point (P=0.99) EPCs in patients who survived less than 6 months compared to patient who survived more than 6 months. There was a significant difference in EPCs in trial patients with a survival over 6 months at treatment end point compared to baseline (P=0.01). There was no significant difference in EPCs in trial patients with a survival under 6 months at treatment end point compared to baseline (P=0.65).

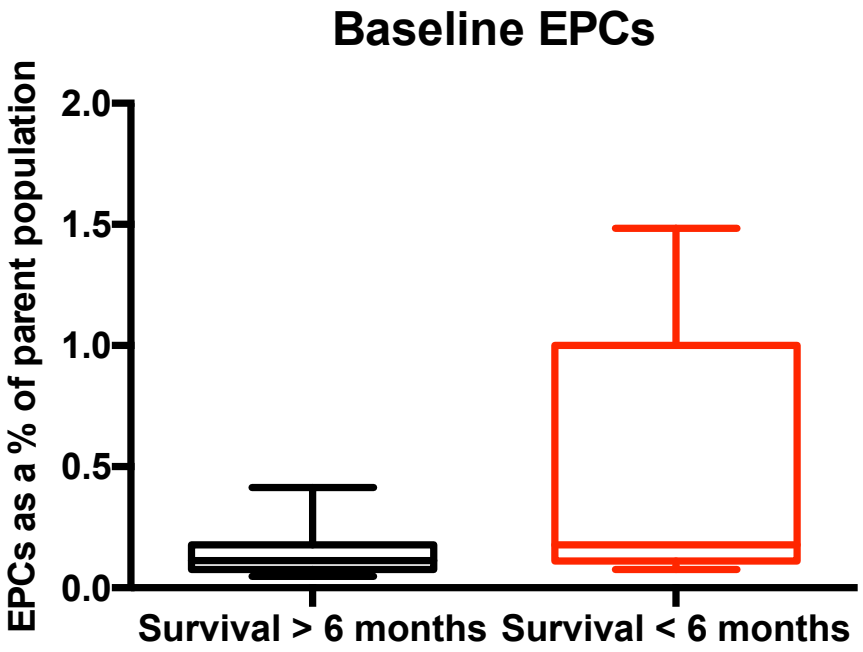

Figure 13.23. Box plot of baseline EPCs in trial patients who had an OS of less or more than 6 months. Whiskers are from minimum to maximum. There was no significant difference in baseline EPCs in patients who survived less than 6 months compared to those who survived more than 6 months (P=0.1, 95% CI= -0.064 – 0.662).

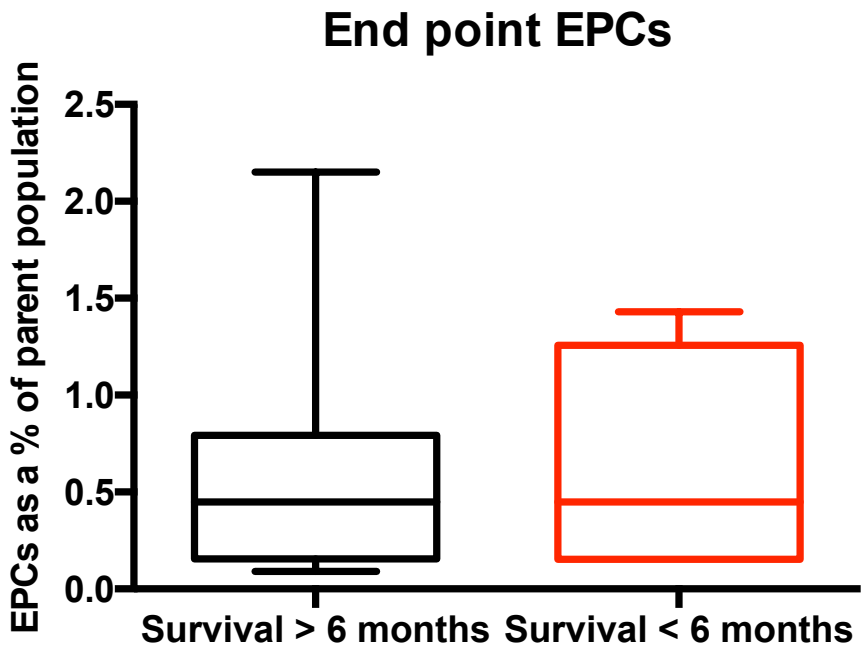

Figure 13.24. Box plot of end point EPCs in trial patients who had an OS of less or more than 6 months. Whiskers are from minimum to maximum. There was no significant difference in end point EPCs in patients who survived less than 6 months compared to those who survived more than 6 months (P=0.99, 95% CI= -0.751 – 0.755).

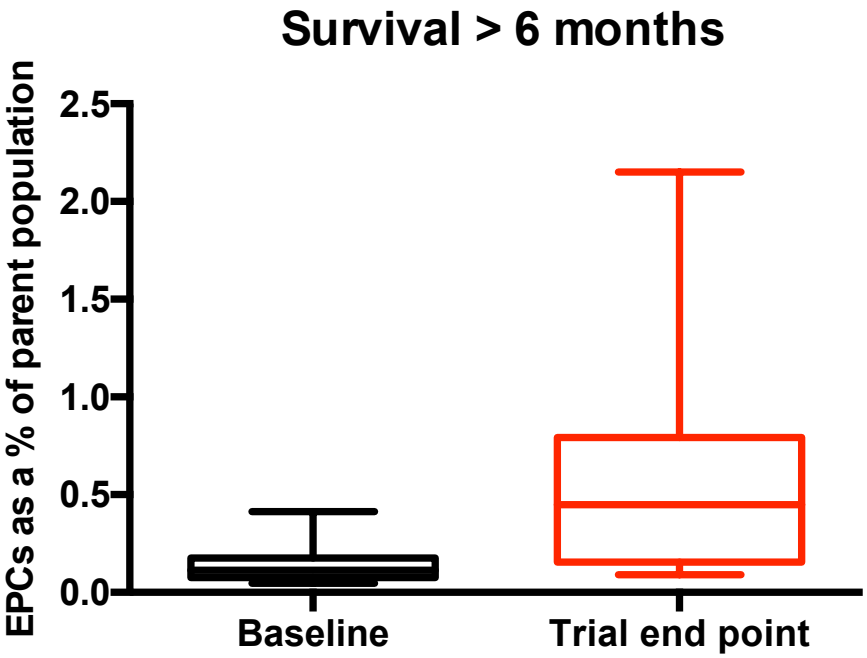

Figure 13.25. Box plot of EPCs at baseline and trial end point in trial patients who had an OS of more than 6 months. Whiskers are from minimum to maximum. There was a significant difference in EPCs in trial patients with a survival over 6 months at treatment end point compared to baseline (P=0.01, 95% CI= 0.093 – 0.833).

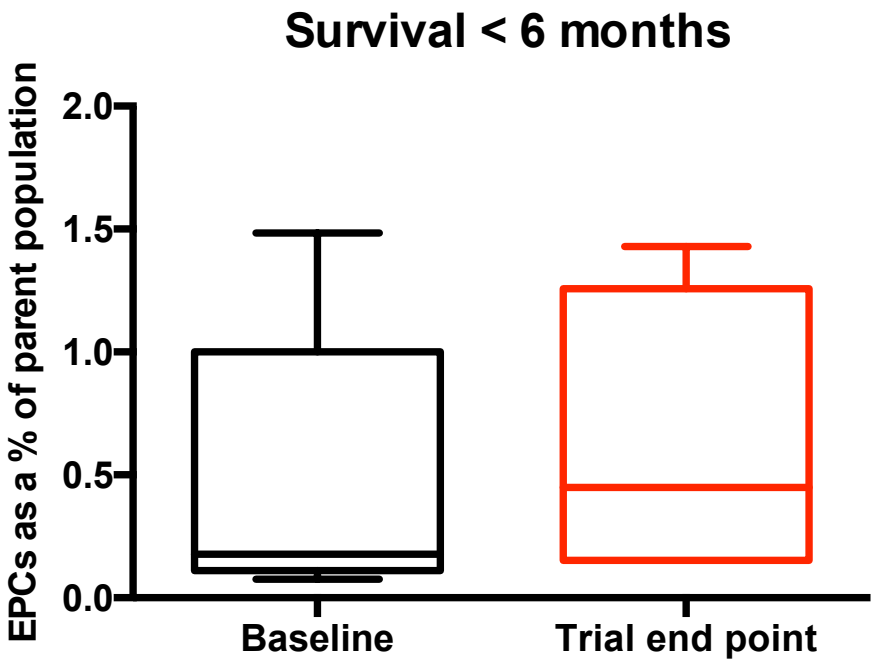

Figure 13.26. Box plot of EPCs at baseline and trial end point in trial patients who had an OS of less than 6 months. Whiskers are from minimum to maximum. There was no significant difference in EPCs in trial patients with a survival under 6 months at treatment end point compared to baseline (P=0.65, 95% CI= -0.648 – 0.982).

13.4.3 Trial patients: Regression analysis

A mixed effects logistic regression analysis was performed on all trial patient samples. There was a significant increase in EPCs over treatment (P=0.0001).

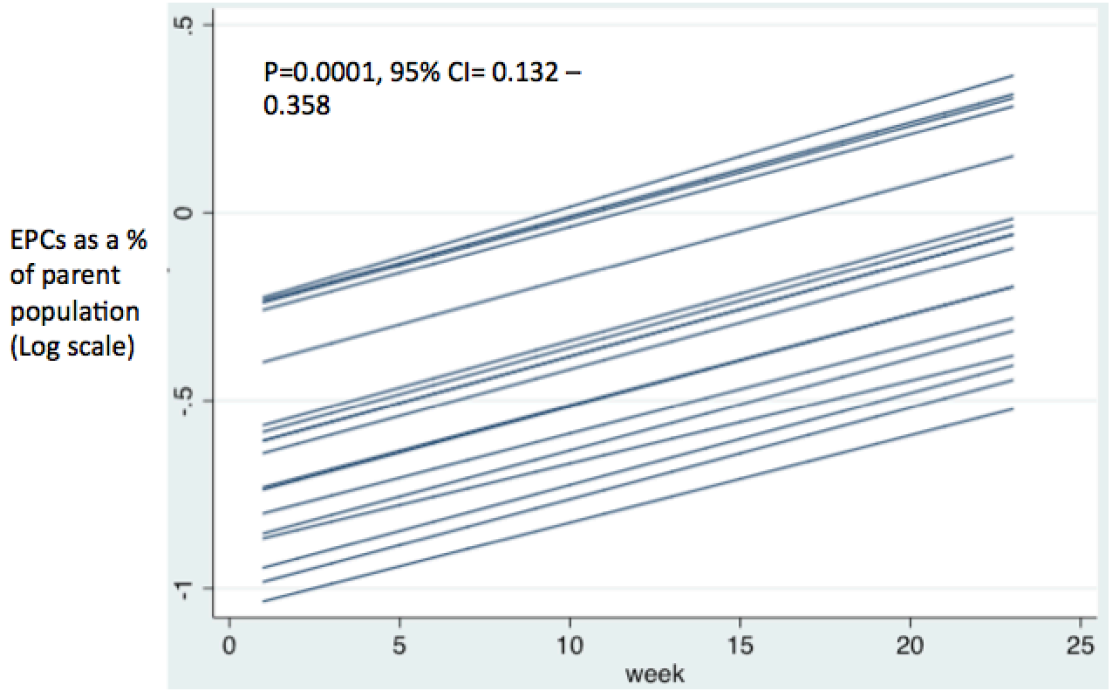

Figure 13.27. Output graph showing regression lines for individual patients plotted against time in weeks following mixed effects logistic regression analysis. EPCs levels are shown on the y axis and are a calculated as a percentage of the parent population (log scale), time in weeks is shown on the x axis. Each regression line represents a patient. One hundred and two time points in eighteen patients were analysed. There was a significant overall increasing trend in EPCs over time (P=0.0001, 95% CI= 0.132 - 0.385).

13.4.4 Trial patients: Survival analysis

The percentage change of EPCs at trial end point compared to baseline was calculated. Patients were divided into two groups, low and high Tregs around the median value percentage change. Kaplan-Meier curves were drawn to examine the relationship of change of EPCs in the PFS and OS of patients. Log rank analysis was used to evaluate the survival curves. 14 patients were eligible for analysis. Patient T10 was excluded from this analysis as the patient became operable and inclusion would have biased the analysis. Patients T7, T12 and T14 were excluded from this analysis, as they had no

sample following a baseline measurement. There was no difference in PFS or OS in patients who had a high or low change in EPCs at trial end point compared to baseline.

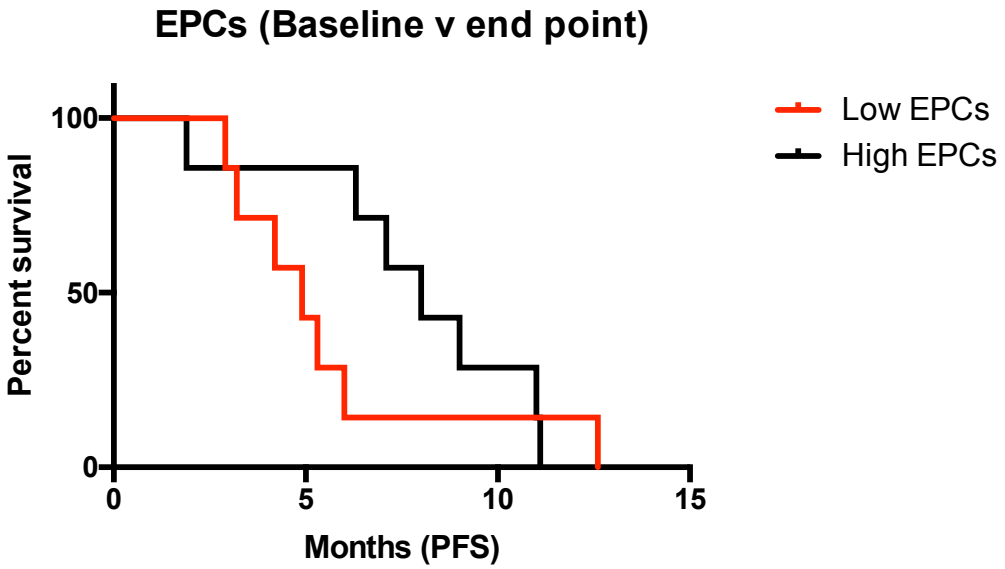

Figure 13.28. There was no significant difference in PFS in patients with a high change in EPCs at treatment end point compared to baseline (log-rank (Mantel-Cox) test, P=0.38). Median survival in patients with low EPCs (N=7) was 4.9 months. Median survival in patients with high EPCs (N=7) was 8 months.

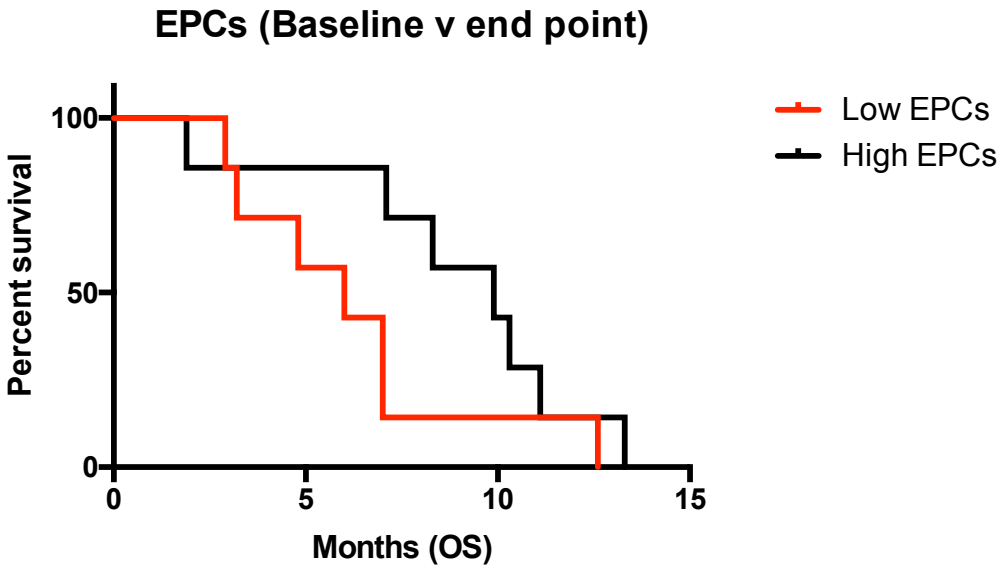

Figure 13.29. There was no significant difference in OS in patients with a high change in EPCs at treatment end point compared to baseline (log-rank (Mantel-Cox) test, P=0.15). Median survival in patients with low EPCs (N=7) was 6 months. Median survival in patients with high EPCs (N=7) was 9.9 months.

13.5 EPCs ($CD45^-$, $CD31^+$and $CD34^+$ EPCs): Control patients

Twenty-four samples were analysed from nine control patients. EPCs were identified as having a $CD45^-$, $CD31^+$and $CD34^+$ phenotype. EPCs were expressed as a percentage of the patient population analysed.

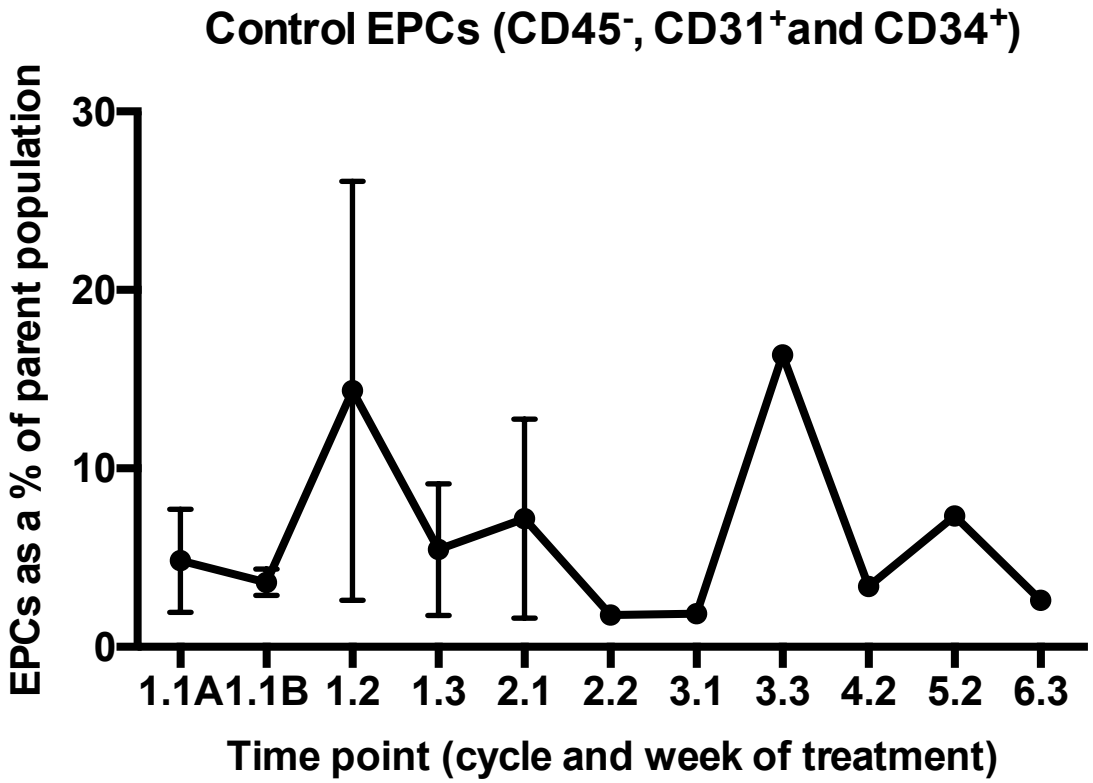

Figure 13.30. Figure showing mean trend line of trial EPCs with range (minimum to maximum). Time point 1.1A is the baseline pre-treatment time point. Time point 1.1B is the post treatment time point.

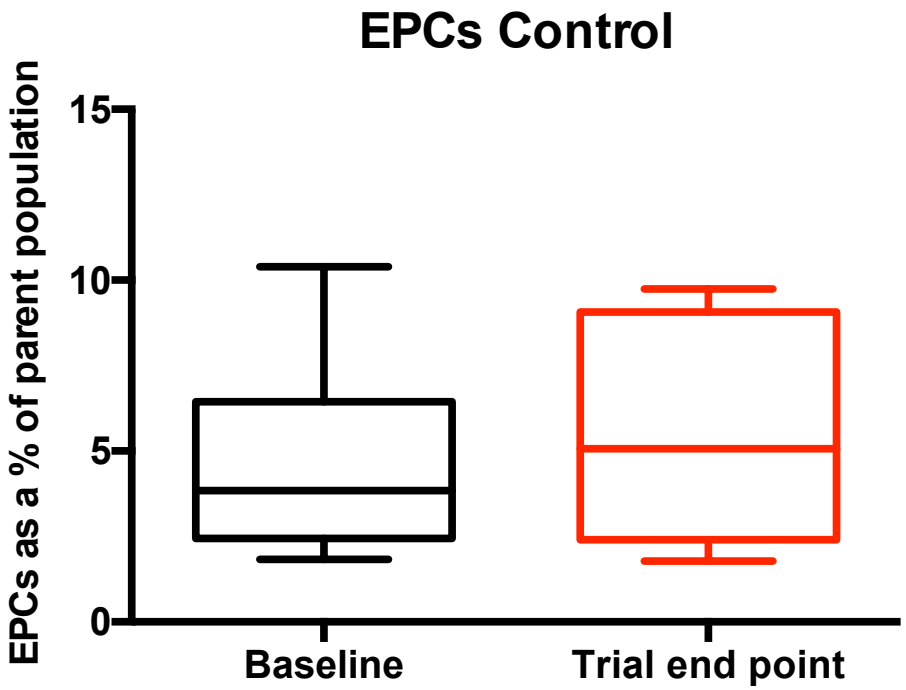

Figure 13.31. Box plot of baseline versus trial end point EPCs in control patients. Whiskers are from minimum to maximum values. There was no significant difference between baseline and trial end point EPCs (P=0.579, 95% CI = -2.492 – 4.271).

13.5.1 Control patients: Regression analysis

A mixed effects logistic regression analysis was performed on all control patient samples. There was a downward trend in EPCs over the treatment but this was not significant (P=0.93).

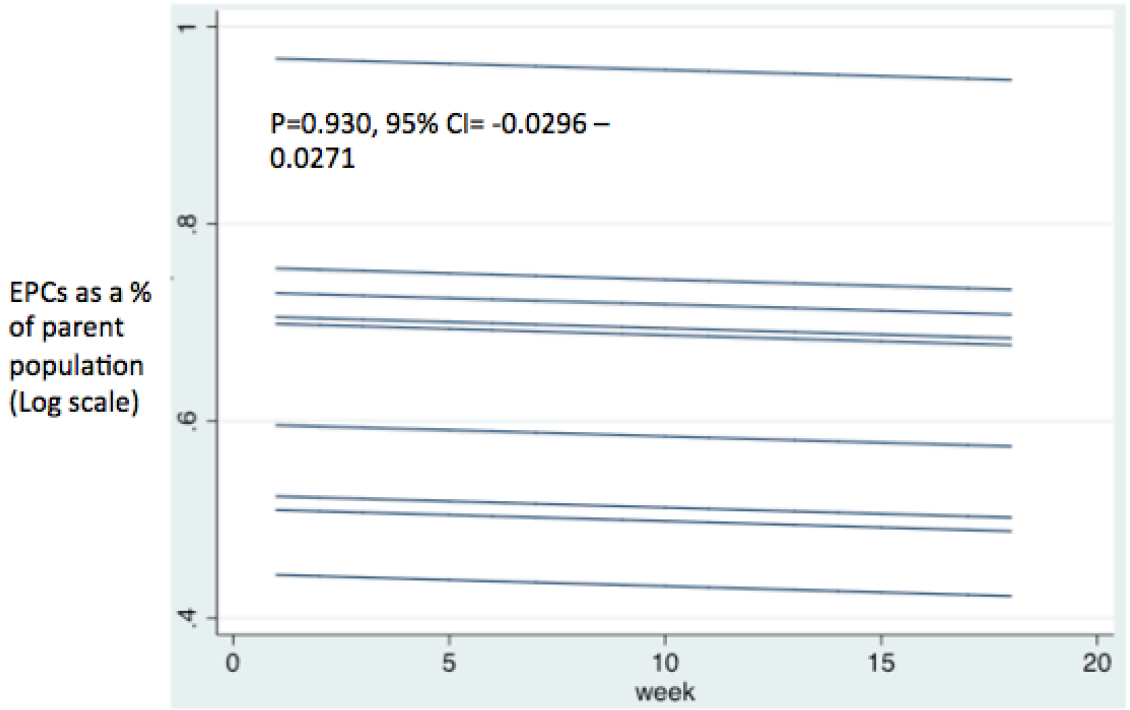

Figure 13.32. Output graph showing regression lines for individual patients plotted against time in weeks following mixed effects logistic regression analysis. EPCs levels are shown on the y axis and are a calculated as a percentage of the parent population (log scale), time in weeks is shown on the x axis. Each regression line represents a patient. Twenty-seven samples in nine patients were analysed. EPCs are calculated as a percentage of the parent population and plotted on a log scale. Twenty-four points in nine patients were analysed. There is a downward trend in EPCs over time, however this was not significant (P=0.930, 95% CI= -0.029 - 0.027).

13.6 EPCs ($CD45^-$, $CD31^+$ and $CD34^+$ EPCs): Comparison analysis

Trial patients were compared to the control cohort. There was a significant increase in baseline EPCs in control versus trial patients (P=0.0001). There was a significant increase in end point EPCs in control versus trial patients (P=0.0001).

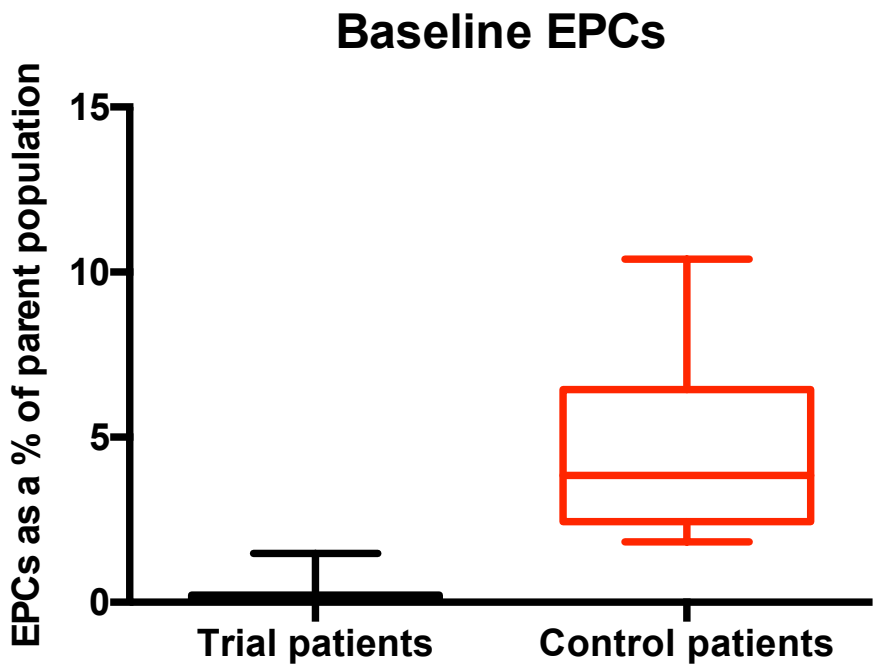

Figure 13.33. Box plot of baseline trial versus control patients EPCs. Whiskers are from minimum to maximum values. Control patients had a significantly higher number of baseline EPCs compared to trial patients (P=0.0001, 95% CI = 3.022 – 5.704).

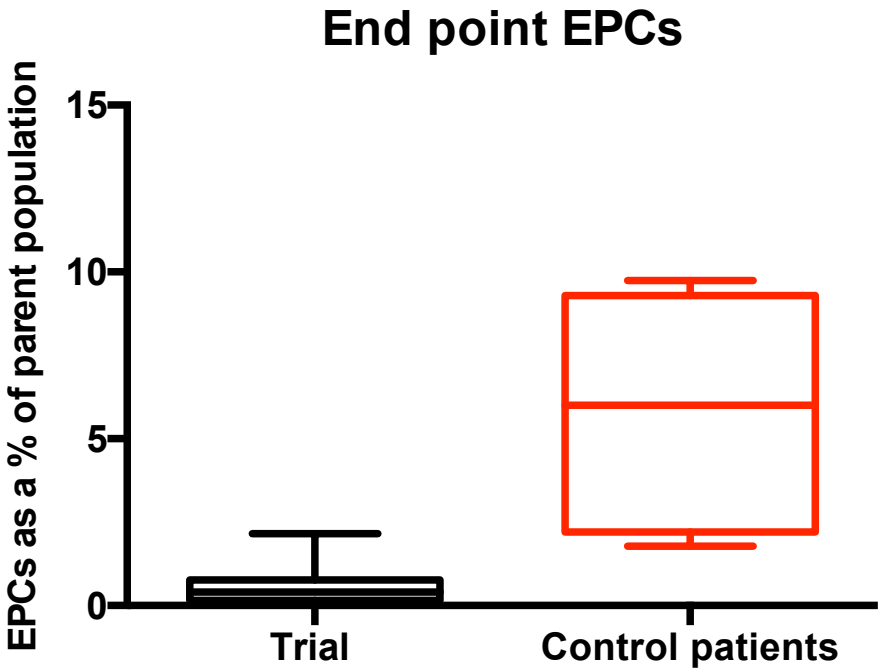

Figure 13.34. Box plot of end point trial versus control patients EPCs. Whiskers are from minimum to maximum values. Control patients had a significantly higher number of end point EPCs compared to trial patients (P=0.0001, 95% CI = 3.215 – 7.194).

13.6.1 Comparison survival analysis

EPCs in both trial and control patients were divided into two groups (low and high change groups) around the median percentage change in EPCs between baseline and end point. OS and PFS of trial and control patients were analysed in the low and high change groups. Patient T10 was excluded from this analysis as the patient became operable and inclusion would bias the analysis. Patients C5, C7, C9, T7, T12 and T14 were excluded from this analysis, as they had no sample following a baseline measurement. There was no significant difference in PFS in patients with a low change in EPCs in trial versus control patients (P=0.42). There was a significant difference in PFS in patients with a high change in EPCs in trial versus control patients (P=0.012), suggesting a survival benefit with an increase in EPC. There was no difference in OS in patients with a low or high change in EPCs.

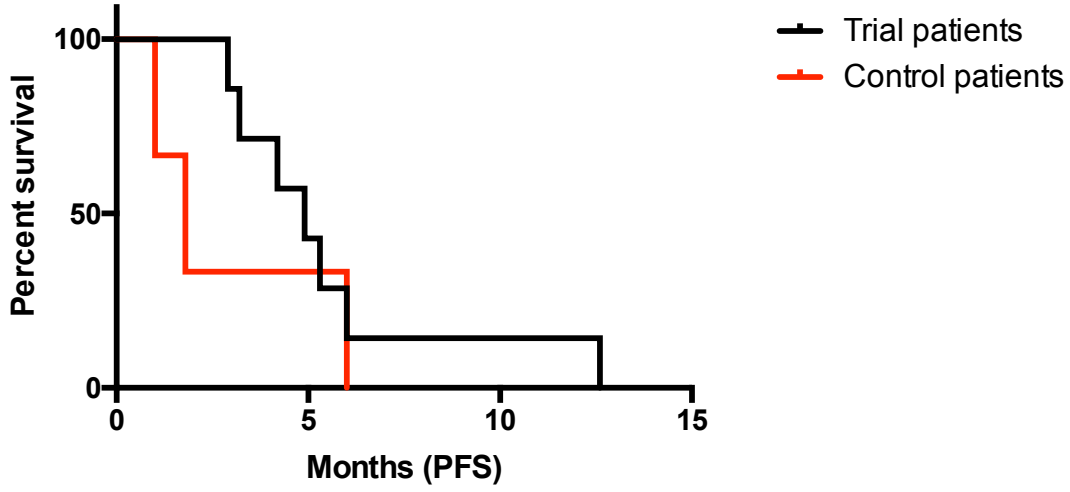

Figure 13.35. There was no significant difference in PFS in patients with a low change in EPCs in trial versus control patients (log-rank (Mantel-Cox) test, P=0.42). Median survival in trial patients (N=7) was 4.9 months. Median survival in control patients (N=3) was 1.8 months.

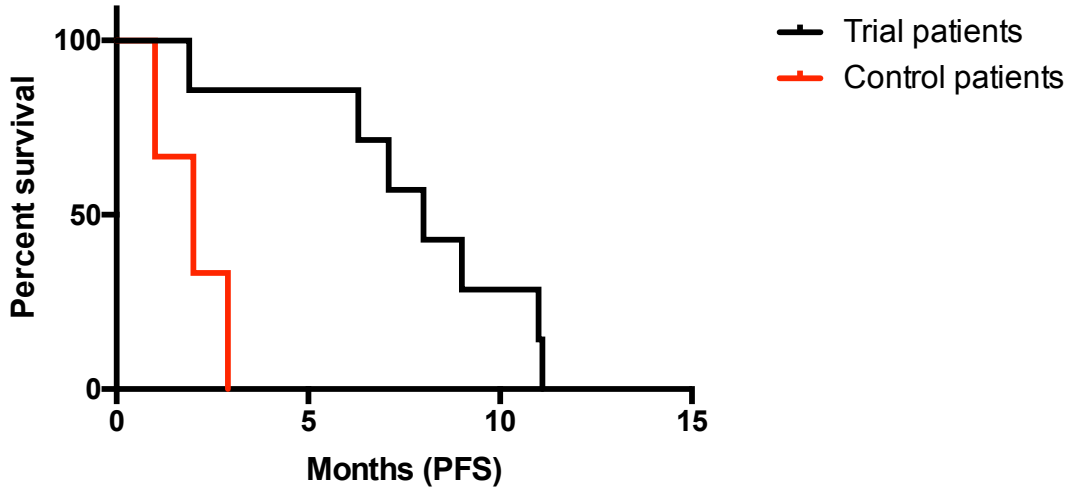

Figure 13.36. There was a significant difference in PFS in patients with a high change in EPCs in trial versus control patients (log-rank (Mantel-Cox) test, P=0.012). Median survival in trial patients (N=7) was 8 months. Median survival in control patients (N=3) was 2 months

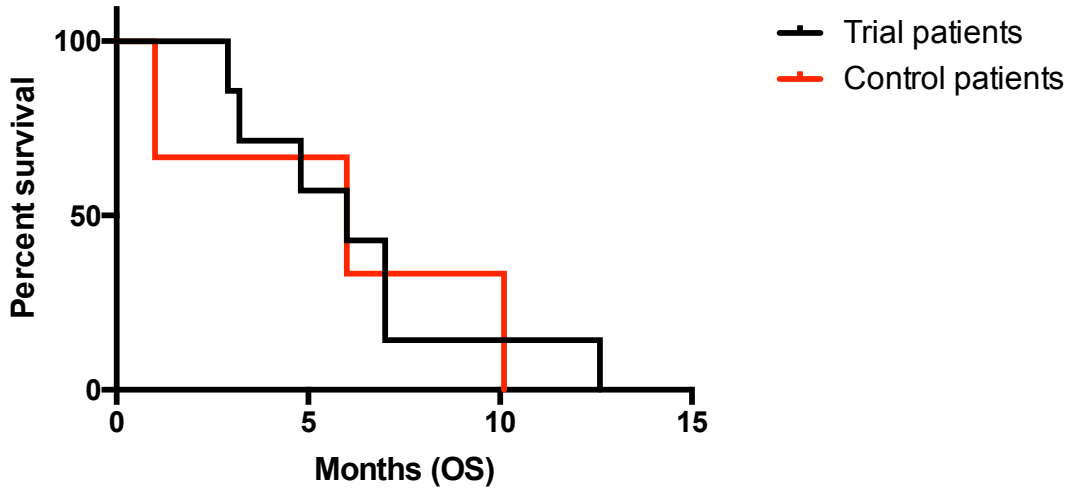

Figure 13.37. There was no significant difference in OS in patients with a low change in EPCs in trial versus control patients (log-rank (Mantel-Cox) test, P=0.82). Median survival in trial patients (N=7) was 6 months. Median survival in control patients (N=3) was 6 months

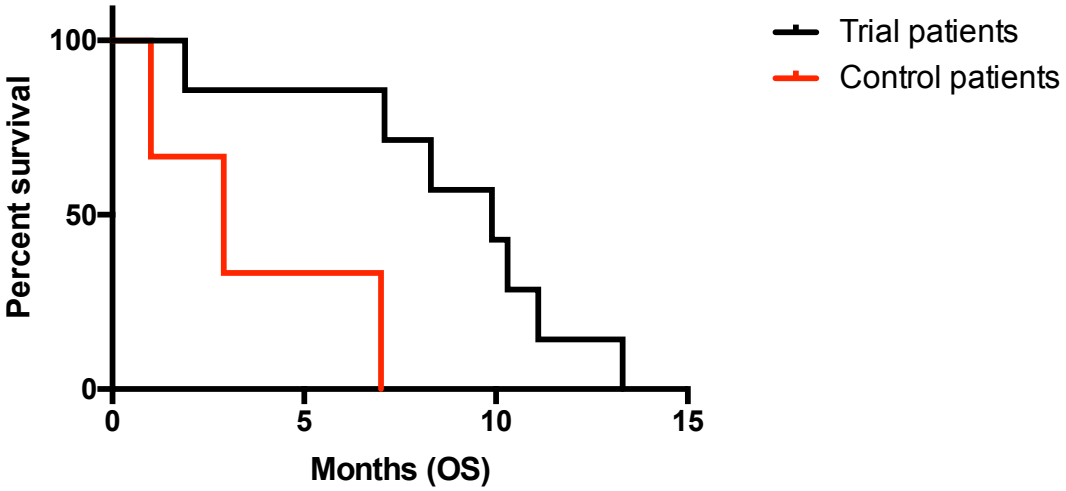

Figure 13.38. There was no significant difference in OS in patients with a high change in EPCs in trial versus control patients (log-rank (Mantel-Cox) test, P=0.012). Median survival in trial patients (N=7) was 9.9 months. Median survival in control patients (N=3) was 2.9 months.

13.6.2 Regression analysis

Mixed effects logistic regression analysis was used to compare EPCs between the trial and control patients. One hundred and twenty-nine time points in twenty-seven patients were included for analysis. The effect of the cycle was analysed between the two groups. There was a significant difference between trial and control patients in cycle one (P=0.021), however this was not seen in subsequent cycles. The effect of the week between trial and control groups was analysed in cycle one. There was no significance between week one (P=0.161, 95% CI=-0.6624 – 3.9837), and week two (P=0.075, 95% CI=-5.1246 – 0.2451), however there was a significant difference between trial and control group in week three (P=0.0001, 95% CI=-7.4808 - -2.9212). Overall there was a statistically significant difference between the trial and control patients over time (P=0.0001).

13.7 EPCs ($CD45^-$, $CD34^+$, $CD31^+$and $CD133^+$ EPCs): Trial patients

One hundred and two samples were analysed from eighteen trial patients. EPCs were identified as having a $CD45^-$, $CD34^+$, $CD31^+$ and $CD133^+$ phenotype. EPCs were expressed as a percentage of the patient population analysed.

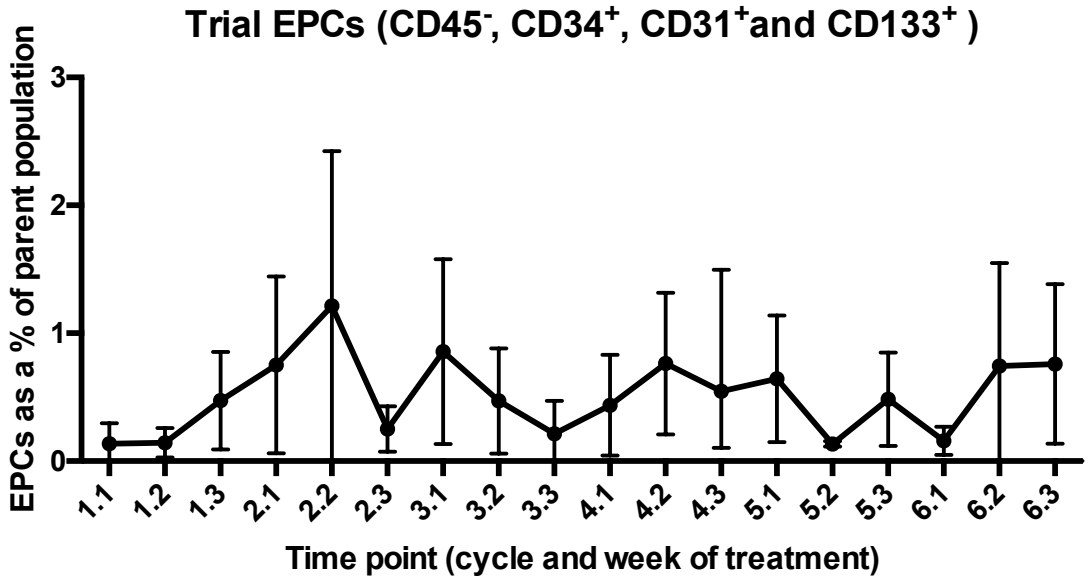

Figure 13.39. Figure showing mean trend line of trial EPCs with a $CD45^-$, $CD34^+$, $CD31^+$ and $CD133^+$ phenotype, with trend (minimum to maximum).

13.7.1 Baseline versus post treatment EPCs at one month and trial end point

EPCs were analysed at baseline compared to one-month post treatment and trial end point. There was a significant increase in EPCs at one-month post treatment compared to baseline (P=0.001), and at end point compared to baseline (P=0.015).

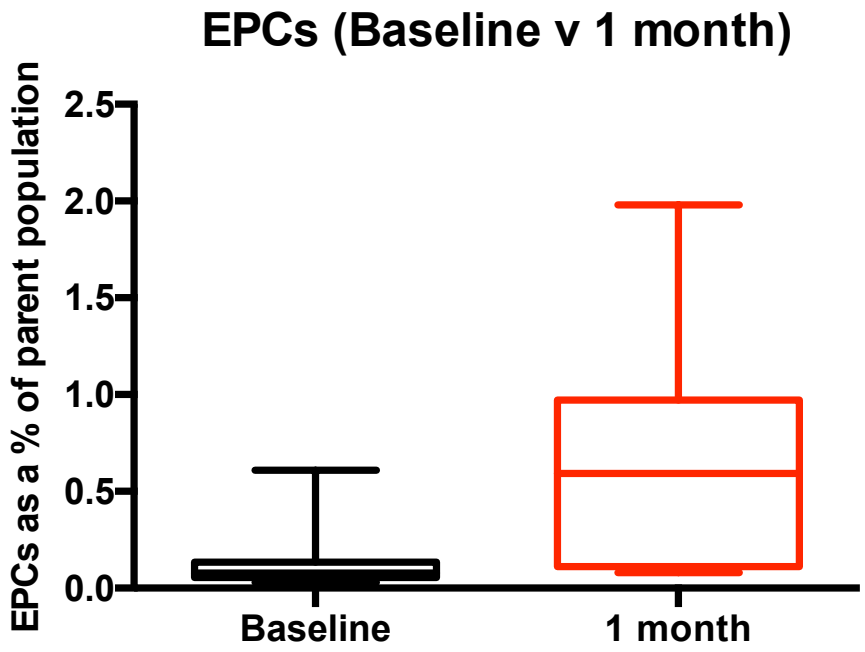

Figure 13.40. Box plot of EPCs at baseline and following 1 month of treatment. Whiskers are from minimum to maximum. There was a significant difference in EPCs in trial patients at one month following treatment compared to baseline (P=0.001, 95% CI= 0.196 – 0.763).

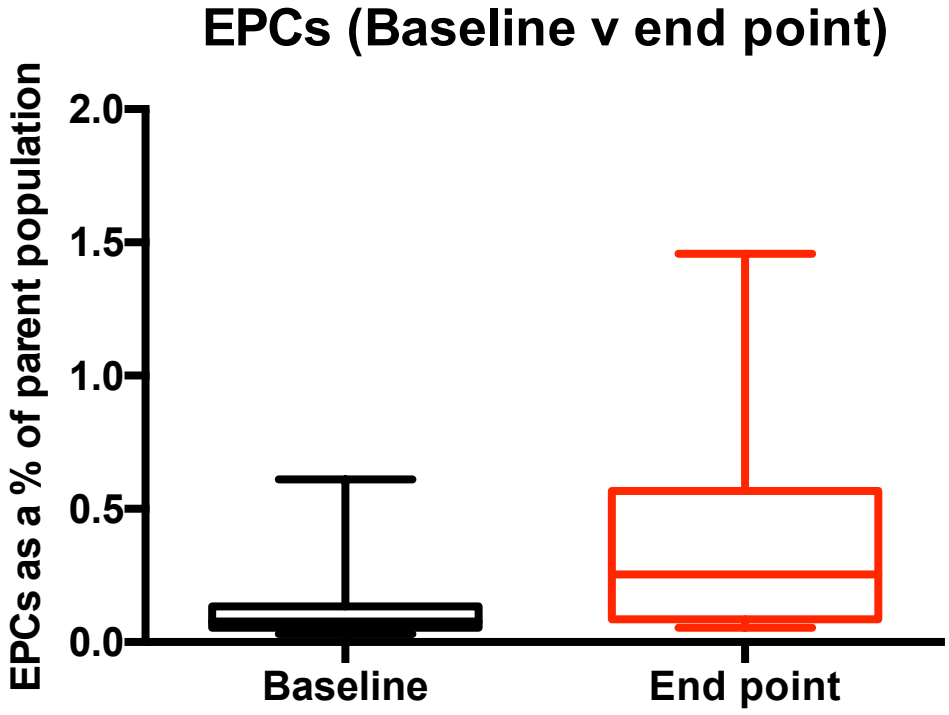

Figure 13.41. Box plot of EPCs at baseline and treatment end point. Whiskers are from minimum to maximum. There was a significant difference in EPCs in trial patients at end point following treatment compared to baseline (P=0.015, 95% CI= 0.055 – 0.479).

13.7.2 Baseline and end point EPCs compared to patient overall survival

Trial patients were divided into two groups around an OS of six months. EPCs at baseline and end point were compared in these two groups. There was no significant difference in baseline or end point EPCs in patients who survived less than 6 months compared to those who survived more than 6 months. There was a significant difference in EPCs in trial patients with a survival over 6 months at treatment end point compared to baseline (P=0.025). There was no significant difference in EPCs in trial patients with a survival under 6 months at treatment end point compared to baseline.

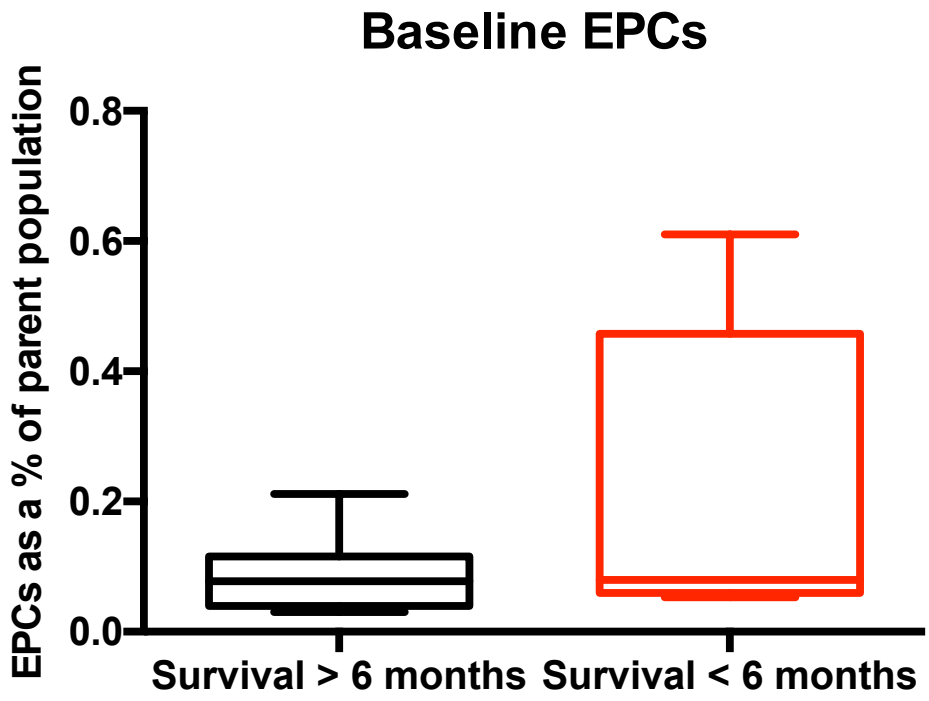

Figure 13.42. Box plot of baseline EPCs in trial patients who had an OS of less or more than 6 months. Whiskers are from minimum to maximum. There was no significant difference in baseline EPCs in patients who survived Less than 6 months compared to those who survived more than 6 months (P=0.106 95% CI= -0.028 – 0.272).

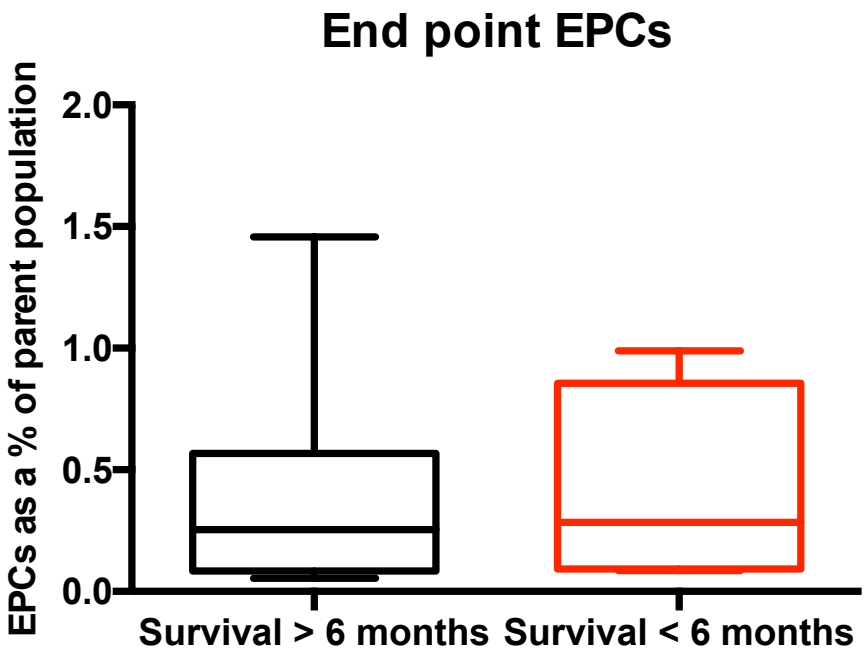

Figure 13.43. Box plot of end point EPCs in trial patients who had an OS of less or more than 6 months. Whiskers are from minimum to maximum. There was no significant difference in end point EPCs in patients who survived Less than 6 months compared to those who survived more than 6 months (P=0.954, 95% CI= -0.519 – 0.548).

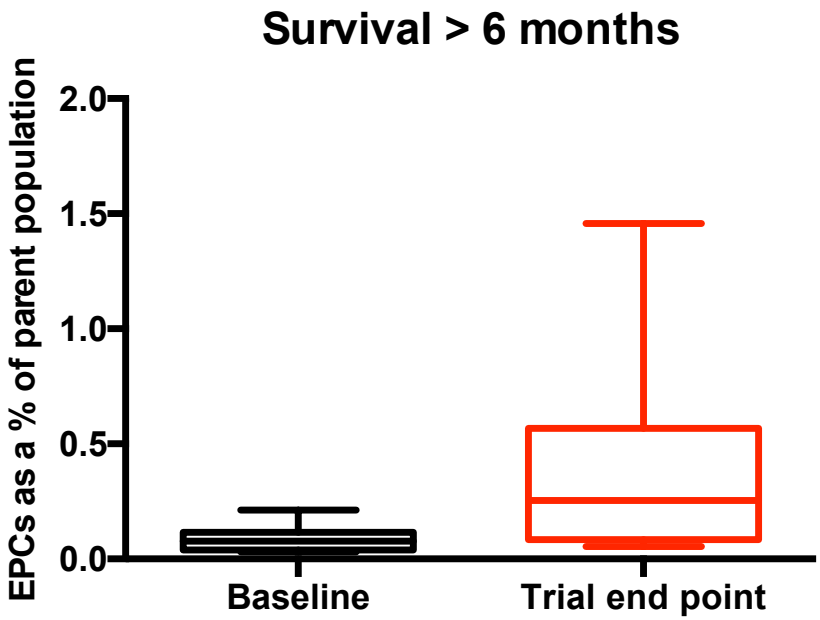

Figure 13.44. Box plot of baseline EPCs in trial patients who had an OS of more than 6 months. Whiskers are from minimum to maximum. There was a significant difference in EPCs in trial patients with a survival over 6 months at treatment end point compared to baseline (P=0.025, 95% CI= 0.047 – 0.573).

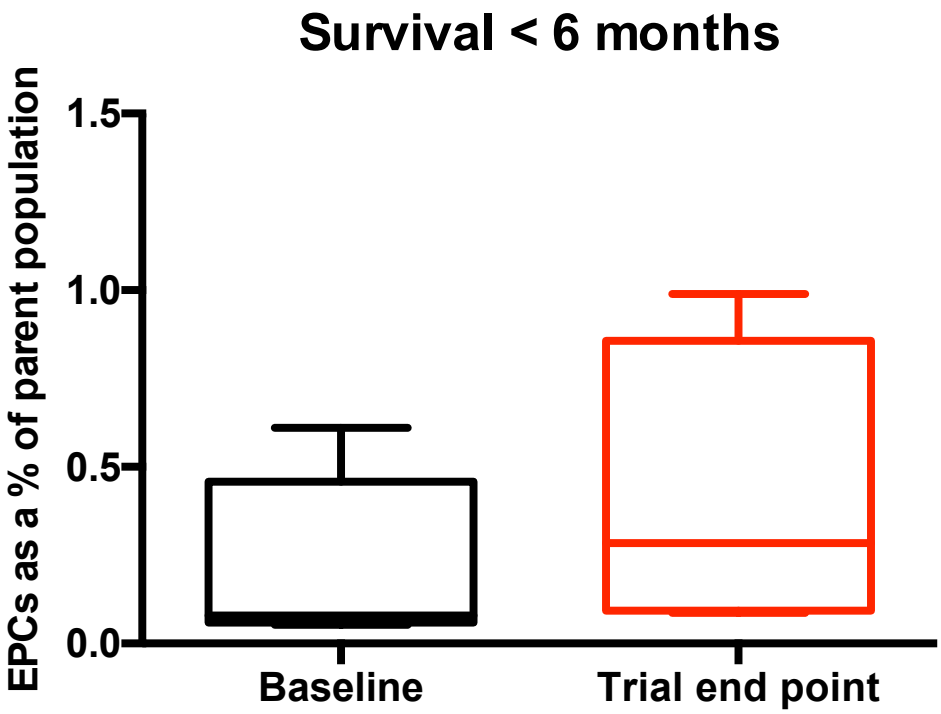

Figure 13.45. Box plot of EPCs at baseline and trial end point in trial patients who had an OS of less than 6 months. Whiskers are from minimum to maximum. There was no significant difference in EPCs in trial patients with a survival under 6 months at treatment end point compared to baseline (P=0.317, 95% CI= -0.230 – 0.637).

13.7.3 Trial patients: Regression analysis

Mixed effects logistic regression analysis was performed on all trial patient samples. There was a significant increase in EPCs over treatment (P=0.007).

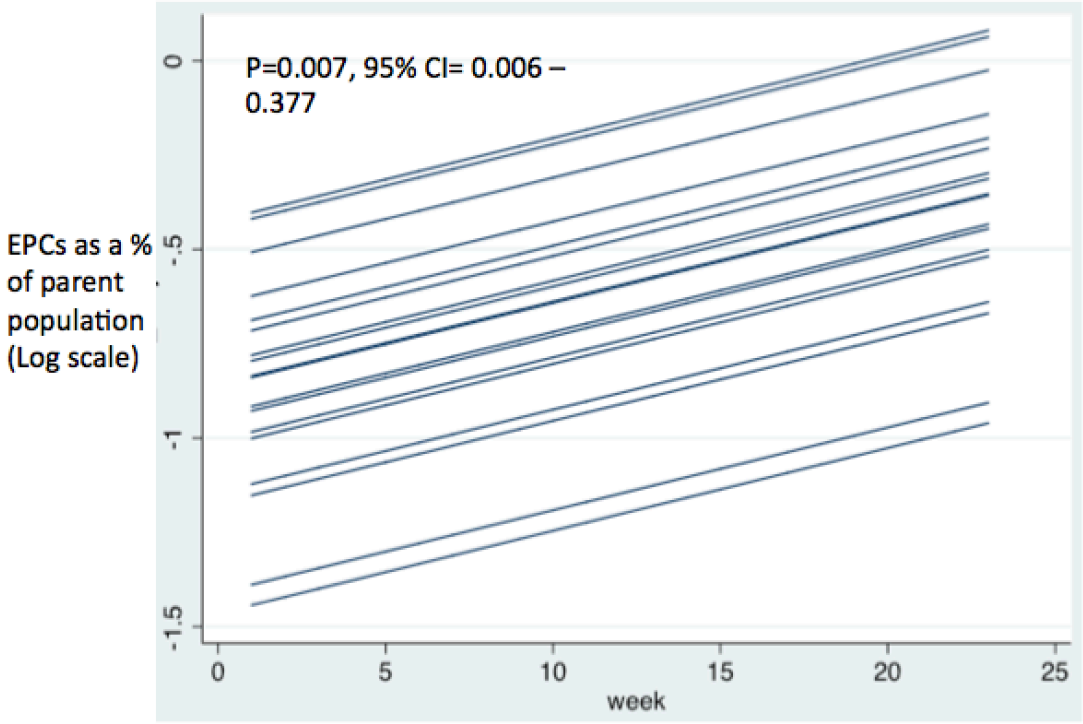

Figure 13.46. Output graph showing regression lines for individual patients plotted against time in weeks following mixed effects logistic regression analysis. EPCs levels are shown on the y axis and are a calculated as a percentage of the parent population (log scale), time in weeks is shown on the x axis. Each regression line represents a patient. Twenty-seven samples in nine patients were analysed. EPCs are calculated as a percentage of the parent population and plotted on a log scale. One hundred and three time points in eighteen patients were analysed. There is a significant increase in EPCs over time (P=0.007, 95% CI= 0.006 - 0.377).

13.7.4 Trial patients: Survival analysis

The percentage change of EPCs at trial end point compared to baseline was calculated. Patients were divided into two groups, low and high Tregs around the median value percentage change. Kaplan-Meier curves were drawn to examine the relationship of change in Tregs with patients PFS and OS. Log rank analysis was used to evaluate the survival curves. 14 patients were eligible for analysis. Patient T10 was excluded from this analysis as the patient became operable and inclusion would have biased the analysis. Patients T7, T12 and T14 were excluded from this analysis, as they had no sample following a baseline measurement. There was no difference in PFS or OS in patients who had a high or low change in EPCs at trial end point compared to baseline.

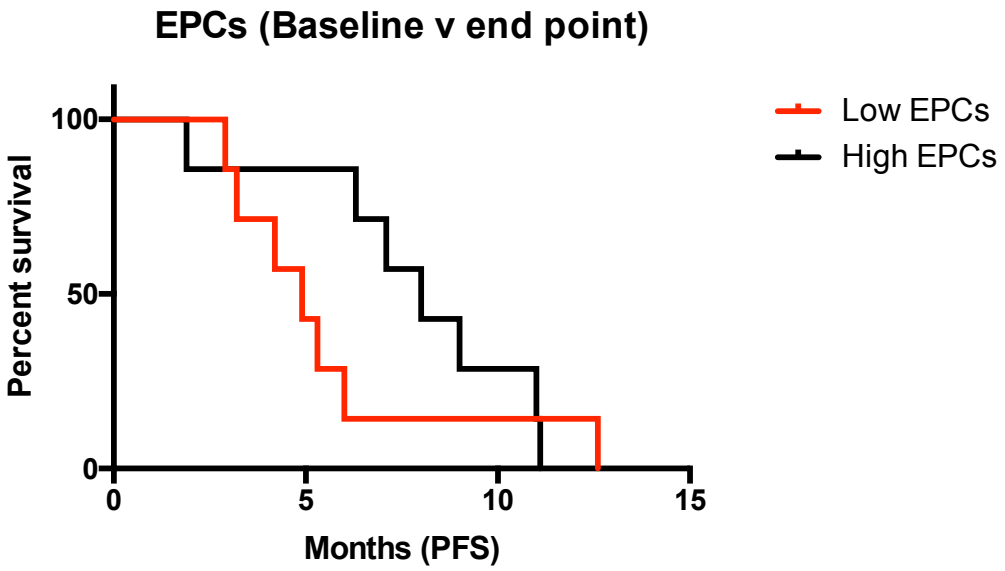

Figure 13.47. There was no significant difference in PFS in patients with a high change in EPCs following one month of treatment compared to baseline (log-rank (Mantel-Cox) test, P=0.38). Median survival in patients with low EPCs (N=7) was 4.9 months. Median survival in patients with high EPCs (N=7) was 8 months.

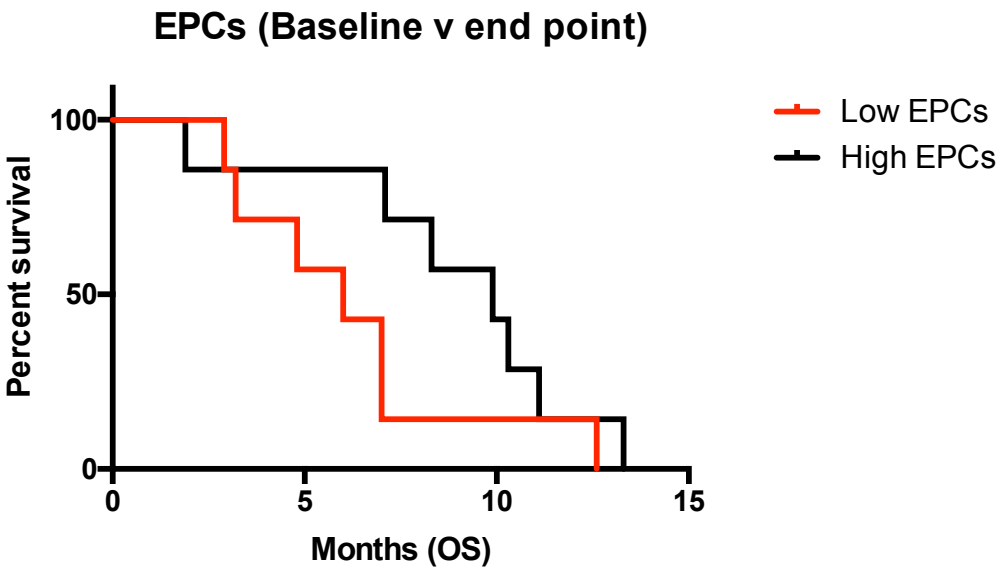

Figure 13.48. There was no significant difference in OS in patients with a high change in EPCs following one month of treatment compared to baseline (log-rank (Mantel-Cox) test, P=0.153). Median survival in patients with low EPCs (N=7) was 6 months. Median survival in patients with high EPCs (N=7) was 9.9 months.

13.8 EPCs ($CD45^-$, $CD34^+$, $CD31^+$ and $CD133^+$ EPCs): Control patients

Twenty-four samples were analysed from nine control patients. EPCs were identified as having a $CD45^-$, $CD34^+$, $CD31^+$ and $CD133^+$ phenotype. EPCs were expressed as a percentage of the patient population analysed.

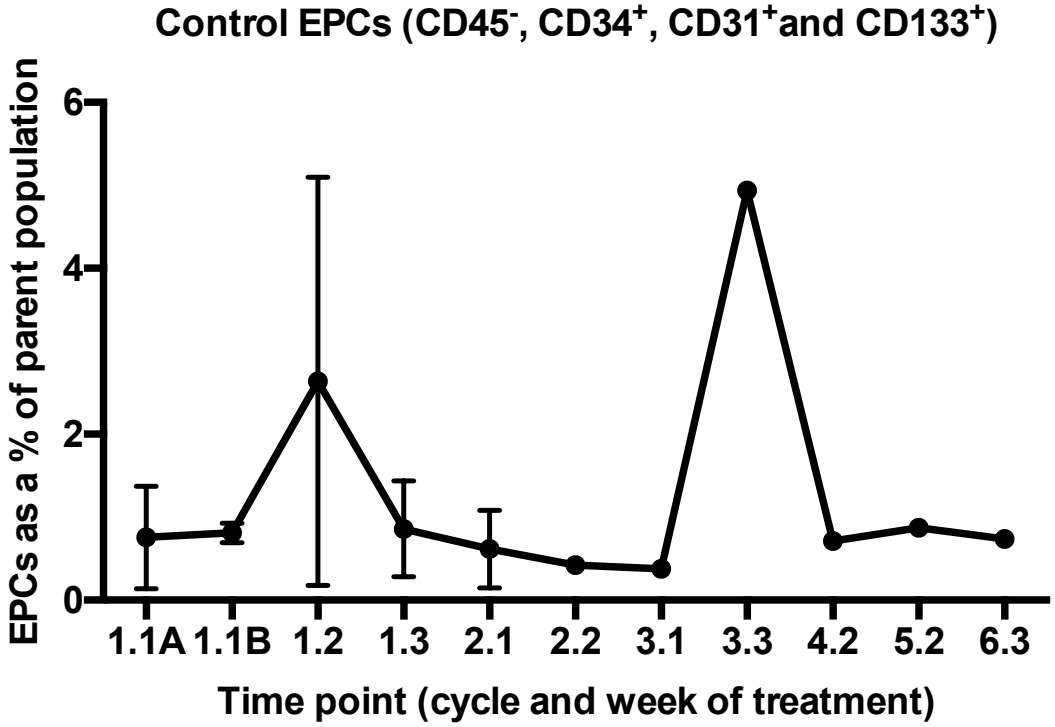

Figure 13.49. Figure showing mean trend line of control EPCs with a $CD45^-$, $CD34^+$, $CD31^+$ and $CD133^+$, with range (minimum to maximum).

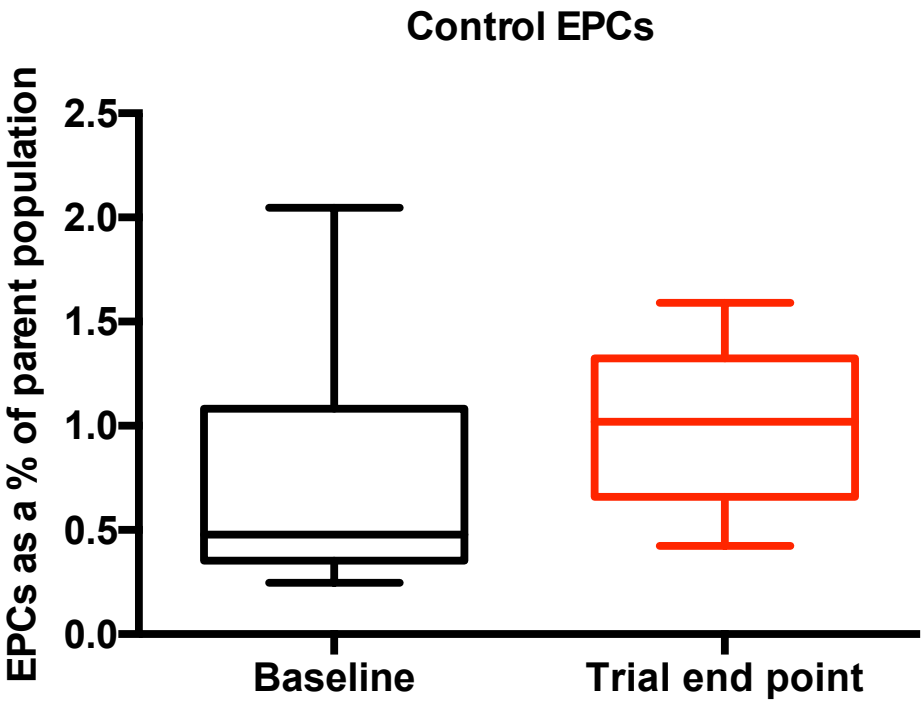

Figure 13.50. Box plot of baseline versus trial end point EPCs in control patients. Whiskers are from minimum to maximum values. There was no significant difference between baseline and trial end point EPCs (P=0.374 95% CI = -0.340 – 0.843).

13.8.1 Control patients: Regression analysis

Logistic regression analysis was performed on all control patient samples. There was a non-significant increasing trend in EPCs over the treatment (P=0.358).

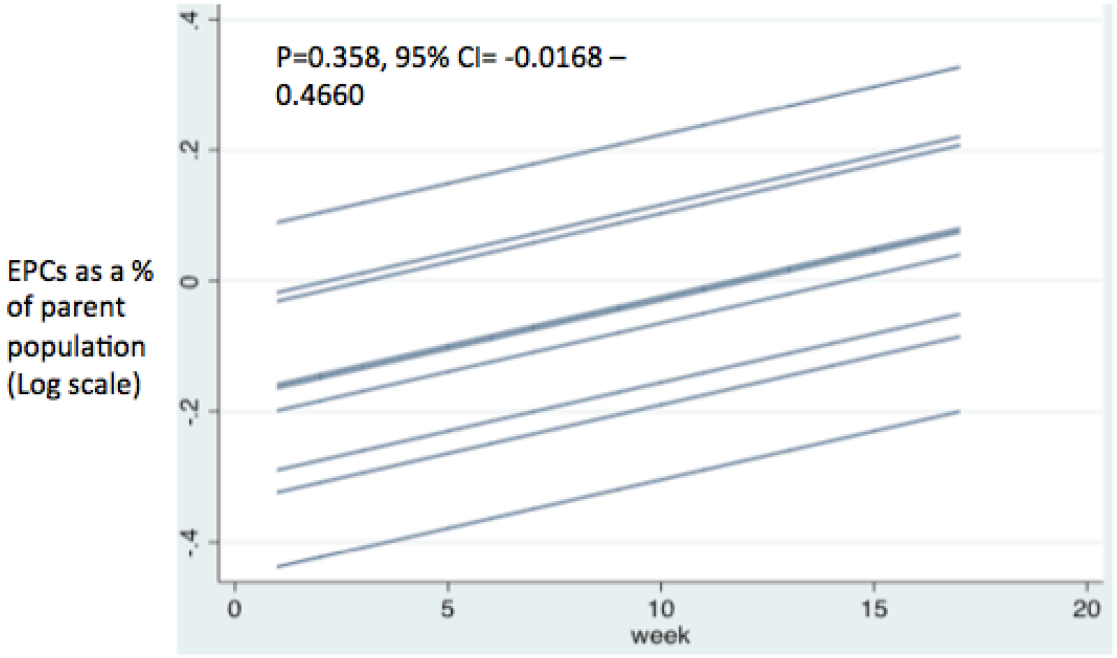

Figure 13.51. Output graph showing regression lines for individual patients plotted against time in weeks following mixed effects logistic regression analysis. EPCs levels are shown on the y axis and are a calculated as a percentage of the parent population (log scale), time in weeks is shown on the x axis. Each regression line represents a patient. Twenty-seven samples in nine patients were analysed. EPCs are calculated as a percentage of the parent population and plotted on a log scale. Twenty-four points in nine patients were analysed. There was a non-significant increase seen in EPCs (P=0.358, 95% CI= -0.016 - 0.466).

13.9 EPCs ($CD45^-$, $CD34^+$, $CD31^+$ and $CD133^+$ EPCs): Comparison analysis

Trial patients were compared to the control cohort. There was a significant increase in baseline EPCs in control versus trial patients (P=0.0002), and there was a significant increase in end point EPCs in control versus trial patients (P=0.006).

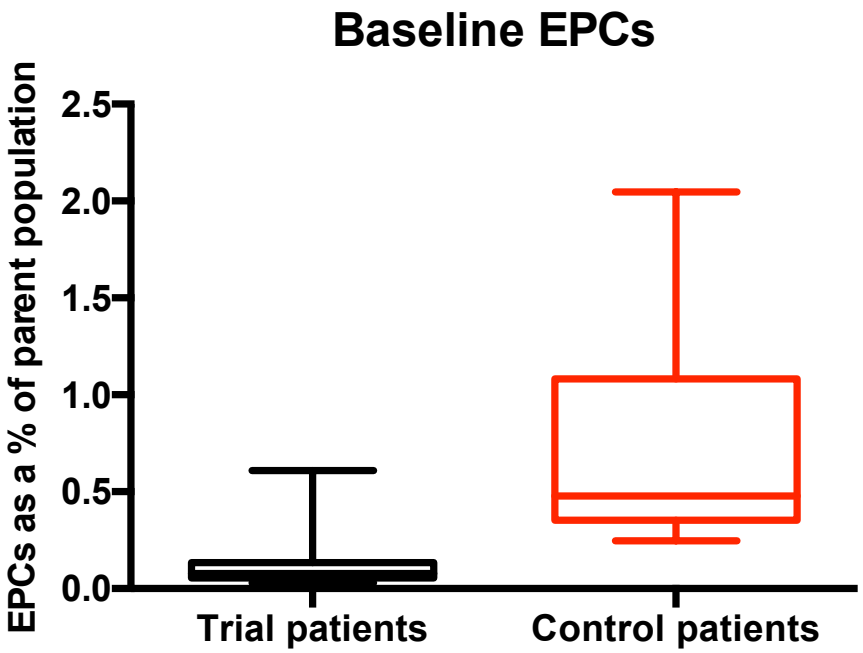

Figure 13.52. Box plot of baseline trial versus control patients $CD45^-$, $CD31^+$, $CD133^+$ and $CD34^+$ EPCs. Whiskers are from minimum to maximum values. There was a significant increase in control baseline EPCs versus trial patients (P=0.0002, 95% CI = 0.323 -0.914).

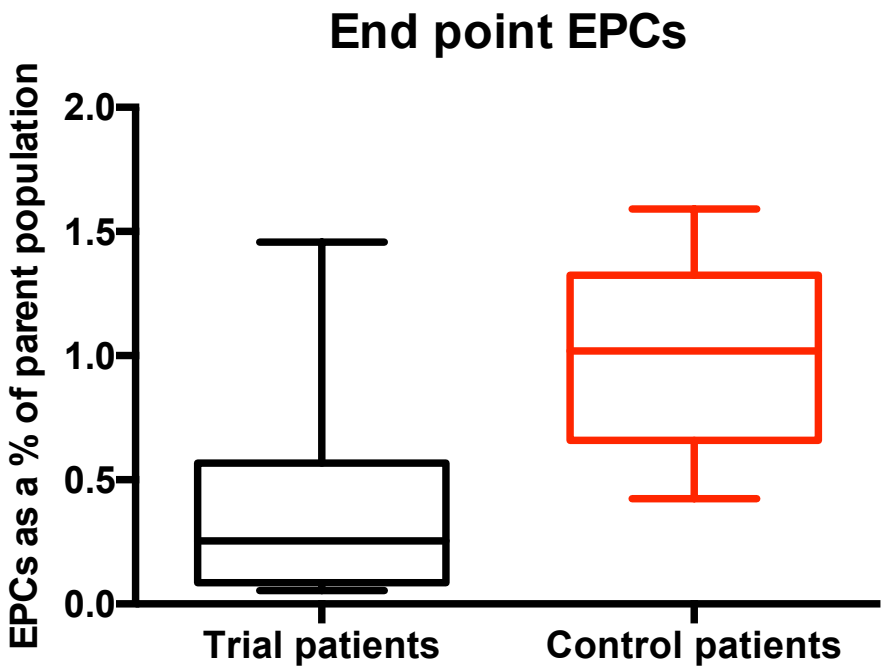

Figure 13.53. Box plot of end point trial versus control patients $CD45^-$, $CD31^+$, $CD133^+$ and $CD34^+$ EPCs. Whiskers are from minimum to maximum values. There was a significant increase in control endpoint EPCs versus trial patients (P=0.006, 95% CI = 0.1907 -1.017).

13.9.1 Comparison survival analysis

EPCs in both trial and control patients were divided into two groups (low and high change groups) around the median percentage change of EPCs between baseline and end point. OS and PFS of trial and control patients were compared in the low and high change groups. Patient T10 was excluded from this analysis as the patient became operable and inclusion would have biased the analysis. Patients C5, C7, C9, T7, T12 and T14 were excluded from this analysis, as they had no sample following a baseline measurement. There was a significant difference in PFS in patients with a low change in EPCs in trial versus control patients (P=0.0008). In addition there was a significant difference in PFS in patients with a high change in EPCs in trial versus control patients (P=0.012). There was no difference in OS in patients with a low or high change in EPCs in trial versus control patients.

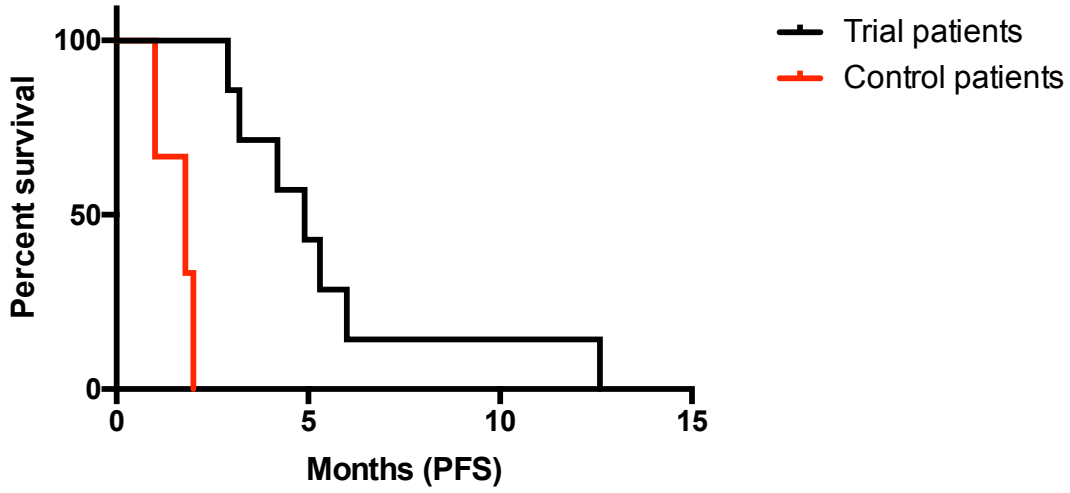

Figure 13.54. There was a significant difference in PFS in patients with a low change in EPCs in trial versus control patients (log-rank (Mantel-Cox) test, P=0.0008). Median survival in trial patients (N=7) was 4.9 months. Median survival in control patients (N=3) was 1.8 months.

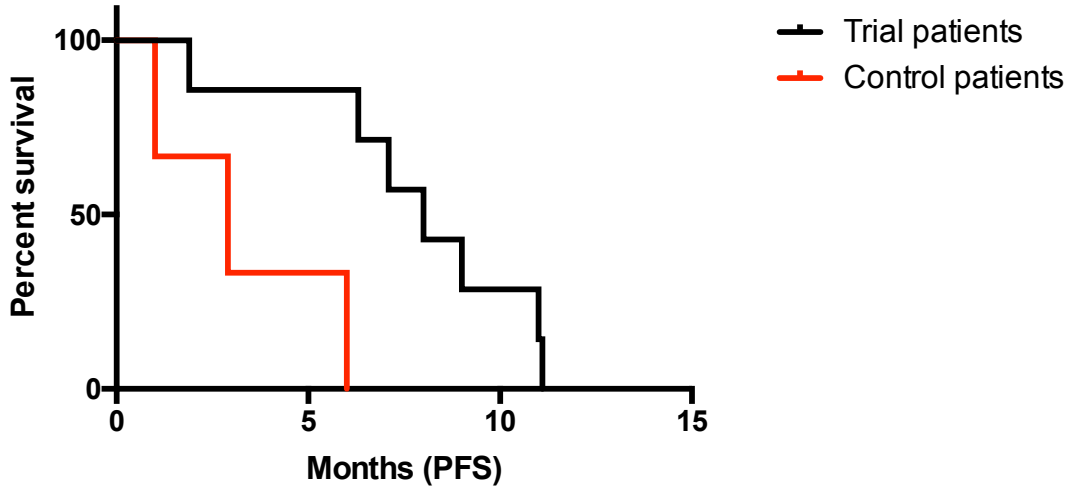

Figure 13.55. There was a significant difference in PFS in patients with a high change in EPCs in trial versus control patients (log-rank (Mantel-Cox) test, P=0.012). Median survival in trial patients (N=7) was 8 months. Median survival in control patients (N=3) was 2.9 months.

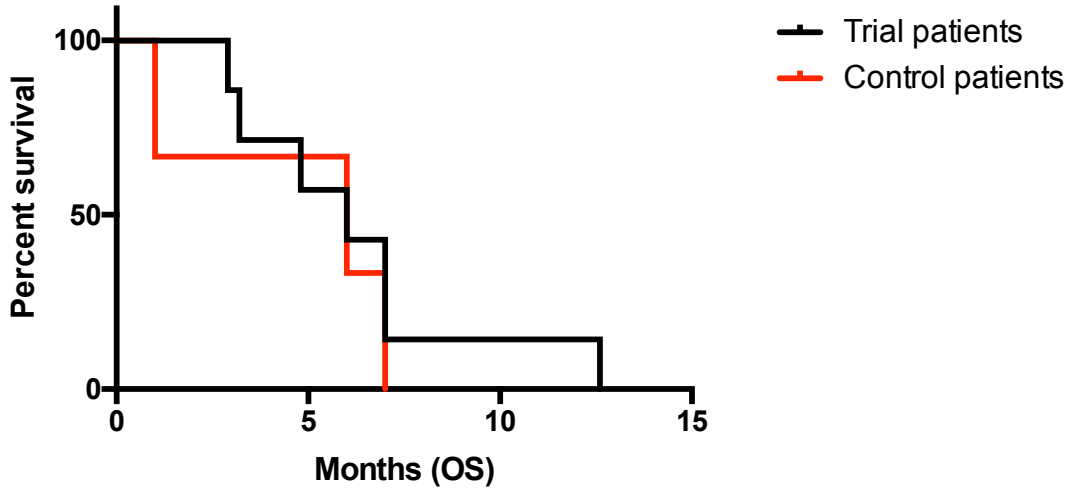

Figure 13.56. There was no significant difference in OS in patients with a low change in EPCs in trial versus control patients (log-rank (Mantel-Cox) test, P=0.647). Median survival in trial patients (N=7) was 6 months. Median survival in control patients (N=3) was 6 months.

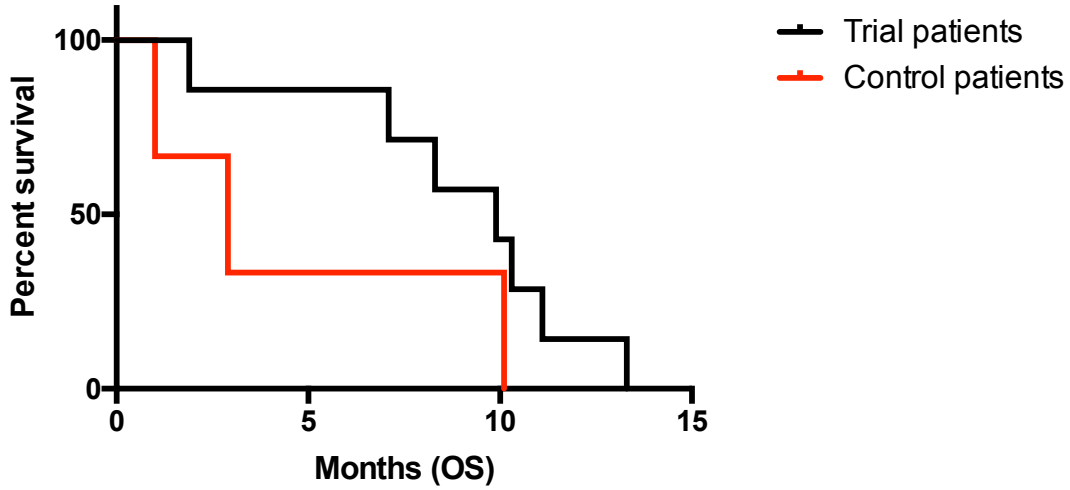

Figure 13.57. There was no significant difference in OS in patients with a high change in EPCs in trial versus control patients (log-rank (Mantel-Cox) test, P=0.17). Median survival in trial patients (N=7) was 9.9 months. Median survival in control patients (N=3) was 2.9 months.

13.9.2 Regression analysis

A mixed effects logistic regression analysis was conducted to compare EPCs between the trial and control patients. One hundred and twenty-nine time points in twenty-seven patients were included for analysis. The effect of the cycle was analysed

between the two groups. There was no difference between trial and control groups between individual cycles. The effect of the week between trial and control groups was analysed in cycle one. There was no difference between week one (P=0.256, 95% CI=-0.3043 – 1.1421), and week two (P=0.396, 95% CI=-0.4711 – 1.1872), however there was a significant difference between trial and control group in week three (P=0.0001, 95% CI=--2.0569 - -0.6283). Overall there was a significant difference between the trial and control patients over time (P=0.0001).

14 Chapter Fourteen: Micro RNA (miRNA) Results

Micro RNA analysis was carried out on 108 trial patient samples (N=17) and 31 control patient samples (N=9). Patient T1 was omitted from the analysis as the samples were misplaced. Six micro RNA's were analysed (miRNA-21, miRNA-146a, miRNA-155, miRNA-196a, miRNA-210 & miRNA-221). This is the first trial to analyse each patient treatment time point and therefore is a robust analysis of miRNA levels. The trial and control patient samples were analysed individually to determine if there was an overall trend over treatment. Trial and control patients were then compared to determine if there was a difference between the two groups. Data was analysed with mixed effects logistic regression models.

14.1 MiRNA-21: Trial patients

There was no significant change in miRNA-21 levels in trial or control patients over the trial.

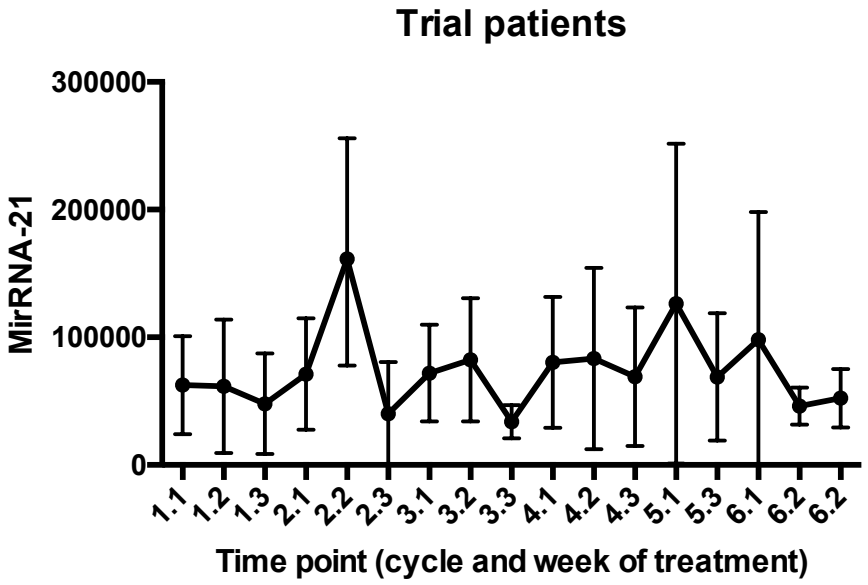

Figure 14.1. Figure showing mean miRNA-21 trend line with range (minimum to maximum).

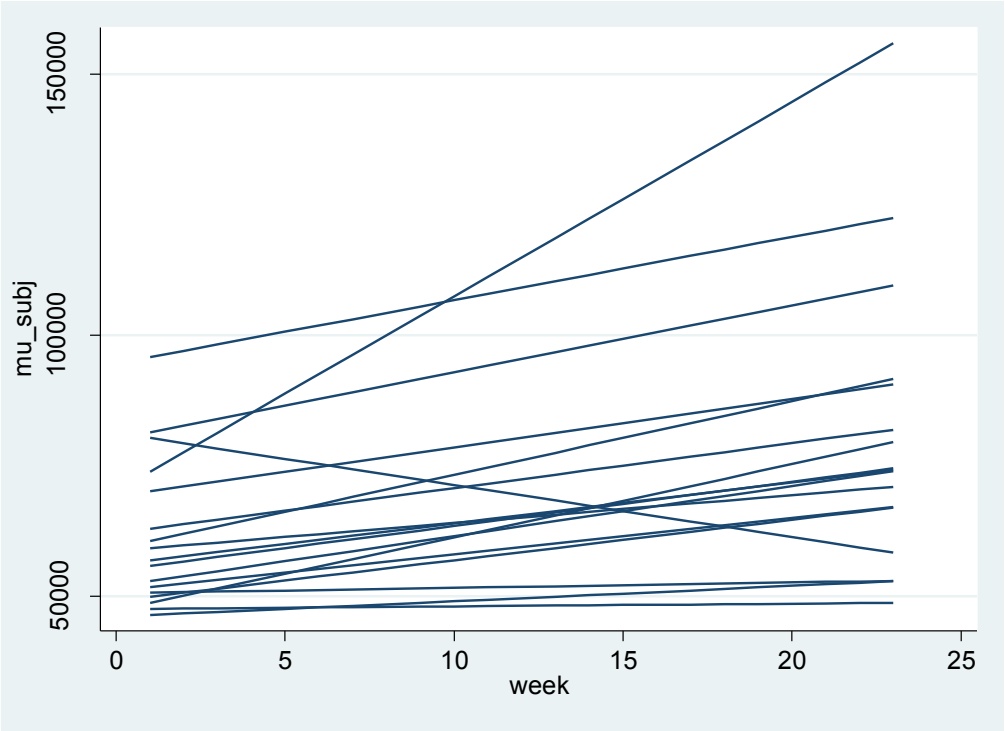

Figure 14.2. Graph showing regression lines for individual patients plotted against time in weeks following mixed effects logistic regression analysis. Micro RNA levels are shown on the y axis (mu_subj), and time in weeks is shown on the x axis. Each regression line represents a patient. There was no statistical significance in miRNA-21 levels in the trial patients (P=0.400, 95% CI = (-1163.809 - 2915.311).

14.2 MiRNA-21: Control patients

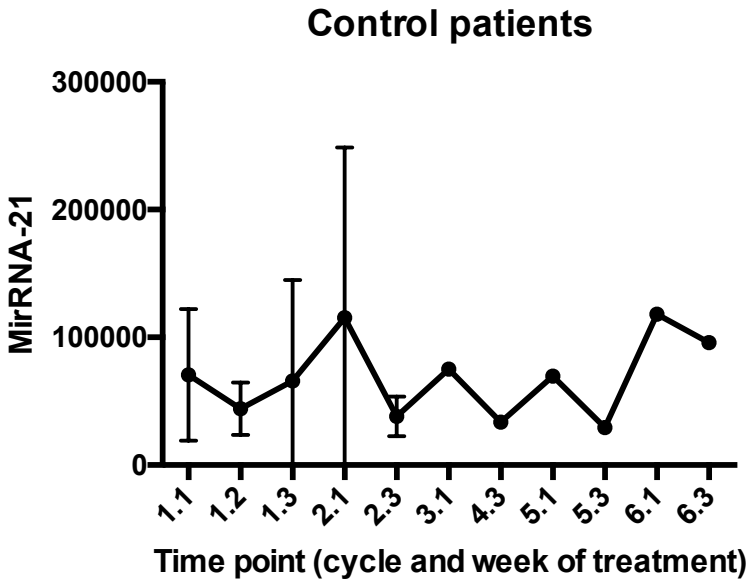

Figure 14.3. Figure showing mean miRNA-21 trend line with range (minimum to maximum).

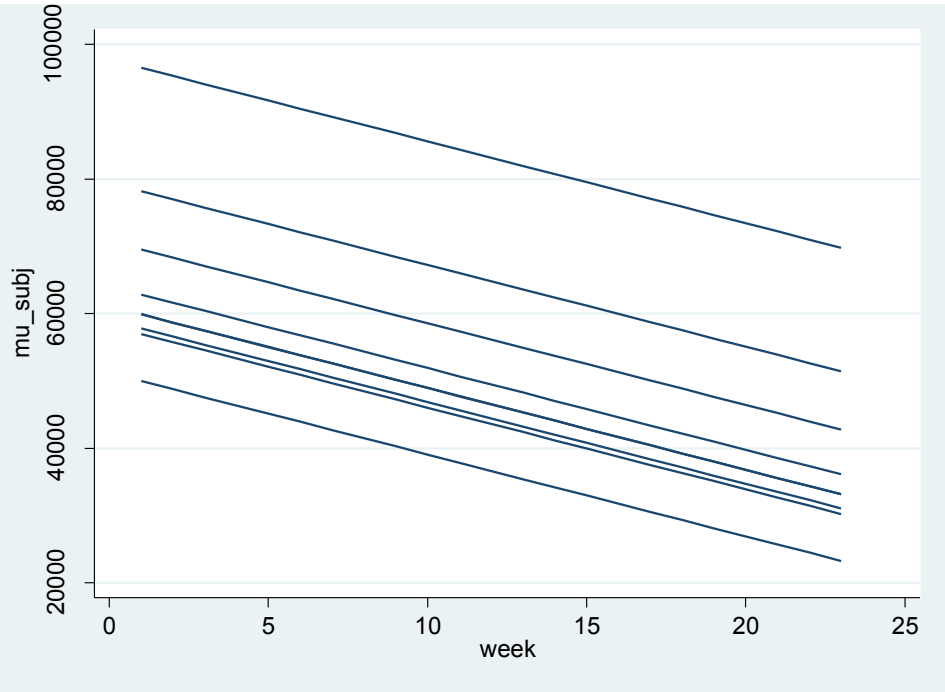

Figure 14.4. Graph showing regression lines for individual patients plotted against time in weeks following mixed effects logistic regression analysis. Micro RNA levels are shown on the y axis (mu_subj), and time in weeks is shown on the x axis. Each regression line represents a patient. There is a downward trend however there was no significant change in miRNA-21 levels in the control patients (P=0.494, 95% CI= (-4699.334 - 2267.271).

14.3 MiRNA-146a: Trial patients

There was no significant change in miRNA-146a levels in trial or control patients over the trial.

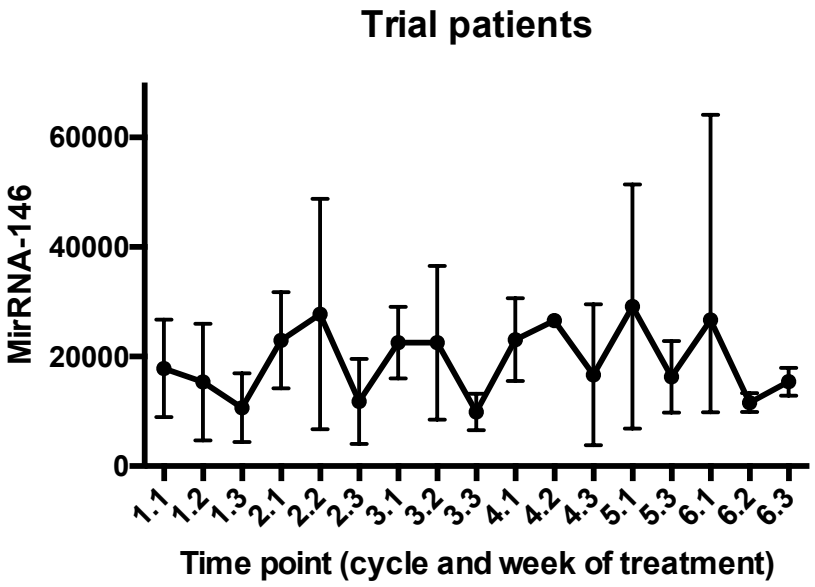

Figure 14.5. Figure showing mean miRNA-146a trend line with range (minimum to maximum).

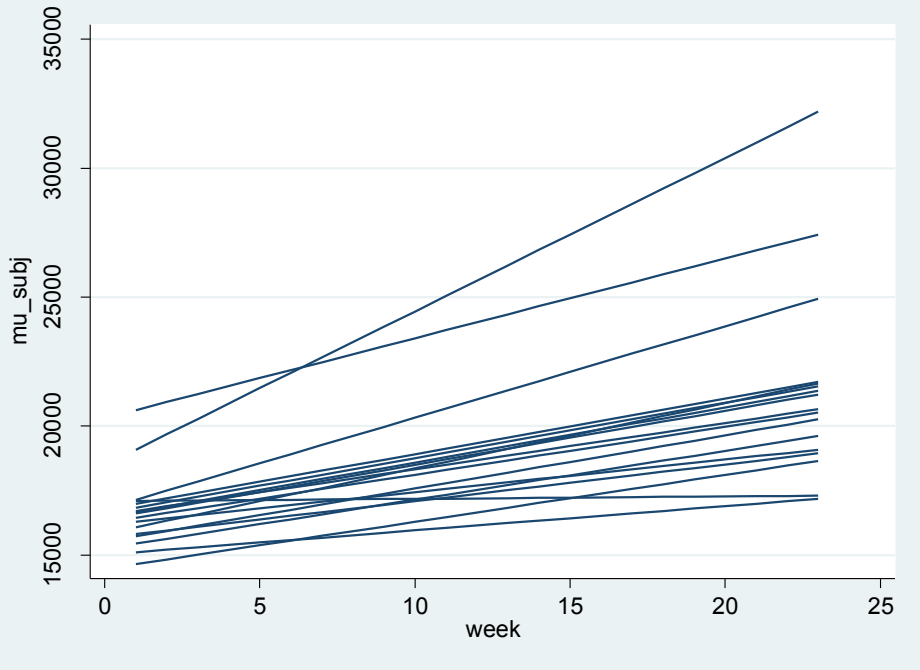

Figure 14.6. Graph showing regression lines for individual patients plotted against time in weeks following mixed effects logistic regression analysis. Micro RNA levels are shown on the y axis (mu_subj), and time in weeks is shown on the x axis. Each regression line represents a patient. There is a upward trend however there was no significant change in miRNA-146a levels in the trial patients (P=0.268, 95% CI = (-166.305 - 599.431).

14.4 MiRNA-146a: Control patients

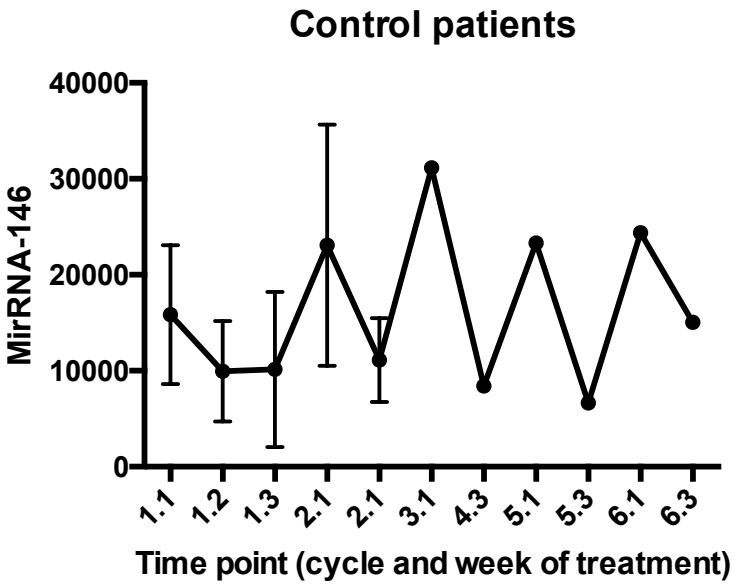

Figure 14.7. Figure showing mean miRNA-146a trend line with range (minimum to maximum).

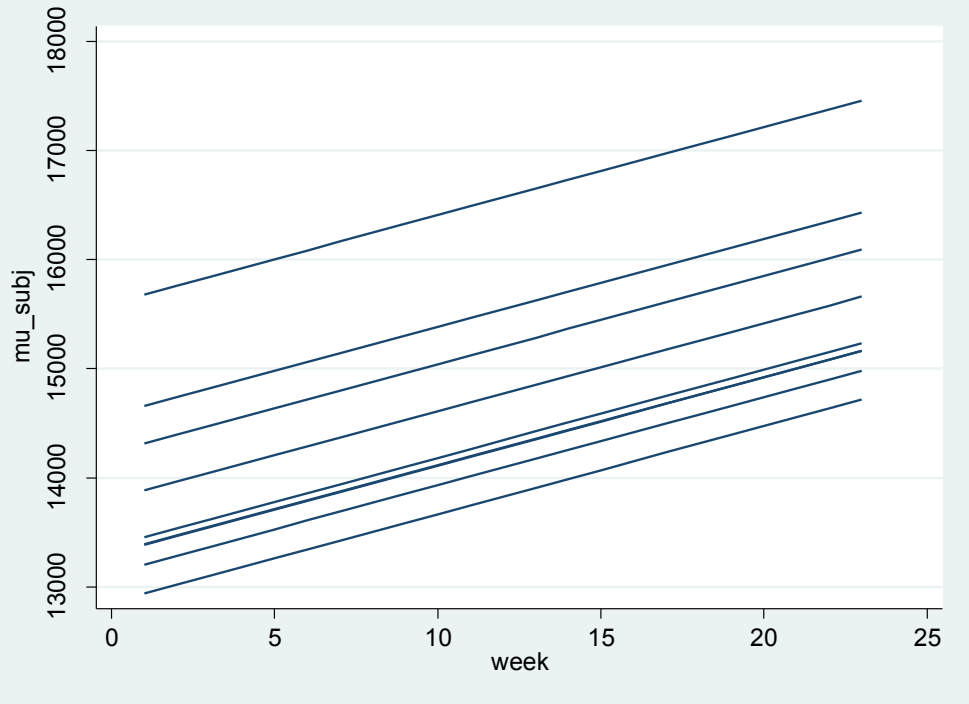

Figure 14.8. Graph showing regression lines for individual patients plotted against time in weeks following mixed effects logistic regression analysis. Micro RNA levels are shown on the y axis (mu_subj), and time in weeks is shown on the x axis. Each regression line represents a patient. There is a upward trend however there was no significant change in miRNA-146a levels in the control patients (P=0.743, 95% CI = (-402.233 - 563.825).

14.5 MiRNA-155: Trial patients

There was no significant change in miRNA-155 levels in trial or control patients over the trial.

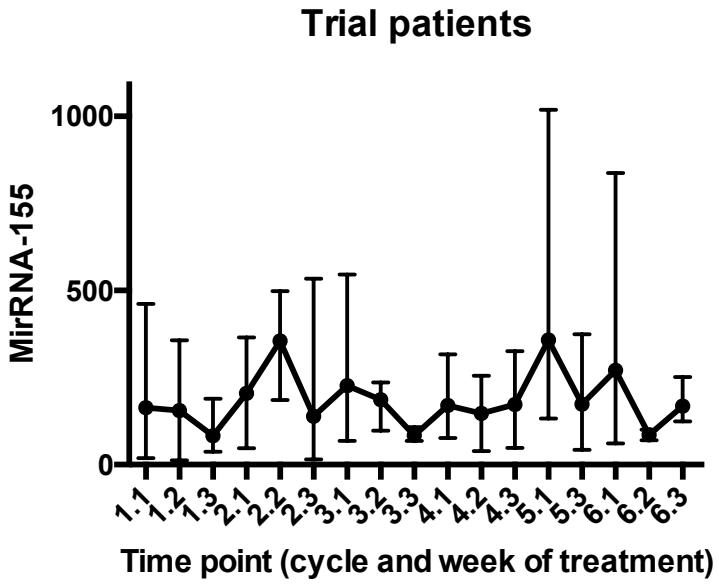

Figure 14.9. Figure showing mean miRNA-155 trend line with range (minimum to maximum).

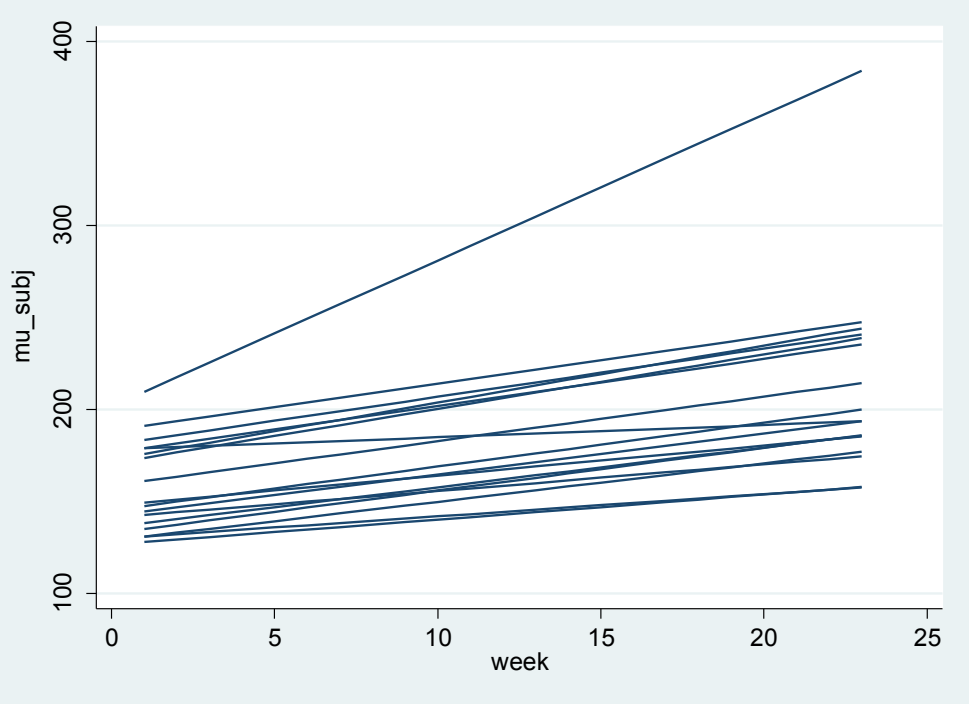

Figure 14.10. Graph showing regression lines for individual patients plotted against time in weeks following mixed effects logistic regression analysis. Micro RNA levels are shown on the y axis (mu_subj), and time in weeks is shown on the x axis. Each regression line represents a patient. There is an upward trend however there was no significant change in miRNA-155 levels in the trial patients (P=0.362, 95% CI = (-2.813 - 7.714).

14.6 MiRNA-155: Control patients

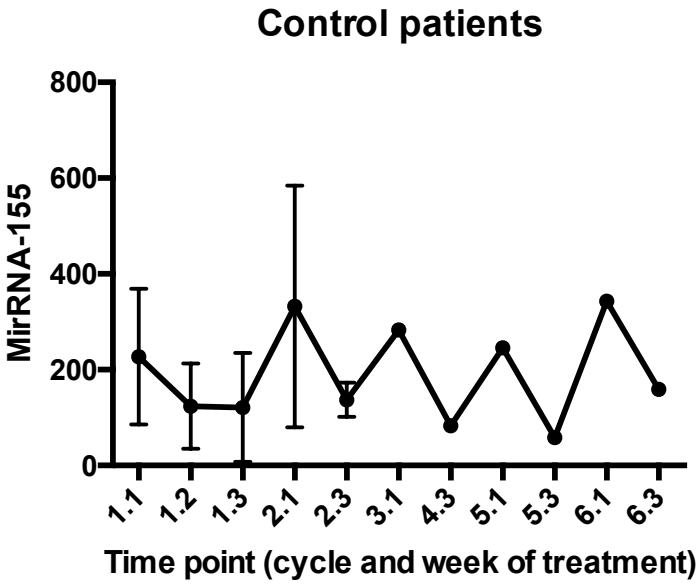

Figure 14.11. Figure showing mean miRNA-155 trend line with range (minimum to maximum).

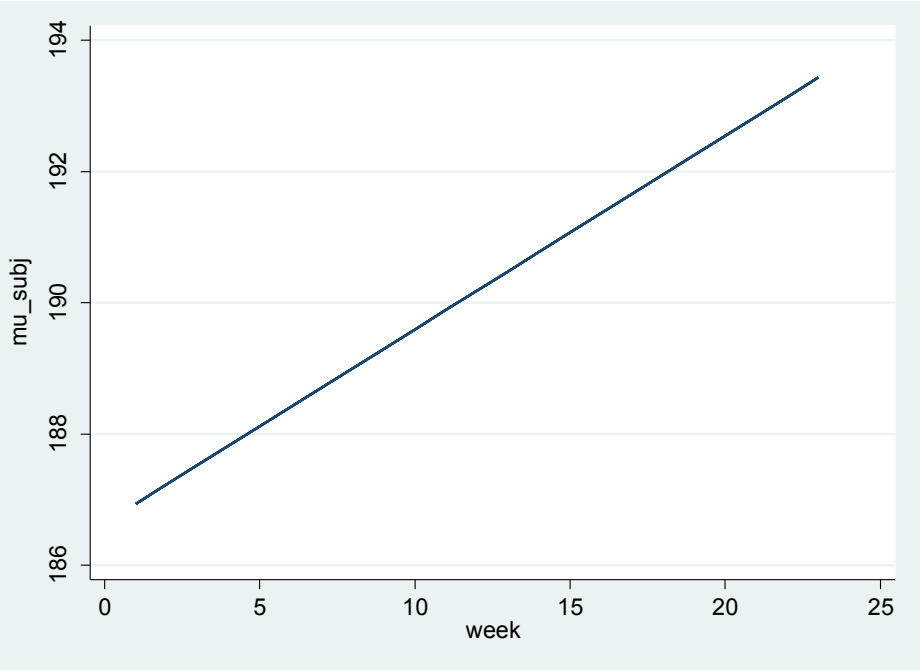

Figure 14.12. Graph showing regression lines for individual patients plotted against time in weeks following mixed effects logistic regression analysis. Micro RNA levels are shown on the y axis (mu_subj), and time in weeks is shown on the x axis. Each regression line represents a patient. There is only one line as the regression lines are very close together the model has combined all regression lines into one. There is a upward trend however there was no significant change in miRNA-155 levels in the control patients (P=0.939, 95% CI = (-7.226 - 7.817)

14.7 MiRNA-196a: Trial patients

There was no significant change in miRNA-196a levels in trial or control patients over the trial.

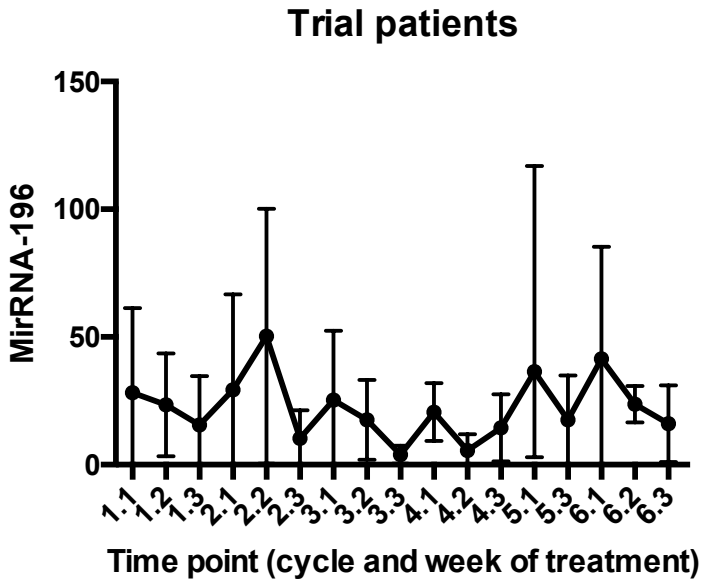

Figure 14.13. Figure showing mean miRNA-196a trend line with range (minimum to maximum).

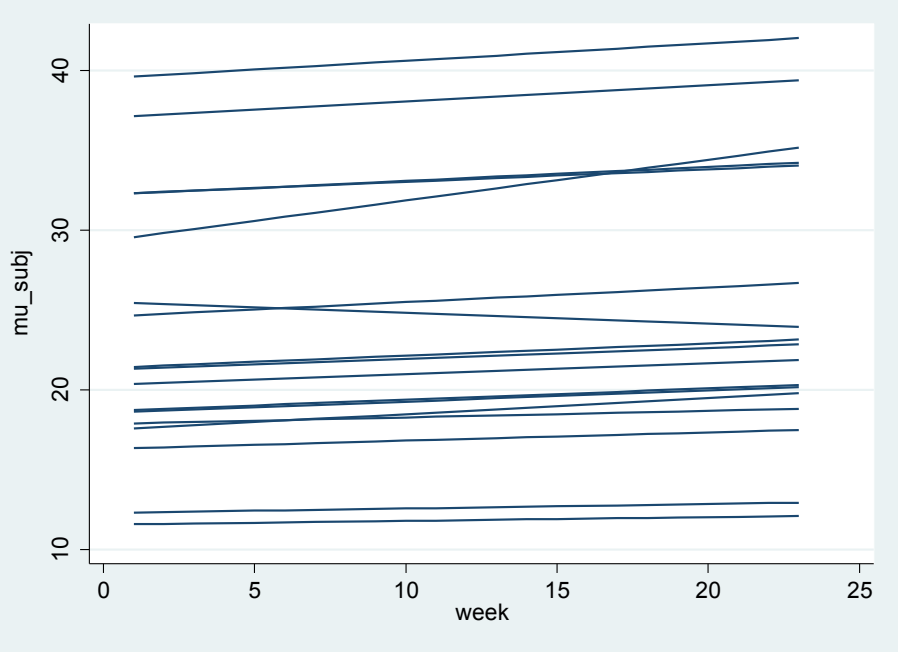

Figure 14.14. Graph showing regression lines for individual patients plotted against time in weeks following mixed effects logistic regression analysis. Micro RNA levels are shown on the y axis (mu_subj), and time in weeks is shown on the x axis. Each regression line represents a patient. There was no significant change in miRNA-196a levels in the trial patients (P=0.857, 95% CI = (-0.730 - 0.878).

14.8 MiRNA-196a: Control patients

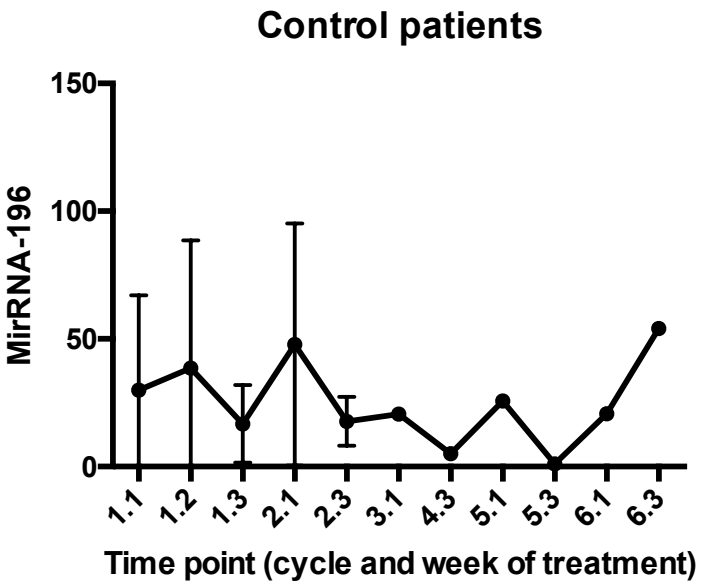

Figure 14.15. Figure showing mean miRNA-196a trend line with range (minimum to maximum).

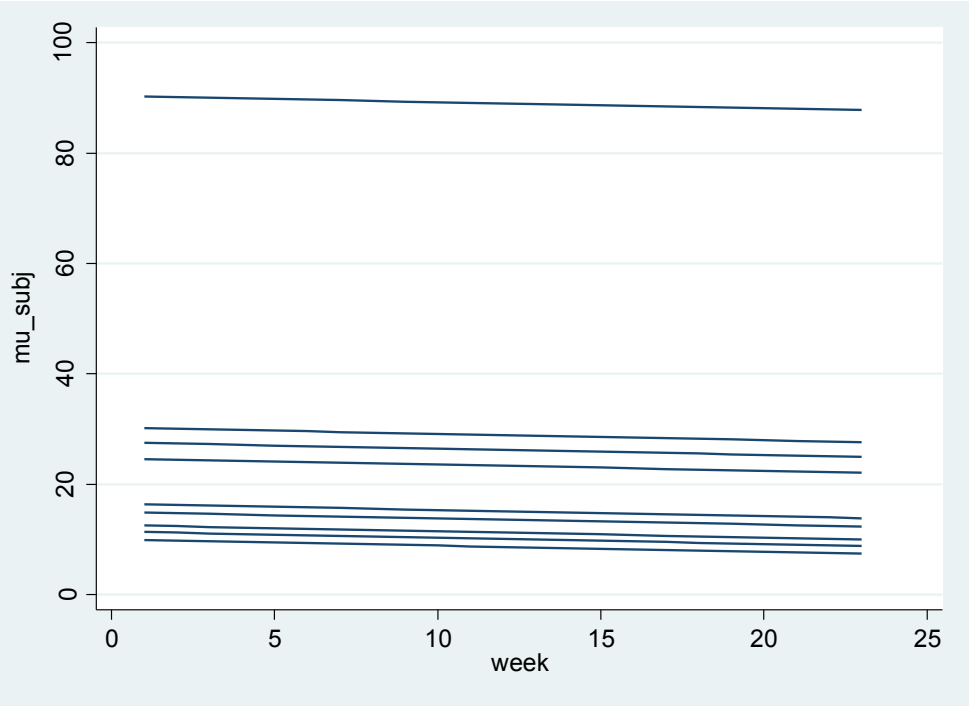

Figure 14.16. Graph showing regression lines for individual patients plotted against time in weeks following mixed effects logistic regression analysis. Micro RNA levels are shown on the y axis (mu_subj), and time in weeks is shown on the x axis. Each regression line represents a patient. There was no significant change in miRNA-196a levels in the control patients (P=0.885, 95% CI = (-1.643 - 1.417).

14.9 MiRNA-210: Trial patients

There was no significant change in miRNA-210 levels in trial or control patients over the trial.

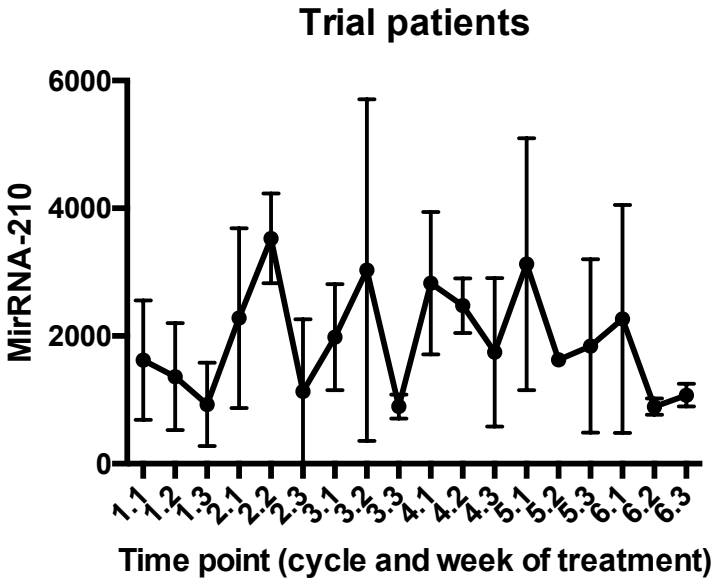

Figure 14.17. Figure showing mean miRNA-210 trend line with range (minimum to maximum).

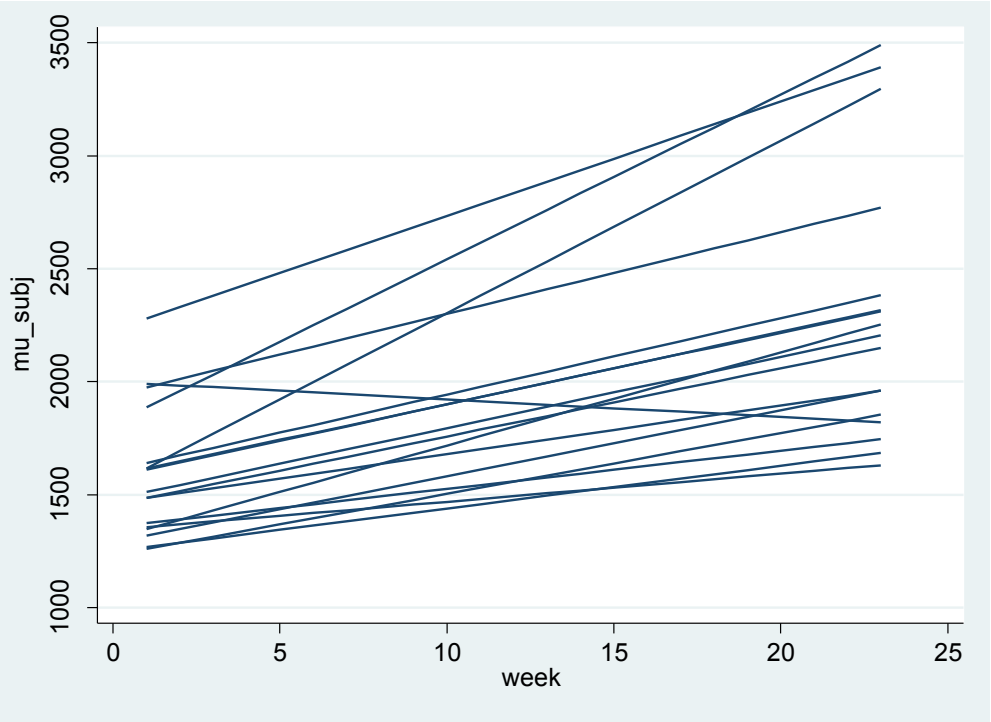

Figure 14.18. Graph showing regression lines for individual patients plotted against time in weeks following mixed effects logistic regression analysis. Micro RNA levels are shown on the y axis (mu_subj), and time in weeks is shown on the x axis. Each regression line represents a patient. There is an upward trend in values but there was no significant change in miRNA-210 levels in the trial patients (P=0.169, 95% CI = (-13.887 - 79.143).

14.10 MiRNA-210: Control patients

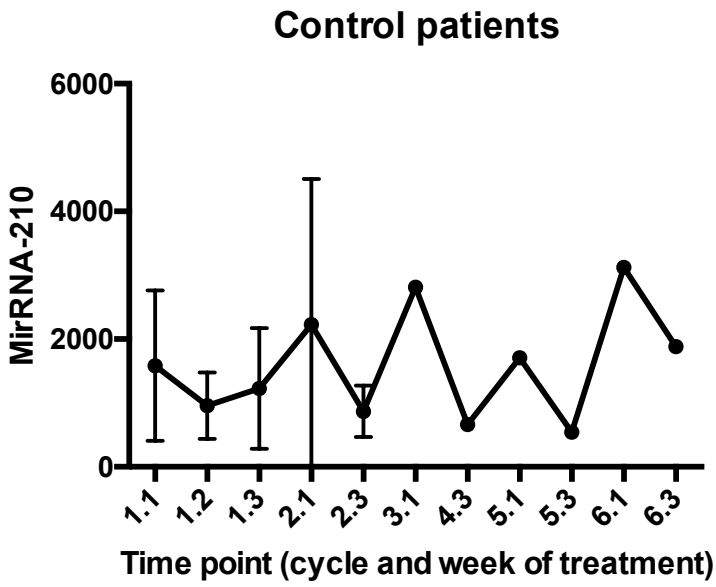

Figure 14.19. Figure showing mean miRNA-210 trend line with range (minimum to maximum).

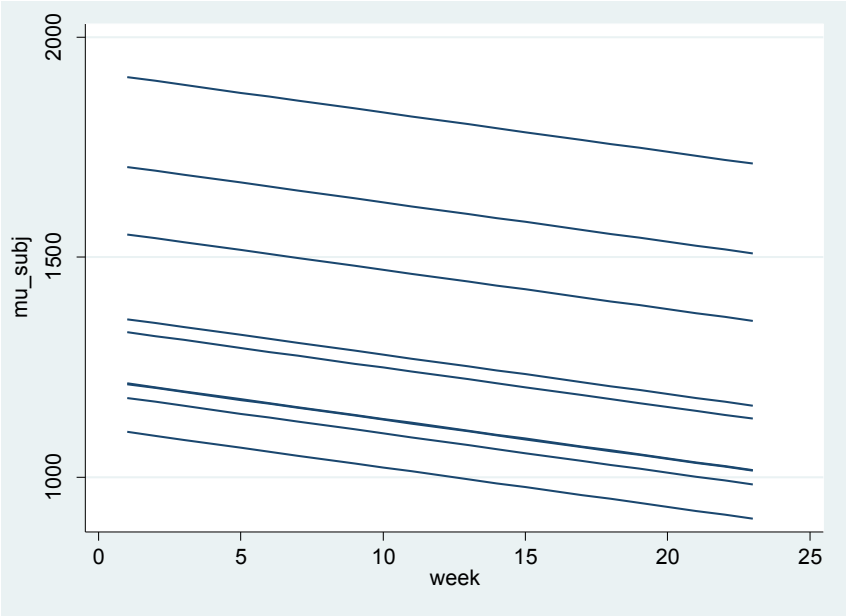

Figure 14.20. Graph showing regression lines for individual patients plotted against time in weeks following mixed effects logistic regression analysis. Micro RNA levels are shown on the y axis (mu_subj), and time in weeks is shown on the x axis. Each regression line represents a patient. There is a downward trend in values but there was no significant change in miRNA-210 levels in the control patients (P=0.791, 95% CI = (-75.286- 57.375).

14.11 MiRNA-221: Trial patients

There was no significant change in miRNA-221 levels in trial or control patients over the trial.

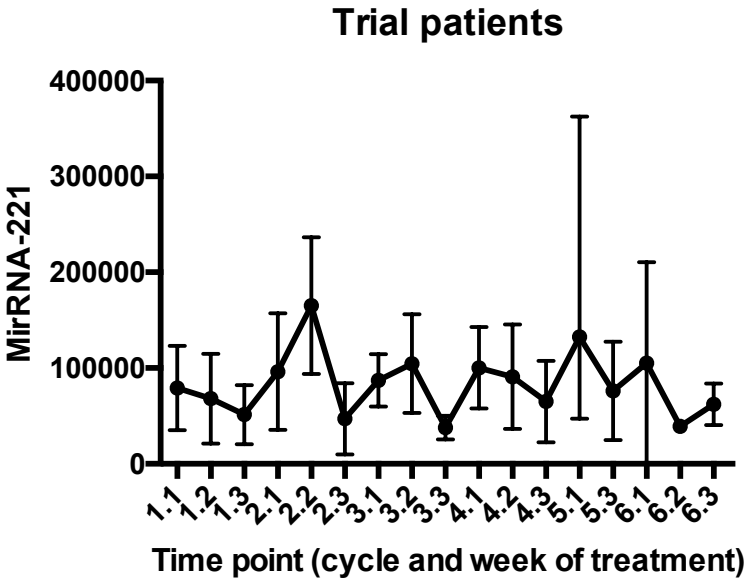

Figure 14.21. Figure showing mean miRNA-221 trend line with range (minimum to maximum).

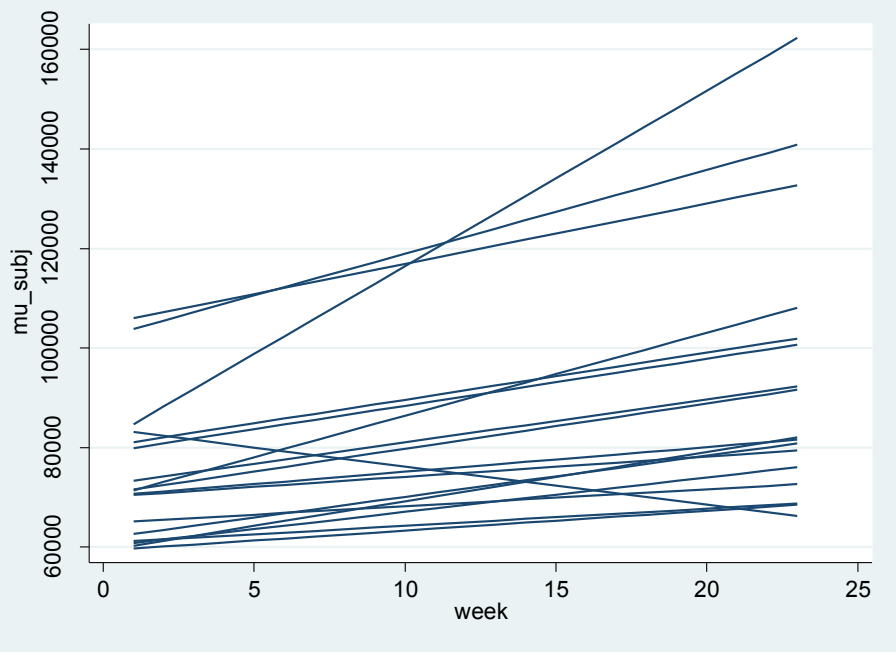

Figure 14.22. Graph showing regression lines for individual patients plotted against time in weeks following mixed effects logistic regression analysis. Micro RNA levels are shown on the y axis (mu_subj), and time in weeks is shown on the x axis. Each regression line represents a patient. There is an upward trend in values but there was no significant change in miRNA-221 levels in the trial patients (P=0.380, 95% CI = (-1123.677 - 2945.008).

14.12 MiRNA-221: Control patients

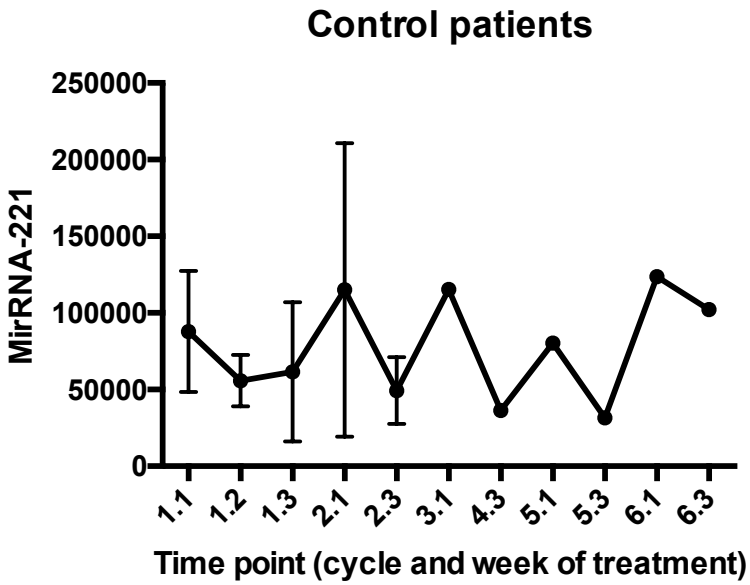

Figure 14.23. Figure showing mean miRNA-221 trend line with range (minimum to maximum).

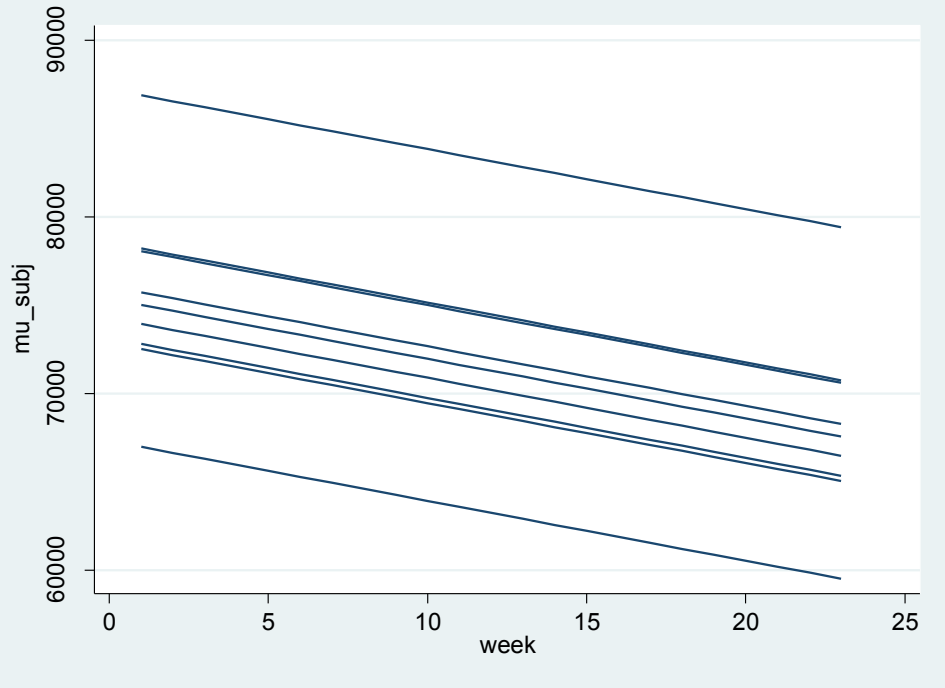

Figure 14.24. Graph showing regression lines for individual patients plotted against time in weeks following mixed effects logistic regression analysis. Micro RNA levels are shown on the y axis (mu_subj), and time in weeks is shown on the x axis. Each regression line represents a patient. There is a downward trend in values but there was no significant change in miRNA-221 levels in the trial patients (P=0.798, 95% CI = (-2935.561 - 2256.829).

14.13 Micro RNA: Comparison analysis

Trial and control patients were compared using a bespoke mixed effects logistic regression model. A tabulated summary of results is seen below.

Cohort analysed	Micro RNA					
	21	**146**	**155**	**196**	**210**	**221**
Trial patients	P=0.400, 95%CI = (-1163.809 - 2915.311)	P=0.268, 95% CI = (-166.305 - 599.431)	P=0.362, 95% CI = (-2.813 - 7.714)	P=0.857, 95%CI = (-0.730 - 0.878)	P=0.169, 95%CI = (-13.887 - 79.143)	P=0.380, 95%CI = (-1123.677 - 2945.0)
Control patients	P=0.494 95%CI = (-4699.334 - 2267.271)	P=0.743 95%CI = (-402.239 - 563.825)	P=0.939 95 % CI = (-7.226 - 7.817)	P=0.885, 95%CI = (-1.643 - 1.417)	P=0.791, 95%CI = (-75.286 - 57.375)	P=0.798, 95%CI = (-2935.561 - 2256.829)
Comparison analysis of trial and control patients	P=0.5559	P=0.7364	P=0.3949	P=0.5639	P=0.6487	P=0.5344

Table 14.1. Summary of all micro RNA results analysed. There was no significant change in all micro RNA analysed in both the trial and control patients. There were no significant changes in miRNAs analysed between trial and control patients.

15 Chapter Fifteen: Discussion

The aim of this study was to assess the effects of administering intravenous ω-3FAs in combination with gemcitabine chemotherapy on immunological cells and specific miRNAs in patients with APC compared to gemcitabine chemotherapy alone. Previous published data have demonstrated that intravenous administration of ω-3FAs is well tolerated[438], results in a rapid uptake into cell membranes and improves patient's quality of life[409–412,439] in advanced cancers. This pilot study has some obvious criticisms. Firstly the trial and control groups are unmatched, with eighteen in the trial cohort and nine in the control cohort. Recruitment stopped at nine control patients as a result of the standard chemotherapy regime being changed following the introduction of nab-paclitaxel as a chemotherapy addition to gemcitabine[20]. Nab-paclitaxel was subsequently removed as standard treatment in England by the National Institute of Health and Care Excellence department, who stated that it was not a cost effective treatment for APC in the National Health Service setting. In addition this was a pilot study and compared treatment in two cohorts with patients recruited in succession as they presented. Randomisation of patients and treatment would have reduced the possibility of selection bias. As a result of the unmatched groups the control cohort had a lower median age (64 versus 70 years) and a significantly lower total number of treatment time points (38 versus 146).

This study investigated the addition of Lipidem to standard gemcitabine chemotherapy. Lipidem contains 20 g ω-3FAs and 8.6-17.2g of EPA and DHA in 1000mls. In addition to this it contains medium chain triglycerides, soya-bean oil and omega 6 fatty acids. Ideally a more refined investigational product that contained a purer form of ω-3FAs in a lower total volume would have been selected. This product is currently not available on the market and we are currently in the process of developing a refined product with the manufacturer. Lipidem was administered following gemcitabine treatment and patients would receive up to 500ml over 4 hours. This was often quite exhausting for patients who were occasionally critical of the time scale it took to receive the treatment. The use of a smaller volume and more refined

product would improve compliance and ensure a high dose of ω-3FAs was administered in a shorter time frame without unnecessary volume. Lipidem was also administered following the gemcitabine treatment as per standard protocol on days 1, 8 and 15, which was followed by a rest week. This was a result of the ethics review that did not want to inconvenience patient's treatment. Ideally patients would have received intravenous ω-3FAs every week in order to maintain levels, however this would potentially result in, reduced recruitment, an increased drop-out rate and reduced compliance. A high dose oral supplement that could be administered in addition to intravenous treatment is a possible alternative treatment strategy.

Lipidem was selected as a source of omega-3-acid triglycerides as it was already an established medication with MHRA approval and was selected during trial development. There are other commercially available sources of omega-3 but as this trial was a continuation of a Phase II trial already in progress it was not possible to amend the treatment protocol. Likewise the use of refined EPA and or DHA was not possible due the treatment protocol.

The use of a trial product with additional levels of medium chain triglycerides and soya-bean oil is controversial. The added products does provides a cachectic cohort of patients with additional calories and can possibly help explain the improved quality of life scores seen in trial patents by improving nutrition and energy levels. It is unknown what he exact effect these additional calories had on patients and this effect could be analyzed further in future studies. In addition patients were not asked to keep food diaries. All patients were encouraged to have full nutritional intake and were assessed regularly by dedicated specialized pancreatic dieticians. No patient in the trial arm further supplemented their omega-3 intake with oral supplements and obtained their omega-3 from lipidem alone. There is no robust evidence that any of the additional products in Lipidem have demonstrated an anti-tumorigenic effect and the evidence provided of increased uptake, decreased omega-3:omega-6 ratio and effect on immune modulatory cells provided evidence of the anti-tumorigenic effect of omega-3. All patients were taking pancreatic enzyme replacement therapy in addition to a proton pump inhibitor. This is standard practice for the department and all pancreatic

cancer patients. It is unknown if supplementation of pancreatic enzymes increases absorption of oral omega-3 supplements and this is the subject of an ongoing trial within the department. This will have ramifications on further trials that would use oral and intravenous omega-3 supplementation.

15.1 Clinical data

Although this study was not powered for survival analysis, overall there was a significant difference in PFS between trial and control patients with a median PFS in the trial cohort of 5.65 months compared to 1.8 months in the control cohort. There was no significant benefit in OS in the trial compared to control group. This is likely to be the result of the small sample size and unmatched cohorts and the fact this pilot study was not powered to survival.

This study is the first to analyse immune regulatory cells and micro RNA at multiple treatment points in patients receiving intravenous ω-3FAs. Most other studies only analyse baseline levels and either one, two or three treatment points. As demonstrated in various figures there is variability in immune regulatory cell levels and micro RNAs at each treatment point. This study therefore provides an essential and robust analysis of the immune regulatory cell levels and micro RNA levels over treatment.

15.2 MDSCs

MDSCs are immature cells in a constant state of development and therefore difficult to phenotypically define. Two MDSCs phenotypes were studied. MDSCs with a $Lin1^-$, $HLA\text{-}DR^-$, $CD33^+$, and $CD11b^+$ phenotype demonstrated a significant decrease in trial patients on regression analysis. There was no significant change in control patients on regression analysis. ω-3FAs therefore significantly reduce MDSCs with a $Lin1^-$, $HLA\text{-}DR^-$, $CD33^+$, and $CD11b^+$ phenotype in APC. However comparative regression analysis did not demonstrate a significant difference between trial and control cohorts. This is possibly the result of small comparison cohorts. Interestingly there was a significant

difference in cycles one, three and six between trial and control patients. Control patients had a significantly lower baseline level of MDSCs compared to trial patients, however this was not seen at end point. There was no benefit in PFS or OS in trial patients who had a high or low number of MDSCs at treatment end point compared to baseline. In addition there was no significant benefit in PFS or OS when comparing trial and control patients who had a high or low change in MDSCs.

MDSCs with a $Lin1^-$, $HLA\text{-}DR^-$ and $CD11b^+$ phenotype demonstrated a significant decrease in trial patients on regression analysis. In comparison there was no significant decrease in MDSCs in the control cohort overall. ω-3FAs therefore significantly reduce MDSCs with a $Lin1^-$, $HLA\text{-}DR^-$ and $CD11b^+$ phenotype in APC and this was also seen on comparative regression analysis. In addition on comparison there was a statistically significant difference in cycle two, three, four and five between trial and control patients. Within cycle one there was a significant difference in week one and two of treatments between the two cohorts. MDSCs with a $Lin1^-$, $HLA\text{-}DR^-$ and $CD11b^+$ phenotype in trial patients were significantly reduced at one month and end point. In addition trial patients who survived over six months had a significant decrease in MDSCs at end point.

Overall there was a significant reduction in patients MDSCs (both $Lin1^-$, $HLA\text{-}DR^-$, $CD33^+$, $CD11b^+$ and $Lin1^-$, $HLA\text{-}DR^-$ and $CD11b^+$ phenotypes) treated with ω-3FAs with no change demonstrated in control patients MDSCs. In addition there was a significant reduction in $Lin1^-$, $HLA\text{-}DR^-$ and $CD11b^+$ MDSCs on comparison regression analysis of trial versus control patients. This is the first time MDSCs have been studied in a clinical setting where APC patients have been treated with intravenous ω-3FAs. There is a profound inflammatory response seen in the tumour microenvironment of APC and MDSCs are key promoters of this inflammatory response. There are increased levels of MDSCs in APC, with levels correlating with disease progression. The precise mechanism underlying the reduction in MDSCs by ω-3FAs may be a result of a reduction in the pro-inflammatory mediators present in APC. Pro-inflammatory mediators, which include cytokines, eicosanoids and growth factors, drive the recruitment and expansion of MDSCs in APC. As discussed ω-3FAs reduce these pro-

inflammatory factors predominantly by their incorporation into the cell membrane from which they are subsequently metabolised to less inflammatory mediators thereby shifting the balance and reducing the amount of pro-inflammatory eicosanoids. By reducing the number of MDSCs it can be postulated that there will be a subsequent reduction in their actions such as the inhibition of CTLs, TH1 $CD4^+$ and TH17 $CD4^+$ T cells, M1 macrophages, the secretion of pro inflammatory cytokines such as IL-10, growth factors such as VEGF and particularly their role in expanding Tregs. A reduction in the pro-inflammatory response seen in APC could reduce tumour progression and ω-3FA treatment offers a safe and well-tolerated treatment that acts upstream of these mediators with the ability to act on multiple pathways. Studies have shown that ω-3FAs promote the accumulation of MDSCs in cell culture and mice models[415], which resulted in a more pronounced tumour growth[416]. These studies offer conflicting evidence to the results presented and demonstrate that there may be a multitude of downstream actions of ω-3FAs and any therapeutic benefit needs to be specifically investigated for its targeted pathology. The low number within the peripheral circulation limits measurement of circulating immune regulatory cells. The examination of local cell population frequencies within pancreatic tissue would be an alternative option, however this is technically and ethically difficult to justify. Pancreatic biopsies are not without significant risk of morbidity and mortality and ethical approval for repeated biopsy would be unlikely to be granted. In addition the refinement of a peripheral investigation is much more likely to be accepted by patients in future studies.

15.3 Tregs

There was a non-significant change in trial Tregs on regression analysis but a significant increase in Tregs in control patients on regression analysis. However regression analysis comparing the two cohorts demonstrated no significant difference over treatment. Treatment with ω-3FAs therefore results in stability of Tregs while patients treated with gemcitabine alone had a significant increase in Tregs. ω-3FAs result in the decrease in MDSCs and this could explain the observed non-increase and stable levels of Tregs. It may be that there were insufficient numbers of patients to demonstrate a

reduction but it can be postulated that an increase in Tregs is associated with a decreased survival as described in the literature. Indeed, in trial patients who had an OS of less than 6 months there was a significant increase in end point Tregs compared to baseline. In addition a low level of Tregs is associated with improved survival. We have demonstrated that in patients with a low change in Tregs at end point compared to baseline there was a statistically significant PFS in trial compared to control patients. MDSCs are significantly elevated in patients with PAC and their levels correlate with Treg levels[78]. In addition inhibition of MDSC function has been shown to abrogate Treg proliferation[241]. There was a significant increase in Tregs seen in the control patients. There was no decrease in MDSCs seen in control patients and the on-going expansion on MDSCs in this group (albeit not significant) may be a possible explanation for the Treg increase.

Tregs are increased in PAC and their levels correlate with a significantly reduced survival[216,440]. Although Homma et al[218] demonstrated a significant reduction in Tregs in patients receiving gemcitabine chemotherapy this was in comparison to patients receiving best supportive treatment. This study compared two cohorts that received effective comparable evidence based treatment and although there was a small sample size there were multiple measurements of Tregs resulting in a more robust evidence base. We can therefore conclude that intravenous ω-3FAs treatment results in the significant reduction of MDSCs, which results in stabilisation of Treg levels. Treatment with gemcitabine therapy only results in the non-significant reduction of MDSCs and a significant increase in Treg levels. Treatment with ω-3FAs therefore results in reduction of the potent pro inflammatory circulating cells (MDSCs) and stability of Tregs in patients with APC.

Patients with APC would be expected to have increasing levels of Tregs correlating with progressive disease, however this was not seen in trial patients, where a non significant increase was demonstrated on regression analysis of one hundred and five samples (P=0.23). It could be debated that this stabilisation is simply the effect of advanced cancer and Treg levels would have plateaued regardless, however this is contrary to published literature which demonstrates an increase in Tregs with

developing tumour stage[216]. Additional analysis is required to determine this effect within a randomised control trial.

15.4 EPCs

All three EPC phenotypes were significantly increased in the trial patients but not control patients. In addition EPCs ($CD45^-$, $CD31^+$, $CD34^+$ and $CD45^-$, $CD34^+$, $CD31^+$, $CD133^+$ phenotype) were significantly reduced compared to control on comparison regression analysis. An increase in EPCs had been demonstrated following ω-3FAs administration[429,430]. Theoretically if ω-3FAs reduce the numerous pro-angiogenic mediators there would be a reduction in EPCs over ω-3FA treatment. However ω-3FAs appear to increase EPCs over treatment and the exact pathways producing this are currently undetermined. It can be hypothesised that the reduction in pro-inflammatory mediators and environment established as a result of ω-3FA treatment allows the expansion and recruitment of EPCs by alternative PAC mediators. Although reduction of the hypoxic stroma and inflammatory cuff seen in PAC should theoretically limit EPC expansion, there are clearly alternative mechanisms behind the EPC expansion seen with ω-3FA treatment, and this requires further investigation. An increase in EPCs may actually have a survival benefit. Interestingly there was a survival benefit seen with an increase in EPCs in trial patients with a high change of EPCs compared to control patients. In EPCs with a $CD45^-$, $CD31^+$, $CD133^+$ and $CD45^-$, $CD31^+$ and $CD34^+$ phenotype there was a significant PFS and OS seen in trial patients with a high change of EPCs compared to control patients.

The reduction in trial MDSCs, stabilisation of Tregs and increase in EPCs had been hypothesised to be secondary to the anti tumorigenic effect of Omega-3 fatty acids. However this study had unmatched groups and low number of control patients and in addition patients in the trial group had significantly longer chemotherapy cycles then the control cohort. It can be therefore be hypothesised that treatment with gemcitabine alone was responsible for the effects observed. This cannot be irrefutably denied which is why a phase three randomised trial with the utilisation of refined omega-3 treatment would build on the results demonstrated in this pilot study to conclusively answer this.

15.5 Micro RNA.

There was no significant difference in any of the miRNA analysed in both trial and control patients. It may be that selection of specific miRNAs resulted in the omission of miRNAs that would have demonstrated dysregulation. The six miRNAs selected were chosen as they had the largest evidence base of dysregulation in APC. Additional studies utilising micro RNA arrays may result in successful miRNA dysregulation analysis.

15.6 Learning points and future consideration

This pilot study was performed within part of a phase two study that was previously on-going. On reflection if I were to perform the study again I would have designed the study differently in several ways. Firstly, I would have adopted the use of a more refined omega-3 product. The use of an unrefined product has provided an element of doubt and possible bias into this study and the use of a pure omega-3 product would eliminate this. Secondly I would have ensured matched groups over similar recruiting time frames. This would have ensured more comparable cohorts and data sets. This study was severely limited by the poor outcome and unmatched control group leading to difficult data analysis and extrapolation of results implication in their clinical context. This pilot study does benefit from some very robust sample analysis. All samples taken from each patient were analysed in full. This included analysing each sample for each individual antibody as well as combination stains. Although this provided a thorough analysis for this sample cohort, it could be optimised in the future by analysing only cycle one and cycle three samples in treatment month. Based on this preliminary data it would provide an appropriate analytical time frame to determine trends in sample analysis. On reflection in addition to the immunological cells measured I would measure circulating tumour cells. This would include all potential circulating tumour cell markers of immunological dysfunction. In addition to this I would perform a comprehensive micro RNA analysis of all potential dysregulated micro RNAs. This would enable comprehensive analysis of micro RNA dysregulation in both cohorts. This is obviously an expensive analysis and would need appropriately

planned in collaboration with an expert scientific team. This pilot study has established a robust platform of methodological, clinical and scientific data that can be utilised and developed within a phase three randomised trial.

15.7 Conclusion

Administration of ω-3FAs with gemcitabine chemotherapy in APC results in the significant decrease of MDSCs and stability of Tregs. This may be secondary to the reduction of pro inflammatory mediators. The evidence that omega-3 supplementation in advanced pancreatic cancer reduces key immune modulatory mediators clearly demonstrate that a phase three randomised trial is warranted to further validate these results.

16 Chapter Sixteen: Appendix 1

16.1 Eastern Cooperative Oncology Group performance status.

Grade Description	
0	Fully active, able to carry on all pre-disease performance without restriction
1	Restricted in physically strenuous activity but ambulatory and able to carry out work of a light or sedentary nature, e.g., light house work, office work
2	Ambulatory and capable of all self-care but unable to carry out any work activities; up and about more than 50% of waking hours
3	Capable of only limited self-care; confined to bed or chair more than 50% of waking hours
4	Completely disabled; cannot carry on any self-care; totally confined to bed or chair
5	Dead

16.2 RECIST Criteria: Response Evaluation Criteria In Solid Tumours - Evaluation of target lesions (version 1.1)

* Complete Response (CR):	Disappearance of all target lesions and no appearance of new lesions. Each must be documented on two separate occasions separated by at least 4 weeks.
* Partial Response (PR):	At least a 30% decrease in the sum of the LD of target lesions, taking as reference the baseline sum LD
* Progressive Disease (PD):	At least a 20% increase in the sum of the LD of target lesions, taking as reference the smallest sum LD recorded since the treatment started or the appearance of one or more new lesions

* Stable Disease (SD):	Neither sufficient shrinkage to qualify for PR nor sufficient increase to qualify for PD, taking as reference the smallest sum LD since the treatment started

16.3 RECIST Criteria; Response Evaluation Criteria In Solid Tumours - Evaluation of non-target lesions (version 1.1)

Complete Response (CR):	Disappearance of all non-target lesions and normalization of tumor marker level
Incomplete Response/ Stable Disease (SD):	Persistence of one or more non-target lesion(s) or/and maintenance of tumor marker level above the normal limits
Progressive Disease (PD):	Appearance of one or more new lesions and/or unequivocal progression of existing non-target lesions

17 Chapter Seventeen: Bibliography

1. Statistics, O. for N. Mortality Statistics: Cause: England and Wales. (2007).
2. Miller, K. D. et al. Cancer treatment and survivorship statistics, 2016. CA. Cancer J. Clin. **66,** 271–89 (2016).
3. Siegel, R., Ma, J., Zou, Z. & Jemal, A. Cancer statistics, 2014. CA. Cancer J. Clin. **64,** 9–29 (2014).
4. Neuzillet, C. et al. State of the art and future directions of pancreatic ductal adenocarcinoma therapy. Pharmacol. Ther. **155,** 80–104 (2015).
5. Ryan, D. P., Hong, T. S. & Bardeesy, N. Pancreatic Adenocarcinoma. N. Engl. J. Med. **371,** (2014).
6. CHARI, S. et al. Probability of Pancreatic Cancer Following Diabetes: A Population-Based Study. Gastroenterology **129,** 504–511 (2005).
7. Progress, M. & Hidalgo, M. Pancreatic Cancer. 1605–1617 (2010).
8. Shi, C. et al. Familial pancreatic cancer. Arch. Pathol. Lab. Med. **133,** 365–374 (2009).
9. Tersmette, A. C. et al. Increased risk of incident pancreatic cancer among first-degree relatives of patients with familial pancreatic cancer. Clin. Cancer Res. **7,** 738–44 (2001).
10. DiMagno, E. P., Reber, H. A. & Tempero, M. A. AGA technical review on the epidemiology, diagnosis, and treatment of pancreatic ductal adenocarcinoma. American Gastroenterological Association. Gastroenterology **117,** 1464–84 (1999).
11. Li, D., Xie, K., Wolff, R. & Abbruzzese, J. L. Pancreatic cancer. Lancet (London, England) **363,** 1049–1058 (2004).
12. Jemal, A. et al. Global cancer statistics. CA. Cancer J. Clin. **61,** 69–90 (2011).
13. Gillen, S., Schuster, T., Meyer zum Büschenfelde, C., Friess, H. & Kleeff, J. Preoperative/Neoadjuvant Therapy in Pancreatic Cancer: A Systematic Review and Meta-analysis of Response and Resection Percentages. PLoS Med. **7,** e1000267 (2010).
14. Thota, R., Pauff, J. M. & Berlin, J. D. Treatment of metastatic pancreatic adenocarcinoma: a review. Oncology (Williston Park). **28,** 70–4 (2014).

15. Burris III, H. A. et al. Improvements in Survival and Clinical Benefit With Gemcitabine as First-Line Therapy for Patients With Advanced Pancreas Cancer : A Randomized Trial. J. Clin. Oncol. **15,** 2403–2413 (1997).
16. Moore, M. J. et al. Erlotinib Plus Gemcitabine Compared With Gemcitabine Alone in Patients With Advanced Pancreatic Cancer: A Phase III Trial of the National Cancer Institute of Canada Clinical Trials Group. J. Clin. Oncol. **25,** 1960–1966 (2007).
17. Cunningham, D. et al. Phase III Randomized Comparison of Gemcitabine Versus Gemcitabine Plus Capecitabine in Patients With Advanced Pancreatic Cancer. J. Clin. Oncol. **27,** 5513–5518 (2009).
18. Ueno, H. et al. Randomized phase III study of gemcitabine plus S-1, S-1 alone, or gemcitabine alone in patients with locally advanced and metastatic pancreatic cancer in Japan and Taiwan: GEST study. J. Clin. Oncol. **31,** 1640–8 (2013).
19. Gourgou-bourgade, S. et al. FOLFIRINOX versus Gemcitabine for Metastatic Pancreatic Cancer. N. Engl. J. Med. **364,** 1817–1825 (2011).
20. Von Hoff, D. D. et al. Increased survival in pancreatic cancer with nab-paclitaxel plus gemcitabine. N. Engl. J. Med. **369,** (2013).
21. Neoptolemos, J. P. et al. Comparison of adjuvant gemcitabine and capecitabine with gemcitabine monotherapy in patients with resected pancreatic cancer (ESPAC-4): a multicentre, open-label, randomised, phase 3 trial. Lancet **389,** 1011–1024 (2017).
22. Yang, Z. et al. Gemcitabine Plus Erlotinib for Advanced Pancreatic Cancer : A Systematic Review with Meta-Analysis. **8,** 1–10 (2013).
23. Herrmann, R. et al. Gemcitabine Plus Capecitabine Compared With Gemcitabine Alone in Advanced Pancreatic Cancer: A Randomized, Multicenter, Phase III Trial of the Swiss Group for Clinical Cancer Research and the Central European Cooperative Oncology Group. J. Clin. Oncol. **25,** 2212–2217 (2007).
24. Scheithauer, W. et al. Biweekly high-dose gemcitabine alone or in combination with capecitabine in patients with metastatic pancreatic adenocarcinoma: a randomized phase II trial. Ann. Oncol. Off. J. Eur. Soc. Med. Oncol. **14,** 97–104 (2003).
25. <p>Muhammad Wasif Saif, C. P. C. J. R. Is S-1 a Potential Game Changer in

Adjuvant Therapy of Pancreatic Cancer? JOP. J. Pancreas

26. Yardley, D. A. nab-Paclitaxel mechanisms of action and delivery. J. Control. Release **170,** 365–372 (2013).
27. Von Hoff, D. D. et al. Gemcitabine plus nab-paclitaxel is an active regimen in patients with advanced pancreatic cancer: a phase I/II trial. J. Clin. Oncol. **29,** 4548–54 (2011).
28. Berlin, J. D. et al. Phase III Study of Gemcitabine in Combination With Fluorouracil Versus Gemcitabine Alone in Patients With Advanced Pancreatic Carcinoma: Eastern Cooperative Oncology Group Trial E2297. J. Clin. Oncol. **20,** 3270–3275 (2002).
29. Colucci, G. et al. Gemcitabine alone or with cisplatin for the treatment of patients with locally advanced and/or metastatic pancreatic carcinoma: a prospective, randomized phase III study of the Gruppo Oncologia dell'Italia Meridionale. Cancer **94,** 902–10 (2002).
30. Ducreux, M. et al. A randomised trial comparing 5-FU with 5-FU plus cisplatin in advanced pancreatic carcinoma. Ann. Oncol. Off. J. Eur. Soc. Med. Oncol. **13,** 1185–91 (2002).
31. Bramhall, S. R. et al. A double-blind placebo-controlled, randomised study comparing gemcitabine and marimastat with gemcitabine and placebo as first line therapy in patients with advanced pancreatic cancer. Br. J. Cancer **87,** 161–167 (2002).
32. Van Cutsem, E. et al. Phase III Trial of Gemcitabine Plus Tipifarnib Compared With Gemcitabine Plus Placebo in Advanced Pancreatic Cancer. J. Clin. Oncol. **22,** 1430–1438 (2004).
33. Oettle, H. et al. A phase III trial of pemetrexed plus gemcitabine versus gemcitabine in patients with unresectable or metastatic pancreatic cancer. Ann. Oncol. **16,** 1639–1645 (2005).
34. Louvet, C. et al. Gemcitabine in combination with oxaliplatin compared with gemcitabine alone in locally advanced or metastatic pancreatic cancer: results of a GERCOR and GISCAD phase III trial. J. Clin. Oncol. **23,** 3509–16 (2005).
35. Heinemann, V. et al. Randomized Phase III Trial of Gemcitabine Plus Cisplatin Compared With Gemcitabine Alone in Advanced Pancreatic Cancer. J. Clin.

Oncol. **24,** 3946–3952 (2006).

36. Abou-Alfa, G. K. et al. Randomized Phase III Study of Exatecan and Gemcitabine Compared With Gemcitabine Alone in Untreated Advanced Pancreatic Cancer. J. Clin. Oncol. **24,** 4441–4447 (2006).
37. Stathopoulos, G. P. et al. A multicenter phase III trial comparing irinotecan-gemcitabine (IG) with gemcitabine (G) monotherapy as first-line treatment in patients with locally advanced or metastatic pancreatic cancer. Br. J. Cancer **95,** 587–592 (2006).
38. Eckhardt, S. G. et al. Patient-Reported Outcomes as a Component of the Primary Endpoint in a Double-Blind, Placebo-Controlled Trial in Advanced Pancreatic Cancer. J. Pain Symptom Manage. **37,** 135–143 (2009).
39. Van Cutsem, E. et al. Phase III Trial of Bevacizumab in Combination With Gemcitabine and Erlotinib in Patients With Metastatic Pancreatic Cancer. J. Clin. Oncol. **27,** 2231–2237 (2009).
40. Poplin, E. et al. Phase III, randomized study of gemcitabine and oxaliplatin versus gemcitabine (fixed-dose rate infusion) compared with gemcitabine (30-minute infusion) in patients with pancreatic carcinoma E6201: a trial of the Eastern Cooperative Oncology Group. J. Clin. Oncol. **27,** 3778–85 (2009).
41. Ciuleanu, T. E. et al. A randomised Phase III trial of glufosfamide compared with best supportive care in metastatic pancreatic adenocarcinoma previously treated with gemcitabine. Eur. J. Cancer **45,** 1589–1596 (2009).
42. Dahan, L. et al. Combination 5-fluorouracil, folinic acid and cisplatin (LV5FU2-CDDP) followed by gemcitabine or the reverse sequence in metastatic pancreatic cancer: final results of a randomised strategic phase III trial (FFCD 0301). Gut **59,** 1527–1534 (2010).
43. Kindler, H. L. et al. Gemcitabine plus bevacizumab compared with gemcitabine plus placebo in patients with advanced pancreatic cancer: phase III trial of the Cancer and Leukemia Group B (CALGB 80303). J. Clin. Oncol. **28,** 3617–22 (2010).
44. Philip, P. A. et al. Phase III Study Comparing Gemcitabine Plus Cetuximab Versus Gemcitabine in Patients With Advanced Pancreatic Adenocarcinoma: Southwest Oncology Group–Directed Intergroup Trial S0205. J. Clin. Oncol. **28,** 3605–3610

(2010).

45. Goncalves, A. et al. BAYPAN study: a double-blind phase III randomized trial comparing gemcitabine plus sorafenib and gemcitabine plus placebo in patients with advanced pancreatic cancer. Ann. Oncol. **23,** 2799–2805 (2012).
46. Heinemann, V. et al. Gemcitabine plus erlotinib followed by capecitabine versus capecitabine plus erlotinib followed by gemcitabine in advanced pancreatic cancer: final results of a randomised phase 3 trial of the 'Arbeitsgemeinschaft Internistische Onkologie' (AIO-PK0104). Gut **62,** 751–759 (2013).
47. Rougier, P. et al. Randomised, placebo-controlled, double-blind, parallel-group phase III study evaluating aflibercept in patients receiving first-line treatment with gemcitabine for metastatic pancreatic cancer. Eur. J. Cancer **49,** 2633–2642 (2013).
48. Middleton, G. et al. Gemcitabine and capecitabine with or without telomerase peptide vaccine GV1001 in patients with locally advanced or metastatic pancreatic cancer (TeloVac): an open-label, randomised, phase 3 trial. Lancet Oncol. **15,** 829–840 (2014).
49. Fuchs, C. S. et al. A phase 3 randomized, double-blind, placebo-controlled trial of ganitumab or placebo in combination with gemcitabine as first-line therapy for metastatic adenocarcinoma of the pancreas: the GAMMA trial. Ann. Oncol. **26,** 921–927 (2015).
50. Deplanque, G. et al. A randomized, placebo-controlled phase III trial of masitinib plus gemcitabine in the treatment of advanced pancreatic cancer. Ann. Oncol. **26,** 1194–1200 (2015).
51. Yamaue, H. et al. Randomized phase II/III clinical trial of elpamotide for patients with advanced pancreatic cancer: PEGASUS-PC Study. Cancer Sci. **106,** 883–90 (2015).
52. O'Neil, B. H. et al. A phase II/III randomized study to compare the efficacy and safety of rigosertib plus gemcitabine versus gemcitabine alone in patients with previously untreated metastatic pancreatic cancer. Ann. Oncol. **26,** 1923–1929 (2015).
53. Wang-Gillam, A. et al. Nanoliposomal irinotecan with fluorouracil and folinic acid in metastatic pancreatic cancer after previous gemcitabine-based therapy

(NAPOLI-1): a global, randomised, open-label, phase 3 trial. Lancet **387,** 545–557 (2016).

54. Lee, H. S. et al. A randomized, multicenter, phase III study of gemcitabine combined with capecitabine versus gemcitabine alone as first-line chemotherapy for advanced pancreatic cancer in South Korea. Medicine (Baltimore). **96,** e5702 (2017).
55. Okusaka, T. et al. Updated results from GEST study: a randomized, three-arm phase III study for advanced pancreatic cancer. J. Cancer Res. Clin. Oncol. (2017). doi:10.1007/s00432-017-2349-y
56. Sahin, I. H., Iacobuzio-Donahue, C. A. & O'Reilly, E. M. Molecular signature of pancreatic adenocarcinoma: an insight from genotype to phenotype and challenges for targeted therapy. Expert Opin. Ther. Targets **20,** 341–359 (2016).
57. Ottaiano, A. et al. Gemcitabine mono-therapy versus gemcitabine plus targeted therapy in advanced pancreatic cancer: a meta-analysis of randomized phase III trials. Acta Oncol. (Madr). **56,** 377–383 (2017).
58. Tian, X., Chen, B. & Liu, X. Telomere and Telomerase as Targets for Cancer Therapy. Appl. Biochem. Biotechnol. **160,** 1460–1472 (2010).
59. Murakami, H. et al. Phase 1 study of ganitumab (AMG 479), a fully human monoclonal antibody against the insulin-like growth factor receptor type I (IGF1R), in Japanese patients with advanced solid tumors. Cancer Chemother. Pharmacol. **70,** 407–14 (2012).
60. Beltran, P. J. et al. AMG 479, a fully human anti-insulin-like growth factor receptor type I monoclonal antibody, inhibits the growth and survival of pancreatic carcinoma cells. Mol. Cancer Ther. **8,** 1095–1105 (2009).
61. Humbert, M. et al. Masitinib combined with standard gemcitabine chemotherapy: in vitro and in vivo studies in human pancreatic tumour cell lines and ectopic mouse model. PLoS One **5,** e9430 (2010).
62. Mitry, E. et al. Safety and activity of masitinib in combination with gemcitabine in patients with advanced pancreatic cancer. Cancer Chemother. Pharmacol. **66,** 395–403 (2010).
63. Korc, M. Pathways for aberrant angiogenesis in pancreatic cancer. Mol. Cancer **2,** 8 (2003).

64. Miyazawa, M. et al. Phase I clinical trial using peptide vaccine for human vascular endothelial growth factor receptor 2 in combination with gemcitabine for patients with advanced pancreatic cancer. Cancer Sci. **101,** 433–9 (2010).
65. Nuthalapati, S. et al. Preclinical Pharmacokinetic and Pharmacodynamic Evaluation of Novel Anticancer Agents, ON01910.Na (Rigosertib, Estybon^{TM}) and ON013105, for Brain Tumor Chemotherapy. Pharm. Res. **29,** 2499–2511 (2012).
66. Middleton, G. et al. Gemcitabine and capecitabine with or without telomerase peptide vaccine GV1001 in patients with locally advanced or metastatic pancreatic cancer (TeloVac): an open-label, randomised, phase 3 trial. Lancet Oncol. **15,** 829–840 (2014).
67. Yamaue, H. et al. Randomized phase II/III clinical trial of elpamotide for patients with advanced pancreatic cancer: PEGASUS-PC Study. Cancer Sci. **106,** 883–890 (2015).
68. Ciliberto, D. et al. Systematic review and meta-analysis on targeted therapy in advanced pancreatic cancer. Pancreatology **16,** 249–258 (2016).
69. Rahib, L., Fleshman, J. M., Matrisian, L. M. & Berlin, J. D. Evaluation of Pancreatic Cancer Clinical Trials and Benchmarks for Clinically Meaningful Future Trials. JAMA Oncol. **2,** 1209 (2016).
70. Matrisian, L. M. & Berlin, J. D. The Past, Present, and Future of Pancreatic Cancer Clinical Trials. Am. Soc. Clin. Oncol. Educ. B. **36,** e205–e215 (2016).
71. Thota, R., Maitra, A. & Berlin, J. D. Preclinical Rationale for the Phase III Trials in Metastatic Pancreatic Cancer. Pancreas **46,** 143–150 (2017).
72. Balkwill, F. & Mantovani, A. Inflammation and cancer: back to Virchow? Lancet **357,** 539–545 (2001).
73. Mohamed, A. et al. Pancreatic cancer in patients with chronic calcifying pancreatitis: Computed tomography findings – a retrospective analysis of 48 patients. Eur. J. Radiol. **86,** 206–212 (2017).
74. Sarles, H. et al. Chronic calcifying pancreatitis (CCP). Mechanism of formation of the lesions. New data and critical study. Monogr. Pathol. **21,** 48–66 (1980).
75. Farrow, B. et al. Inflammatory mechanisms contributing to pancreatic cancer development. Ann. Surg. **239,** 763-9-71 (2004).
76. Ino, Y. et al. Immune cell infiltration as an indicator of the immune

microenvironment of pancreatic cancer . Br. J. Cancer **108,** 914–923 (2013).

77. Chen, M.-L. et al. Regulatory T cells suppress tumor-specific CD8 T cell cytotoxicity through TGF- signals in vivo. Proc. Natl. Acad. Sci. **102,** 419–424 (2005).
78. Chang, J. H., Jiang, Y. & Pillarisetty, V. G. Role of immune cells in pancreatic cancer from bench to clinical application. Medicine (Baltimore). **95,** e5541 (2016).
79. Ene-Obong, A. et al. Activated pancreatic stellate cells sequester CD8+ T cells to reduce their infiltration of the juxtatumoral compartment of pancreatic ductal adenocarcinoma. Gastroenterology **145,** 1121–32 (2013).
80. BURNET, M. Cancer: a biological approach. III. Viruses associated with neoplastic conditions. IV. Practical applications. Br. Med. J. **1,** 841–7 (1957).
81. Dunn, G. P., Bruce, A. T., Ikeda, H., Old, L. J. & Schreiber, R. D. Cancer immunoediting: from immunosurveillance to tumor escape. Nat. Immunol. **3,** 991–998 (2002).
82. Gabitass, R. F. et al. Elevated myeloid-derived suppressor cells in pancreatic, esophageal and gastric cancer are an independent prognostic factor and are associated with significant elevation of the Th2 cytokine interleukin-13 . Cancer Immunol. Immunother. **60,** 1419–1430 (2011).
83. Clark, C. E., Beatty, G. L. & Vonderheide, R. H. Immunosurveillance of pancreatic adenocarcinoma : Insights from genetically engineered mouse models of cancer. Cancer Lett. **279,** 1–7 (2009).
84. Smyth, M. J. et al. Perforin-mediated cytotoxicity is critical for surveillance of spontaneous lymphoma. J. Exp. Med. **192,** 755–60 (2000).
85. Dighe, A. S., Richards, E., Old, L. J. & Schreiber, R. D. Enhanced in vivo growth and resistance to rejection of tumor cells expressing dominant negative IFN gamma receptors. Immunity **1,** 447–56 (1994).
86. Baumgart, S., Ellenrieder, V. & Fernandez-Zapico, M. E. Oncogenic transcription factors: cornerstones of inflammation-linked pancreatic carcinogenesis. Gut **62,** 310–316 (2013).
87. Sideras, K. et al. Role of the immune system in pancreatic cancer progression and immune modulating treatment strategies. Cancer Treat. Rev. **40,** 513–22

(2014).

88. Wörmann, S. M., Diakopoulos, K. N., Lesina, M. & Algül, H. The immune network in pancreatic cancer development and progression. Oncogene **33,** 2956–67 (2014).

89. Borish, L. C. & Steinke, J. W. 2. Cytokines and chemokines. J. Allergy Clin. Immunol. **111,** S460-75 (2003).

90. Okada, S. et al. Elevated serum interleukin-6 levels in patients with pancreatic cancer. Jpn. J. Clin. Oncol. **28,** 12–5 (1998).

91. Tjomsland, V. et al. Interleukin 1α sustains the expression of inflammatory factors in human pancreatic cancer microenvironment by targeting cancer-associated fibroblasts. Neoplasia **13,** 664–75 (2011).

92. Smirne, C., Camandona, M., Alabiso, O., Bellone, G. & Emanuelli, G. [High serum levels of Transforming Growth Factor-beta1, Interleukin-10 and Vascular Endothelial Growth Factor in pancreatic adenocarcinoma patients]. Minerva Gastroenterol. Dietol. **45,** 21–7 (1999).

93. Bellone, G. et al. Tumor-associated transforming growth factor-beta and interleukin-10 contribute to a systemic Th2 immune phenotype in pancreatic carcinoma patients. Am. J. Pathol. **155,** 537–47 (1999).

94. Chen, Y. et al. Interleukin-8, a promising predictor for prognosis of pancreatic cancer. World J. Gastroenterol. **18,** 1123–9 (2012).

95. Monti, P. et al. The CC chemokine MCP-1/CCL2 in pancreatic cancer progression: regulation of expression and potential mechanisms of antimalignant activity. Cancer Res. **63,** 7451–61 (2003).

96. Li, A. et al. Overexpression of CXCL5 is associated with poor survival in patients with pancreatic cancer. Am. J. Pathol. **178,** 1340–9 (2011).

97. Hiraoka, N. et al. CXCL17 and ICAM2 are associated with a potential anti-tumor immune response in early intraepithelial stages of human pancreatic carcinogenesis. Gastroenterology **140,** 310–21 (2011).

98. Feig, C. et al. Targeting CXCL12 from FAP-expressing carcinoma-associated fibroblasts synergizes with anti-PD-L1 immunotherapy in pancreatic cancer. Proc. Natl. Acad. Sci. U. S. A. **110,** 20212–7 (2013).

99. Rozenblum, E. et al. Tumor-suppressive pathways in pancreatic carcinoma.

Cancer Res. **57,** 1731–4 (1997).

100. McGrath, J. P. et al. Structure and organization of the human Ki-ras proto-oncogene and a related processed pseudogene. Nature **304,** 501–6
101. Ijichi, H. et al. Inhibiting Cxcr2 disrupts tumor-stromal interactions and improves survival in a mouse model of pancreatic ductal adenocarcinoma. J. Clin. Invest. **121,** 4106–4117 (2011).
102. Goggins, M., Kern, S. E., Offerhaus, J. A. & Hruban, R. H. Progress in cancer genetics: lessons from pancreatic cancer. Ann. Oncol. Off. J. Eur. Soc. Med. Oncol. **10 Suppl 4,** 4–8 (1999).
103. Disis, M. L. Immune regulation of cancer. J. Clin. Oncol. **28,** 4531–4538 (2010).
104. Ryschich, E. et al. Control of T-cell-mediated immune response by HLA class I in human pancreatic carcinoma. Clin. Cancer Res. **11,** 498–504 (2005).
105. von Bernstorff, W. et al. Pancreatic cancer cells can evade immune surveillance via nonfunctional Fas (APO-1/CD95) receptors and aberrant expression of functional Fas ligand. Surgery **125,** 73–84 (1999).
106. Uyttenhove, C. et al. Evidence for a tumoral immune resistance mechanism based on tryptophan degradation by indoleamine 2,3-dioxygenase. Nat. Med. **9,** 1269–74 (2003).
107. Basso, D. et al. Pancreatic Tumors and Immature Immunosuppressive Myeloid Cells in Blood and Spleen: Role of Inhibitory Co-Stimulatory Molecules PDL1 and CTLA4. An In Vivo and In Vitro Study. PLoS One **8,** e54824 (2013).
108. Moo-Young, T. A. et al. Tumor-derived TGF-beta mediates conversion of CD4+Foxp3+ regulatory T cells in a murine model of pancreas cancer . J. Immunother. (Hagerstown, Md. 1997) **32,** 12–21 (2009).
109. Ochi, A. et al. Toll-like receptor 7 regulates pancreatic carcinogenesis in mice and humans. J. Clin. Invest. **122,** 4118–29 (2012).
110. Tang, D. et al. High expression of Galectin-1 in pancreatic stellate cells plays a role in the development and maintenance of an immunosuppressive microenvironment in pancreatic cancer. Int. J. cancer **130,** 2337–48 (2012).
111. Gabrilovich, D. I. et al. The Terminology Issue for Myeloid-Derived Suppressor Cells. Cancer Res. **67,** 425–425 (2007).
112. Strober, S. Natural Suppressor (NS) Cells, Neonatal Tolerance, and Total

Lymphoid Irradiation: Exploring Obscure Relationships. Annu. Rev. Immunol. **2,** 219–237 (1984).

113. Pan, W. et al. Highlights on mechanisms of drugs targeting MDSCs: providing a novel perspective on cancer treatment. Tumor Biol. **36,** 3159–3169 (2015).
114. Youn, J., Nagaraj, S., Collazo, M. & Gabrilovich, D. I. Subsets of Myeloid-Derived Suppressor Cells in Tumor-Bearing Mice. (2012).
115. Bronte, V. Myeloid-derived suppressor cells in inflammation: Uncovering cell subsets with enhanced immunosuppressive functions. Eur. J. Immunol. **39,** 2670–2672 (2009).
116. Ochando, J. C. & Hsia, S. Myeloid-derived suppressor cells in transplantation and cancer. 275–285 (2012). doi:10.1007/s12026-012-8335-1
117. Ardi, V. C., Kupriyanova, T. A., Deryugina, E. I. & Quigley, J. P. Human neutrophils uniquely release TIMP-free MMP-9 to provide a potent catalytic stimulator of angiogenesis. Proc. Natl. Acad. Sci. **104,** 20262–20267 (2007).
118. Brandau, S., Moses, K. & Lang, S. The kinship of neutrophils and granulocytic myeloid-derived suppressor cells in cancer: Cousins, siblings or twins? Semin. Cancer Biol. **23,** 171–182 (2013).
119. Mucha, J., Majchrzak, K., Taciak, B., Hellmén, E. & Król, M. MDSCs Mediate Angiogenesis and Predispose Canine Mammary Tumor Cells for Metastasis via IL-28/IL-28RA (IFN-λ) Signaling. PLoS One **9,** e103249 (2014).
120. Gabrilovich, D. I. & Nagaraj, S. Myeloid-derived suppressor cells as regulators of the immune system. Nat. Rev. **9,** 162–174 (2009).
121. Ostrand-rosenberg, S., Sinha, P. & Alerts, E. Myeloid-derived suppressor cells: linking inflammation and cancer. J. Immunol. **182,** 4499–4506 (2009).
122. Goedegebuure, P. et al. Myeloid-derived suppressor cells: general characteristics and relevance to clinical management of pancreatic cancer. Curr. Cancer Drug Targets **11,** 734–751 (2011).
123. Ochoa, A. C., Zea, A. H., Hernandez, C. & Rodriguez, P. C. Arginase, prostaglandins, and myeloid-derived suppressor cells in renal cell carcinoma. Clin. Cancer Res. **13,** 721s–726s (2007).
124. Almand, B. et al. Increased Production of Immature Myeloid Cells in Cancer Patients: A Mechanism of Immunosuppression in Cancer. (2012).

125. Kusmartsev, S., Nefedova, Y., Yoder, D. & Gabrilovich, D. I. Antigen-specific inhibition of CD8+ T cell response by immature myeloid cells in cancer is mediated by reactive oxygen species. J. Immunol. **172,** 989–99 (2004).
126. Schmielau, J. & Finn, O. J. Activated granulocytes and granulocyte-derived hydrogen peroxide are the underlying mechanism of suppression of t-cell function in advanced cancer patients. Cancer Res. **61,** 4756–60 (2001).
127. Khaled, Y. S., Ammori, B. J. & Elkord, E. Increased levels of granulocytic myeloid-derived suppressor cells in peripheral blood and tumour tissue of pancreatic cancer patients. J. Immunol. Res. **2014,** 879897 (2014).
128. Annels, N. E. et al. The effects of gemcitabine and capecitabine combination chemotherapy and of low-dose adjuvant GM-CSF on the levels of myeloid-derived suppressor cells in patients with advanced pancreatic cancer. Cancer Immunol. Immunother. **63,** 175–83 (2014).
129. Clark, C. E. et al. Dynamics of the immune reaction to pancreatic cancer from inception to invasion. Cancer Res. **67,** 9518–9527 (2007).
130. Diaz-Montero, C. M. et al. Increased circulating myeloid-derived suppressor cells correlate with clinical cancer stage, metastatic tumor burden, and doxorubicin-cyclophosphamide chemotherapy. Cancer Immunol. Immunother. **58,** 49–59 (2009).
131. Markowitz, J. et al. Patients with pancreatic adenocarcinoma exhibit elevated levels of myeloid-derived suppressor cells upon progression of disease. Cancer Immunol. Immunother. (2014). doi:10.1007/s00262-014-1618-8
132. Bronte, V. et al. Recommendations for myeloid-derived suppressor cell nomenclature and characterization standards. Nat. Commun. **7,** 12150 (2016).
133. Coussens, L. M. & Werb, Z. Inflammation and cancer. Nature **420,** 860–867 (2002).
134. Nagaraj, S., Schrum, A. G., Cho, H. & Gabrilovich, D. I. Mechanism of T Cell Tolerance Induced by Myeloid-Derived Suppressor Cells. (2012). doi:10.4049/jimmunol.0902661
135. Nagaraj, S. et al. Altered recognition of antigen is a mechanism of CD8+ T cell tolerance in cancer. Nat. Med. **13,** 828–35 (2007).
136. Molon, B. et al. Chemokine nitration prevents intratumoral infiltration of

antigen-specific T cells. J. Exp. Med. **208,** 1949–62 (2011).

137. Gabrilovich, D. I., Ostrand-rosenberg, S. & Bronte, V. Coordinated regulation of myeloid cells by tumours. Nat. Publ. Gr. **12,** 253–268 (2012).
138. Rodriguez, P. C. et al. Arginase I Production in the Tumor Microenvironment by Mature Myeloid Cells Inhibits T-Cell Receptor Expression and Antigen-Specific T-Cell Responses. Cancer Res. **64,** 5839–5849 (2004).
139. Rodríguez, P. C. & Ochoa, A. C. Arginine regulation by myeloid derived suppressor cells and tolerance in cancer: mechanisms and therapeutic perspectives. Immunol. Rev. **222,** 180–191 (2008).
140. Liu, C.-Y. et al. Population alterations of L-arginase- and inducible nitric oxide synthase-expressed CD11b+/CD14$^-$/CD15+/CD33+ myeloid-derived suppressor cells and CD8+ T lymphocytes in patients with advanced-stage non-small cell lung cancer. J. Cancer Res. Clin. Oncol. **136,** 35–45 (2010).
141. Rodriguez, P. C. et al. Regulation of T cell receptor CD3zeta chain expression by L-arginine. J. Biol. Chem. **277,** 21123–9 (2002).
142. Zea, A. H. et al. Arginase-producing myeloid suppressor cells in renal cell carcinoma patients: a mechanism of tumor evasion. Cancer Res. **65,** 3044–8 (2005).
143. Sinha, P., Clements, V. K., Bunt, S. K., Albelda, S. M. & Ostrand-Rosenberg, S. Cross-talk between myeloid-derived suppressor cells and macrophages subverts tumor immunity toward a type 2 response. J. Immunol. **179,** 977–83 (2007).
144. Yang, L. et al. Abrogation of TGF beta signaling in mammary carcinomas recruits Gr-1+CD11b+ myeloid cells that promote metastasis. Cancer Cell **13,** 23–35 (2008).
145. Movahedi, K. et al. Identification of discrete tumor-induced myeloid-derived suppressor cell subpopulations with distinct T cell-suppressive activity. Blood **111,** 4233–4244 (2008).
146. Murdoch, C., Muthana, M., Coffelt, S. B. & Lewis, C. E. The role of myeloid cells in the promotion of tumour angiogenesis. Nat. Rev. **8,** 618–631 (2008).
147. Connolly, M. K. et al. Distinct populations of metastases-enabling myeloid cells expand in the liver of mice harboring invasive and preinvasive intra-abdominal tumor. **87,** (2010).

148. Melani, C., Chiodoni, C., Forni, G. & Colombo, M. P. Myeloid cell expansion elicited by the progression of spontaneous mammary carcinomas in c-erbB-2 transgenic BALB/c mice suppresses immune reactivity. Blood **102,** 2138–45 (2003).
149. Yang, L. et al. Expansion of myeloid immune suppressor Gr+CD11b+ cells in tumor-bearing host directly promotes tumor angiogenesis. Cancer Cell **6,** 409–21 (2004).
150. Kaplan, R. N. et al. VEGFR1-positive haematopoietic bone marrow progenitors initiate the pre-metastatic niche. Nature **438,** 820–827 (2005).
151. Ellis, L. M. & Hicklin, D. J. VEGF-targeted therapy: mechanisms of anti-tumour activity. Nat. Rev. Cancer **8,** 579–591 (2008).
152. Psaila, B. & Lyden, D. The metastatic niche: adapting the foreign soil. Nat. Rev. Cancer **9,** 285–293 (2009).
153. Peinado, H. et al. Pre-metastatic niches: organ-specific homes for metastases. Nat. Rev. Cancer **17,** 302–317 (2017).
154. Mantovani, A., Allavena, P., Sica, A. & Balkwill, F. Cancer-related inflammation. Nature **454,** 436–444 (2008).
155. Young, M. R. & Wright, M. A. Myelopoiesis-associated immune suppressor cells in mice bearing metastatic Lewis lung carcinoma tumors: gamma interferon plus tumor necrosis factor alpha synergistically reduces immune suppressor and tumor growth-promoting activities of bone marrow cells and diminishes tumor recurrence and metastasis. Cancer Res. **52,** 6335–40 (1992).
156. Baniyash, M. TCR zeta-chain downregulation: curtailing an excessive inflammatory immune response. Nat. Rev. Immunol. **4,** 675–87 (2004).
157. Sinha, P., Clements, V. K., Fulton, A. M. & Ostrand-Rosenberg, S. Prostaglandin E2 Promotes Tumor Progression by Inducing Myeloid-Derived Suppressor Cells. Cancer Res. **67,** 4507–4513 (2007).
158. Song, X. et al. CD11b+/Gr-1+ immature myeloid cells mediate suppression of T cells in mice bearing tumors of IL-1beta-secreting cells. J. Immunol. **175,** 8200–8 (2005).
159. Bunt, S. K. et al. Reduced Inflammation in the Tumor Microenvironment Delays the Accumulation of Myeloid-Derived Suppressor Cells and Limits Tumor

Progression Accumulation of Myeloid-Derived Suppressor Cells and Limits Tumor Progression. (2007). doi:10.1158/0008-5472.CAN-07-2354

160. Alleva, D. G., Burger, C. J. & Elgert, K. D. Tumor growth increases Ia- macrophage synthesis of tumor necrosis factor-alpha and prostaglandin E2: changes in macrophage suppressor activity. J. Leukoc. Biol. **53,** 550–8 (1993).
161. Taketo, M. M. Cyclooxygenase-2 inhibitors in tumorigenesis (Part II). J. Natl. Cancer Inst. **90,** 1609–20 (1998).
162. Wang, D. & DuBois, R. N. Pro-inflammatory prostaglandins and progression of colorectal cancer. Cancer Lett. **267,** 197–203 (2008).
163. Foell, D., Wittkowski, H., Vogl, T. & Roth, J. S100 proteins expressed in phagocytes: a novel group of damage-associated molecular pattern molecules. J. Leukoc. Biol. **81,** 28–37 (2006).
164. Hiratsuka, S., Watanabe, A., Aburatani, H. & Maru, Y. Tumour-mediated upregulation of chemoattractants and recruitment of myeloid cells predetermines lung metastasis. Nat. Cell Biol. **8,** 1369–1375 (2006).
165. Turovskaya, O. et al. RAGE, carboxylated glycans and S100A8/A9 play essential roles in colitis-associated carcinogenesis. Carcinogenesis **29,** 2035–43 (2008).
166. Cheng, P. et al. Inhibition of dendritic cell differentiation and accumulation of myeloid-derived suppressor cells in cancer is regulated by S100A9 protein. J. Exp. Med. **205,** 2235–49 (2008).
167. Sinha, P. et al. Proinflammatory S100 proteins regulate the accumulation of myeloid-derived suppressor cells. J. Immunol. **181,** 4666–75 (2008).
168. Markiewski, M. M. & Lambris, J. D. The Role of Complement in Inflammatory Diseases From Behind the Scenes into the Spotlight. Am. J. Pathol. **171,** 715–727 (2007).
169. Guo, R.-F. & Ward, P. A. ROLE OF C5A IN INFLAMMATORY RESPONSES. Annu. Rev. Immunol. **23,** 821–852 (2005).
170. Markiewski, M. M. et al. Modulation of the antitumor immune response by complement. Nat. Immunol. **9,** 1225–1235 (2008).
171. Parker, K. H., Beury, D. W. & Ostrand-Rosenberg, S. Myeloid-Derived Suppressor Cells: Critical Cells Driving Immune Suppression in the Tumor Microenvironment. Adv. Cancer Res. **128,** 95–139 (2015).

172. Parker, K. H. et al. HMGB1 enhances immune suppression by facilitating the differentiation and suppressive activity of myeloid-derived suppressor cells. Cancer Res. **74,** 5723–33 (2014).
173. Voronov, E. et al. IL-1 is required for tumor invasiveness and angiogenesis. Proc. Natl. Acad. Sci. U. S. A. **100,** 2645–50 (2003).
174. Bunt, S. K., Sinha, P., Clements, V. K., Leips, J. & Ostrand-Rosenberg, S. Inflammation induces myeloid-derived suppressor cells that facilitate tumor progression. J. Immunol. **176,** 284–90 (2006).
175. Bunt, S. K., Clements, V. K., Hanson, E. M., Sinha, P. & Ostrand-Rosenberg, S. Inflammation enhances myeloid-derived suppressor cell cross-talk by signaling through Toll-like receptor 4. J. Leukoc. Biol. **85,** 996–1004 (2009).
176. Johnston, F. M. et al. Circulating Mesothelin Protein and Cellular Antimesothelin Immunity in Patients with Pancreatic Cancer. Clin. Cancer Res. **15,** 6511–6518 (2009).
177. Kubuschok, B. et al. Naturally Occurring T-Cell Response against Mutated p21 Ras Oncoprotein in Pancreatic Cancer. Clin. Cancer Res. **12,** 1365–1372 (2006).
178. Yanagimoto, H. et al. Immunological evaluation of personalized peptide vaccination with gemcitabine for pancreatic cancer. Cancer Sci. **98,** 605–611 (2007).
179. Swann, J. B. & Smyth, M. J. Immune surveillance of tumors. J. Clin. Invest. **117,** 1137–1146 (2007).
180. Dunn, G. P., Koebel, C. M. & Schreiber, R. D. Interferons, immunity and cancer immunoediting. Nat. Rev. Immunol. **6,** 836–848 (2006).
181. Emmrich, J. et al. Immunohistochemical characterization of the pancreatic cellular infiltrate in normal pancreas, chronic pancreatitis and pancreatic carcinoma. Digestion **59,** 192–8 (1998).
182. Ademmer, K. et al. Effector T lymphocyte subsets in human pancreatic cancer: detection of CD8+CD18+ cells and CD8+CD103+ cells by multi-epitope imaging. Clin. Exp. Immunol. **112,** 21–6 (1998).
183. Fukunaga, A. et al. CD8+ tumor-infiltrating lymphocytes together with CD4+ tumor-infiltrating lymphocytes and dendritic cells improve the prognosis of patients with pancreatic adenocarcinoma. Pancreas **28,** e26-31 (2004).

184. Kim, J. S. et al. Inhibition of human pancreatic tumor growth by cytokine-induced killer cells in nude mouse xenograft model. Immune Netw. **12,** 247–52 (2012).
185. Ashida, A. et al. Expression profiling of esophageal squamous cell carcinoma patients treated with definitive chemoradiotherapy: clinical implications. Int. J. Oncol. **28,** 1345–52 (2006).
186. Pagès, F. et al. In situ cytotoxic and memory T cells predict outcome in patients with early-stage colorectal cancer. J. Clin. Oncol. **27,** 5944–51 (2009).
187. Galon, J. et al. Type, Density, and Location of Immune Cells Within Human Colorectal Tumors Predict Clinical Outcome. Science (80-.). **313,** 1960–1964 (2006).
188. Kawai, O. et al. Predominant infiltration of macrophages and CD8(+) T Cells in cancer nests is a significant predictor of survival in stage IV nonsmall cell lung cancer. Cancer **113,** 1387–95 (2008).
189. Nakano, O. et al. Proliferative activity of intratumoral CD8(+) T-lymphocytes as a prognostic factor in human renal cell carcinoma: clinicopathologic demonstration of antitumor immunity. Cancer Res. **61,** 5132–6 (2001).
190. Xu, Y.-F. et al. Abnormal distribution of peripheral lymphocyte subsets induced by PDAC modulates overall survival. Pancreatology **14,** 295–301 (2014).
191. Bellone, G. et al. Impact of surgery and chemotherapy on cellular immunity in pancreatic carcinoma patients in view of an integration of standard cancer treatment with immunotherapy. Int. J. Oncol. **34,** 1701–15 (2009).
192. Pignatelli, M. et al. Loss of membranous E-cadherin expression in pancreatic cancer: correlation with lymph node metastasis, high grade, and advanced stage. J. Pathol. **174,** 243–8 (1994).
193. Friess, H. et al. Enhanced expression of transforming growth factor beta isoforms in pancreatic cancer correlates with decreased survival. Gastroenterology **105,** 1846–56 (1993).
194. Shunrong Ji, X. Y. et al. CD8+ T Cells Are Compromised In Human Pancreatic Cancer. Transl. Med. **2,** (2012).
195. Dong, H. et al. Tumor-associated B7-H1 promotes T-cell apoptosis: a potential mechanism of immune evasion. Nat. Med. **8,** 793–800 (2002).

196. Fogar, P. et al. Pancreatic cancer alters human CD4+ T lymphocyte function: a piece in the immune evasion puzzle. Pancreas **40,** 1131–7 (2011).
197. Suzuki, D., Furukawa, K., Kimura, F. & Shimizu, H. Effects of perioperative immunonutrition on cell-mediated immunity , T helper type 1 (Th1)/ Th2 differentiation , and Th17 response after pancreaticoduodenectomy. Surgery **148,** 573–581
198. Fridman, W. H., Pagès, F., Sautès-Fridman, C. & Galon, J. The immune contexture in human tumours: impact on clinical outcome. Nat. Rev. Cancer **12,** 298–306 (2012).
199. De Monte, L. et al. Intratumor T helper type 2 cell infiltrate correlates with cancer-associated fibroblast thymic stromal lymphopoietin production and reduced survival in pancreatic cancer. J. Exp. Med. **208,** 469–78 (2011).
200. Tassi, E. et al. Carcinoembryonic antigen-specific but not antiviral CD4+ T cell immunity is impaired in pancreatic carcinoma patients. J. Immunol. **181,** 6595–603 (2008).
201. Sakaguchi, S., Sakaguchi, N., Asano, M., Itoh, M. & Toda, M. Immunologic self-tolerance maintained by activated T cells expressing IL-2 receptor alpha-chains (CD25). Breakdown of a single mechanism of self-tolerance causes various autoimmune diseases. J. Immunol. **155,** 1151–64 (1995).
202. Curotto de Lafaille, M. A. & Lafaille, J. J. Natural and Adaptive Foxp3+ Regulatory T Cells: More of the Same or a Division of Labor? Immunity **30,** 626–635 (2009).
203. Hori, S., Nomura, T. & Sakaguchi, S. Control of regulatory T cell development by the transcription factor Foxp3. Science **299,** 1057–1061 (2003).
204. Fontenot, J. D., Gavin, M. A. & Rudensky, A. Y. Foxp3 programs the development and function of CD4+CD25+ regulatory T cells. Nat. Immunol. **4,** 330–336 (2003).
205. Huang, B. et al. Gr-1+CD115+ immature myeloid suppressor cells mediate the development of tumor-induced T regulatory cells and T-cell anergy in tumor-bearing host. Cancer Res. **66,** 1123–1131 (2006).
206. Hiraoka, N., Onozato, K. & Kosuge, T. Prevalence of FOXP3 + Regulatory T Cells Increases During the Progression of Pancreatic Ductal Adenocarcinoma and Its Premalignant Lesions Prevalence of FOXP3 + Regulatory T Cells Increases During and Its Premalignant Lesions. (2006). doi:10.1158/1078-0432.CCR-06-0369

207. Chen, W. et al. Conversion of peripheral CD4+CD25- naive T cells to CD4+CD25+ regulatory T cells by TGF-beta induction of transcription factor Foxp3. J. Exp. Med. **198,** 1875–86 (2003).

208. Ghiringhelli, F. et al. Tumor cells convert immature myeloid dendritic cells into TGF-β–secreting cells inducing CD4 $^{+}$ CD25 $^{+}$ regulatory T cell proliferation. J. Exp. Med. **202,** 919–929 (2005).

209. Brunkow, M. E. et al. Disruption of a new forkhead/winged-helix protein, scurfin, results inthe fatal lymphoproliferative disorder of the scurfy mouse. Nat. Genet. **27,** 68–73 (2001).

210. Gavin, M. A. et al. Single-cell analysis of normal and FOXP3-mutant human T cells: FOXP3 expression without regulatory T cell development. Proc. Natl. Acad. Sci. U. S. A. **103,** 6659–64 (2006).

211. Bennett, C. L. et al. The immune dysregulation, polyendocrinopathy, enteropathy, X-linked syndrome (IPEX) is caused by mutations of FOXP3. Nat. Genet. **27,** 20–1 (2001).

212. Liyanage, U. K. et al. Prevalence of Regulatory T Cells Is Increased in Peripheral Blood and Tumor Microenvironment of Patients with Pancreas or Breast Adenocarcinoma 1. (2002).

213. Sasada, T., Kimura, M., Yoshida, Y., Kanai, M. & Takabayashi, A. CD4+CD25+ regulatory T cells in patients with gastrointestinal malignancies. Cancer **98,** 1089–1099 (2003).

214. Ormandy, L. A. et al. Increased populations of regulatory T cells in peripheral blood of patients with hepatocellular carcinoma. Cancer Res. **65,** 2457–64 (2005).

215. Liotta, F. et al. Frequency of regulatory T cells in peripheral blood and in tumour-infiltrating lymphocytes correlates with poor prognosis in renal cell carcinoma. BJU.Int. **107,** 1500–1506 (2011).

216. Ikemoto, T. et al. Clinical roles of increased populations of Foxp3+CD4+ T cells in peripheral blood from advanced pancreatic cancer patients. Pancreas **33,** 386–90 (2006).

217. Yamamoto, T. et al. Circulating CD4+CD25+ regulatory T cells in patients with pancreatic cancer . Pancreas **41,** 409–415 (2012).

218. Homma, Y. et al. Changes in the immune cell population and cell proliferation in peripheral blood after gemcitabine-based chemotherapy for pancreatic cancer. Clin. Transl. Oncol. **16,** 330–335 (2014).
219. Cretney, E., Kallies, A. & Nutt, S. L. Differentiation and function of Foxp3 + effector regulatory T cells. Trends Immunol. **4,** 1–7 (2012).
220. Sojka, D. K., Huang, Y.-H. & Fowell, D. J. Mechanisms of regulatory T-cell suppression - a diverse arsenal for a moving target. Immunology **124,** 13–22 (2008).
221. Azuma, T., Takahashi, T., Kunisato, A., Kitamura, T. & Hirai, H. Human CD4+ CD25+ regulatory T cells suppress NKT cell functions. Cancer Res. **63,** 4516–20 (2003).
222. Ghiringhelli, F. et al. CD4 $^{+}$ CD25 $^{+}$ regulatory T cells inhibit natural killer cell functions in a transforming growth factor–β–dependent manner. J. Exp. Med. **202,** 1075–1085 (2005).
223. Orentas, R. J., Kohler, M. E. & Johnson, B. D. Suppression of anti-cancer immunity by regulatory T cells : Back to the future. **16,** 137–149 (2006).
224. Thornton, A. M. & Shevach, E. M. CD4+CD25+ immunoregulatory T cells suppress polyclonal T cell activation in vitro by inhibiting interleukin 2 production. J. Exp. Med. **188,** 287–96 (1998).
225. Antony, P. A. & Restifo, N. P. CD4+CD25+ T regulatory cells, immunotherapy of cancer, and interleukin-2. J. Immunother. **28,** 120–8
226. Tan, W. et al. Tumour-infiltrating regulatory T cells stimulate mammary cancer metastasis through RANKL-RANK signalling. Nature **470,** 548–53 (2011).
227. Amedei, A. et al. Ex vivo analysis of pancreatic cancer-infiltrating T lymphocytes reveals that ENO-specific Tregs accumulate in tumor tissue and inhibit Th1/Th17 effector cell functions. Cancer Immunol. Immunother. **62,** 1249–1260 (2013).
228. Yu, P. et al. Intratumor depletion of CD4 $^{+}$ cells unmasks tumor immunogenicity leading to the rejection of late-stage tumors. J. Exp. Med. **201,** 779–791 (2005).
229. Trzonkowski, P., Szmit, E., Myśliwska, J., Dobyszuk, A. & Myśliwski, A. CD4+CD25+ T regulatory cells inhibit cytotoxic activity of T CD8+ and NK lymphocytes in the direct cell-to-cell interaction. Clin. Immunol. **112,** 258–67 (2004).

230. Tan, M. C. B. et al. Disruption of CCR5-dependent homing of regulatory T cells inhibits tumor growth in a murine model of pancreatic cancer. J. Immunol. **182,** 1746–55 (2009).
231. Liyanage, U. K. et al. Increased prevalence of regulatory T cells (Treg) is induced by pancreas adenocarcinoma . J. Immunother. (Hagerstown, Md. 1997) **29,** 416–424 (2006).
232. Nummer, D. et al. Role of tumor endothelium in CD4+ CD25+ regulatory T cell infiltration of human pancreatic carcinoma . J. Natl. Cancer Inst. **99,** 1188–1199 (2007).
233. Viehl, C. T. et al. Depletion of CD4+CD25+ Regulatory T Cells Promotes a Tumor-Specific Immune Response in Pancreas Cancer–Bearing Mice. Ann. Surg. Oncol. **13,** 1252–1258 (2006).
234. Aida, K. et al. Suppression of Tregs by anti-glucocorticoid induced TNF receptor antibody enhances the antitumor immunity of interferon-α gene therapy for pancreatic cancer. Cancer Sci. **105,** 159–167 (2014).
235. Royal, R. E. et al. Phase 2 trial of single agent Ipilimumab (anti-CTLA-4) for locally advanced or metastatic pancreatic adenocarcinoma. J. Immunother. **33,** 828–33 (2010).
236. Brahmer, J. R. et al. Phase I Study of Single-Agent Anti–Programmed Death-1 (MDX-1106) in Refractory Solid Tumors: Safety, Clinical Activity, Pharmacodynamics, and Immunologic Correlates. J. Clin. Oncol. **28,** 3167–3175 (2010).
237. Game, D. S., Hernandez-Fuentes, M. P. & Lechler, R. I. Everolimus and basiliximab permit suppression by human CD4+CD25+ cells in vitro. Am. J. Transplant **5,** 454–64 (2005).
238. Baan, C. C. et al. Differential effect of calcineurin inhibitors, anti-CD25 antibodies and rapamycin on the induction of FOXP3 in human T cells. Transplantation **80,** 110–7 (2005).
239. Beyer, M. et al. Reduced frequencies and suppressive function of CD4+CD25hi regulatory T cells in patients with chronic lymphocytic leukemia after therapy with fludarabine. Blood **106,** 2018–25 (2005).
240. Ghiringhelli, F. et al. CD4+CD25+ regulatory T cells suppress tumor immunity but

are sensitive to cyclophosphamide which allows immunotherapy of established tumors to be curative. Eur. J. Immunol. **34,** 336–44 (2004).

241. Marigo, I., Dolcetti, L., Serafini, P., Zanovello, P. & Bronte, V. Tumor-induced tolerance and immune suppression by myeloid derived suppressor cells. Immunol. Rev. **222,** 162–179 (2008).
242. Rodriguez, P. C., Quiceno, D. G. & Ochoa, A. C. L-arginine availability regulates T-lymphocyte cell-cycle progression. Blood **109,** 1568–73 (2007).
243. Lu, T. et al. Tumor-infiltrating myeloid cells induce tumor cell resistance to cytotoxic T cells in mice. J. Clin. Invest. **121,** 4015–29 (2011).
244. Hanson, E. M., Clements, V. K., Sinha, P., Ilkovitch, D. & Ostrand-Rosenberg, S. Myeloid-Derived Suppressor Cells Down-Regulate L-Selectin Expression on CD4+ and CD8+ T Cells. J. Immunol. **183,** 937–944 (2009).
245. Srivastava, M. K., Sinha, P. & Clements, V. K. Myeloid-Derived Suppressor Cells Inhibit T-Cell Activation by Depleting Cystine and Cysteine Myeloid-Derived Suppressor Cells Inhibit T-Cell Activation. 68–77 (2010). doi:10.1158/0008-5472.CAN-09-2587
246. Lu, T. et al. Tumor-infiltrating myeloid cells induce tumor cell resistance to cytotoxic T cells in mice. J. Clin. Invest. **121,** 4015–29 (2011).
247. Gabrilovich, D. I., Velders, M. P., Sotomayor, E. M. & Kast, W. M. Mechanism of immune dysfunction in cancer mediated by immature Gr-1+ myeloid cells. J. Immunol. **166,** 5398–406 (2001).
248. Otsuji, M., Kimura, Y., Aoe, T., Okamoto, Y. & Saito, T. Oxidative stress by tumor-derived macrophages suppresses the expression of CD3 zeta chain of T-cell receptor complex and antigen-specific T-cell responses. Proc. Natl. Acad. Sci. U. S. A. **93,** 13119–24 (1996).
249. Serafini, P., Mgebroff, S., Noonan, K. & Borrello, I. Myeloid-derived suppressor cells promote cross-tolerance in B-cell lymphoma by expanding regulatory T cells. Cancer Res. **68,** 5439–5449 (2008).
250. Lindau, D. et al. The immunosuppressive tumour network: Myeloid-derived suppressor cells, regulatory T cells and natural killer T cells. Immunology **138,** 105–115 (2013).
251. Yang, R. et al. CD80 in immune suppression by mouse ovarian carcinoma-

associated Gr-1+CD11b+ myeloid cells. Cancer Res. **66,** 6807–15 (2006).

252. de la Puente, P., Muz, B., Azab, F. & Azab, A. K. Cell trafficking of endothelial progenitor cells in tumor progression. Clin. Cancer Res. **19,** 3360–8 (2013).

253. Greenblatt, M. & Shubi, P. Tumor angiogenesis: transfilter diffusion studies in the hamster by the transparent chamber technique. J. Natl. Cancer Inst. **41,** 111–24 (1968).

254. Vizio, B. et al. Pilot study to relate clinical outcome in pancreatic carcinoma and angiogenic plasma factors/circulating mature/progenitor endothelial cells: Preliminary results. Cancer Sci. **101,** 2448–2454 (2010).

255. Ding, Y., Kumar, S. & Yu, D. The role of endothelial progenitor cells in tumour vasculogenesis. Pathobiology **75,** 265–73 (2008).

256. Lin, Y., Weisdorf, D. J., Solovey, A. & Hebbel, R. P. Origins of circulating endothelial cells and endothelial outgrowth from blood. J. Clin. Invest. **105,** 71–7 (2000).

257. Burger, P. E. et al. Fibroblast growth factor receptor-1 is expressed by endothelial progenitor cells. Blood **100,** 3527–35 (2002).

258. Rafii, S., Lyden, D., Benezra, R., Hattori, K. & Heissig, B. Vascular and haematopoietic stem cells: novel targets for anti-angiogenesis therapy? Nat. Rev. Cancer **2,** 826–835 (2002).

259. Fadini, G. P., Losordo, D. & Dimmeler, S. Critical reevaluation of endothelial progenitor cell phenotypes for therapeutic and diagnostic use. Circ. Res. **110,** 624–637 (2012).

260. Asahara, T. et al. Isolation of putative progenitor endothelial cells for angiogenesis. Science **275,** 964–7 (1997).

261. Peichev, M. et al. Expression of VEGFR-2 and AC133 by circulating human CD34(+) cells identifies a population of functional endothelial precursors. Blood **95,** 952–958 (2000).

262. Goon, P. K. Y., Lip, G. Y. H., Boos, C. J., Stonelake, P. S. & Blann, A. D. Circulating Endothelial Cells, Endothelial Progenitor Cells, and Endothelial Microparticles in Cancer. Neoplasia **8,** 79–88 (2006).

263. Kocher, A. A. et al. Neovascularization of ischemic myocardium by human bone-marrow-derived angioblasts prevents cardiomyocyte apoptosis, reduces

remodeling and improves cardiac function. Nat. Med. **7,** 430–6 (2001).

264. Asahara, T., Kawamoto, A. & Masuda, H. Concise Review: Circulating Endothelial Progenitor Cells for Vascular Medicine. Stem Cells **29,** 1650–1655 (2011).
265. Hristov, M., Erl, W. & Weber, P. C. Endothelial progenitor cells: isolation and characterization. Trends Cardiovasc. Med. **13,** 201–6 (2003).
266. Shintani, S. et al. Mobilization of endothelial progenitor cells in patients with acute myocardial infarction. Circulation **103,** 2776–9 (2001).
267. Willett, C. G. et al. Direct evidence that the VEGF-specific antibody bevacizumab has antivascular effects in human rectal cancer. Nat. Med. **10,** 145–147 (2004).
268. Carmeliet, P. et al. Abnormal blood vessel development and lethality in embryos lacking a single VEGF allele. Nature **380,** 435–9 (1996).
269. George, M. L., Eccles, S. A., Tutton, M. G., Abulafi, A. M. & Swift, R. I. Correlation of plasma and serum vascular endothelial growth factor levels with platelet count in colorectal cancer: clinical evidence of platelet scavenging? Clin. Cancer Res. **6,** 3147–52 (2000).
270. Hattori, K. et al. Vascular endothelial growth factor and angiopoietin-1 stimulate postnatal hematopoiesis by recruitment of vasculogenic and hematopoietic stem cells. J. Exp. Med. **193,** 1005–14 (2001).
271. Asahara, T. et al. Bone marrow origin of endothelial progenitor cells responsible for postnatal vasculogenesis in physiological and pathological neovascularization. Circ. Res. **85,** 221–8 (1999).
272. Yamaguchi, J. et al. Stromal cell-derived factor-1 effects on ex vivo expanded endothelial progenitor cell recruitment for ischemic neovascularization. Circulation **107,** 1322–8 (2003).
273. Lonardo, E., Hermann, P. C. & Heeschen, C. Pancreatic cancer stem cells e update and future perspectives. Mol. Oncol. **4,** 431–442 (2010).
274. Starzynska, T. et al. An intensified systemic trafficking of bone marrow-derived stem/progenitor cells in patients with pancreatic cancer. J Cell Mol Med **17,** 792–799 (2013).
275. Bertolini, F., Shaked, Y., Mancuso, P. & Kerbel, R. R. S. The multifaceted circulating endothelial cell in cancer: towards marker and target identification. Nat. Rev. Cancer **6,** 835–845 (2006).

276. Beerepoot, L. V et al. Increased levels of viable circulating endothelial cells are an indicator of progressive disease in cancer patients. Ann. Oncol. Off. J. Eur. Soc. Med. Oncol. **15,** 139–45 (2004).

277. Ko, A. H. et al. A phase II study of bevacizumab plus erlotinib for gemcitabine-refractory metastatic pancreatic cancer. Cancer Chemother. Pharmacol. **66,** 1051–1057 (2010).

278. Bertolini, F. et al. Maximum tolerable dose and low-dose metronomic chemotherapy have opposite effects on the mobilization and viability of circulating endothelial progenitor cells. Cancer Res. **63,** 4342–6 (2003).

279. Buckstein, R. et al. High-Dose Celecoxib and Metronomic "Low-dose" Cyclophosphamide Is an Effective and Safe Therapy in Patients with Relapsed and Refractory Aggressive Histology Non-Hodgkin's Lymphoma. Clin. Cancer Res. **12,** 5190–5198 (2006).

280. Schuch, G. et al. Endostatin inhibits the vascular endothelial growth factor-induced mobilization of endothelial progenitor cells. Cancer Res. **63,** 8345–50 (2003).

281. Capillo, M. et al. Continuous infusion of endostatin inhibits differentiation, mobilization, and clonogenic potential of endothelial cell progenitors. Clin. Cancer Res. **9,** 377–82 (2003).

282. Mancuso, P. et al. Resting and activated endothelial cells are increased in the peripheral blood of cancer patients. Blood **97,** 3658–61 (2001).

283. Kim, H. K. et al. Circulating numbers of endothelial progenitor cells in patients with gastric and breast cancer. Cancer Lett. **198,** 83–8 (2003).

284. Lyden, D. et al. Impaired recruitment of bone-marrow-derived endothelial and hematopoietic precursor cells blocks tumor angiogenesis and growth. Nat. Med. **7,** 1194–201 (2001).

285. Garmy-Susini, B. & Varner, J. A. Circulating endothelial progenitor cells. Br. J. Cancer **93,** 855–858 (2005).

286. Stoll, B. R., Migliorini, C., Kadambi, A., Munn, L. L. & Jain, R. K. A mathematical model of the contribution of endothelial progenitor cells to angiogenesis in tumors: implications for antiangiogenic therapy. Blood **102,** 2555–61 (2003).

287. Khan, S. S., Solomon, M. A. & McCoy, J. P. Detection of circulating endothelial

cells and endothelial progenitor cells by flow cytometry. Cytom. Part B Clin. Cytom. **64B,** 1–8 (2005).

288. Gehling, U. M. et al. In vitro differentiation of endothelial cells from AC133-positive progenitor cells. Blood **95,** 3106–3112 (2000).
289. Danova, M., Comolli, G., Manzoni, M., Torchio, M. & Mazzini, G. Flow cytometric analysis of circulating endothelial cells and endothelial progenitors for clinical purposes in oncology: A critical evaluation (Review). Mol. Clin. Oncol. **4,** 909–917 (2016).
290. Sakamori, Y. et al. Increase in circulating endothelial progenitor cells predicts response in patients with advanced non-small-cell lung cancer. Cancer Sci. **103,** 1065–70 (2012).
291. Morita, R. et al. Endothelial progenitor cells are associated with response to chemotherapy in human non-small-cell lung cancer. J. Cancer Res. Clin. Oncol. **137,** 1849–1857 (2011).
292. Steurer, M. et al. Quantification of circulating endothelial and progenitor cells: comparison of quantitative PCR and four-channel flow cytometry. BMC Res. Notes **1,** 71 (2008).
293. Roodhart, J. M. et al. Late release of circulating endothelial cells and endothelial progenitor cells after chemotherapy predicts response and survival in cancer patients. Neoplasia **12,** 87–94 (2010).
294. Li, A. et al. CXCR2-Dependent Endothelial Progenitor Cell Mobilization in Pancreatic Cancer Growth. Transl. Oncol. **4,** 20–28 (2011).
295. Starlinger, P. et al. Discrimination between Circulating Endothelial Cells and Blood Cell Populations with Overlapping Phenotype Reveals Distinct Regulation and Predictive Potential in Cancer Therapy. Neoplasia **13,** 980–990 (2011).
296. Lin, C.-C. et al. Profiles of circulating endothelial cells and serum cytokines during adjuvant chemoradiation in rectal cancer patients. Clin. Transl. Oncol. **15,** 855–860 (2013).
297. Fuereder, T. et al. Circulating endothelial progenitor cells in castration resistant prostate cancer: a randomized, controlled, biomarker study. PLoS One **9,** e95310 (2014).
298. DuBois, S. G. et al. Circulating endothelial cells and circulating endothelial

precursor cells in patients with osteosarcoma. Pediatr. Blood Cancer **58,** 181–4 (2012).

299. Corsini, E. et al. Decrease in circulating endothelial progenitor cells in treated glioma patients. J. Neurooncol. **108,** 123–9 (2012).
300. Kim, Y. B. et al. Circulating endothelial progenitor cells in gynaecological cancer. J. Int. Med. Res. **41,** 293–299 (2013).
301. Bhatt, R. S. et al. Increased mobilisation of circulating endothelial progenitors in von Hippel-Lindau disease and renal cell carcinoma. Br. J. Cancer **105,** 112–117 (2011).
302. Ha, X. et al. Identification and clinical significance of circulating endothelial progenitor cells in gastric cancer. Biomarkers **18,** 487–492 (2013).
303. Marlicz, W. et al. Effect of colorectal cancer on the number of normal stem cells circulating in peripheral blood. Oncol. Rep. **36,** 3635–3642 (2016).
304. Shim, Y., Nam, M. H., Hyuk, S. W., Yoon, S. Y. & Song, J. M. Concurrent hypermulticolor monitoring of CD31, CD34, CD45 and CD146 endothelial progenitor cell markers for acute myocardial infarction. Anal. Chim. Acta **853,** 501–507 (2015).
305. DeLisser, H. M. et al. Involvement of endothelial PECAM-1/CD31 in angiogenesis. Am. J. Pathol. **151,** 671–7 (1997).
306. Bühring, H. J. et al. Expression of novel surface antigens on early hematopoietic cells. Ann. N. Y. Acad. Sci. **872,** 25-38–9 (1999).
307. Zimmerlin, L., Donnenberg, V. S., Rubin, J. P. & Donnenberg, A. D. Mesenchymal markers on human adipose stem/progenitor cells. Cytom. Part A **83A,** 134–140 (2013).
308. Hernandez, Y. G. & Lucas, A. L. MicroRNA in pancreatic ductal adenocarcinoma and its precursor lesions. World J. Gastrointest. Oncol. **8,** 18–29 (2016).
309. Sethi, S. et al. Comprehensive molecular oncogenomic profiling and miRNA analysis of prostate cancer. Am. J. Transl. Res. **5,** 200–11 (2013).
310. Ang, J. I. N. W., En, S. U. S., Wang, J. & Sen, S. MicroRNA functional network in pancreatic cancer: from biology to biomarkers of disease. J. Biosci. **36,** 481–491 (2011).
311. Rachagani, S., Kumar, S. & Batra, S. K. MicroRNA in pancreatic cancer:

pathological, diagnostic and therapeutic implications. Cancer Lett. **292,** 8–16 (2010).

312. Cai, X., Hagedorn, C. H. & Cullen, B. R. Human microRNAs are processed from capped, polyadenylated transcripts that can also function as mRNAs. RNA **10,** 1957–66 (2004).
313. Shah, M. S., Davidson, L. A. & Chapkin, R. S. Mechanistic insights into the role of microRNAs in cancer: Influence of nutrient crosstalk. Front. Genet. **3,** 1–14 (2012).
314. Harfe, B. D. MicroRNAs in vertebrate development. Curr. Opin. Genet. Dev. **15,** 410–415 (2005).
315. Calin, G. A. et al. Frequent deletions and down-regulation of micro- RNA genes miR15 and miR16 at 13q14 in chronic lymphocytic leukemia. Proc. Natl. Acad. Sci. U. S. A. **99,** 15524–15529 (2002).
316. McManus, M. T. MicroRNAs and cancer. Semin. Cancer Biol. **13,** 253–258 (2003).
317. Lu, J. et al. MicroRNA expression profiles classify human cancers. Nature **435,** 834–838 (2005).
318. Mayr, C. & Bartel, D. P. Widespread Shortening of 3'UTRs by Alternative Cleavage and Polyadenylation Activates Oncogenes in Cancer Cells. Cell **138,** 673–684 (2009).
319. Lee, E. J. et al. Expression profiling identifies microRNA signature in pancreatic cancer. Int. J. cancer.Journal Int. du cancer **120,** 1046–1054 (2007).
320. Zhang, Y. et al. Profiling of 95 MicroRNAs in pancreatic cancer cell lines and surgical specimens by real-time PCR analysis. World J. Surg. **33,** 698–709 (2009).
321. Piepoli, A. et al. Mirna Expression Profiles Identify Drivers in Colorectal and Pancreatic Cancers. PLoS One **7,** e33663 (2012).
322. Szafranska, A. E. et al. Analysis of microRNAs in pancreatic fine-needle aspirates can classify benign and malignant tissues. Clin. Chem. **54,** 1716–1724 (2008).
323. Davidson, L. A. et al. n-3 Polyunsaturated fatty acids modulate carcinogen-directed non-coding microRNA signatures in rat colon. Carcinogenesis **30,** 2077–2084 (2009).
324. Yang, Y., Chaerkady, R., Beer, M. A., Mendell, J. T. & Pandey, A. Identification of miR-21 targets in breast cancer cells using a quantitative proteomic approach.

Proteomics **9,** 1374–1384 (2009).

325. Moriyama, T. et al. MicroRNA-21 modulates biological functions of pancreatic cancer cells including their proliferation, invasion, and chemoresistance. Mol. Cancer Ther. **8,** 1067–1074 (2009).
326. Dillhoff, M., Liu, J., Frankel, W., Croce, C. & Bloomston, M. MicroRNA-21 is overexpressed in pancreatic cancer and a potential predictor of survival. J. Gastrointest. Surg. **12,** 2171–6 (2008).
327. Bloomston, M. et al. MicroRNA expression patterns to differentiate pancreatic adenocarcinoma from normal pancreas and chronic pancreatitis. JAMA **297,** 1901–8 (2007).
328. Park, J.-K., Lee, E. J., Esau, C. & Schmittgen, T. D. Antisense inhibition of microRNA-21 or -221 arrests cell cycle, induces apoptosis, and sensitizes the effects of gemcitabine in pancreatic adenocarcinoma. Pancreas **38,** e190-9 (2009).
329. Giovannetti, E., Funel, N., Peters, G. J., Chiaro, M. Del & Erozenci, L. A. MicroRNA-21 in Pancreatic Cancer : Correlation with Clinical Outcome and Pharmacologic Aspects Underlying Its Role in the Modulation of Gemcitabine Activity MicroRNA-21 in Pancreatic Cancer : Correlation with Clinical Outcome and Pharmacologic Aspects Und. (2010). doi:10.1158/0008-5472.CAN-09-4467
330. Li, Y. et al. Abstract 5703: Up-regulation of miR-146a contributes to the inhibition of invasion of pancreatic cancer cells. Cancer Res. **70,** 5703–5703 (2010).
331. Li, Y. et al. miR-146a Suppresses Invasion of Pancreatic Cancer Cells. Cancer Res. **70,** 1486–1495 (2010).
332. John, J. et al. MicroRNA expression alterations are linked to tumorigenesis and non-neoplastic processes in pancreatic ductal adenocarcinoma. Oncogene **26,** 4442–4452 (2007).
333. Bloomston, M., Frankel, W. L. & Petrocca, F. MicroRNA Expression Patterns to Differentiate Pancreatic Adenocarcinoma From Normal. (2010). doi:10.1001/jama.297.17.1901
334. Ryu, J. K. et al. Aberrant microRNA-155 expression is an early event in the multistep progression of pancreatic adenocarcinoma. Pancreatology **10,** 66–73

(2010).

335. Gironella, M. et al. Tumor protein 53-induced nuclear protein 1 expression is repressed by miR-155, and its restoration inhibits pancreatic tumor development. Proc. Natl. Acad. Sci. **104,** 16170–16175 (2007).
336. Greither, T. et al. Elevated expression of microRNAs 155, 203, 210 and 222 in pancreatic tumors is associated with poorer survival. Int. J. Cancer **126,** 73–80 (2010).
337. Kawaguchi, T. et al. Clinical impact of circulating miR-221 in plasma of patients with pancreatic cancer. Br. J. Cancer **108,** 361–369 (2013).
338. Fish, J. E. & Srivastava, D. MicroRNAs: Opening a New Vein in Angiogenesis Research. Sci. Signal. **2,** pe1-pe1 (2009).
339. Ivan, M., Harris, A. L., Martelli, F. & Kulshreshtha, R. Hypoxia response and microRNAs: no longer two separate worlds. J. Cell. Mol. Med. **12,** 1426–31 (2008).
340. Ho, A. S. et al. Circulating miR-210 as a Novel Hypoxia Marker in Pancreatic Cancer. Transl. Oncol. **3,** 109–113 (2010).
341. Hu, S. et al. MicroRNA-210 as a Novel Therapy for Treatment of Ischemic Heart Disease. Circulation **122,** S124–S131 (2010).
342. Takikawa, T. et al. MiR-210 regulates the interaction between pancreatic cancer cells and stellate cells. Biochem. Biophys. Res. Commun. **437,** 433–439 (2013).
343. Chen, Y. et al. Regulation of the expression and activity of the antiangiogenic homeobox gene GAX/MEOX2 by ZEB2 and microRNA-221. Mol. Cell. Biol. **30,** 3902–13 (2010).
344. Lorenzen, J. M. et al. Circulating miR-210 Predicts Survival in Critically Ill Patients with Acute Kidney Injury. Clin. J. Am. Soc. Nephrol. **6,** 1540–1546 (2011).
345. Patel, S., Leal, A. D. & Gorski, D. H. The Homeobox Gene Gax Inhibits Angiogenesis through Inhibition of Nuclear Factor- B-Dependent Endothelial Cell Gene Expression. Cancer Res. **65,** 1414–1424 (2005).
346. Wang, J. et al. MicroRNAs in Plasma of Pancreatic Ductal Adenocarcinoma Patients as Novel Blood-Based Biomarkers of Disease MicroRNAs in Plasma of Pancreatic Ductal Adenocarcinoma Patients as Novel Blood-Based Biomarkers of Disease. 807–813 (2009). doi:10.1158/1940-6207.CAPR-09-0094

347. Liu, R. et al. Serum microRNA expression profile as a biomarker in the diagnosis and prognosis of pancreatic cancer. Clin. Chem. **58,** 610–618 (2012).
348. El Gazzar, M. microRNAs as potential regulators of myeloid-derived suppressor cell expansion. Innate Immun. **20,** 227–38 (2014).
349. Chen, S., Zhang, Y., Kuzel, T. M. & Zhang, B. Regulating Tumor Myeloid-Derived Suppressor Cells by MicroRNAs. Cancer cell Microenviron. **2,** (2015).
350. Boldin, M. P. et al. miR-146a is a significant brake on autoimmunity, myeloproliferation, and cancer in mice. J. Exp. Med. **208,** 1189–201 (2011).
351. Li, L. et al. MicroRNA-155 and MicroRNA-21 promote the expansion of functional myeloid-derived suppressor cells. J. Immunol. **192,** 1034–43 (2014).
352. Chen, S. et al. Host miR155 Promotes Tumor Growth through a Myeloid-Derived Suppressor Cell-Dependent Mechanism. Cancer Res. **75,** 519–531 (2015).
353. Cui, T. X. et al. Myeloid-Derived Suppressor Cells Enhance Stemness of Cancer Cells by Inducing MicroRNA101 and Suppressing the Corepressor CtBP2. Immunity **39,** 611–621 (2013).
354. Kromann, N. & Green, A. Epidemiological studies in the Upernavik district, Greenland. Incidence of some chronic diseases 1950-1974. Acta Med. Scand. **208,** 401–6 (1980).
355. Hardman, W. E. on Food , Nutrition & Cancer Omega-3 Fatty Acids to Augment Cancer Therapy 1. 3508–3512 (2002).
356. Calder, P. C. & Yaqoob, P. Understanding Omega-3 Polyunsaturated Fatty Acids. Postgrad. Med. **121,** 148–157 (2009).
357. Calder, P. C. Mechanisms of Action of (n-3) Fatty Acids. J. Nutr. **142,** 592S–599S (2012).
358. Murphy, M. G. Dietary fatty acids and membrane protein function. J. Nutr. Biochem. **1,** 68–79 (1990).
359. Stubbs, C. D. & Smith, A. D. The modification of mammalian membrane polyunsaturated fatty acid composition in relation to membrane fluidity and function. Biochim. Biophys. Acta **779,** 89–137 (1984).
360. Yaqoob, P. The Nutritional Significance of Lipid Rafts. Annu. Rev. Nutr. **29,** 257–282 (2009).
361. Miles, E. A. & Calder, P. C. Modulation of immune function by dietary fatty acids.

Proc. Nutr. Soc. **57,** 277–92 (1998).

362. Yaqoob, P., Pala, H. S., Cortina-Borja, M., Newsholme, E. A. & Calder, P. C. Encapsulated fish oil enriched in alpha-tocopherol alters plasma phospholipid and mononuclear cell fatty acid compositions but not mononuclear cell functions. Eur. J. Clin. Invest. **30,** 260–74 (2000).
363. Simopoulos, A. P. The importance of the omega-6/omega-3 fatty acid ratio in cardiovascular disease and other chronic diseases. Exp. Biol. Med. (Maywood). **233,** 674–688 (2008).
364. Marsen, T. A., Pollok, M., Oette, K. & Baldamus, C. A. Pharmacokinetics of omega-3-fatty acids during ingestion of fish oil preparations. Prostaglandins. Leukot. Essent. Fatty Acids **46,** 191–6 (1992).
365. Blonk, M. C. et al. Dose-response effects of fish-oil supplementation in healthy volunteers. Am. J. Clin. Nutr. **52,** 120–7 (1990).
366. Okami, J. et al. Overexpression of cyclooxygenase-2 in carcinoma of the pancreas. Clin. Cancer Res. **5,** 2018–24 (1999).
367. Calder, P. & Grimble, R. Polyunsaturated fatty acids, inflammation and immunity. Eur. J. Clin. Nutr. **56,** S14–S19 (2002).
368. Calder, P. C. Use of fish oil in parenteral nutrition: Rationale and reality. Proc. Nutr. Soc. **65,** 264–277 (2006).
369. Lee, T. H. et al. Effect of dietary enrichment with eicosapentaenoic and docosahexaenoic acids on in vitro neutrophil and monocyte leukotriene generation and neutrophil function. N. Engl. J. Med. **312,** 1217–24 (1985).
370. von Schacky, C., Kiefl, R., Jendraschak, E. & Kaminski, W. E. n-3 fatty acids and cysteinyl-leukotriene formation in humans in vitro, ex vivo, and in vivo. J. Lab. Clin. Med. **121,** 302–9 (1993).
371. Sperling, R. I. et al. Dietary omega-3 polyunsaturated fatty acids inhibit phosphoinositide formation and chemotaxis in neutrophils. J. Clin. Invest. **91,** 651–660 (1993).
372. Goldman, D. W., Pickett, W. C. & Goetzl, E. J. Human neutrophil chemotactic and degranulating activities of leukotriene B5 (LTB5) derived from eicosapentaenoic acid. Biochem. Biophys. Res. Commun. **117,** 282–8 (1983).
373. Waitzberg, D. L., Torrinhas, R. S. & Jacintho, T. M. New parenteral lipid

emulsions for clinical use. JPEN.Journal Parenter. Enter. Nutr. **30,** 351–367 (2006).

374. Sanderson, P. & Calder, P. C. Dietary fish oil appears to prevent the activation of phospholipase C-gamma in lymphocytes. Biochim. Biophys. Acta **1392,** 300–8 (1998).
375. Poynter, M. E. & Daynes, R. A. Peroxisome proliferator-activated receptor alpha activation modulates cellular redox status, represses nuclear factor-kappaB signaling, and reduces inflammatory cytokine production in aging. J. Biol. Chem. **273,** 32833–41 (1998).
376. Ross, J. A., Moses, A. G. & Fearon, K. C. The anti-catabolic effects of n-3 fatty acids. Curr. Opin. Clin. Nutr. Metab. Care **2,** 219–26 (1999).
377. Bordin, L. et al. Arachidonic acid-induced IL-6 expression is mediated by PKC alpha activation in osteoblastic cells. Biochemistry **42,** 4485–91 (2003).
378. De Caterina, R., Cybulsky, M. I., Clinton, S. K., Gimbrone, M. A. & Libby, P. The omega-3 fatty acid docosahexaenoate reduces cytokine-induced expression of proatherogenic and proinflammatory proteins in human endothelial cells. Arterioscler. Thromb. a J. Vasc. Biol. **14,** 1829–36 (1994).
379. Priante, G., Bordin, L., Musacchio, E., Clari, G. & Baggio, B. Fatty acids and cytokine mRNA expression in human osteoblastic cells: a specific effect of arachidonic acid. Clin. Sci. (Lond). **102,** 403–9 (2002).
380. Trebble, T. M. et al. Prostaglandin E2 production and T cell function after fish-oil supplementation: response to antioxidant cosupplementation. Am. J. Clin. Nutr. **78,** 376–82 (2003).
381. Trebble, T. et al. Inhibition of tumour necrosis factor-alpha and interleukin 6 production by mononuclear cells following dietary fish-oil supplementation in healthy men and response to antioxidant co-supplementation. Br. J. Nutr. **90,** 405–12 (2003).
382. Serhan, C. N. Novel eicosanoid and docosanoid mediators: resolvins, docosatrienes, and neuroprotectins. Curr. Opin. Clin. Nutr. Metab. Care **8,** 115–21 (2005).
383. Geelen, A. et al. Fish consumption, n-3 fatty acids, and colorectal cancer: a meta-analysis of prospective cohort studies. Am. J. Epidemiol. **166,** 1116–1125

(2007).

384. Chang, W. L., Chapkin, R. S. & Lupton, J. R. Fish oil blocks azoxymethane-induced rat colon tumorigenesis by increasing cell differentiation and apoptosis rather than decreasing cell proliferation. J. Nutr. **128,** 491–7 (1998).

385. Kachroo, P. et al. Classification of diet-modulated gene signatures at the colon cancer initiation and progression stages. Dig. Dis. Sci. **56,** 2595–604 (2011).

386. Davidson, L. A. et al. Identification of Actively Translated mRNA Transcripts in a Rat Model of Early-Stage Colon Carcinogenesis. Cancer Prev. Res. **2,** 984–994 (2009).

387. Dimri, M., Bommi, P. V., Sahasrabuddhe, A. A., Khandekar, J. D. & Dimri, G. P. Dietary omega-3 polyunsaturated fatty acids suppress expression of EZH2 in breast cancer cells. Carcinogenesis **31,** 489–495 (2010).

388. Hall, M. N., Chavarro, J. E., Lee, I.-M., Willett, W. C. & Ma, J. A 22-year prospective study of fish, n-3 fatty acid intake, and colorectal cancer risk in men. Cancer Epidemiol. Biomarkers Prev. **17,** 1136–43 (2008).

389. Whelan, J. & McEntee, M. F. Dietary (n-6) PUFA and intestinal tumorigenesis. J. Nutr. **134,** 3421S–3426S (2004).

390. Larsson, S. C., Kumlin, M., Ingelman-sundberg, M. & Wolk, A. Dietary long-chain n Ⲭ 3 fatty acids for the prevention of cancer : a review of potential mechanisms 1 – 3. (2004).

391. Hamid, R., Singh, J., Reddy, B. S. & Cohen, L. A. Inhibition by dietary menhaden oil of cyclooxygenase-1 and -2 in N-nitrosomethylurea-induced rat mammary tumors. Int. J. Oncol. **14,** 523–8 (1999).

392. Lala, P. K. & Chakraborty, C. Role of nitric oxide in carcinogenesis and tumour progression. Lancet Oncol. **2,** 149–156 (2001).

393. Jadeski, L. C., Chakraborty, C. & Lala, P. K. Role of nitric oxide in tumour progression with special reference to a murine breast cancer model. Can. J. Physiol. Pharmacol. **80,** 125–35 (2002).

394. Ohata, T., Fukuda, K., Takahashi, M., Sugimura, T. & Wakabayashi, K. Suppression of nitric oxide production in lipopolysaccharide-stimulated macrophage cells by omega 3 polyunsaturated fatty acids. Jpn. J. Cancer Res. **88,** 234–7 (1997).

395. Murray, N. R. et al. Protein kinase C βII and TGFβRII in ω-3 fatty acid–mediated inhibition of colon carcinogenesis. J. Cell Biol. **157,** 915–920 (2002).
396. Cockbain, A. J. et al. Anticolorectal cancer activity of the omega-3 polyunsaturated fatty acid eicosapentaenoic acid. Gut 1–9 (2014). doi:10.1136/gutjnl-2013-306445
397. Watson, H. et al. Measurement of red blood cell eicosapentaenoic acid (EPA) levels in a randomised trial of EPA in patients with colorectal cancer liver metastases. Prostaglandins, Leukot. Essent. Fat. Acids **115,** 60–66 (2016).
398. Falconer, J. S. et al. Effect of eicosapentaenoic acid and other fatty acids on the growth in vitro of human pancreatic cancer cell lines. Br. J. Cancer **69,** 826–832 (1994).
399. Zhang, W., Long, Y., Zhang, J. & Wang, C. Modulatory effects of EPA and DHA on proliferation and apoptosis of pancreatic cancer cells. J. Huazhong Univ. Sci. Technol. Sci. = Hua zhong ke ji da xue xue bao.Yi xue Ying wen ban = Huazhong keji daxue xuebao.Yixue Yingdewen ban **27,** 547–550 (2007).
400. Dekoj, T. et al. G2/M cell-cycle arrest and apoptosis by n-3 fatty acids in a pancreatic cancer model. J. Surg. Res. **139,** 106–12 (2007).
401. Hering, J. et al. Inhibition of proliferation by omega-3 fatty acids in chemoresistant pancreatic cancer cells. Ann. Surg. Oncol. **14,** 3620–3628 (2007).
402. Funahashi, H. et al. Opposing Effects of n-6 and n-3 Polyunsaturated Fatty Acids on Pancreatic Cancer Growth. Pancreas **36,** 353–362 (2008).
403. O'Connor, T. P. et al. Effect of dietary omega-3 and omega-6 fatty acids on development of azaserine-induced preneoplastic lesions in rat pancreas. J. Natl. Cancer Inst. **81,** 858–863 (1989).
404. Heukamp, I. et al. Influence of Different Dietary Fat Intake on Liver Metastasis and Hepatic Lipid Peroxidation in BOP-Induced Pancreatic Cancer in Syrian Hamsters. Pancreatology **6,** 96–102 (2006).
405. Falconer, J. S., Fearon, K. C., Ross, J. A. & Carter, D. C. Polyunsaturated fatty acids in the treatment of weight-losing patients with pancreatic cancer. World Rev. Nutr. Diet. **76,** 74–6 (1994).
406. Wigmore, S. J. et al. The effect of polyunsaturated fatty acids on the progress of cachexia in patients with pancreatic cancer. Nutrition **12,** S27-30 (1996).

407. Fearon, K. C. H. et al. Effect of a protein and energy dense N-3 fatty acid enriched oral supplement on loss of weight and lean tissue in cancer cachexia: a randomised double blind trial. Gut **52,** 1479–86 (2003).

408. Barber, M. D., McMillan, D. C., Preston, T., Ross, J. a & Fearon, K. C. Metabolic response to feeding in weight-losing pancreatic cancer patients and its modulation by a fish-oil-enriched nutritional supplement. Clin. Sci. (Lond). **98,** 389–399 (2000).

409. Arshad, A. et al. Intravenous ω-3 Fatty Acids Plus Gemcitabine. J. Parenter. Enter. Nutr. **41,** 398–403 (2017).

410. Arshad, A., Chung, W. Y., Steward, W., Metcalfe, M. S. & Dennison, A. R. Reduction in circulating pro-angiogenic and pro-inflammatory factors is related to improved outcomes in patients with advanced pancreatic cancer treated with gemcitabine and intravenous omega-3 fish oil. HPB (Oxford). **15,** 428–32 (2013).

411. Arshad, A. et al. Cellular and plasma uptake of parenteral omega-3 rich lipid emulsion fatty acids in patients with advanced pancreatic cancer. Clin. Nutr. **33,** 895–899 (2014).

412. Eltweri, A. M. et al. Plasma and erythrocyte uptake of omega-3 fatty acids from an intravenous fish oil based lipid emulsion in patients with advanced oesophagogastric cancer. Clin. Nutr. **36,** 768–774 (2017).

413. Dupuis, F., Desplat, V., Praloran, V. & Denizot, Y. Effects of lipidic mediators on the growth of human myeloid and erythroid marrow progenitors. J. Lipid Mediat. Cell Signal. **16,** 117–25 (1997).

414. Varney, M. E., Hardman, W. E. & Sollars, V. E. Omega 3 fatty acids reduce myeloid progenitor cell frequency in the bone marrow of mice and promote progenitor cell differentiation. Lipids Health Dis. **8,** 9 (2009).

415. Yan, D. et al. Polyunsaturated fatty acids promote the expansion of myeloid-derived suppressor cells by activating the JAK/STAT3 pathway. Eur. J. Immunol. **43,** 2943–2955 (2013).

416. Xia, S. et al. Chronic intake of high fish oil diet induces myeloid-derived suppressor cells to promote tumor growth. Cancer Immunol. Immunother. **63,** 663–73 (2014).

417. Yessoufou, A., Plé, A., Moutairou, K., Hichami, A. & Khan, N. A. Docosahexaenoic

acid reduces suppressive and migratory functions of CD4 CD25 regulatory T-cells. **50,** 2377–2388 (2009).

418. Spencer, L. et al. The effect of omega-3 FAs on tumour angiogenesis and their therapeutic potential. Eur. J. Cancer **45,** 2077–2086 (2009).
419. Terano, T., Shiina, T. & Tamura, Y. Eicosapentaenoic acid suppressed the proliferation of vascular smooth muscle cells through modulation of various steps of growth signals. Lipids **31 Suppl,** S301-4 (1996).
420. Fox, P. L. & DiCorleto, P. E. Fish oils inhibit endothelial cell production of platelet-derived growth factor-like protein. Science **241,** 453–6 (1988).
421. Jeyarajah, D. R., Kielar, M., Penfield, J. & Lu, C. Y. Docosahexaenoic acid, a component of fish oil, inhibits nitric oxide production in vitro. J. Surg. Res. **83,** 147–150 (1999).
422. Tsuzuki, T., Shibata, A., Kawakami, Y., Nakagaya, K. & Miyazawa, T. Anti-angiogenic effects of conjugated docosahexaenoic acid in vitro and in vivo. Biosci. Biotechnol. Biochem. **71,** 1902–1910 (2007).
423. Matsuzaki, M. et al. Incremental effects of eicosapentaenoic acid on cardiovascular events in statin-treated patients with coronary artery disease. Circ. J. **73,** 1283–90 (2009).
424. GISSI-HF investigators, L. et al. Effect of n-3 polyunsaturated fatty acids in patients with chronic heart failure (the GISSI-HF trial): a randomised, double-blind, placebo-controlled trial. Lancet **372,** 1223–1230 (2008).
425. He, K. et al. Accumulated Evidence on Fish Consumption and Coronary Heart Disease Mortality: A Meta-Analysis of Cohort Studies. Circulation **109,** 2705–2711 (2004).
426. Rizos, E. C., Ntzani, E. E., Bika, E., Kostapanos, M. S. & Elisaf, M. S. Association between omega-3 fatty acid supplementation and risk of major cardiovascular disease events: a systematic review and meta-analysis. JAMA **308,** 1024–33 (2012).
427. De Caterina, R. n–3 Fatty Acids in Cardiovascular Disease. N. Engl. J. Med. **364,** 2439–2450 (2011).
428. Devaraj, S., Chien, A., Rao, B., Chen, X. & Jialal, I. Modulation of endothelial progenitor cell number and function with n-3 polyunsaturated fatty acids.

Atherosclerosis **228,** 94–7 (2013).

429. Spigoni, V. et al. N-3 PUFA increase bioavailability and function of endothelial progenitor cells. Food Funct. **5,** 1881 (2014).
430. Wu, S.-Y., Mayneris-Perxachs, J., Lovegrove, J. A., Todd, S. & Yaqoob, P. Fish-oil supplementation alters numbers of circulating endothelial progenitor cells and microparticles independently of eNOS genotype. Am. J. Clin. Nutr. **100,** 1232–43 (2014).
431. Faragó, N., Fehér, L. Z., Kitajka, K., Das, U. N. & Puskás, L. G. MicroRNA profile of polyunsaturated fatty acid treated glioma cells reveal apoptosis-specific expression changes. Lipids Health Dis. **10,** 173 (2011).
432. Vinciguerra, M. et al. Unsaturated fatty acids inhibit the expression of tumor suppressor phosphatase and tensin homolog(PTEN) via microRNA-21 up-regulation in hepatocytes. Hepatology **49,** 1176–1184 (2009).
433. Mandal, C. C., Ghosh-Choudhury, T., Dey, N., Choudhury, G. G. & Ghosh-Choudhury, N. miR-21 is targeted by omega-3 polyunsaturated fatty acid to regulate breast tumor CSF-1 expression. Carcinogenesis **33,** 1897–1908 (2012).
434. Macey, M. G. & Perry, A. E. Flow Cytometry. Comprehensive Biotechnology **1,** (Elsevier B.V., 2007).
435. Mukherjee, S. et al. Gemcitabine-based or capecitabine-based chemoradiotherapy for locally advanced pancreatic cancer (SCALOP): a multicentre , randomised , phase 2 trial. **14,** 317–326 (2013).
436. Korn, R. L. & Crowley, J. J. Overview: progression-free survival as an endpoint in clinical trials with solid tumors. Clin. Cancer Res. **19,** 2607–12 (2013).
437. Klionsky, D. J. et al. Guidelines for the use and interpretation of assays for monitoring autophagy (3rd edition). doi.org 1–222 (2016). doi:10.1080/15548627.2015.1100356
438. Simoens, C. M., Deckelbaum, R. J., Massaut, J. J. & Carpentier, Y. A. Inclusion of 10% fish oil in mixed medium-chain triacylglycerol-long-chain triacylglycerol emulsions increases plasma triacylglycerol clearance and induces rapid eicosapentaenoic acid (20:5n-3) incorporation into blood cell phospholipids. Am. J. Clin. Nutr. **88,** 282–8 (2008).
439. Arshad, a, Al-Leswas, D., Stephenson, J., Metcalfe, M. & Dennison, A. Potential

applications of fish oils rich in n-3 fatty acids in the palliative treatment of advanced pancreatic cancer. Br. J. Nutr. **106,** 795–800 (2011).

440. Ino, Y. et al. Immune cell infiltration as an indicator of the immune microenvironment of pancreatic cancer. Br. J. Cancer **108,** 914–923 (2013).